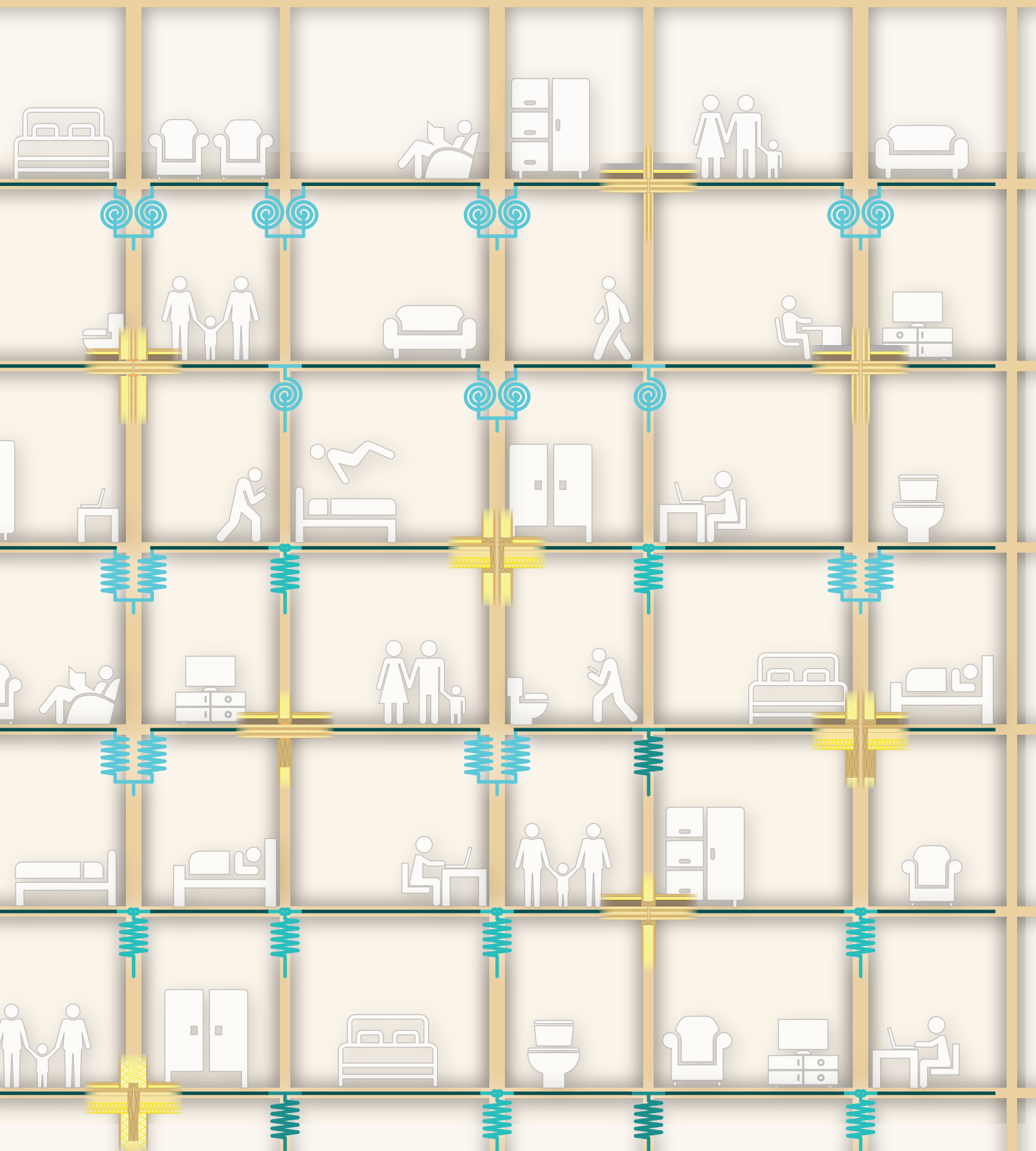


Walking-induced vibration control in multifamily timber buildings

Analysis of floor configurations and support conditions
using classical vibration theory



Robin (T.J.) Oonk



Walking-induced vibration control in multifamily timber buildings

Analysis of floor configurations and support conditions using
classical vibration theory

by

Robin T. J. Oonk

to obtain the degree of Master of Science
at the Delft University of Technology,
to be defended publicly on Wednesday June 10, 2020 at 11:00 AM.

Student number: 4140389
Project duration: April 9, 2019 – November 1, 2019
Thesis committee: Prof. dr. ir. J. W. G. van de Kuilen TU Delft (chairman)
Dr. ir. G. J. P. Ravenshorst TU Delft
Dr. ir. P. C. J. Hoogenboom TU Delft
Ir. M. A. Visscher Royal HaskoningDHV

An electronic version of this thesis is available at <http://repository.tudelft.nl/>.



*“If you had to invent a machine,
which gives you a renewable
supply of building materials
while also reducing carbon
levels,
it would be a tree.”*

ANDREW WAUGH

Preface

Humans live most of our lifetime inside buildings, and these creatures are the souvenirs of them that may last forever representing the society and culture even if the ones who have built it are no longer there. They define the world we are living in nowadays and in the future, which fascinated me already during my childhood, and therefore studying Architecture in Delft being an obvious choice. Later on, I gained more interest in the technical aspects of buildings and enjoying the 'maths' made decide to follow a master at the faculty of Civil Engineering this thesis being the final chapter of that fantastic study journey.

That journey either made me realise what impact the construction sector has on the environment and that the planet pays the price for the souvenirs we are building. When I learned about timber structures, I became aware of that we have to build with nature to save nature like we did thousands of years ago. Only by creating a better version of the homes the hunters and gathers were living in would enable us to keep this planet habitable the coming thousands of years.

I would like to thank Geert Ravenshorst and Jan-Willem van der Kuilen for inspiring me regarding timber structures and guidance with their knowledge for this thesis. I also want to thank Pierre Hoogenboom for providing me other perspectives upon the topic, despite that the research deviated from his knowledge field along the way. Furthermore, I want to thank Michiel Visscher for giving me the right assignments or contacts during the research process to bring back the clarity into my mind.

I am grateful to the colleagues at Royal HaskoningDHV for the inspiring and enjoyable working environment, and especially to Sander Meijers for his support regarding structural dynamics and Falko Noortman for helping me out with SCIA engineer. Besides, I want to thank my friends for the joyful times we had in Delft and the valuable insights they gave me and that I will take with me the rest of my life.

At last, I want to thank my family for enabling me to study in Delft and the confidence in choices I made during my studies. Your unconditional confidence empowered me to be whom I have become.

*Robin T. J. Oonk
Delft, June 2020*

Abstract

Practical combinations of floor configurations and support conditions are studied for the development of a lightweight timber building method that is suitable for multi-family residential buildings. Classical vibration theory forms the base for a methodology that is developed to assess transmittance of vibrations to adjoining floor fields. Especially when the source is out of sight, humans tend to classify vibrations as annoying for low vibration levels. With the introduction of new engineered timber products made wood a more suitable and used material for residential buildings. Strength- and stiffness variation is reduced by homogenizing the material and regarding soundproofing innovative concepts have been improved, such as floating screeds and resilient materials. Based on these products and acoustic concepts, 32 design combinations are studied. A distinction between forced- and free vibrations is made and related to low- and high-frequency floors. Forced vibrations are in structural dynamics described by the particular solution, and free vibrations by the homogeneous solution of the equation of motion. This solution is found through the method of separation of variables, which multiplies the space- and time-related parts. Mode shapes are studied regarding transmittance and effective measures for prevention. Fundamental frequencies of floors supported either rigid and flexible are determined with one-dimensional undamped continuous systems where supported beams are represented by equivalent springs. All floors are transformed into Single Degree of Freedom systems to include damping. These systems are assessed making use of modal superposition, for steady-state and transient response. The behaviour of floors under walking load harmonics provides the resonant response, and free vibration of the system due to initial conditions the transient response. Since the perception of vibrations by humans is frequency-dependent, vibrations are weighted accordingly. Eurocodes currently available are found to provide guidance regarding human-induced vibrations of lightweight structures marginally. Non-timber Eurocodes do not provide an assessment method, EN1990 only provides requirements when no assessment has to be done, and current code for timber structures prescribe criteria that are not sufficient as found in the literature. The future revision of Eurocode 5 holds several methods for assessment of vibrations but is generally focussed on rigidly supported floors. In extending to this code methods are developed to acquire fundamental frequencies of flexible, supported floors, and by transformation into SDOF systems an equation is developed for the appropriate determination of modal mass for two-span or beam supported floors using a simple formula. 32 combinations of floor configurations and support conditions are assessed at the excited field and at adjoining floor fields, where both steady-state and transient response are combined. Based on this assessment, transient responses are found to contribute significantly for low-frequency floors, where generally is assumed that the mass is sufficient to neglect this response.

Keywords: walking vibrations, timber structures, steady-state response, transient response

Contents

List of Tables	xi
List of Figures	xiii
1 Introduction	1
1.1 Relevance of research	2
1.2 Problem statement	3
1.3 Research question and objective	3
1.4 Methodology	4
2 Structural dynamics of Human induced vibrations	7
2.1 Introduction	8
2.2 Continuous systems	9
2.3 Single degree of freedom systems	12
2.3.1 Homogeneous solution for free vibrations	13
2.3.2 Particular solution for forced vibrations	14
2.3.3 Relation of SDOF with Multiple DOF systems	15
2.4 Response of lightweight floors to walking loads	17
2.4.1 Single step load curve	17
2.4.2 Resonant response of low-frequency floors	19
2.4.3 Transient response of high-frequency floors	22
2.5 Human perception of motion	24
2.5.1 Frequency weighting	24
2.5.2 Vibration assessment methods	25
2.6 Main parameters and vibration comfort	29
2.6.1 Steady-state and transient response	30
2.7 Natural frequency of LFF & HFF floor fields	32
3 Vibrations in Eurocodes	35
3.1 Eurocode 5 (EN 1995-1-1)	36
3.1.1 Fundamental frequency	37
3.1.2 Static deflection	37

3.1.3	Unit impulse velocity response	38
3.2	Vibration assessment in non-timber Eurocodes	39
3.2.1	Buildings	39
3.2.2	Footbridges	39
3.3	Revision of EN 1995-1-1	40
3.3.1	Vibrations of all floor types	40
3.3.2	Floors with a permanent weight of at least 50 kg/m ²	42
3.3.3	Shortcomings revised EC5	44
4	Building with timber	47
4.1	Engineered wood products	48
4.2	Timber building methods	50
4.2.1	Floor types	50
4.2.2	Types of load-bearing structures	50
4.2.3	Damping in timber structures	51
4.3	Acoustic performance of dwellings	53
4.3.1	Soundproofing measures	55
4.4	Junction typologies	57
4.4.1	Introduction of floor configurations	57
5	Parameter study	61
5.1	Explanation of system	63
5.1.1	Multi-family residential timber buildings	63
5.1.2	Maple model	64
5.2	Translational stiffness support	69
5.2.1	Translational model	69
5.2.2	Location of force	69
5.2.3	Beam height at home-separating junction	73
5.2.4	Beam height at internal junction	75
5.2.5	Spanning length of supporting beam	77
5.3	Rotational stiffness support	79
5.3.1	Rotational model	79
5.3.2	Location of force	82
5.3.3	Thickness home-separating CLT wall	83
5.3.4	Thickness internal CLT wall	85
5.4	Floor configuration	87
5.4.1	Floor stiffness	87
5.4.2	Additional mass by non-structural floor layers	90
5.5	Comparison with future EC5 revision	91
6	Assessment of junction typologies	93
6.1	Transformation of floors into SDOF systems	95
6.1.1	Methodology	96
6.1.2	SDOF properties of all floors	98
6.1.3	Comparison with revised Eurocode 5	99
6.2	Comfort levels of combined response	102
6.2.1	Methodology	102
6.2.2	Quantification using root-mean-square values	108
6.2.3	Contribution transient response	111
6.2.4	Classification using response factors	111
6.3	Sensitivity response factors for damping ratio	114
6.4	Comparison results with other methods	116
7	Conclusion	121
7.1	Conclusion	122
7.2	Discussion	123
7.3	Recommendations	123

Bibliography	125
A Junction details and properties	131
B Dataholz datasheets	141
C Boundary- and interface conditions	153

List of Tables

2.1	Boundary conditions for a beam in bending [27]	11
2.2	Difference between homogeneous- and particular solution	13
2.3	K-values for different frequencies [63]	18
2.4	Cut-off frequencies for residential purpose adopted by different authors and guidelines	19
2.5	Design parameters for walking forces due to one person [17, 54]	20
2.6	Mean and design values of footfall harmonics [72]	22
2.7	Criteria for acceptable ranges of velocity (mm/s) adopted by different guidelines [63]	27
2.8	Vibration classes proposed by Toratti and Talja [66]	28
2.9	Design limits for vibration classes [66]	28
2.10	Fundamental frequencies	34
3.1	Multiplication factor $k_{e,1}$	41
3.2	Response factors R and motion criteria according to floor performance level [5]	43
3.3	Floor requirements depending on floor class [4, 13]	44
3.4	Recommended requirements for frequency, stiffness and acceleration criteria [4]	44
4.1	Damping ratios after Abeysekera [1] and values proposed for revised Eurocode 5 [5]	52
4.2	Criteria for sound insulation with an external source [36]	53
4.3	Main classes of sound insulation criteria in Danish standard (DS 490). Summarised by Rasmussen [56]	55
4.4	Properties of floors	58
4.5	Properties of walls after Dataholz [15]	59
5.1	Dynamic clamping moment and required normal forces for standard quantities of the junctions	82
5.2	Comparison of fundamental frequencies from model with future revision EC5	92
6.1	Static deflection and corresponding effective width	97
6.2	Steady-state response input variables for model and revision EC5	100
6.3	Transient response input variables for model and revision EC5	101
6.4	Response factors as given in revision of EC5 [5] and newly determined for combined response	112
6.5	Damping ratios used for sensitivity study	114

6.6	Comparison of steady-state and transient responses from model with revision EC5	117
6.7	Input values of equivalent SDOF for 'De Karel Doorman'	118
6.8	v_{rms} quantile values from model for 'De Karel Doorman'	118
C.1	Boundary- and interface conditions for rotational model	154
C.2	Boundary- and interface conditions for translational model	155

List of Figures

1.1	Impression of using timber to vertically extend existing buildings [28]	2
1.2	Schematization of the problem	3
2.1	Vibrations of a simply supported beam as a continuous system (after Zegers [76], edited by Oonk)	9
2.2	Amplitude response and phase angle for a damped SDOF system excited by a harmonic force [6]	14
2.3	FRF magnitude for a damped MDOF system. The dashed lines illustrate the three uncoupled modal SDOF systems [10]	15
2.4	Load-time functions for different activities [71]	17
2.5	Normalized step loads	18
2.6	Series of footfall forces applied by (a) both feet of a walking person and (b) the resulting force on the floor (dashed line) [63]	19
2.7	Resonant response for $f_s = 2$ Hz	19
2.8	Dynamic Load Factors dependent on the walking frequency [63]	21
2.9	DLF according to Wilford	21
2.10	Transient response for $f_s = 2$ Hz	22
2.11	Effective Impulse by Young	23
2.12	Weighting values for human perception	25
2.13	ISO 10137 [17]	25
2.14	OS-RMS ₉₀ design charts for three modal damping values [8]	26
2.15	Response affection by varying the panel height and their envelopes (dashed line)	30
2.16	Response affection by varying the distributed mass and their envelopes (dashed line)	31
2.17	Response affection by varying the damping ratio and their envelopes (dashed line)	31
2.18	Timber structure of a multi-family apartment building	32
3.1	Recommended range of and relationship between a and b [39]	36
3.2	Magnitude of force depending on the fundamental frequency of the floor (after Hamm and Richter [13])	42
4.1	Wood directions [58]	48
4.2	Engineered wood products	49
4.3	Floor types	50

4.4	Load-bearing structures	51
4.5	Visualization of direct (solid line) and flanking paths (dashed line)	54
4.6	Two screed types types [13]	56
4.7	Application of resilient interlayer between walls and floor [60]	56
4.8	Overview of junction details for all floors and their supports (after Dataholz, edited by Oonk)	60
5.1	Apartment	63
5.2	Physical representation of the model	64
5.3	Mode shape ϕ_1 , ϕ_2 and ϕ_3 of a simply-supported beam [27]	66
5.4	Flowchart of Maple sheets for chapter 5	68
5.5	Double leaf junction	70
5.6	Single leaf junction with interrupted floor field	70
5.7	Single leaf junction with continuous floor field	70
5.8	Mechanical schemes for translational model	71
5.9	Vibration shapes of beam supported floor for various force locations	72
5.10	Vibration shapes of timber-frame supported floors for various force locations	72
5.11	Vibration shapes of floor 2 supported by beams (F2-SB) for varying beam height at home-separating junctions	73
5.12	Vibration shapes of floor 3 supported by beams (F3-SB) for varying beam height at home-separating junctions	73
5.13	Natural frequencies for varying beam height at home-separating junctions	74
5.14	Modal mass area for varying beam height at home-separating junctions	74
5.15	Vibration shapes of floor 2 supported by beams (F2-SB) for varying beam height at internal junctions	75
5.16	Vibration shapes of floor 3 supported by beams (F3-SB) for varying beam height at internal junctions	75
5.17	Natural frequencies for varying beam height at internal junctions	76
5.18	Modal mass area for varying beam height at internal junctions	76
5.19	Vibration shapes of floor 2 supported by beams (F2-SB) for varying spanning length of supporting beam	77
5.20	Vibration shapes of floor 3 supported by beams (F3-SB) for varying spanning length of supporting beam	77
5.21	Natural frequencies for varying beam spanning length of supporting beam	78
5.22	Modal mass area for varying beam spanning length of supporting beam	78
5.23	Double leaf junction	80
5.24	Single leaf junction with interrupted floor field	80
5.25	Single leaf junction with continuous floor field	80
5.26	Mechanical schemes for rotational model	81
5.27	Vibration shapes of CLT wall supported floor for various force locations	82
5.28	Vibration shapes of floor 1 supported by CLT walls (F1-CLT) for varying structural thickness of home-separating wall	83
5.29	Vibration shapes of floor 2 supported by CLT walls on elastomers (F2-CLT) for varying structural thickness of home-separating wall	83
5.30	Natural frequencies for varying thickness of home-separating wall	84
5.31	Modal mass area for varying thickness of home-separating wall	84
5.32	Vibration shapes of floor 1 supported by CLT walls (F1-CLT) for varying structural thickness of internal wall	85
5.33	Vibration shapes of floor 2 supported by CLT walls on elastomers (F2-CLT) for varying structural thickness of internal wall	85
5.34	Natural frequencies for varying thickness of internal wall	86
5.35	Modal mass area for varying thickness of internal wall	86
5.36	Vibration shapes of floor 2 supported by beams (F2-SB) for varying floor stiffness	88
5.37	Vibration shapes of floor 3 supported by beams (F3-SB) for varying floor stiffness	88
5.38	Vibration shapes of floor 2 supported by timber-frame (F2-TF) for varying floor stiffness	88
5.39	Vibration shapes of floor 3 supported by timber-frame (F3-TF) for varying floor stiffness	88
5.40	Natural frequencies for varying thickness of structural CLT floor	89

5.41	Natural frequencies for varying height of I-joists	89
5.42	Natural frequencies for varying mass of non-structural floor layers	90
6.1	Flowchart of Maple sheets for chapter 6	94
6.2	Natural frequencies of floor typologies	95
6.3	Static deflection definition	98
6.4	Equivalent SDOF system for steady-state vibration	102
6.5	Maximum steady-state response of floor 2 with timber-frame walls (F2-TF) and double leaf continuous floor field (DC)	104
6.6	Equivalent SDOF system for transient vibration	104
6.7	Maximum transient response	105
6.8	aRMS-values within the walking frequency range	107
6.9	vRMS-values within the walking frequency range	107
6.10	Probability of aRMS-values	107
6.11	Probability of vRMS-values	107
6.12	a_{rms} values of floor typologies	109
6.13	v_{rms} values of floor typologies	110
6.14	Contribution of transient to total response	111
6.15	Response factor	113
6.16	Response factors of combined responses for $0,5\zeta$ to 2ζ	115
6.17	Results from model for 'De Karel Doorman' as designed	119
6.18	Results from model for 'De Karel Doorman' as built	119
6.19	Home-separating junction of 'De Karel Doorman' [14]	119
A.1	Junctions of CLT floors with a wet screed on CLT walls without elastomeric interlayer	132
A.2	Junctions of CLT floors with a dry screed on CLT walls with elastomeric interlayer	133
A.3	Junctions of CLT floors with a dry screed on supporting LVL beam with elastomeric interlayer	134
A.4	Junctions of CLT floors with a dry screed on timber-frame wall with elastomeric interlayer	135
A.5	Junctions of joist floor with fill on supporting LVL beam with elastomeric interlayer	136
A.6	Junctions of joist floor with fill on timber-frame wall with elastomeric interlayer	137
A.7	Junctions of joist floor without fill on supporting LVL beam with elastomeric interlayer	138
A.8	Junctions of joist floor without fill on timber-frame wall with elastomeric interlayer	139

1

Introduction

1.1 RELEVANCE OF RESEARCH

In the Netherlands, about 75% of the population lives in urban areas, and an additional 1,5 million people will settle in metropolitan areas in the coming decades [32]. Cities have to densify to accommodate these people without extensively enlarging the urban area leading to the preservation of green spaces, and use of existing infrastructure like streets, cables and plumbing. Urban densification can be established by building on top of buildings, above highways, railroads, and on soils with low bearing capacity[14]. These areas are not suitable for construction using traditional (heavy concrete) methods, but the development of new lightweight construction methods facilitates the addition of increased living area at locations where they are most expensive. Other beneficial aspects of building lightweight include less foundation material and having lower transportation- and lifting costs.

Royal HaskoningDHV (RHDHV) proved with 'De Karel Doorman' the feasibility of extending an existing building vertically by activating unused load-bearing potential of existing concrete structure in combination with adding a lightweight structure. The concrete lift shaft resists lateral wind loads, and the steel frame introduces the vertical imposed loads applied on timber floors to the concrete columns of the existing structure [14]. The architect aspired to add 16 apartment floors which is achieved using an ultra-lightweight building concept. During construction, however, excessive dynamic behaviour come to light setting the project on hold, such that independent research organisation TNO could investigate the vibrations for useful measures to reduce vibration transmittance. [22]. The weight minimisation results in challenges regarding vibration comfort since mass damps vibrations and lowers amplitudes in general. Not the strength nor static deflection appear to be the governing design criteria, but dynamic behaviour is guiding for lightweight structures.

Transmittance of vibrations to adjacent floor fields is a relatively new field, and more extensive research has yet to be done upon this subject. Most studies focus on situations where both the source and receiver are on the same floor field or within the same apartment. 'De Karel Doorman' proved current standards to be insufficient regarding transmittance to adjoining floor fields when supported by structural beams. Therefore, TNO developed criteria for adjoining apartments based on innovative guidelines to ensure 'De Karel Doorman' fulfils the set demands [22].

Cobelens [7] did research, based on these guidelines, into vibrational problems with 'De Karel Doorman' and the adjustments made during construction. He investigated the effect of several measures for vibration control in multi-house dwellings – like span, mass and stiffness variation of timber joist floor fields and rigidity improvements of the floor supporting steel-frame. Steel being the main bearing structure, the question rises how to control vibration levels of timber structures since it potentially performs better than steel due to its higher damping ratio, and comparable stiffness-to-weight ratio. Furthermore, building with timber regained interest due to new innovative timber products entering the market last decade – like Cross-Laminated Timber (CLT), I-joists and Laminated-Veneer Lumber (LVL) beams and panels. The products introduced new timber building methods and its wide variety in combinations of floor configurations and support conditions.

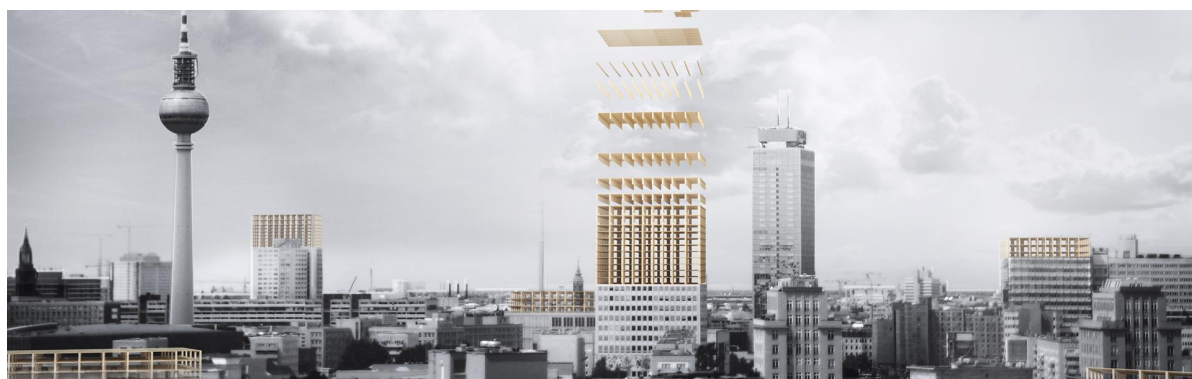


Figure 1.1: Impression of using timber to vertically extend existing buildings [28]

1.2 PROBLEM STATEMENT

The 'Karel Doorman' is an inspiring project covering the socially relevant topic of urban densification. Responding to this need, RHDHV came up with an innovative approach for vertical extension using steel as the main load-bearing structure. However, this also led to new challenges regarding vibration comfort of a lightweight building system where current standards do not provide sufficient assessment methods.

Even though vibrations in timber structures are studied more comprehensively than steel, especially after regaining interest with the introduction of new engineered timber products, more research regarding transmittance to adjoining floor fields is necessary. Most studies focus on single spanning floor fields on rigid supports, which are cases where vibrations do not transmit. However, when one replaces the rigid wall with a flexible supporting beam to increase plan flexibility or applies a two-span floor field vibrations may annoy neighbours.

To enable lightweight building using timber as the main load-bearing structure, a preliminary study is necessary to find the most promising combinations of floor configurations and support conditions. Freedom of form resulted in many commonly applied junctions which all do perform differently when suspected to human-induced loading. Besides, the stiffness and mass of standard floor configurations vary widely though they are the main variables when it comes to vibrations, so study is required into the best measures to take for appropriate vibration levels.

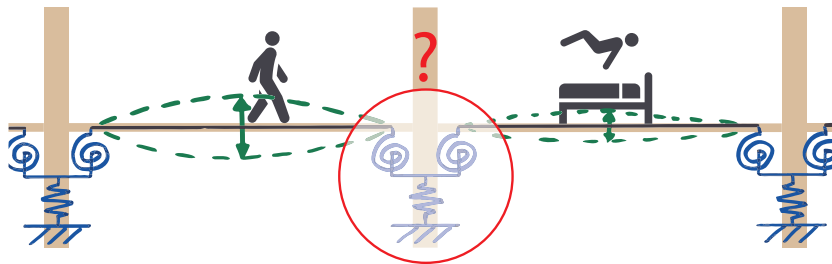


Figure 1.2: Schematization of the problem

1.3 RESEARCH QUESTION AND OBJECTIVE

The answer to the following question contributes to solving previously mentioned problem:

How do floor configurations and support conditions affect fundamental frequencies and transmittance of human-induced vibrations to adjoining floor fields, and which combinations are suitable for multi-family buildings?

This thesis aims to enable engineers to make better design decisions by providing a framework using static deflection for preliminary assessment of structures regarding human-induced vibrations. Besides, the work studies the effects of adjusting floor- and support parameters upon fundamental frequencies and transmittance to adjoining floor fields. Both the framework and parameter study are compared with the validation method proposed for future revision of Eurocode 5 for timber structures.

1.4 METHODOLOGY

Chapter 1: Introduction

The first chapter gives a general introduction to the thesis. It describes the academic value of researching the topic and depicting the related problem, which results in a research question and research objective. The methodology formulates several sub-questions to answer the main question, and it illustrates the process used to derive reported conclusions.

Chapter 2: Structural dynamics of Human induced vibrations

This chapter elaborates on the phenomenon of vibrations by looking at the structure, source and their interaction. First, classical vibration theory of continuous- and single degrees of freedom systems explain the manner structures vibrate. After that, the theory is related to timber floors making a distinction between low- and high-frequency floors. Finally, the way humans perceive vibrations is described. This chapter addresses the following sub-questions:

- 2.1 How does the classical vibration theory relate to structures?
- 2.2 How to use continuous systems to describe vibrations of multiple floor fields?
- 2.3 In which manner can SDOF systems be used to represent vibrations in floors?
- 2.4 What load does a human apply on the floor when walking?
- 2.5 How does the human-induced load excite low- and high-frequency floors?
- 2.6 How to incorporate the human perception of vibrations?

Chapter 3: Vibrations in Eurocodes

The assessment methods for dynamic serviceability limit state provided by various Eurocodes are investigated in this chapter. It sums up the general guidance regarding structural design given in EN1990, and the vibration verification method for steel structures and footbridges are given. After that, serviceability criteria by Eurocode 5 for timber structures are elaborated for the current EC5 as well as the drafts for the future revision of EC5 expected after 2020. The following sub-questions are answered:

- 3.1 What do non-timber Eurocodes prescribe related to vibrations?
- 3.2 In which manner are the serviceability criteria for vibrations verified in EN 1995-1-1?
- 3.3 How is state-of-the-art research implemented in the revised version for EN 1995-1-1?

Chapter 4: Building with timber

This chapter describes the engineered timber products and their practical application. The microscale structure of wood led to innovative products in the last decade that solved several timber building problems. These products introduced new building methods for timber structures requiring investigation regarding their vibrational behaviour at the supports and fulfilment of soundproofing. With these findings, four floor-layer configurations are introduced that follow from the engineered wood products. The chapter aims to answer the following questions:

- 4.1 What are the characteristics of wood as construction material?
- 4.2 Which timber products on the market are suitable for structural application under dynamic loading?
- 4.3 What are the generally applied timber building methods and how is the soundproofing achieved?
- 4.4 Which potentially useful junctions can be made using engineered wood products?

Chapter 5: Parameter study

The previous chapter brings several design combinations of interest, and this chapter studies the effects in the space-domain of varying specific parameters regarding the support and floor configurations. The undamped continuous models are solved using Maple, showing the manner in which vibrations transmit to adjacent floor fields. Besides this, it studies the effect of varying the parameters upon eigenfrequencies of floors. This study aims to answer the following sub-questions:

- 5.1 How to translate the support conditions at the junctions into representative interface conditions for the continuous model?
- 5.2 How do support condition parameters affect transmittance of vibrations by the junction?
- 5.3 What is the influence of floor configuration parameters on eigenfrequencies of floor fields?
- 5.4 How does the floor area that contributes to the modal mass change by varying the floor- and support stiffnesses?
- 5.5 How do the fundamental frequencies compare to the ones provided by the revised Eurocode 5?

Chapter 6: Assessment of junction typologies

The second part of the study focusses on the assessment of low- and high frequency floors for walking. It quantifies the steady-state and transient response of combinations of floor configurations and support conditions in terms of comfort levels. The proposed framework is compared with assessment according to the future revision of Eurocode 5. This study aims to answer the following sub-questions:

- 6.1 How do low- and high-frequency floors compare to one another for various human activities?
- 6.2 Are the vibration levels according to the revised Eurocode 5 comparable to the used method?
- 6.3 Which combinations of typology and support conditions perform promising regarding dynamic serviceability, acoustic behaviour and mass?

Chapter 7: Conclusion

The main findings of the research are summarized in this chapter by answering the research question and its sub-questions. Moreover, conclusions and recommendations for future research upon the subject are given.

2

Structural dynamics of Human induced vibrations

2.1 INTRODUCTION

Vibrations have been of interest to humanity for centuries ever since the first musical instruments were developed and played. Galileo Galilei is the first person to scientifically describe their dynamics in 'Dialogues concerning two new sciences' in 1638, where he discussed harmonic displacing bodies such as pendulums and vibrating strings. With the term *sympathetic vibrations* he therein referred to the phenomenon we now know as resonance.

The next important contribution to the field of dynamics was made by Sir Isaac Newton with the publication of its work 'Philosophiae Naturalis Principia Mathematica' in 1687. It was published in 1686 and contains the three laws of motion: 1) objects in motion tend to stay in motion unless acted upon by a force 2) force equals mass times acceleration ($f(t) = m \cdot a(t)$) and 3) for every action there is an equal and opposite reaction [48].

Four different forces act upon a structure representing the vibration of an object as shown in equation 2.1. The force resulting from a velocity change of a mass ($F_m = m\ddot{x}(t)$), is one of the forces acting on an object in motion following from Newton's Laws of Motion. The force bringing the mass back to its resting position is due to bending of the beam, which can be represented by a spring following Hooke's Law ($F_k = kx(t)$). The force acting on a moving rigid body causing vibrations to decay over time is the damping and a frictional force proportional to the velocity ($F_c = c\dot{x}(t)$). Finally, the external applied force exiting the object ($F(t)$). The equilibrium of the upper defined forces give the equation of motion of a rigid body:

$$F_m + F_c + F_k = m\ddot{x}(t) + c\dot{x}(t) + kx(t) = F(t) \quad (2.1)$$

This chapter will discuss several aspects of floor vibrations due to human activities. First the theorem of continuous systems and its boundary conditions are elaborated for an undamped situation. Thereafter, damping is introduced for Single Degree of Freedom systems explaining the (mathematical) difference between free vibrations and steady-state responses. The cause of these vibrations (i.e. a walking load) is discussed by studying the load profile, and elaborates the manner timber floors—and lightweight floors in general—respond to human activity. Finally, the way perception by humans is incorporated in assessment criteria is shortly explained.

2.2 CONTINUOUS SYSTEMS

As with static situations, vibrations of beam elements are described by the Euler-Bernoulli beam theory, providing a continuous and analytical approach of vibration analysis. Their theory results in an equation of motion which describes the vibration shape of a beam once it is solved for its boundary conditions. Since the system is solved using separation of space and time damping can, unfortunately, not be taken into account. However, it is useful for describing the vibration shape and the transmittance to adjoining floor fields.

This section shows the procedure for solving the equation of motion for the case of a prismatic simply supported beam (see figure 2.1) obtaining the harmonic form of displacement. After that, boundary conditions are given for other cases, which can be solved using the same procedure.

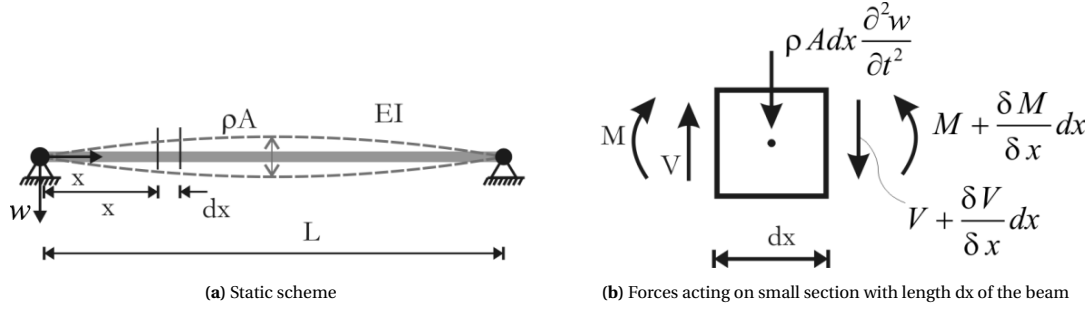


Figure 2.1: Vibrations of a simply supported beam as a continuous system (after Zegers [76], edited by Oonk)

At first, the general equation of motion for an undamped Euler-Bernoulli beam is given by the equilibrium of dynamic forces:

$$\rho A(x) \frac{\partial^2 w(x, t)}{\partial t^2} + \frac{\partial^2}{\partial x^2} \left[EI(x) \frac{\partial^2 w(x, t)}{\partial x^2} \right] = p(x, t) \quad (2.2)$$

The deflection of the beam is given by $w(x, t)$, the first derivative of $w(x, t)$ over time is the velocity and the second derivative over time acceleration of the beam element. Furthermore, $\rho A(x)$ is the mass per unit length, and $EI(x)$ the bending stiffness per unit length. In this work the beams are considered to have a uniform cross-section over length and thus, all three parameters are independent of x and since no uniform dynamic load is applied along the beam is the external force equal to zero: $p(x, t) = 0$. This gives the following homogeneous differential equation of the fourth order for describing the free vibration of a beam:

$$\rho A \frac{\partial^2 w(x, t)}{\partial t^2} + EI \frac{\partial^4 w(x, t)}{\partial x^4} = 0 \quad (2.3)$$

In general, free vibration is assumed to be a synchronic harmonic motion and thus, it has a homogeneous solution. To solve this differential equation that is dependent on two variables one has to apply the method of separation of variables, and search for the solution of the differential problem through its space- and time-related components:

$$w(x, t) = W(x)\Psi(t) \quad (2.4)$$

Substituting equation 2.4 into the homogeneous equation of motion—and dividing by $W \cdot \Psi$ —gives:

$$\frac{1}{\Psi} \frac{\partial^2 \Psi}{\partial t^2} + a^2 \frac{1}{W} \frac{\partial^4 W}{\partial x^4} = 0 \quad \text{Where: } a^2 = \frac{EI}{\rho A} \quad (2.5)$$

Since the first term in equation 2.5 depends on time only, whereas the second term only on the x -coordinate, this equation can be satisfied if and only if these terms are equal to a separation constant ω^2 :

$$\begin{cases} \frac{1}{\Psi} \frac{\partial^2 \Psi}{\partial t^2} = -\omega^2 \\ a^2 \frac{1}{W} \frac{\partial^4 W}{\partial x^4} = \omega^2 \end{cases} \quad (2.6)$$

The general solution to the time-related part, i.e. $\frac{\partial^2 \Psi}{\partial t^2} = -\omega^2 \Psi$, reads:

$$\Psi(t) = A \sin(\omega t) + B \cos(\omega t) \quad (2.7)$$

The second equation describing the space-related part of the solution that is given by the set of equations 2.6 can be rewritten as:

$$\frac{\partial^4 W}{\partial x^4} - \frac{a^2}{\omega^2} \frac{1}{W} = 0 \quad (2.8)$$

The general solution of this equation can be written as:

$$W(x) = \sum_{n=1}^4 \tilde{C}_n e^{s_n x} \quad (2.9)$$

Substituting equation 2.8 into equation 2.8 provides the characteristic equation (equation 2.10). The solutions for s_n , i.e. the characteristic roots, are given in equation 2.11.

$$s_n^4 - \frac{\omega^2}{a^2} = 0 \quad (2.10)$$

$$s_1 = \beta, \quad s_2 = -\beta, \quad s_3 = i\beta, \quad s_4 = -i\beta \quad \text{Where: } \beta^4 = \omega^2 \frac{\rho A}{EI} \quad (2.11)$$

Substituting the characteristic exponents s_n into equation 2.9, we find the general solution to the differential problem:

$$\begin{aligned} W(x) &= \tilde{C}_1 e^{\beta x} + \tilde{C}_2 e^{-\beta x} + \tilde{C}_3 e^{i\beta x} + \tilde{C}_4 e^{-i\beta x} \\ &= C_1 \sin(\beta x) + C_2 \cos(\beta x) + C_3 \sinh(\beta x) + C_4 \cosh(\beta x) \end{aligned} \quad (2.12)$$

$C_1 \dots C_4$ are unknown constants that can be solved by substituting the harmonic form of displacement into the boundary conditions.

Boundary conditions

In reality a variety of beams are found each with their own specific boundary conditions. In table 2.1 the kinetic and dynamic relations for boundaries are given for left- and right-ends of beams. By solving the general solution (equation 2.12) for specific boundary conditions one obtains the solution for that case.

Further on in the work boundary conditions given in table 2.1 will be used to determine interface conditions that describe the relation between the left end of one field and the right end of another.

Table 2.1: Boundary conditions for a beam in bending [27]

	Left-end boundary ($x = x_l$)	Right-end boundary ($x = x_r$)	
Displacement	$W(x_l) = A$		$W(x_r) = B$
Slope	$\frac{\partial W(x_l)}{\partial x} = -\theta_A$		$\frac{\partial W(x_r)}{\partial x} = \theta_B$
Bending moment	$M = EI \frac{\partial^2 W(x_l)}{\partial x^2}$		$M = -EI \frac{\partial^2 W(x_r)}{\partial x^2}$
Shear force	$P = EI \frac{\partial^3 W(x_l)}{\partial x^3}$		$P = -EI \frac{\partial^3 W(x_r)}{\partial x^3}$
Rotational spring	$EI \frac{\partial^2 W(x_l)}{\partial x^2} = r \frac{\partial W(x_l)}{\partial x}$		$EI \frac{\partial^2 W(x_r)}{\partial x^2} = -r \frac{\partial W(x_r)}{\partial x}$
Translational spring	$EI \frac{\partial^3 W(x_l)}{\partial x^3} = -kW(x_l)$		$EI \frac{\partial^3 W(x_r)}{\partial x^3} = kW(x_r)$

2.3 SINGLE DEGREE OF FREEDOM SYSTEMS

Systems with just one degree of freedom are dynamic systems of its most elementary form and require only one coordinate to describe the systems position at any instant of time. Thus, they can be described with one equation of motion for that specific coordinate. SDOF in its purest form do not exist in reality, but in some cases do they approximate the behaviour closely. An advantage of these systems is its easy solvability and its easy incorporation of damping. Therefore, this theorem of SDOF systems will be used further on in this work for assessing the floor- and support configurations regarding vibrations.

The general solution to the equation of motion including damping (equation 2.1) consists out of a particular solution in which the system is subjected to harmonic loading, $w_p(t)$ and in a homogeneous part with no load involved, $w_h(t)$:

$$w(t) = w_p(t) + w_h(t) \quad (2.13)$$

For solving the problem, first the free vibration (i.e. homogeneous solution) of a SDOF system is considered, so the external force is set equal to zero like in previous section. The solution is searched in the form $u_h = e^{s_n t}$, where s_n can be both real and imaginary, substituted into the equation of motion and through the characteristic equation following eigenvalues are found:

$$s_{1,2} = \frac{-c \pm \sqrt{c^2 - 4km}}{2m} \quad (2.14)$$

The vibrations of an excited structure reduce over time (and eventually stop) due to dissipation of the introduced energy and the transfer of vibration by junctions to adherent structural elements. The damping of a system can be caused by internal friction of the material, external friction with other elements or an installed viscous damper. For a single beam the damping can easily be measured by reduction of the amplitude in time. However, within structural designs it is hard to predict the absorbing elements of the structure and especially the amount of energy that is dissipated.

Labonnote studied the damping of timber structures by testing 11 solid wood beams and 11 glulam beams made of Norway spruce using the impact test method. She concluded from the results that the material damping of timber beams is governed by shear deformation [24]. Since glulam has a higher shear modulus its damping was found to be 20 % higher than for the solid wood beams. Shear deformation depends largely on the cross-section of the beam, where its height especially contributes. Thus can be stated that higher damping values can be reached when one applies higher height-to-width ratios for the same cross-sectional area. Also was found that the damping ratio increases for higher modes, shorter spans and edgewise orientation of glulam compared to flatwise and the density had no influence on the amount of damping.

Another manner of energy dissipation is through dry friction, which occurs at the interface of two elements for example at the support or between the decking and joist. This form of damping is called Coulomb damping, and amount of damping is proportional with the inner area of the stress-strain relationship.

When the discriminant (under the square root) of equation 2.14 is negative, eigenvalues s_n are a complex number, and therefore resulting in decreasing oscillation. The critical damping is found when the discriminant is set equal to zero ($c_{cr} = 2\sqrt{km}$). For the level of damping is the damping ratio ζ introduced:

$$\zeta = \frac{c}{c_{cr}} \quad (2.15)$$

Equation 2.15 can be rewritten into:

$$c = 2\zeta\sqrt{km} = 2\zeta m\omega_n \quad (2.16)$$

The damping ratio distinguishes four different damping scenarios, where the first is the hypothetical case of an undamped system ($\zeta = 0$) with indefinitely continuing free vibrations which is shown in section 2.2. Second is the realistic case of underdamping ($\zeta < 1$) and applicable to most structures, like all floors studied in this work. Underdamped systems still oscillate around its rest position but the amplitude decays over time as energy is withdrawn from the structure. A system is called overdamped ($\zeta > 1$) if the displaced mass slowly returns to its rest position without oscillations and can in practice be found in e.g. door closers. The

last case is for $\zeta = 1$ and such systems are named critically damped since these return to its equilibrium without oscillations, similar to overdamped systems, however, they do so in the shortest possible time, which is desirable for many applications such as car suspensions. For now, the damping ratio is always smaller than one, i.e. an underdamped structure, which will be explained in section 4.2.3.

The principles of a single degree of freedom system will be demonstrated including viscous damping. First, the homogeneous solution will be determined for free vibrations, and thereafter, the particular solution representing forced vibrations is found. This will be done for the following equation of motion for a damping SDOF system:

$$\ddot{w}(t) + 2\zeta\omega_n\dot{w}(t) + \omega_n^2 w(t) = \frac{f(t)}{m} \quad (2.17)$$

Where: ζ Damping ratio, defined as $\zeta = \frac{c}{2\sqrt{km}}$

ω_n Angular natural frequency of vibration, defined as $\omega_n = (n\pi)^2 \sqrt{\frac{k}{m}} = 2\pi f_n$

$f(t)$ of equation 2.17 depends on the excitation source, which differs for the homogeneous and particular solution. As a consequence do both have another equation of motion as is shown in table 2.2, and therefore different solutions for $w(t)$ have to be substituted to solve to problem. For the homogeneous solution this procedure is elaborated in section 2.3.1, and section 2.3.2 provides the particular solution to the equation of motion.

Table 2.2: Difference between homogeneous- and particular solution

Solution	Excitation source	f(t)	Equation of motion
Homogeneous	Initial conditions	0	$\ddot{w}(t) + 2\zeta\omega_n\dot{w}(t) + \omega_n^2 w(t) = 0$
Particular	External force	$F_0 \sin(\Omega t)$	$\ddot{w}(t) + 2\zeta\omega_n\dot{w}(t) + \omega_n^2 w(t) = \frac{F_0}{m} \sin(\Omega t)$

2.3.1 Homogeneous solution for free vibrations

Free vibrations of SDOF systems are known as the resulting oscillation after an initial disturbance and the structure is left to vibrate on its own without external forces acting on the system. This disturbance can be a initial displacement caused by something or someone bringing the mass away from its equilibrium or an initial velocity resulting from an impact and giving the mass momentum.

In both cases the structure will start to vibrate in a pattern that is a summation of all the structures' modes, and therefore, no excitation force is applied to the system. The homogeneous solution of a harmonic motion is found for the differential problem given in equation 2.18.

$$\ddot{w}_h(t) + 2\zeta\omega_n\dot{w}_h(t) + \omega_n^2 w_h(t) = 0 \quad (2.18)$$

The homogeneous part of the solution for underdamped systems can be written as:

$$w_h(t) = e^{-\zeta\omega_1 t} [A \cos(\omega_D t) + B \sin(\omega_D t)] \quad (2.19)$$

Where the damped natural frequency is given by $\omega_D = \omega_1 \sqrt{1 - \zeta^2}$. The damping ratio of timber structures is generally low (1 to 6 percent) [8] and therefore, the damped natural frequency is about equal to the undamped ω_n . The constants A and B of the homogeneous part are determined by substituting equation 2.19 into the initial $w_h(0) = x_0$ and $\dot{w}_h(0) = v_0$ and resolving the so-obtained system of two algebraic equations:

$$A = x_0 \quad B = \frac{v_0}{\omega_1} + \zeta x_0$$

By substitution of these into the homogeneous solution given by equation 2.19 and rewriting the equation, one obtains the displacement-time curve of a SDOF system in free vibration:

$$w_h(t) = \sqrt{x_0^2 + \left(\frac{v_0}{\omega_1} + \zeta x_0\right)^2} \cdot e^{-\zeta\omega_1 t} \cos \left[\omega_1 t - \tan^{-1} \left(\frac{v_0 + \zeta\omega_1 x_0}{x_0\omega_1} \right) \right] \quad (2.20)$$

2.3.2 Particular solution for forced vibrations

If a system is subjected to an external force, the resulting vibration is known as a forced vibration. The external force is introduced into the equation of motion by $F(t)$ with an forcing frequency Ω and mean force F_0 , resulting in the following equation of motion:

$$\ddot{w}_p(t) + 2\zeta\omega_n\dot{w}_p(t) + \omega_n^2 w_p(t) = \frac{F_0}{m} \sin(\Omega t) \quad (2.21)$$

The response of a system to a harmonic force is also a harmonic one, and because of linearity and superposition, the shape of the response is a summation of eigenmodes of the system.

$$w_p(t) = W_{p,d} \sin(\Omega t - \phi) \quad (2.22)$$

$W_{p,d}$ is the amplitude of the particular solution and found by a multiplication of the static displacement and the amplitude response $H(\Omega)$, also known as the Dynamic Modification Factor (DMF). The phase response $\phi(\Omega)$ of the system to a forced harmonic load could be described as system's delay due to damping. Both the phase angle and DMF curves are displayed in figure 2.2 for Ω/ω_1 .

$$W_{p,d}(\omega) = w_s \cdot H(\Omega) = w_s \cdot \frac{1}{\sqrt{\left[1 - \left(\frac{\Omega}{\omega_n}\right)^2\right]^2 + \left[2\zeta\frac{\Omega}{\omega_n}\right]^2}} \quad \phi(\Omega) = \arctan\left(\frac{2\zeta\frac{\Omega}{\omega_n}}{1 - \left(\frac{\Omega}{\omega_n}\right)^2}\right) \quad (2.23)$$

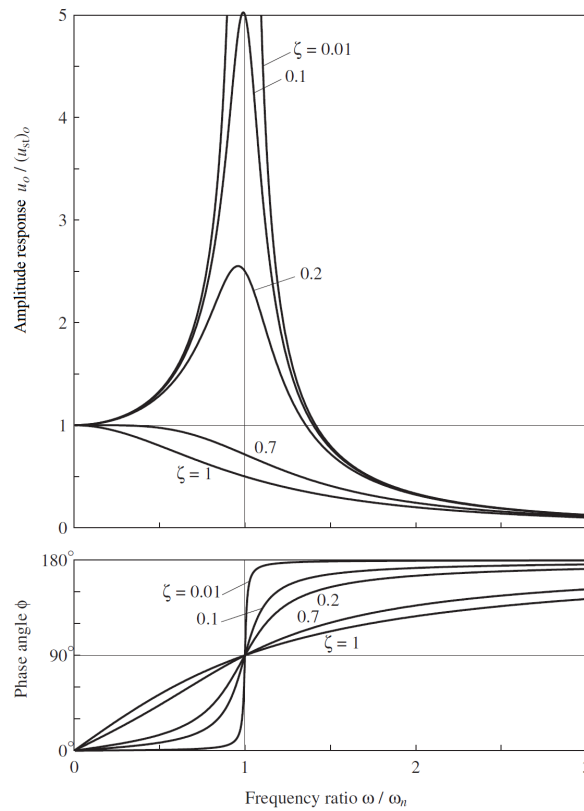


Figure 2.2: Amplitude response and phase angle for a damped SDOF system excited by a harmonic force [6]

Using the amplitude response $H(\Omega)$ and the phase response $\phi(\Omega)$, as defined in equation 2.23, one can find the frequency response function (FRF). It is a complex non-dimensional relationship between a system's input and its output:

$$G(\omega) = H(\Omega) e^{-i\phi(\Omega)} \quad (2.24)$$

Commonly used frequency response functions are compliance, mobility and acceleration that express displacement, velocity and acceleration over frequency respectively. All of these terms are mathematically related to each other and it is easy to move between these different functions by integrating or differentiating the FRF plot display [64].

2.3.3 Relation of SDOF with Multiple DOF systems

As already mentioned do SDOF systems rarely exist in reality since structures consist out of multiple elements with varying fundamental frequencies creating a multiple degree of freedom system (MDOF). These kind of systems can be analysed as well from SDOF perspective using superposition.

Starting point for finding the MDOF FRF is the uncoupled system resulting from modal analysis excited by a synchronous harmonic load. The frequency response $H_{u_i F_p}(\Omega)$ represents n^2 different frequency response functions and are often summarized in a matrix. Each frequency response function from this non-symmetrical matrix of a simple type, equal to a damped system with one degree of freedom.

$$H_{u_i F_p}(\Omega) = \frac{\hat{u}_i}{\hat{F}_p} = \frac{1}{\sqrt{(1 - (\Omega/\omega_i)^2)^2 + (2\xi_i \Omega/\omega_i)}} \frac{1}{\omega_i^2} \frac{\hat{x}_{pi}}{m_{ii}^*} \quad (2.25)$$

Subsequently this equation shows the behaviour of a certain degree of freedom under a specific loading. However, the vibration of a certain degree of freedom under all present loads is of interest. For this we can make use of the modal superposition and sum all the frequency response functions of $x_q(t)$ for the different dynamic loads. The FRF for the MDOF system is given by summing the DMF graphs [10], like is shown in figure 2.3.

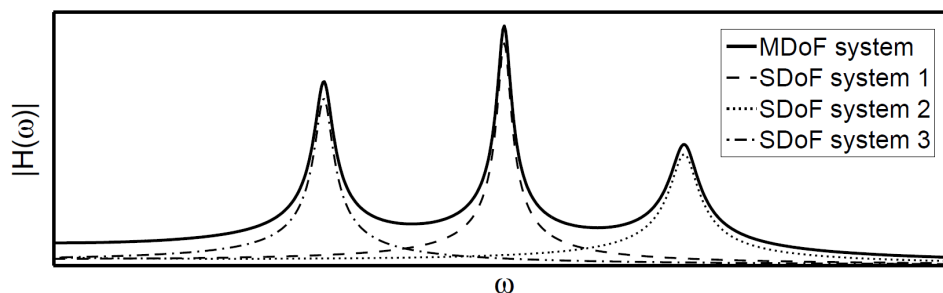


Figure 2.3: FRF magnitude for a damped MDOF system. The dashed lines illustrate the three uncoupled modal SDOF systems [10]

When a structure is subjected to a dynamic force with a frequency close to one of its fundamental frequencies, it can be seen in figure 2.3 that the amplitude can rise significantly. This phenomenon is that of resonance. In absence of any damping, the amplitude gradually increases towards infinity. In reality, however, there is always some damping present in structures (internal friction, friction at the joints) preventing these uncontrolled oscillations from occurring.

Especially resonance for the first few natural frequencies results in annoyance for inhabitants, since these modes contain almost all of the vibration energy of the system. Thus, it is wanted to have the fundamental frequency faraway from the loading frequency to prevent resonance of the system. Even if the loading frequency is far-off, a structure consisting out of multiple elements with natural frequencies close to each other could still result in excessively vibrations by different elements resonating one another. Therefore it is desirable to, for example, design a floor and its supporting beam such the fundamental frequencies of each are not interfering too much.

Fundamental frequency of plates

An example of a MDOF system which is especially relevant to this work is a plate, which has (at least) two degrees of freedom in both in-plane directions of the plate. Through the ratios of stiffnesses and size of both directions the magnitude of vibrations can be found, and since one direction influences the other is it known as a coupled system.

The natural frequencies $f_{m,n}$ of rectangular orthotropic plates of size $l \times b$ and simply supported along all four edges are given by the following equation:

$$f_{m,n} = \frac{\pi}{2l^2\sqrt{\rho}} \sqrt{D_x m^4 + 2D_{xy} m^2 n^2 \left(\frac{l}{b}\right)^2 + D_y n^4 \left(\frac{l}{b}\right)^4} \quad (2.26)$$

where m and n correspond with the mode in the x- and y-directions respectively, ρ is the mass density per square meter and D is the flexural plate stiffness in different directions, where $D_x > D_y$, and defined as:

$$D_x = \frac{E_x t^3}{12(1 - \nu_x \nu_y)}; \quad D_y = \frac{E_y t^3}{12(1 - \nu_x \nu_y)} \quad \text{and} \quad D_{xy} = D_x \nu_y \frac{1}{6} G t^3 \quad (2.27)$$

where E is the modulus of elasticity in their directions, G the shear modulus and ν_x and ν_y the Poisson ratio is x- and y- direction respectively. This equation was in 1988 simplified ($D_{xy} \approx D_y$) by Ohlsson [49] for calculating natural frequencies of first order modes to:

$$f_{1,n} = f_n = \frac{\pi}{2l^2} \sqrt{\frac{D_x}{\rho}} \sqrt{1 + \left[2n^2 \left(\frac{l}{b}\right)^2 + n^4 \left(\frac{l}{b}\right)^4 \right] \left(\frac{D_y}{D_x}\right)} \quad (2.28)$$

The equation shows that for lower degrees of isotropy, i.e. stiffness ratio D_y/D_x , the number of first order modes in the lower frequency spectrum increases, and thus become natural frequencies closer together. The same holds if the ratio of l over b is decreased that contributes to the power 4. Concluding, since it is beneficial to have less natural frequencies in the spectrum of interest, i.e. the lower excited range, the behaviour of a floor can significantly be improved by increasing the floor stiffness in transverse direction or reducing the width of the floor.

2.4 RESPONSE OF LIGHTWEIGHT FLOORS TO WALKING LOADS

The main source of dynamic excitation of floors in residential buildings is human activities, such as walking, running, dancing or jumping, of which walking is the most common, and therefore the one this thesis focusses on. Besides the activity, the force from a step also depends on the persons characteristics like walking style and body weight. The type of shoe, and the flexibility of its sole has, on the other hand, a negligible influence on the load functions [63].

2.4.1 Single step load curve

People have in general a walking frequency between 1,2 and 2,4 Hz, i.e. 1,2 to 2,4 steps per second. Though, during studies frequencies of 3,5 Hz have been observed. When people are walking in larger groups the spread is smaller and the frequency lies in the range 1,5–2,8 Hz.

In figure 2.4 are normalized load-time functions shown for different activities and walking speeds. The resulting contact force, as reaction of the floor to the uplifting force from the persons foot, on the floor are higher for more intense activities. Especially for activities characterised by a complete lift-off (running and jumping) the vertical ground force may rise to 2 to 3 times the body weight. These activities are characterised by a single load maximum, whereas walking induced vertical load shows by two load maxima.

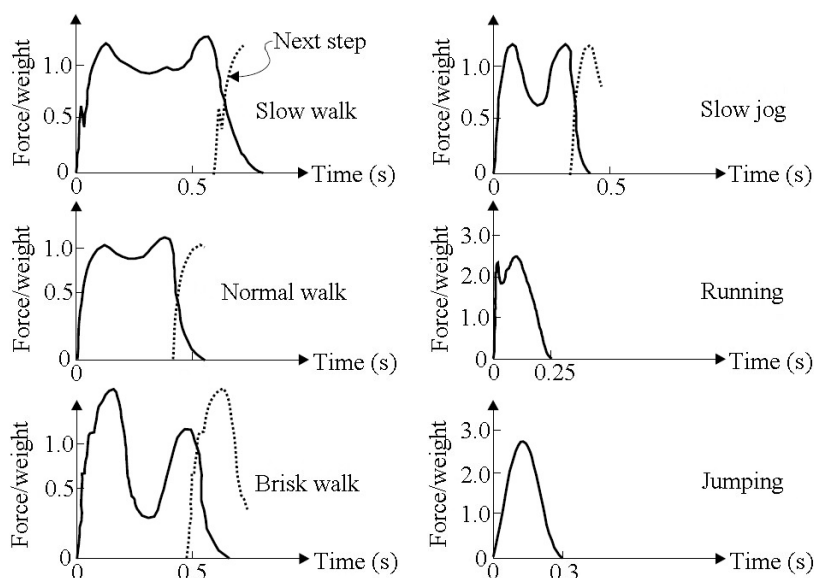


Figure 2.4: Load-time functions for different activities [71]

Polynomial function for the contact force due to a single footstep was first proposed by Sedlacek et al. [63], whom studied the load progression. They measured the load-time function for 5 persons walking along a 20m long walkway and fitted equation 2.29 upon the data. The K-coefficients are dependent on the step frequency and can be found in table 2.3.

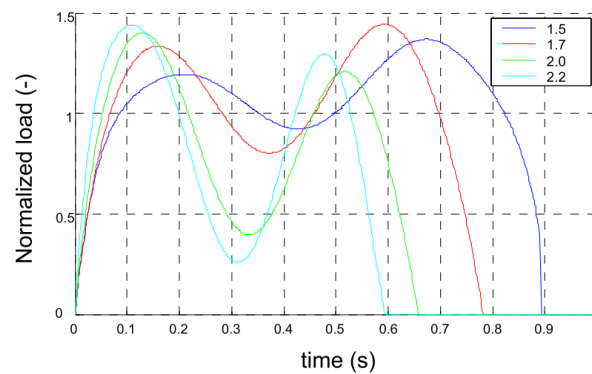
$$F_{1-step}(t, m_p, f_s) = m_p \sum_{n=1}^8 K_n(f_s) * t^n \quad (2.29)$$

Where: f_s Walking step frequency
 m_p Body weight

Body weight is a scalar within the force function, where the step frequency changes the shape of the function. Thus, an increasing weight only influences the amplitude of the human-induced vibrations linearly. However, when the step frequency approaches one of the natural frequencies the amplitude of the vibration changes as well as the proportion of each modal shape.

Table 2.3: K-values for different frequencies [63]

Coefficient	Step frequency ranges		
	$f_s \leq 1,75 \text{ Hz}$	$1,75 < f_s \leq 2 \text{ Hz}$	$f_s \geq 2 \text{ Hz}$
K_1	$-8f_s + 38$	$24f_s - 18$	$75f_s - 120$
K_2	$376f_s - 844$	$-404f_s + 521$	$-1720f_s + 3153$
K_3	$-2804f_s + 6025$	$4224f_s - 6274$	$17055f_s - 31936$
K_4	$6308f_s - 16573$	$-29144f_s + 45468$	$-94265f_s + 175710$
K_5	$1732f_s + 13619$	$109976f_s - 175808$	$298940f_s - 553736$
K_6	$-24648f_s + 16045$	$-217424f_s + 353403$	$-529390f_s + 977335$
K_7	$31836f_s + 33614$	$212776f_s - 350259$	$481665f_s - 888037$
K_8	$-12948f_s + 15532$	$-81572f_s + 135624$	$-174265f_s + 321008$

**Figure 2.5:** Step load normalized to body weight for four different step frequencies

The body moves slightly up and down when one goes from one step to the next, ultimately moving the body forward. First, gravity attracts a body downwards, the body mass accelerates in the same direction and the resulting inertia force is applied as contact force on the floor. This is recognized as the first peak in figure 2.5. Once the vertical velocity of the person is zero (through between the peaks), the body is accelerated upwards to enable the next step, which applies another contact force at the floor (second peak). This phenomenon can be distinguished in the load-time functions by the two peaks whom become more clear for more intense activities (i.e. higher step frequencies).

Series of footfalls

In reality the imposed load on a floor does not consist out of just one footstep. Its a sequence of multiple single footfall load curves each shifted by the time interval $\Delta t = 1/f_s$ (see figure 2.6a, $\Delta t \approx 0.6$ s). This series of loads is summed to get the resulting load, where the overlapping single step loads are causing peaks for the periods in time both feet are in contact with the ground. The magnitude of these peaks is about twice the persons weight, as one can see in figure 2.6b. Besides, it has a strongly harmonic shape oscillating around ± 1.3 times the body weight.

The first 4 harmonics have a significant impact and contain enough energy to bring the structure in excitation, so for a walking pace of 2,5 Hz the excitation frequency can be up to 10 Hz. To make an distinction between high- (HFF) and low-frequency floors (LFF), Sedlacek et al. proposed to use a cut-off frequency of 10 Hz [63]. The threshold frequency varies significantly for different authors and design guidelines, as shown in table 2.4, which endorses the complexity of making a distinction between low- and high-frequency floors.

This grey area where to split for LFF and HFF has its origin in the transition from resonant response (see figure 2.7) into a transient one (figure 2.10). Reflecting on the previous section about SDOF system does this response distinction relate to the particular and homogeneous solution, which are summed to obtain the general solution given by equation 2.13. For the fundamental frequency of the floor going upwards the response shifts from steady-stated dominated into a transient dominated response.

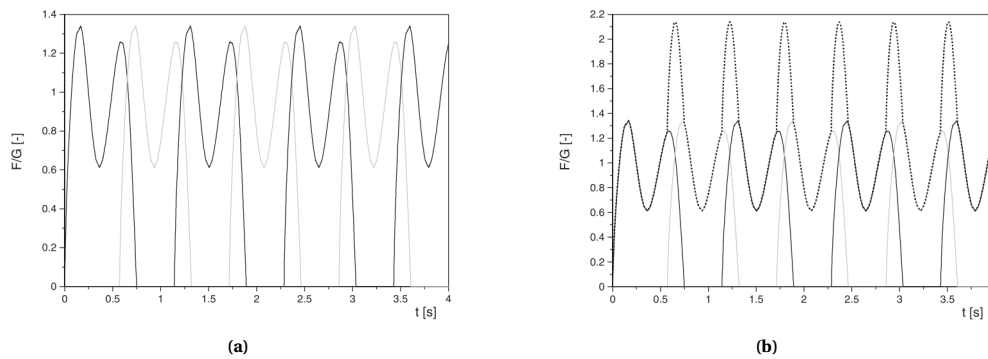


Figure 2.6: Series of footfall forces applied by (a) both feet of a walking person and (b) the resulting force on the floor (dashed line) [63]

Table 2.4: Cut-off frequencies for residential purpose adopted by different authors and guidelines

Author(s)	Material	Year	Cut-off frequency
Ohlsson [50]	General	1988	8 Hz
Wyatt and Dier [74]	Steel	1989	7 Hz
Allen and Murray [2]	General	1993	9 Hz
The concrete society [52]	Concrete	2001	10 Hz
Sedlacek et al. [63]	Steel	2006	10 Hz
The concrete centre [72]	Concrete	2006	10 Hz
The Steel Construction Institute P354 [65]	Steel	2009	8 Hz
Americal institute of steel [31]	Steel	2016	9 Hz

2.4.2 Resonant response of low-frequency floors

Floors with low natural frequencies responds strongly to the walking load harmonics causing a steady-state response, like is shown in figure 2.7. These type of vibrations are analysed from load perspective by looking for its response to each load frequency, i.e. for each harmonic. For excitation from walking activities, this kind of response occurs for floors with a fundamental natural frequency less than 9-10 Hz [8, 65], where the relative contribution of higher harmonics increases since its frequency approaches the natural frequency. Magnitude of these higher harmonics is, however, significantly less than the lower ones, which is expressed by the Dynamic Load Factor.

Dynamic load factors

The walking load $f(t)$ given by equation 2.29 is strongly harmonic and thus, very appropriate for Fourier analysis. Any periodic loading can be represented as the sum of a series of simple harmonic components and the response of a linear structural system will occur at these same frequencies [30]. Jacobs et al. [18] were in 1972 the first ones proposing, in the biomechanics field of study, to represent the walking force function by Fourier series. This method was later on adopted for application in civil engineering to footbridges and widely accepted and known under the name *Dynamic forcing function*. Equation 2.30 consists of two part; a

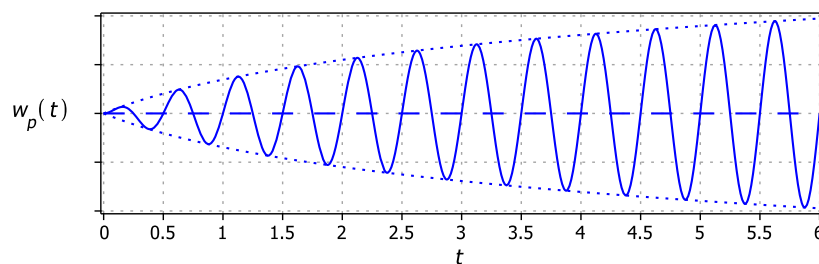


Figure 2.7: Resonant response for $f_s = 2$ Hz

Table 2.5: Design parameters for walking forces due to one person [17, 54]

Harmonic number, n	Rainer et al. (1988)		ISO 10137:2007	
	Frequency range, nf [Hz]	Dynamic Load Factor, α_n [-]	Frequency range, nf [Hz]	Dynamic Load Factor, α_n [-]
1	1,6 to 2,2	0,5	1,2 to 2,4	$0,37 f_s - 0,37$
2	3,2 to 4,4	0,2	2,4 to 4,8	0,1
3	4,8 to 6,6	0,1	3,6 to 7,2	0,06

static part representing the dead weight of the person and a dynamic time-varying part related to the dynamic behaviour:

$$F(t)/G = \underbrace{\frac{1}{2}\alpha_0}_{\text{Static}} + \underbrace{\sum_{n=1}^N [\alpha_n \sin(2\pi n f_s t - \varphi_n)]}_{\text{Dynamic}} \quad (2.30)$$

For each n^{th} harmonic, the length of the cycle is equal to T/n , where T is given by $1/f_s$ and thus, the amount of cycles in one period is equal n . φ_n describes the phase lag and α_n are Fourier coefficients giving weight of each harmonic (also known as the Dynamic Load Factor - DLF), which are found by integration over the interval T :

$$\alpha_n = \frac{2}{T} \int_T f(t) \cos\left(\frac{2\pi n t}{T}\right) dt$$

The first research into the DLF was performed by Rainer et al. in 1988 (table 2.5), and they found the DLF for the first harmonic to be constant by picking the average over the range [54]. However, following studies [17, 63, 72, 80] found it to be linear with respect to the frequency resulting in a higher α_1 for higher walking paces.

The standard for verification of serviceability of buildings against vibrations, ISO 10137:2007, prescribes numerical coefficients for DLF as well and are presented in table 2.5. The values given by the International Organization of Standardisation are significantly lower than the ones found in other studies by Wilford et al. and Sedlacek et al., and might therefore underestimate the amplitude of a walking force.

Sedlacek et al. transformed the graph with series of polynomial footfall forces, as shown in figure 2.6b, into its spectral density function using Fast Fourier Transform (FFT). For each pace frequency the Fourier coefficients a_n are determined by taking the peak values and appending phase angles. These are used for the finding the necessary number of harmonics to represent the load curve adequately according to formula 2.30. Sedlacek et al. conclude from these results that it is sufficiently accurate to consider only the Fourier-coefficients of the first three harmonics (α_1 , α_2 and α_3) to match the dynamic walking behaviour. The relations between walking pace and the DLF of harmonics are given in figure 2.8.

Extensive research into several studies regarding the Dynamic Load Factor has been performed by Wilford and Young [72]. They combined the literature of Kerr, Galbraith and Barton, Wheeler, Ohlsson, Rainer and Ellis into a scatter plot (figure 2.9) and fitted mean and design values (i.e. 25% chance of exceedance, see table 2.6) for the DLFs. Their study and others indicate to use the first four harmonics for appropriate representation of a walking load [72, 75].

Since these combine multiple studies such a large test group is acquired, will the design value functions for Dynamic Load Factors by Wilford and Young be used in this work. Besides, there is no consensus for the necessary number of harmonics to accurately represent the walking load, and therefore choosing to use the first four harmonics being on the conservative side.

By decomposing the walking load into harmonics the steady-state response of a low-frequency floor can be analysed. The total response is found by superposition of the responses to each harmonic, where the magnitude of the harmonic depends on the Dynamic Load Factor.

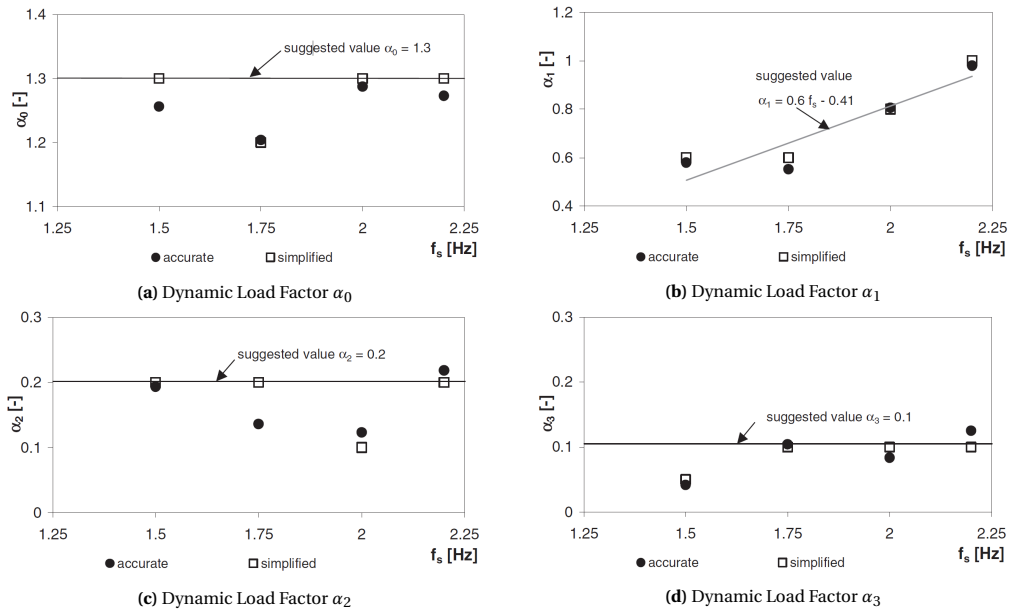


Figure 2.8: Dynamic Load Factors dependent on the walking frequency [63]

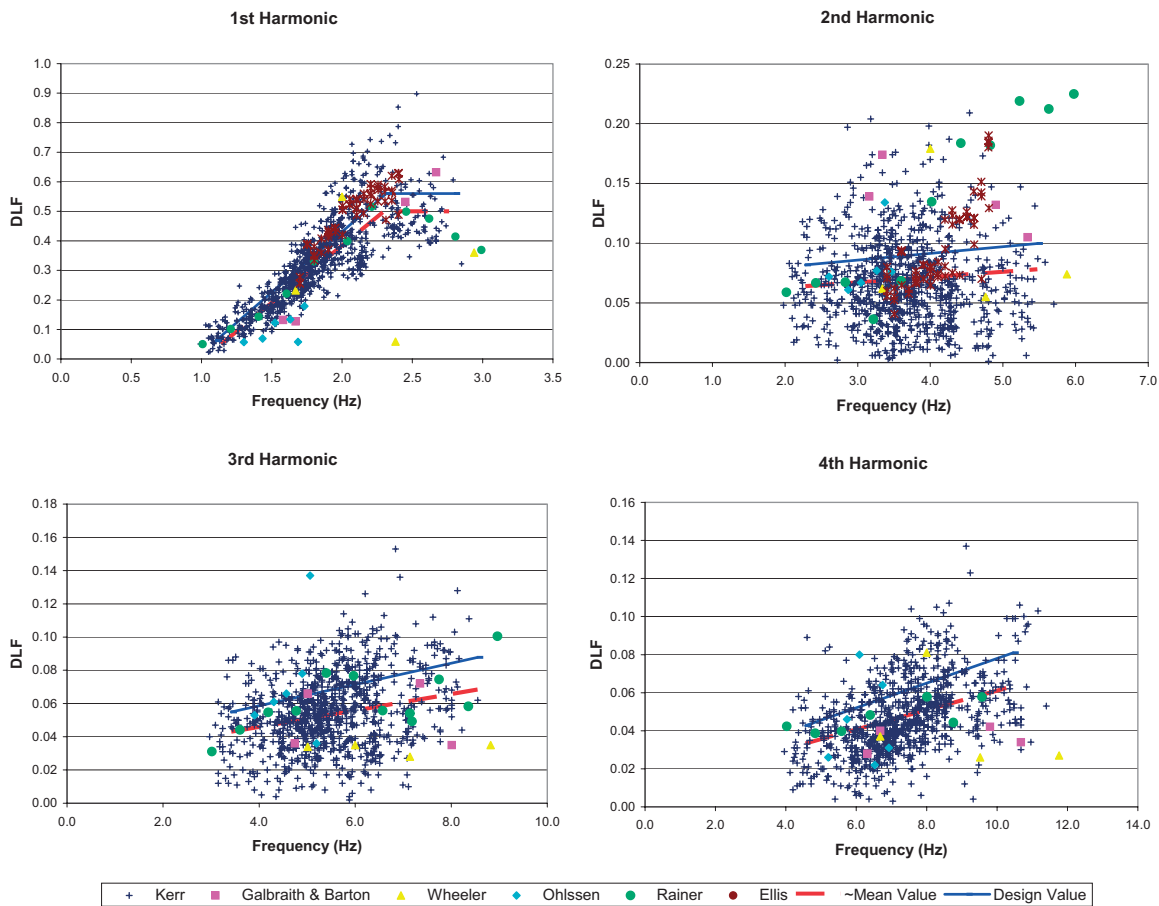


Figure 2.9: Scatter plot of multiple studies for DLFs combined by Wilford et al. [72]

Table 2.6: Mean and design values of footfall harmonics [72]

Harmonic number, n	Frequency range, nf [Hz]	Mean value DLF [-]	CoV	Design value DLF, α_n [-]
1	1,0–2,8	$0,37f_s - 0,35$	0,17	$0,41f_s - 0,390$
2	2,0–5,6	$0,0044 \cdot 2f_s + 0,054$	0,40	$0,0056 \cdot 2f_s + 0,069$
3	3,0–8,4	$0,0050 \cdot 3f_s + 0,026$	0,40	$0,0064 \cdot 3f_s + 0,033$
4	4,0–11,2	$0,0051 \cdot 4f_s + 0,010$	0,40	$0,0065 \cdot 4f_s + 0,013$

Resonant build-up

As one can observe from figure 2.7 does the structure not resonate fully from the start of loading (i.e. walking). It takes a number of loading cycles to built up resonance, which may not be reached because the required number of steps cannot be taken within the spanning length of the floor. In practice, by the time the required numbers of steps have been taken the pedestrian may have moved off the structure completely, or at least he or she is likely to have moved away from the maximum point on the mode shape.

Therefore the term ρ is introduced, which is the resonant build-up factor accounting for the fact that there may be an insufficient number of loading cycles for steady-state response to occur.

$$\rho = 1 - e^{-2\pi f_1 \zeta T_w} \quad (2.31)$$

Where T_w is the walking duration in seconds defined as the longer of the floor's plan dimensions L over the walking velocity ($T_w = L/V$). The latter is in m/s and given by:

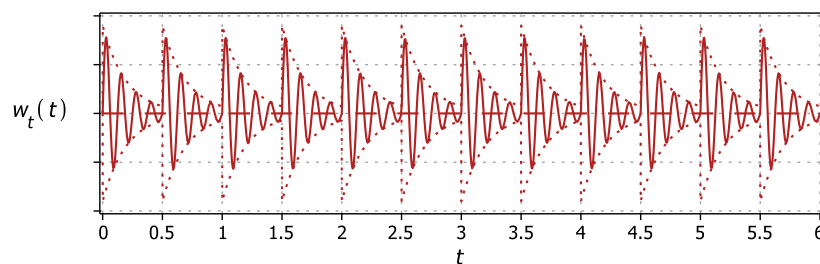
$$V = 1.67f_s^2 - 4.83f_s + 4.5 \quad (2.32)$$

For an open plan building, or when the dimensions still are unknown, the factor ρ can conservatively taken as 1,0.

2.4.3 Transient response of high-frequency floors

When the fundamental frequency of the floor is high compared to the forcing frequencies, the steady-state part will be insignificant to the transient response. The floor responds to the excitation as if it is a series of impulses, with the vibration due to one foot step dying away—in case there is sufficient damping available—before the next step impulse. This effect is caused by the impulses setting the mass of the floor in motion, which will vibrate at its natural frequency and decaying rapidly as energy is dispersed over the floor as a whole; this response is shown in figure 2.10 [8, 65]. This makes that, for high-frequency floors, only the transient response has to be considered [19].

For transient responses walking load shape does not influence the behaviour since these forces are modelled as impulses. The mathematical model of a unit impulse is an infinite force over an infinitesimal time, with the multiple of force and time equal to 1. This is not physically correct, but represent reality quite accurately making impulses a useful tool in vibration analysis.

**Figure 2.10:** Transient response for $f_s = 2$ Hz

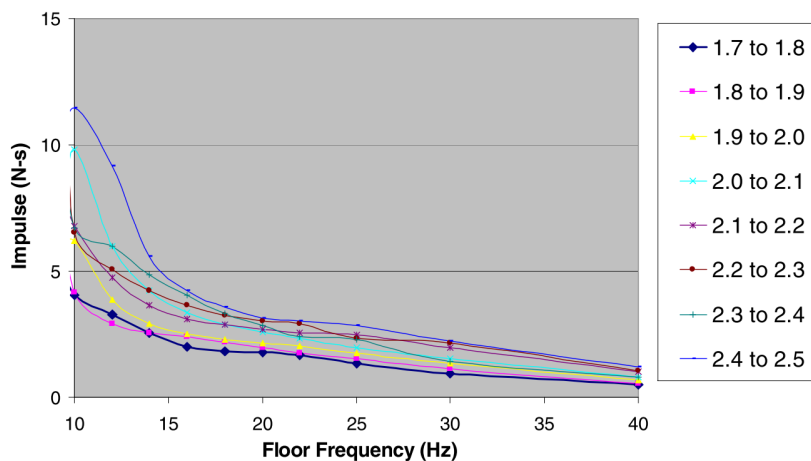


Figure 2.11: Effective impulse for varying walking paces (after Young [75])

Young developed a formula to determine the effective impulse using the footfall traces from experiments by Kerr [75]. The initial velocity of a floor mode excited by an impulsive action is found by dividing the impulse value by the modal mass, and therefore, the initial velocity being equal to the applied impulse for a modal mass of 1 kg. This provides a method for determining the 'effective impulse' as Young has proposed.

He analysed the 880 continuous walking force-time histories recorded for 40 individuals stepping on a force plate from Kerr's experiment by calculating the velocity response in the time domain for different natural frequencies (each having a modal mass of 1.0), and extracting the peak velocities of the vibration. The latter are the numerical values of the effective impulse of that footfall, of which the mean values of different walking paces are plotted separately for varying floor frequencies (see figure 2.11). From this graph can be concluded that the effective impulse reduces for increasing floor fundamental frequency and decreasing walking pace, both intuitively being correct.

For design purposes a formula for calculation of the effective impulse is proposed by Young, having a 25% chance of exceedance (like the design value DLFs proposed by Wilford and Young in table 2.6) with a coefficient of variation of 0,4. The effective impulse depends on the ratio of the walking pace f_p and natural frequency of the floor f_n :

$$I_{eff,mean} = 42 \frac{f_p^{1,43}}{f_n^{1,3}} \quad (2.33a)$$

$$I_{eff,design} = 54 \frac{f_p^{1,43}}{f_n^{1,3}} \quad (2.33b)$$

Mohammed et al. [29] propose an improved modelling procedure based on the effective impulse method. Contrary to the model by Young they consider the damping effect, to incorporate the slight amplification of HFF induced by near-resonance response of higher harmonics. This effect has, according to their paper, a minor effect on the impulse value. The complexity of their proposed method does not outweigh increased accuracy, and therefore equation 2.33b will be used in this work to determine the transient responses of high-frequency floors.

2.5 HUMAN PERCEPTION OF MOTION

Extensive research in the area of human perception of whole-body vibration, and human response to such vibration have been carried out and found to be a hard to predict, complex subject. The way people perceiving vibrations react depends on their position (e.g. moving, sitting, sleeping), their activity (e.g. reading, working), their health, their mindset, their gender, their expectations, awareness and eventually even their emotional state [23]. These physiological factors interfere with physical characteristics of structural vibration - i.e. fear of building collapse, perceived source of vibration and the persons attitude to the source -, which together determines the level of disturbance people experience [51]. The response to vibrations depends on a large number of variables making predictions of responses of individuals difficult and not likely to be highly accurate. Besides, the perception of vibrations is also highly subjective since there is variability between responses of different individuals (inter-subject variability) and the response of an individual on different occasions varies as well [34].

The annoyance humans perceive from vibrations has been found to be dependent on the relative control a subject has over the source. Therefore, Ohlsson [49] suggests to distinguish three different cases. The first one is the self-induced vibration of a floor, and since the annoyed person has full control over the source of vibration (i.e. himself or herself) is this type of vibration commonly accepted. In 1989, Whyatt [73] pointed out that the nervous system of humans is capable of associating the accelerations with its own walking activity that is in progress, and simply disregards the vibrations. Secondly, when vibrations are caused by another subject, the control onto the source of vibrations is reduced. Though, for situations with both subjects in the same room, dialog is likely, and therefore it is possible to ask the other to stop. Thus, if one has control over the source of vibrations the level of acceptance is relatively high. The situation of neighbour-induced vibration is the last case distinguished by Ohlsson. Since one has almost no influence on the source because no contact is possible, the annoyance is substantially increased. This differentiation with the previous case is backed by Toratti and Talja [66].

2.5.1 Frequency weighting

The manner in which vibration affects health, comfort, perception and motion sickness is dependent on the vibration frequency content. The human body cannot observe very high frequency vibrations, so frequency-dependent weighting factors are developed to correct vibration verification for this measure.

An often applied weighting function is given in ISO 2631-2 as the *Pure frequency weighting*, which is used in the DIN 4150 and SBR guidelines [63] and in many studies [10, 23, 76]. For the weighting of a velocity spectrum it has to be multiplied with equation 2.34 and when one is dealing with acceleration spectra equation 2.35 should be used. Both equations hold an assessment of annoying vibrations by means of two vibration quantities, where the reference frequency $f_0 = 5,6$ Hz and the reference velocity v_0 is equal to 1,0 mm/s. Equations 2.34 and 2.35 are dimensionless because of division by the reference frequency and velocity. Both equations are visualised in figure 2.12 from which can be concluded that humans observe in the lower frequency regions especially accelerations, and for higher frequencies it is the velocity that results in annoyance. Figure 2.12 also shows the perception walking load harmonics, where humans feel the first harmonic most strongly in terms of acceleration and harmonic 4 annoys people most in velocity perspective.

$$H_{W,v}(f) = \frac{1}{v_0} \frac{1}{\sqrt{1 + (f_0/f)^2}} \quad (2.34)$$

$$H_{W,a}(f) = \frac{1}{v_0} \frac{1}{\sqrt{1 + (f/f_0)^2}} \quad (2.35)$$

Another manner for frequency weighting is by application of base curve C1 provided in ISO 10137 [17]. Figure 2.13 gives the vibration criteria for sensitive equipment, but is often interpreted as the level that is just perceptible by humans. The comfort criteria in revised Eurocode 5 is based on this curve through the response factor R (see section 3.3), where the base curve represents $R = 1$ and the value of R from assessment should be classified as R times more perceptible than feeling boundary.

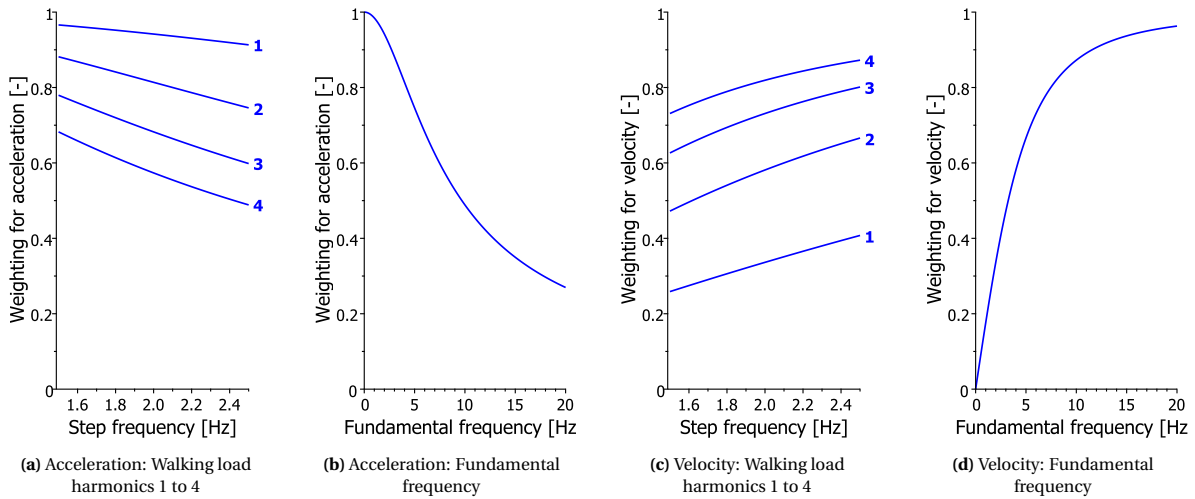


Figure 2.12: Weighting values for human perception

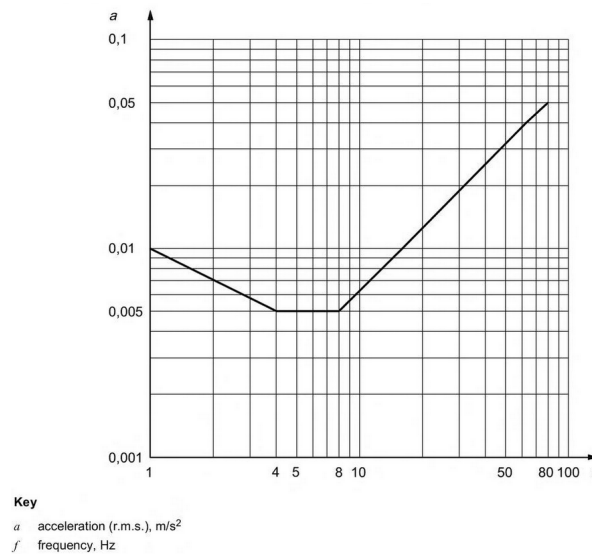


Figure 2.13: ISO 10137 [17]

2.5.2 Vibration assessment methods

The predicted response of a structure is checked with the established acceptance criteria for adequate level of human comfort. Current design guidelines do quantify vibrations in terms of peak acceleration, root-mean-square values for acceleration or velocity, vibration dose value and maximum transient vibration value.

Peak acceleration values

In North American countries and Australia is the AISC/CISC DG11 widely used, which suggests peak acceleration limits for assessment of vibrations. These thresholds are indicated as a percentage of the standard acceleration due to gravity, g , and relate to different environments in line with the base curve recommended by the International Standard Organisation in ISO 10137.

Root-mean-square (r.m.s.)

Vibration is by definition a movement that oscillates about its equilibrium position and therefore, the mean value of a vibration signal will always be zero if measured for an infinite duration, since all positive values will cancel out all negative values. The mean will not signify the magnitude of the signal, which is solved for r.m.s. values by squaring every values, taking the mean of it, and finally taking the square root of this mean value. If

the mean is equal to zero, the root-mean-square value is analogous to standard deviation in statistics [26]. In mathematical terms the root-mean-square for both acceleration and velocity is given by:

$$a_{rms} = \sqrt{\frac{1}{T} \int_0^T a^2(t) dt} \quad (2.36)$$

$$v_{rms} = \sqrt{\frac{1}{T} \int_0^T v^2(t) dt} \quad (2.37)$$

One-Step-RMS-value (OS-RMS₉₀)

This method takes human perception of vibrations and stochastic demographic distribution of walking frequency and body mass into account through the unitless OS-RMS₉₀ value. The latter is defined as the 'One-Step-RMS-value of the velocity for a significant single step covering the intensity of 90% of people's walking steps' [8]. Assessment according this method could be done using design charts or by a transfer function, which can be obtained from finite element analysis and is more accurate. The charts are developed by Waarts [67] and later on implemented by HiVoSS [59] and in the JRC-report for the European commission [8]. When the fundamental frequency, modal mass and damping ratio of a floor is known, the OS-RMS₉₀ value is read from the graph for the specific ζ , which are shown in figure 2.14.

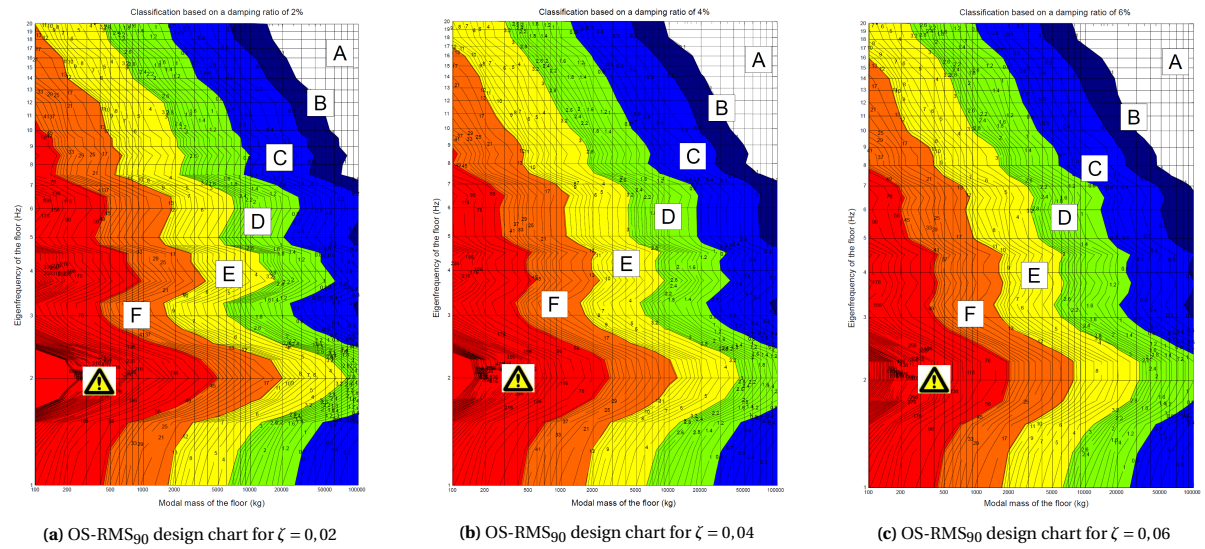


Figure 2.14: OS-RMS₉₀ design charts for three modal damping values [8]

Vibration dose value (VDV)

The r.m.s. method is defined as basic method in ISO 2631-1 but it notes that sometimes additional assessment methods are required, like the vibration dose value and maximum transient vibration value. It is more sensitive to peaks compared to the root-mean-square method for acceleration and it takes the duration effects of the vibration into account.

$$VDV = \left[\int_{t_1}^{t_2} [a_w(t)]^4 dt \right]^{\frac{1}{4}} \quad (2.38)$$

Footfall induced vibration is never of constant amplitude and continuous, which affect people's acceptance of vibration. The Vibration Dose Value is a measure of vibration over a longer period of time that accounts for these factors [72].

Maximum transient vibration value (MTVV)

As mentioned before is the maximum transient vibration value an additional assessment method named in ISO 2631-1. It averages acceleration values as well but its short integration time constant ($\tau = 1$ s is recommended) makes it more sensitive to occasional shocks and transient vibration.

Table 2.7: Criteria for acceptable ranges of velocity (mm/s) adopted by different guidelines [63]

	Residential		Office		Critical working area	
	day	night	day	night	day	night
ISO 2631-2	0,2–0,4	0,14	0,4	0,4	0,1	0,1
DIN 4150-2	0,15–3,0	0,1–0,2	0,4–6,0	0,3–0,6	0,1–3,0	0,1–0,15
SBR	0,2–0,8	0,2–0,4	0,3–1,2	0,3–1,2	0,1	0,1
Dutch practice	0,4	0,4	0,8	0,8	-	-
SCI	0,2–0,4	0,14	0,4	0,4	0,1	0,1
NS 8176	0,1–0,6	0,1–0,6	-	-	-	-

$$a_w(t_0) = \sqrt{\frac{1}{\tau} \int_{t_0-\tau}^{t_0} a_w^2(t) dt} \quad (2.39)$$

$$\text{MTVV} = \max[a_w(t_0)]$$

Crest factor

The crest factor is defined in ISO 2631-2 as "the modulus of the ratio of the maximum instantaneous peak value of the frequency-weighted acceleration signal to its r.m.s. value". It is an useful measure to distinguish whether the response is of a steady-state character, impulsive or a combination of both. Some standards use this value to choose the method of assessment. For example, the Australian standard recommend the r.m.s. method for a crest factor below 6, for a crest factor above 9 only the VDV method should be considered and between 6 and 9 both r.m.s. and VDV are prescribed. In the ISO standard the r.m.s. method is recommended for a crest factor below 9 while above 9 the r.m.s. should be considered plus VDV or MTVV. In the latter case can the discomfort significantly be influenced by peak values and using r.m.s. averaging would lead to underestimation.

$$\text{Crest factor} = \frac{\text{Peak acceleration}}{\text{r.m.s. acceleration}} \quad (2.40)$$

Comfort criteria

Sedlacek et al. have summarized the floor vibration criteria of several guidelines. Although both r.m.s.-values and effective values were given comparisons can be made under the assumption the r.m.s.-value is taken over a small time interval ($T < 1$ s), which is the case when a one-step peak is observed. Furthermore are all criteria mentioned in table 2.7 accompanied by a frequency weighting method [63].

Toratti and Talja researched the relation between both body feeling and sense of perception (hearing and visual) of vibrating objects as well in that study [66]. Besides questioning the subject for perceptibility of vibrations, various objects were imposed by the same vibration, like a coffee cup on a saucer with a spoon inside and a 30 cm high plant. The questionnaire for participants resulted in five vibration classes as given in table 2.8. These classes relate to design limits (table 2.9) which will be compared with the proposed classes for the revised Eurocode 5.

Table 2.8: Vibration classes proposed by Toratti and Talja [66]

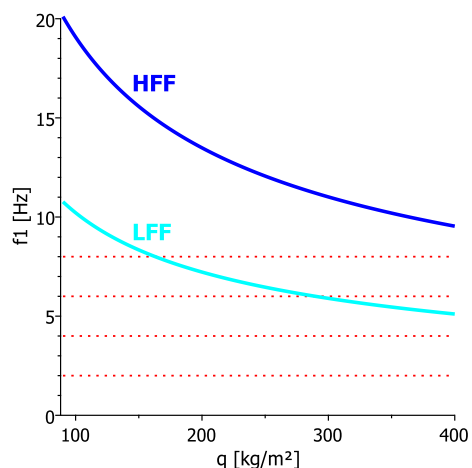
A	Special class for vibrations inside one apartment. Normal class for vibrations transferred from another apartment. The vibration is usually imperceptible.
B	Higher class for vibrations inside one apartment. Lower class for vibrations transferred from another apartment. The vibration may be perceptible but usually it is not annoying (inside one apartment).
C (base class)	Normal class for vibrations inside one apartment. The vibration is often perceptible and some people may feel it annoying (inside one apartment).
D	Lower class for vibrations inside one apartment, e.g. attics and holiday cottages. The vibration is perceptible and most people feel it annoying (inside one apartment).
E	Class without restrictions.

Table 2.9: Design limits for vibration classes [66]

Class	Dynamic vibration values				Static deflection values	
	$f_{1,1} < 10$ Hz	$f_{1,1} > 10$ Hz			Floor plate	
	$a_{w,rms}$ [mm/s ²]	v_{max} [mm/s]	v_{rms} [mm/s]	u_{max} [mm]	δ [mm/kN]	δ_1 [mm/kN]
A	≤ 30	≤ 4	$\leq 0,3$	$\leq 0,05$	$\leq 0,12$	$\leq 0,12$
B	≤ 50	≤ 6	$\leq 0,6$	$\leq 0,1$	$\leq 0,25$	$\leq 0,25$
C	≤ 75	≤ 8	$\leq 1,0$	$\leq 0,2$	$\leq 0,5$	$\leq 0,5$
D	≤ 120	≤ 10	$\leq 1,5$	$\leq 0,4$	$\leq 1,0$	$\leq 1,0$
E	> 120	> 10	$> 1,5$	$> 0,4$	$> 1,0$	$> 1,0$

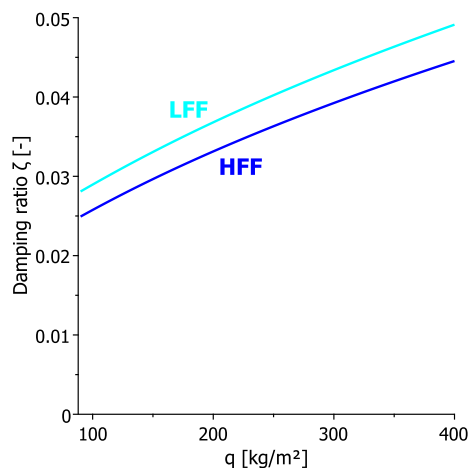
2.6 MAIN PARAMETERS AND VIBRATION COMFORT

Regarding vibrations there are three variables where the level of vibration majorly depends on: flexural stiffness, mass and damping ratio. Since this thesis studies the application of timber structures in situations where the construction has to be as light as possible, the relation of mass to the natural frequency and damping is elaborated first for LFF and HFF. Thereafter, the effects of varying flexural stiffness, distributed mass and damping ratio to the steady-state and transient response is demonstrated.



One of the main parameters determining the comfort level is the floor its natural frequency. In line with above conclusions do HFF have a higher fundamental frequency compared to LFF, which declines for both LFF and HFF with increasing floor mass. The red dotted lines in beside shown figure represent the walking load harmonics. Resonance occurs in the structure if its natural frequency corresponds with one of the harmonics, which explains the distinction between both floor types. LFF are floors which an eigenfrequency below 8 Hz, where HFF have one above that level. Therefore, vibrations of the first type are steady-state dominated and the latter show a transient response. CLT floor in this example can be categorized as LFF if the self-weight is higher than about 160 kg/m².

Another main parameter that is affected by the floor its mass is the level of damping. As already mentioned, is it hard to determine the damping ratio, which depends on many in-situ and connection aspects. This example attempts to describe the relation between mass and level of damping using Rayleigh damping, which estimates the contribution of both mass and stiffness to modal damping of the structure by factor α and β . The values of these factors are found by solving the system of equations describing damping ratios at natural frequency. From the graph shown at the left can be concluded that the damping ratio is slightly higher for low-frequency floors than HFF for an equal mass. This can be explained from the higher transverse stiffness of CLT panels, and therefore, more fibers causing internal friction which increases the level of damping.



Increasing the mass of a structure affects the vibration comfort in two ways. First, the natural frequency decreases which could result in resonance of CLT panel floors (i.e. LFF) besides its transient vibration. High-frequency floors have an eigenfrequency that is high enough to prevent resonance, and therefore depend their response on a free vibration only. Secondly, the damping relies upon the mass as well and rises for increasing mass since energy is dissipated from the system by mass changing direction.

Larger mass improves the damping of a structure, but contrary decreases its natural frequency, which could lead to resonance and cancels out the benefit of increased damping. Once resonance occurs in a structure, increased damping hardly improves the level of comfort as equation 2.23 shows. This Dynamic Modification Factor simplifies to $1/(2\zeta)$ in case the forcing frequency is about equal to the natural frequency (i.e. resonance). This means the amplitude of a floor with $\zeta = 0.05$ (i.e. LFF of 400 kg/m²) decreases to 60% of one with $\zeta = 0.03$ ($q = 100$ kg/m²). However, a CLT floor of 100 kg/m² has an eigenfrequency around 10 Hz, and therefore not resonating with the walking load harmonics. Very heavy CLT floors ($q > 300$ kg/m²) show higher levels of energy dissipation, but also respond more strongly to the 3th harmonic, which is even more powerfully present in walking loads.

2.6.1 Steady-state and transient response

The above described effects upon the vibration comfort follows from the combination of steady-state and transient response. Therefore, the manner these two responses are affected by changing the main parameters – stiffness, mass and damping – is necessary to understand how vibrations can be reduced.

A 5-layer CLT-panel with a thickness of 175mm, distributed mass of 150 kg/m², and a damping ratio of $\zeta = 0.04$ is used for this fictive study. For every main parameter, the values are varied where the other properties are kept equal. There are no values given for the displacement on the y-axis, but the scale is similar for all graphs, since the walking frequency distribution has to be incorporated for realistic results. The purpose of the graphs is to illustrate the effect each parameter by comparing the responses relative to one another.

Flexural stiffness

Figure 2.15a shows the steady-state response for three panel heights, and since the steady-state is a forced vibration, the period is equal for all heights (2 Hz in this case). The amplitude, however, decreases for higher flexural stiffness of the floor, because (1) more energy is required to deflect the floor, analogous to static deflection of floors, and (2) the fundamental frequency increases (shifting away from the forcing frequency), and therefore, the floor resonating less strongly with the external force. Contrary to the steady-state response, the vibration period of the transient response decreases for increasing panel height (see figure 2.15b) since the fundamental frequency increases. This causes the floor to make more oscillations in a time period, and therefore more energy can be dissipated from the system resulting in a faster decay of the amplitude. It can be concluded that increasing the flexural stiffness is beneficial for both the steady-state and transient response.

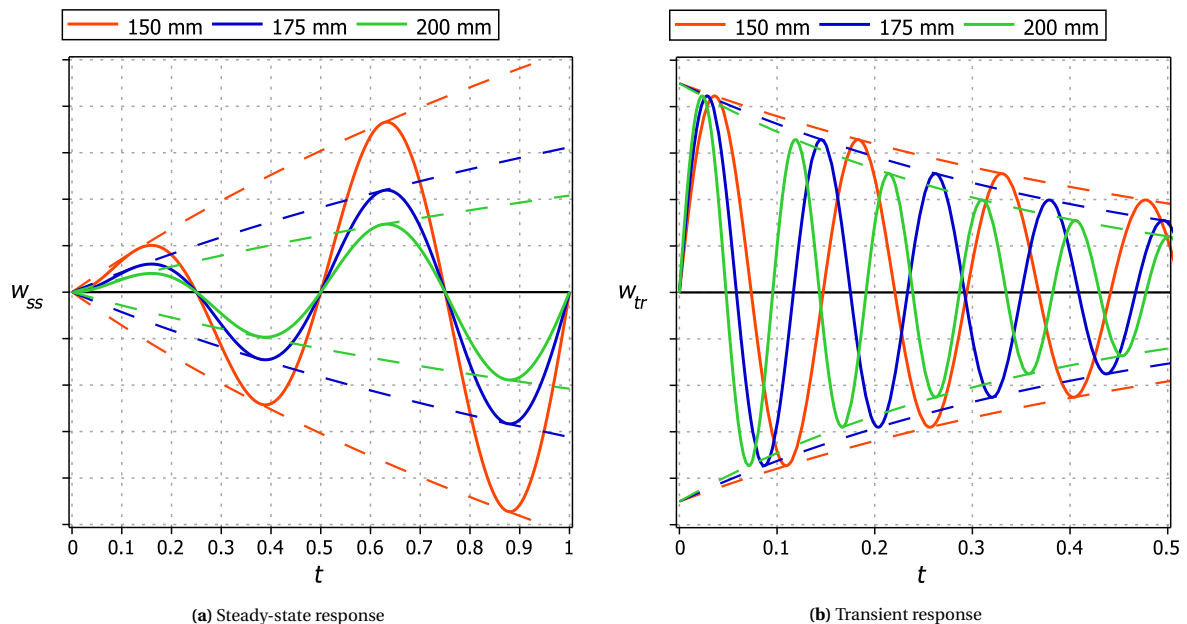


Figure 2.15: Response affection by varying the panel height and their envelopes (dashed line)

Distributed mass

The amplitude decreases of the steady-state response for more increasing mass of floor fields (figure 2.16a), but not as strongly as for the flexural stiffness. Increasing mass results in lowering the fundamental frequency, and therefore the floor resonating more strongly with the external force. It still decreases, however, since more energy required to set the system into motion. The transient response in figure 2.16b shows significant lower amplitudes for a distributed mass of 300 kg/m² compared to 75 kg/m². Higher mass requires more energy into the floor to make it vibrate, which can be observed by the lower initial velocity (i.e. the slope at $t = 0$ sec). Moreover, increasing the mass lowers the fundamental frequency, and therefore the floors making less oscillations over time in free vibration such less energy can be dissipated from the system.

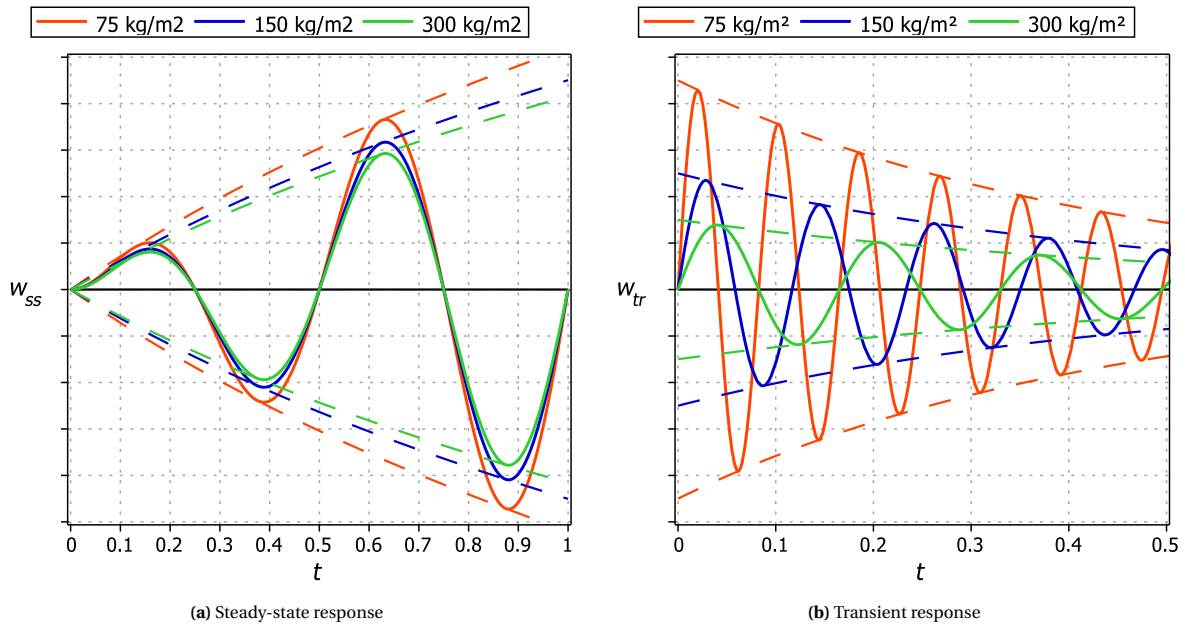


Figure 2.16: Response affection by varying the distributed mass and their envelopes (dashed line)

Damping ratio

As previously noted does the damping ratio increase for higher masses, but in this case the mass is fixed so the damping ratio is fictively changed. In reality, higher levels of damping are the result of more structural or material friction or higher masses. Lower amplitudes are observed in figure 2.17a for the steady-state response when the damping increases, where increasing the damping ratio by 0.02 has more effect for lower ratios (red to blue) than for higher ones (blue to green). The transient response is affected similarly where the initial velocity is equal for all damping ratios, but higher damping results in faster decay of the vibration. Moreover, no significant changes in the vibration period are observed for various damping ratios.

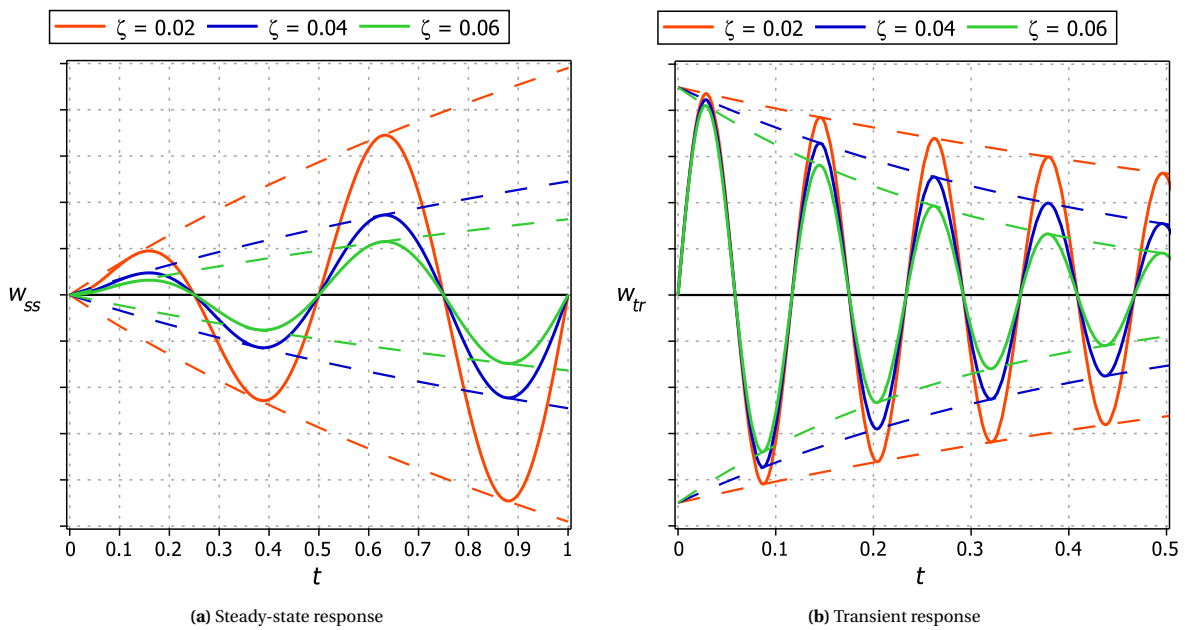


Figure 2.17: Response affection by varying the damping ratio and their envelopes (dashed line)

2.7 NATURAL FREQUENCY OF LFF & HFF FLOOR FIELDS

When one would take off the façade of an apartment building, the structure could look like in figure 2.18a, where one apartment consists of two floor spans and thus, two rooms adjoining the façade. In figure 2.18b these two fields are shown from above in blue, with the corresponding mechanics diagrams shown below which represent the floor as a 1D element, i.e. a beam). The upper diagram shows the case where two separate floor panels are used and therefore, the floor being interrupted at the internal junction. Secondly, the situation is displayed where one panel spans both floor fields with a continuous field at the internal junction.

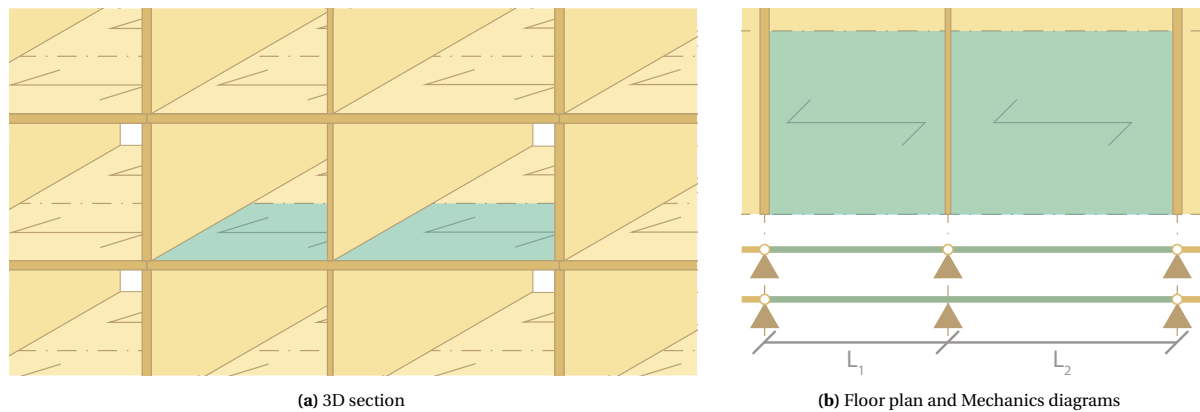


Figure 2.18: Timber structure of a multi-family apartment building

Whether or not both floor fields are physically connected at the internal support affects the natural frequency of the structure, as will be demonstrated in the examples below where the fundamental frequency is calculated for a low-frequency- and high-frequency floor in both single- and double spanning situation.

Floor properties

Below the properties are given for a floor classified as low-frequency floor and one as a high-frequency floor, where EI is the longitudinal stiffness, q the mass and L the larger floor span (i.e. L_2). In all cases is the floor simplified to a beam, where the beam width does not affect the natural frequency since EI and q are both given per unit width, and therefore the width being cancelled out under the square root.

Low-frequency floor (LFF)

Cross-laminated timber floors are generally classified as low-frequency floor due to their low stiffness-to-mass ratio. Therefore, will the fundamental frequency be determined below for a 130 mm thick panel with 5 layers (30-20-30-20-30).

$$EI = 1,734 \cdot 10^6 \text{ Nm}^2/\text{m}$$

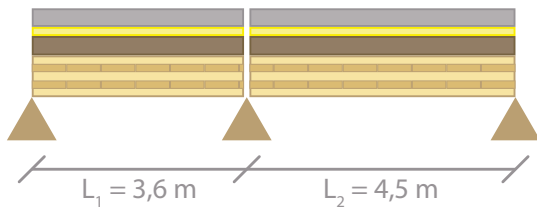
$$q = 280 \text{ kg/m}^2$$

High-frequency floor (HFF)

Floors with a high stiffness-to-mass ratio are classified as a high-frequency floor, which are in practice joist floors with panel decking. For this example, I-joists (FJI89/220@300mm) are chosen with a 27 mm thick LVL panel on top.

$$EI = 6,047 \cdot 10^6 \text{ Nm}^2/\text{m}$$

$$q = 190 \text{ kg/m}^2$$

One-span floor**Low-frequency floor (LFF)**

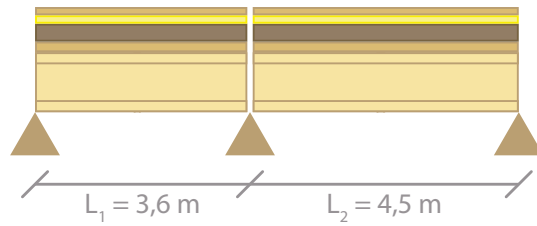
$$EI = 1,734 \cdot 10^6 \text{ Nm}^2/\text{m}$$

$$q = 280 \text{ kg/m}^2$$

$$\beta_1 L = \pi \quad (\text{see equation 5.4})$$

$$f_{1,(L2)} = \frac{(\beta_1 L)^2}{2\pi \cdot (L_2)^2} \sqrt{\frac{EI}{q}} = 6,10 \text{ Hz}$$

$$f_{1,(L1)} = \frac{(\beta_1 L)^2}{2\pi \cdot (L_1)^2} \sqrt{\frac{EI}{q}} = 9,54 \text{ Hz}$$

High-frequency floor (HFF)

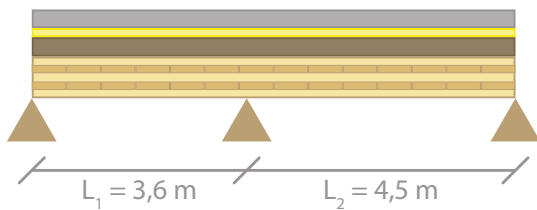
$$EI = 6,047 \cdot 10^6 \text{ Nm}^2/\text{m}$$

$$q = 190 \text{ kg/m}^2$$

$$\beta_1 L = \pi \quad (\text{see equation 5.4})$$

$$f_{1,(L2)} = \frac{(\beta_1 L)^2}{2\pi \cdot (L_2)^2} \sqrt{\frac{EI}{q}} = 13,84 \text{ Hz}$$

$$f_{1,(L1)} = \frac{(\beta_1 L)^2}{2\pi \cdot (L_2)^2} \sqrt{\frac{EI}{q}} = 21,62 \text{ Hz}$$

Two-span floor**Low-frequency floor (LFF)**

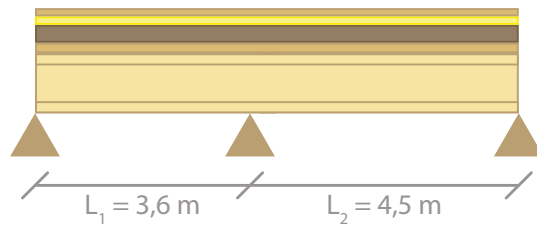
$$EI = 1,734 \cdot 10^6 \text{ Nm}^2/\text{m}$$

$$q = 280 \text{ kg/m}^2$$

$$\beta_1 L = 3,3785 \quad (\text{For } L_1/L_2 = 0,8 \text{ after Zhang et al. (2019)})[78]$$

$$f_{1,(L2)} = \frac{(\beta_1 L)^2}{2\pi \cdot (L_2)^2} \sqrt{\frac{EI}{q}} = 7,06 \text{ Hz}$$

$$f_{2,(L1)} = \frac{(\beta_1 L)^2}{2\pi \cdot (L_1)^2} \sqrt{\frac{EI}{q}} = 11,03 \text{ Hz}$$

High-frequency floor (HFF)

$$EI = 6,047 \cdot 10^6 \text{ Nm}^2/\text{m}$$

$$q = 190 \text{ kg/m}^2$$

$$\beta_1 L = 3,3785 \quad (\text{For } L_1/L_2 = 0,8 \text{ after Zhang et al. (2019)})[78]$$

$$f_{1,(L2)} = \frac{(\beta_1 L)^2}{2\pi \cdot (L_2)^2} \sqrt{\frac{EI}{q}} = 16,00 \text{ Hz}$$

$$f_{2,(L1)} = \frac{(\beta_1 L)^2}{2\pi \cdot (L_1)^2} \sqrt{\frac{EI}{q}} = 25,01 \text{ Hz}$$

Comparison of natural frequencies

Table 2.10 sums all previously determined natural frequencies. For a single spanning floor the fundamental frequencies are given for each separate floor field, where $f_{1,(L2)}$ is the resonance frequency of field L2 and $f_{1,(L1)}$ of field L1. Since the internal junction is interrupted field L2 never resonates on the fundamental frequency of L1. For double spanning cases, however, are both fields connected at the internal junction such they form a single system. Therefore, the floor resonates upon both natural frequencies ($f_{1,(L2)}$ and $f_{2,(L1)}$) independent on the excited floor field. In these case the floor has two natural frequencies in the lower frequency range.

A factor 2,26 higher fundamental frequencies are found for joist floors (HFF) and therefore expected to respond predominantly in a transient manner ($f_1 > 8$ Hz), whereas the CLT floor (LFF) will show a more steady-state dominated response. Additionally, natural frequencies of two-span floors increase by a factor $(\beta_1 L)_{ds}^2 / (\beta_1 L)_{ss}^2 \approx 1,16$ compared to single spanning floors.

	Single spanning		Double spanning	
	$f_{1,(L2)}$	$f_{1,(L1)}$	$f_{1,(L2)}$	$f_{2,(L1)}$
CLT floor (LFF)	6,10 Hz	9,54 Hz	7,06 Hz	11,03 Hz
Joist floor (HFF)	13,84 Hz	21,62 Hz	16,00 Hz	25,01 Hz

Table 2.10: Fundamental frequencies

3

Vibrations in Eurocodes

Previous chapter elaborated the general theorem regarding classical dynamics and human-induced vibrations and the state-of-the-art research that is performed last decades to understand the phenomenon further. Section 2.5 shows the wide variety of quantification measures for the magnitude of vibrations and corresponding comfort criteria. Acceptable comfort levels depend on many factors which vary for each application and due to the complexity, sensitivity and variability of the human body no clearly stated general assessment for acceptable vibrations levels are available. The last 50 years, many studies have been done showing the combination variety of criteria for the development of a general approach for verification of timber floors.

These studies resulted in a verification method for the design of timber structures. This chapter studies the implementation of these studies in Eurocodes by first elaborating on the manner non-timber Eurocodes assess vibrations of both buildings and footbridges, and their level of applicability upon timber structures. After that, the current Eurocode 5 for timber structures, and since it dates from 2005 is most of its verification methods getting outdated with present knowledge. At last, the implementation of state-of-the-art research in the future revision of EN1995-1-1 is studied regarding vibrations, which provides a more comprehensive assessment method.

3.1 EUROCODE 5 (EN 1995-1-1)

Eurocode 5 for the design of timber structures was published in 2004, and comprehensive research regarding human-induced vibrations has been done, ageing out the current code. For example, cross-laminated timber entered the market last decade, which asks for a verification method of low-frequency floors as well, where the current EC5 only defines criteria for floors with a fundamental frequency above 8 Hz.

The vibration requirements specified for HFF by Eurocode 5 (EC5) are based on the static deflection and unit impulse velocity response. Both these limits are related to one another through the parameters a and b , where a relates to the deflection and b defines the velocity limitation. EN1995-1-1 provides a graph (see figure 3.1) for the relation between these parameters and their values are defined in the National Annex [39].

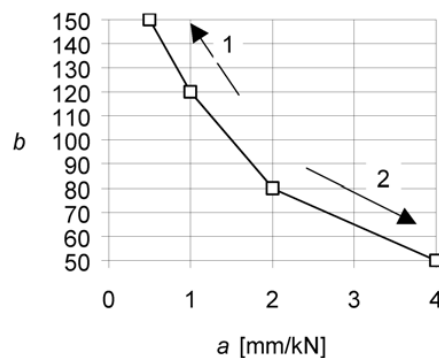


Figure 3.1: Recommended range of and relationship between a and b [39]

Countries using the Eurocode have differing approaches regarding validation of floor vibration design. Fink et al. [9] summarised the overview of Zhang and the survey by CEN, leading to the following insights:

- 36 % (10) of the European countries apply the EC5 as such
- 25 % (7) have nationally recommended values for a and b
- 11 % (3) have only a recommended a value and do not use the velocity criterion
- 29 % (8) have other design methods applied

Weckendorf states [68] that the variety in criteria origins in simplification and disregarding of many response variables and structure properties. Some parameters are hard to measure since they appear not to be variable without changing the others, e.g. the damping ratio. A lot is still unknown about the contribution of damping, and a wide variety of damping ratios are found in the literature for different commonly used timber floorings. This section describes the three criteria given in EC5 for the fundamental frequency, a criterion regarding static deflection (i.e. stiffness) and the unit impulse velocity response. For each is the procedure used in the Netherlands given, and after that, methods used in other countries according to literature study done by Zhang, Rasmussen, Jorissen and Harte.

The German NA applies the research done by Hamm et al. [12] regarding vibrations in floors, including CLT floors. This paper provides design rules and demands regarding the construction to prevent excessive vibrations for three comfort levels, where the lowest class applies to attics and holds no criteria. Higher demands (class I) apply to floors between different units of use, and the base demands (class II) are used for floors within the same unit. Both class I and II hold a frequency- and static load criterion, and demands for floor sublayers to ensure sufficient mass to prevent vibrations. For massive timber (CLT) or timber beam floors, a heavy floating screed (with a fill for higher demands) or light floating screed on a heavy fill should be applied in Germany to add sufficient mass to the structure.

3.1.1 Fundamental frequency

Eurocode for the design of timber structures defines only requirements for residential floors with a fundamental frequency greater than 8 Hz, i.e. only for high-frequency floors with a dominating transient response. For floors where the fundamental frequency condition does not apply, no requirements are defined and "a special investigation should be made", lacking further explanation about appropriate methods for steady-state vibration verification.

A formula for approximating the fundamental frequency of a timber floor is provided (equation 3.1). Although EC5 states it may be used for "simply supported [floors] along all four edges and with timber beams having a span l ", does the equation not apply to a two-span floor since the transverse stiffness is not taken into account. Study by Zhang et al. shows that Austria and Finland both have assigned equation 3.1 to be 2-side support only, and have added an equation that correctly determines the fundamental frequency of 4-side supported floors with an additional factor in line with equation 2.28. It should be noted that the Austrian NA has disregarded the $(l/b)^2$ term, only including the ratio to the power four (probably) for simplification reasons.

$$f_1 = \frac{\pi}{2l^2} \sqrt{\frac{(EI)_l}{m}} \quad (3.1)$$

Where: l Floor span (m)
 $(EI)_l$ Bending stiffness in longitudinal direction (Nm²/m)
 m Mass per unit area (kg/m²)

Furthermore, the Austrian and Finnish NA state that the mass per unit area m should be calculated as the sum of the self-weight of the floor and the quasi-permanent combination of the imposed load, i.e. $\Psi_2 q_k$. This is in line with the design philosophy from EN 1990 [37] where m is defined as the quasi-permanent load added to the dead load. Since vibration design is a serviceability check would it be reasonable to include a particular portion of imposed load (i.e. quasi-permanent) for vibration validation [9] and since timber floors are categorized as lightweight does the quasi-permanent load significantly reduce the fundamental frequency. Though have to be noted that if both the additional effect of the transverse stiffness $(EI)_b$ and the quasi-permanent load combination are considered, the fundamental frequency diverges not much from the one obtained from equation 3.1, because the two effects cancel each other out [77].

3.1.2 Static deflection

Requirement regarding stiffness of floors is given by the unit displacement and limits the one-time deflection of a single footstep [3]. Equations to calculate the static deflection w are not provided in the EC5, only a criterion regarding the deflection is given. This limitation bounds the allowable deflection under a 1 kN point

load by value a [mm/kN], which can be read from figure 3.1 if not defined in the country's National Annex. Equations for determining the static deflection are neither provided in EC5 nor the Dutch National Annex.

However, several countries have adopted alternative equations for determining the static deflection of a floor, as the literature review by Zhang et al. has found [77]. In the National Annexes of Ireland and UK include these equation a factor for shear deflection and slip between floor elements. Austria, Finland, Ireland and the UK consider in their National Annexes the transverse stiffness for redistribution by implementing a multiplication-factor or by determining the effective width.

3.1.3 Unit impulse velocity response

The second criterion for high-frequency floors is the velocity response due to a unit impulse and validates the behaviour of the structure's vibrations imposed by impulses, which corresponds with a damped heel strike of a footfall. v (in $\text{m}/(\text{Ns}^2)$) in equation 3.2 is the maximum initial value of the vertical floor vibration velocity (in m/s) caused by an ideal unit impulse (1 Ns) applied at the point of the floor giving the maximum response.

$$v \leq b f_1 \zeta^{-1} \quad (3.2)$$

In this formula the limitation of the initial velocity is mainly given by b , which is equal to 120 according to the Dutch NA to EN 1995-1-1, f_1 can be obtained from formula 3.1 or a model and ζ is the modal damping ratio. The value v can be obtained from experiments or through a computer model. If these both are not available it could be approximated using equation 3.3:

$$v = \frac{(0,4 + 0,6n_{40})}{\frac{1}{4}(mbl + 200)} \quad \text{Where:} \quad n_{40} = \left[\left(\left(\frac{40}{f_1} \right)^2 - 1 \right) \left(\frac{b}{l} \right)^4 \frac{(EI)_L}{(EI)_T} \right]^{\frac{1}{4}} \quad (3.3)$$

Where: b Width of the floor (m)
 l Span of the floor (m)
 m Mass of the floor per square meter (kg/m^2)
 $(EI)_T$ Equivalent bending stiffness of the floor perpendicular to the span (Nm^2/m)
 $(EI)_L$ Bending stiffness of the floor in spanning direction (Nm^2/m)

This parameter for vibrational serviceability design v is, to quote Zhang et al., "the most mysterious" in EN 1995-1-1 because it is difficult to understand its physical meaning and seems to be determined empirically instead of theoretically or analytically. As a consequence, some countries have disregarded this criterion, e.g. Finland, Germany, Norway and Spain. United Kingdom has adjusted the criterion by increasing the modal damping ratio up to 2%. Zhang et al. suggest to use different damping ratios for each type of flooring system such it reflects realistic situations [77].

3.2 VIBRATION ASSESSMENT IN NON-TIMBER EUROCODES

3.2.1 Buildings

The verification methods provided by different Eurocodes are not sufficient and neither give proper guidance regarding vibrations of lightweight structures. The Dutch National Annex of EN 1990 (A1.4.4 *Vibrations*) [41] states that one can assume vibrations do not exceed the serviceability limit state if the fundamental frequency is equal or higher than 3 Hz. This criterion has not to be fulfilled if the characteristic values of the (quasi-)permanent load is at least 500 kg/m², which is a concrete floor in practice, since it is assumed that the floor cannot be brought into perceptible vibration by walking persons. However, natural frequencies of lightweight structures generally do exceed 3 Hz and these structures have a mass lower than 500 kg/m², but despite meeting the criteria significant vibrations do occur. Furthermore does the NA note that the frequency limitation is necessary to prevent resonance since the highest frequency imposed by walking is 3 Hz, but research shows that higher harmonics of the walking load should also be included for lightweight structures [49, 54, 63, 72].

Annex A1 *Applications to buildings* of EN 1990 [37] states that "the natural frequency of vibrations of the structure or structural member should be kept above appropriate values", where the limitations should be agreed with the client. Furthermore, it states that if it is below the "appropriate value", a more refined analysis of the dynamic response should be performed. Eurocode 3 [40] for the design of steel structures refers to the mentioned Annex A of EN 1990 for guidance, so can be concluded that there is marginal guidance for verification of dynamic effects in non-timber codes related to buildings.

3.2.2 Footbridges

Appendix A2 *Applications to bridges* of EN 1990 [37] also prescribes the number of pedestrians, i.e. 8 to 15 persons, for the general design situation of footbridges depending on the bridge deck area. The comfort criteria regarding acceleration are given in the Dutch National Annex (A2.4.3.2) if the fundamental frequency of the bridge deck is below a limit frequency. The maximum allowable acceleration for vertical vibrations is 0,7 m/s², if $f_1 < 5$ Hz, and in horizontal direction 0,2 m/s² for bridge decks with $f_1 < 2,5$ Hz.

Furthermore, it notes that acceleration calculations are subject to significant uncertainties. In case the comfort margins are not significant, the design should allow for the placement of future dampers to prevent excessive vibrations once the bridge is installed. In EN 1993-2 for the design of steel bridges [43] a similar statement is made regarding future adjustments with the purpose to correct for changing design situations at the end-of-life stage.

In *Eurocode 1: Actions on structures - Part 2: Traffic loads on bridges* [38] loads exerted by pedestrians are given. If the frequencies of these loads are about equal to the natural frequencies of the bridge resonance can occur and thus need to be checked for excessive vibrations. The range of interest for vibrations in the vertical direction is set at 1 to 3 Hz and for horizontal vibrations the frequency range 0,5–1,5 Hz.

The Appendix of the Dutch National Annex of part 2 of Eurocode 1 [42] gives a harmonic load model for crowds footbridges, which uses the equivalent number of pedestrians to incorporate their contribution to damping based on the density. A reduction coefficient is used to include the probability of pace frequency being in the critical range of natural frequencies.

3.3 REVISION OF EN 1995-1-1

The currently used Eurocode 5 is getting outdated due to new findings by state-of-the-art research, especially regarding vibrations, where comprehensive studies were done last decade. Last proposed draft is used for this section, which is Milestone 3 document (31-10-2019) of *Working draft of design of timber structures Eurocode 5-1-1 - Revised section 9.3 Vibrations* proposing criteria for timber floors in general. *Working draft of design of cross-laminated timber in a Eurocode 5-1-1 - Revised section 9.4* (version 13-04-2018) either contains criteria regarding vibrations focussing on floors with a permanent weight of at least 50 kg/m².

3.3.1 Vibrations of all floor types

First, we study the future revision of section 9.3 by CEN TC250 SC5.T3 covering Vibrations of timber floors. The criteria are valid for human-induced vibrations in the categories of use A, B, C1, C3 and D as defined in EN1991-1-1 [5], i.e. residential floors, offices and areas with a moderate amount of people. The provided formulas for fundamental frequency, root-mean-square acceleration and velocity values, and stiffness criteria for maximum static deflection are studied and related to the state-of-the-art research. The manner revised EC5 classifies these vibration criteria elaborated at last.

The floor mass m used for vibrational vibrations should include the self-weight of the structural floor, all supported or suspended horizontal layers of the floor and self-weight of partitions and mass caused by uniform distributed quasi-permanent actions. Partitions should be taken concerning their presence over the long term, their distribution over the floor area and the significance of their influence on the vibrational behaviour. Imposed loads cover movable equipment (such as furniture) contributing to the mass of the floor, and therefore affecting the fundamental frequency. The document proposes only to consider the fraction of the imposed load induced by movable equipment and to limit this additional mass to 10% of the total imposed loads (i.e. 17,5 kg/m² for residential purposes).

Fundamental frequency

The document proposes two equations for determination of the fundamental frequency, one for rigid- (i.e. a wall) and another for non-rigid supports, where non-rigid conditions can be beams. The provided formulas are defined as followed, where expression 3.4a gives f_1 for floors on rigid supports and equation 3.4b for non-rigid conditions:

$$f_1 = k_{e,1} k_{e,2} \frac{\pi}{2l^2} \sqrt{\frac{(EI)_L}{m}} \quad (3.4a)$$

$$f_1 = k_{e,1} k_{e,2} \frac{18}{\sqrt{\delta_{sys}}} \quad (3.4b)$$

$$\text{Where: } k_{e,2} = \sqrt{1 + \left(\frac{l}{b}\right)^4 \frac{(EI)_T}{(EI)_L}}$$

The k-factors in the expressions take the spanning effects into account, where $k_{e,1}$ is a multiplier for two-span floors given in table 3.1. This factor corresponds with βL values found in the study upon two-span floors by Zhang [78]. The second k-factor $k_{e,2}$ accounts for two-way spanning floors using the same multiplier as the current National Annex of Austria prescribes for 4-side supported floors [77]. One can conclude that for decreasing shorter span, the fundamental frequency increases, and likewise, an increasing transverse floor stiffness either increases the fundamental frequency. Parameter δ_{sys} in equation 3.4b for non-rigid supports is the floor deflection under self-weight load, where the load is applied on a single bay only for multi-span floor fields.

Besides equation 3.4b for determination of the fundamental frequency, the document provides another expression for a floor elastically supported on a beam. The system's fundamental frequency is determined from f_1 of each element in that system rigidly supported:

Table 3.1: Factor $k_{e,1}$ for fundamental frequency of two-span floor. l is the longer and l_2 the shorter span

l_2/l	1.0	0.9	0.8	0.7	0.6	0.5	0.4	0.3	0.2
$k_{e,1}$	1.00	1.09	1.16	1.21	1.25	1.28	1.32	1.36	1.41

$$f_{1,res} = \sqrt{\frac{1}{\frac{1}{f_{1,floor}^2} + \frac{1}{3 \cdot f_{1,beam1}^2} + \frac{1}{3 \cdot f_{1,beam2}^2}}} \quad (3.5)$$

The equation holds for several situations, like supported on both sides by a beam or a double or two single span floor – by neglecting one of $f_{1,beam}$ fractions. A floor supported by beams has therefore always a lower fundamental frequency than the same floor rigidly supported. Flexible supports result in a less stiff system, and therefore reducing the natural frequency.

Stiffness criteria

Like in the current EC5 is the static deflection a criterion for assessment of vibrations, this time for both LFF and HFF. Where in the current EC5 only a limitation for unit point load deflection is given, does the future revision of EC5 provide a formula to calculate maximum deflection for single-span floors under a point load of 1 kN, see equation 3.6. Like for the $k_{e,2}$ factor for fundamental frequency is the formula again already prescribed in the current Austrian Annex and takes transverse stiffness contribution into account through the effective width of the floor.

$$w_{1kN} = \frac{Fl^3}{48(EI)_L b_{ef}}, \quad \text{where:} \quad b_{ef} = \min \left\{ \frac{l}{1.1} \sqrt{\frac{(EI)_T}{(EI)_L}}, b \right\} \quad (3.6)$$

For continuous floor beams the provided equation is conservative since additional stiffness from adjoining floor field is not taken into account. Therefore, more accurate deflections are found by replacing equation 3.6 with one that corresponds with two-span floors or calculate the deflection using software. Further, the formula only holds for rigid supports, and therefore, for non-rigid support should the supporting beam's deflection be added to equation 3.6 such that is accounted for the deflection of the system as a whole.

Acceleration criterion

Vibrations of a floor with a fundamental frequency below 8 Hz are assumed resonant and their root-mean-square acceleration should be approximated with equation 3.7. For that equation, a single spanning floor is assumed.

$$a_{rms} = \frac{0,4\alpha F_0}{\sqrt{2}M^*2\zeta} \quad (3.7)$$

Where α is the Fourier coefficient depending on the fundamental frequency, determined by $\alpha = e^{-0,4f_1}$ and ζ the modal damping ratio. M^* is the modal mass of the floor, defined as in equation 3.8 where L_x is the shorter and L_y the longer dimension of L and B .

$$M^* = \frac{mLB}{4} \left(2 - \frac{L_x}{L_y} \right) \quad (3.8)$$

The acceleration criterion is first published by Hamm, Richter and Winter [13] based experiments and adopted in a slightly different manner for EC5. Hamm et al. provide a formula for calculation to determine acceleration, but since for root-mean-square values of sinusoidal shapes $a_{r.m.s.} = a/\sqrt{2}$ holds, formula for acceleration by Hamm et al. is divided by square root 2 such the r.m.s. value is obtained.

Furthermore, the original equation was based on a total dynamic force F_{dyn} , where the weight of the person F_0 is assumed to be 700 N and multiplied with a DLF ($\alpha_1 = 0,4$, $\alpha_2 = 0,2$ and $\alpha_3 = 0,1$) corresponding with the harmonic that ranges the natural frequency, see figure 3.2, upon which is αF_0 fitted such $\alpha = e^{-0,4f_1}$ is obtained. The factor 0.4 is taking into consideration that the force acts only during a limited time (full resonant built-up) and not always at midspan (using mode shapes).

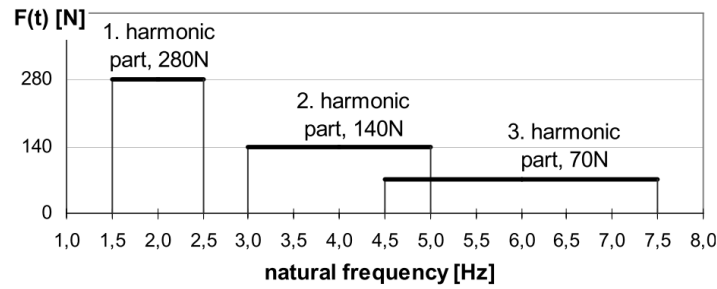


Figure 3.2: Magnitude of force depending on the fundamental frequency of the floor (after Hamm and Richter [13])

Velocity criterion

A transient response is assumed for floors with a fundamental frequency above 8 Hz. Root-mean-square velocities are calculated by a method proposed by Abeyssekeera et al. [1] and uses the mean modal impulse (developed by Young [75], see section 2.4.3):

$$I = 42 \frac{f_w^{1.43}}{f_1^{1.3}} \quad (3.9)$$

$$V_{tot,peak} = K_{imp} \cdot K_{red} \frac{I}{M^* + 70}, \quad \text{where } K_{imp} = 0.48 \left(\frac{b}{l} \right) \left(\frac{(EI)_L}{(EI)_T} \right)^{0.25} \geq 1.0 \quad (3.10)$$

The impulse value of a footfall is used for calculation of the peak velocity in the fundamental mode by dividing it with the modal mass (obtained from equation 3.8) plus the mass of a person, such one obtains the peak velocity at the force location, see equation 3.10. To obtain the total peak velocity one has to correct for the exciting source and sensing person being at a distance from each other with a reduction factor $K_{red} = 0.7$. The effect of higher vibration modes to the floor response is considered by multiplication by the factor K_{imp} .

The root mean square velocity is calculated from the following equation:

$$v_{r.m.s.} = \beta \cdot V_{tot,peak} = (0.65 - 0.01 f_1) (1.22 - 11.0 \zeta) \eta V_{tot,peak} \quad (3.11)$$

$$\text{If } K_{imp} \leq 1.5: \quad \eta = 1.52 - 0.55 \cdot K_{imp}$$

$$\text{Else:} \quad \eta = 0.69$$

The total peak velocity $V_{tot,peak}$ is multiplied with factors incorporating the decaying rate. The amount of energy that is absorbed depends on f_1 (number of vibration cycles per second) and ζ , i.e. the level of damping.

Floor vibration criteria

Contrary to current Eurocode 5, introduces the revision performance levels enabling engineers to design for a specific quality level and type of use. A quality, base and economy choice are given for office and residential purposes, where stricter requirements are set for multi-storey compared to single housing to prevent annoyance at neighbours. Since the purpose of this work is related to multi-family buildings, recommends the document up to level III for quality choice, level IV as base choice and level V is regarded as economy.

Criteria for acceleration and velocity are obtained through response factor R , which is based on the vibration perception base curve given in figure C1 of ISO 10137 [17] (see section 2.5). This R-factor is increasingly being used nowadays for vibrations assessment in buildings [65, 72], where $R = 1$ indicates that the vibration level is just perceptible for an average person while for higher values than one suggest the vibration level to be R times higher than just perceptible.

3.3.2 Floors with a permanent weight of at least 50 kg/m²

Formulas provided in this [4] document for fundamental frequency, acceleration and stiffness are broadly similar to previous chapter. For determination of the fundamental frequency equation 3.4a (for rigid supports, as previously mentioned) is used. Instead of the root-mean-square value the maximum acceleration is proposed for verification, which is similar to equation 3.7 except dividing by $\sqrt{2}$ taking the root-mean-square into account. Requirement regarding maximum deflection w_{1kN} is determined by equation 3.6.

Table 3.2: Response factors R and motion criteria according to floor performance level [5]

	$w_{1kN} \leq$ [mm]	R [-]	$f_1 < 8$ Hz $a_{rms} \leq$ [mm/s ²]	$f_1 \geq 8$ Hz $v_{rms} \leq$ [mm/s]
Level I	0.25	4	20	0.4
Level II	0.25	8	40	0.8
Level III	0.5	16	80	1.6
Level IV	0.8	32	160	3.2
Level V	1.2	64	320	6.4
Level VI	1.6	128	640	12.8

Floor classes

This document distinguishes three floor classes as proposed by Hamm and Richter [12]. They distinguish three demands corresponding with the floor classes, where under the higher demand (class I) vibrations are not perceptible or only when concentrating on them and not classified as annoying. For lower demand floors (class II) vibrations are perceptible but not annoying and for the last demand, corresponding with floor class III, are vibrations clearly perceptible and sometimes annoying. The types of use matching with the floor classes are defined as follow in the document:

- Class I:**
 - Floors between different areas of utilisation
 - Floors between apartments
 - Office floors, computer workstations or conference rooms
 - Corridors with short spans
- Class II:**
 - Floors within the same apartment
 - Floors in one-family dwellings with usual utilisation
- Class III:**
 - Floors underneath rooms without residential purposes or non-developed attics
 - Floors without requirements regarding vibrations

For these floor classes different construction demands are proposed by Hamm et al. as presented in table 3.3. It distinguishes for timber joists- and CLT floors, and wet- and dry screeds. Wet screeds are cementitious materials, like cement, anhydrite or mastic asphalt, and have a usual thickness between 50 and 80 mm. Dry screeds are made of two or three layers of gypsum or wood-based panel boards. Screeds are generally applied as suspended horizontal layer being supported by an acoustic insulating material such a floating screed is created.

Likewise, mass can be added to the floor built-up by applying fill (or ballasting), which does not – in contrast to screed – increase the floor's stiffness, and is often added as sand or gravel. In table 3.3 is a heavy fill defined by a mass per unit area of more than 60 kg/m² and light fills have a mass per unit area between 30 and 60 kg/m². Hamm et al. comment that floating heavy (i.e. wet) screeds are always better than floating light (i.e. dry) screeds regarding floor vibrations because of their increase mass and stiffness.

Recommended requirements

Hamm, Richter and Winter [13] their procedure is, as already mentioned in section 3.1, incorporated in the current National Annex of Germany for verification of CLT panels. Besides, the requirements are proposed for adaptation in the revised Eurocode 5 (see table 3.4), after being slightly changed because of Zimmer and Augustin their research into the relevancy of boundary conditions for dynamic behaviour [79].

Floor meeting a certain level for the fundamental frequency only have to be checked for the stiffness criterion since the floor is classified as high-frequency floor and therefore not oscillating on the footfall harmonics. If the frequency criterion is not met, but the fundamental frequency is still above 4,5 Hz, the acceleration criterion has to be met for the floor.

Table 3.3: Floor requirements depending on floor class [4, 13]

Floor	Screed	Floor class I	Floor class II	Floor class III
Timber joists	Wet	Screed: floating Fill: heavy	Screed: floating Fill: not necessary	-
	Dry	Special verification necessary	Screed: floating Fill: heavy	-
Massive timber	Wet	Screed: floating Fill: heavy or light	Screed: floating Fill: not necessary	-
	Dry	Screed: floating Fill: heavy	Screed: floating Fill: heavy	-

Table 3.4: Recommended requirements for frequency, stiffness and acceleration criteria [4]

Criteria	Floor class I	Floor class II	Floor class III
Stiffness	$f_1 \geq 8$ Hz	$f_1 \geq 6$ Hz	-
	$w_{1kN} \leq 0.25$ mm	$w_{1kN} \leq 0.50$ mm	-
Stiffness	$4.5 \text{ Hz} \leq f_1 \leq 8$ Hz	$4.5 \text{ Hz} \leq f_1 \leq 6$ Hz	-
	$w_{1kN} \leq 0.25$ mm	$w_{1kN} \leq 0.50$ mm	-
Acceleration	$a \leq 5$ mm/s ²	$a \leq 10$ mm/s ²	-

3.3.3 Shortcomings revised EC5

The revision of Eurocode 5 has several shortcomings for appropriate assessment of multiple floor fields in multi-family buildings. In general, can be stated that the future revision of Eurocode 5 focusses on single-span floors on rigid supports. Some additional equations are given for diverging cases, like two-span floors or flexible supports, but for those equations that do not, conservative values are found. Furthermore are for each criterion the deficiencies summed up below.

Fundamental frequency

Fundamental frequencies of flexible supported floors (e.g. on beams) can only be found from the static deflection (equation 3.4b) or Dunkerley's equation (equation 3.5).

Modal mass

The provided formula for determination of modal masses only suits rigid supports, and thus neglects the increased modal mass for beam supported floors. When excitement of one floor field also brings other floor fields in motion, does the mass of the latter fields either contribute to the modal mass.

Acceleration criterion

The given equation for root-mean-square acceleration assumes resonance with one of the harmonics and neglects all others. On itself is this assumption correct since the contribution of this resonating harmonic outweighs the others. However, the used Dynamic Load Factors for determination of α are low compared to the DLF's found in the study performed by Wilford (see table 2.6). Besides, only the first 3 harmonics are considered where the fourth harmonic could resonate with floors having a fundamental frequency higher than 7,5 Hz.

Velocity criterion

A walking frequency of $f_w = 1,5$ Hz is assumed for mean modal impulse I_m , while the impulse increases for higher f_w . Since a mean walking frequency between 1,8 and 2,0 Hz is found in multiple studies does revised Eurocode 5 underestimate the impulse of a heel-strike. Furthermore, the paper by Young [75] proposes the use of design modal impulse for transient response assessment, which results in a $54/42 = 1,29$ times higher impact value.

Floor vibration criteria

A hard-line is drawn between LFF and HFF at 8 Hz to distinct steady-state and transient responses. However, in reality, both responses always exist in a structure, where steady-state dominates for LFF and transient for HFF. Combining both responses may lead to higher response factors, especially for floors with $f_1 \approx 8$ Hz, and thus lower comfort levels. Within the proposed procedure of revised EC5, this could be (partly) taken into account by defining R as the maximum of R_a and R_v , i.e. picking the highest response factor resulting from steady-state (R_a) and transient response (R_v).

Improvements proposed in this work

Therefore proposes this work a more comprehensive method for vibrations of timber floors using $\beta_1 L$ factors. It enables engineers to validate adjacent floor fields of the excited one as well by transformation into mass-spring-dashpot (SDOF) systems. For these systems is the equivalent spring stiffness determined from the static deflection and the modal mass is found by ensuring the SDOF system has the same natural frequencies as the beam. Since support conditions and connected floor fields are captured in these $\beta_1 L$ values, and thus in the natural frequencies, works the proposed method also for modal mass determination of flexible supported floors.

Besides, an alternative procedure for assessing floors is proposed incorporating both steady-state and transient responses, such floors with a fundamental frequency close to 8 Hz can be verified more realistically. From the static deflection, both responses are determined from a mass-spring-dashpot system that is equivalent to the maximum vibrations in a floor structure.

4

Building with timber

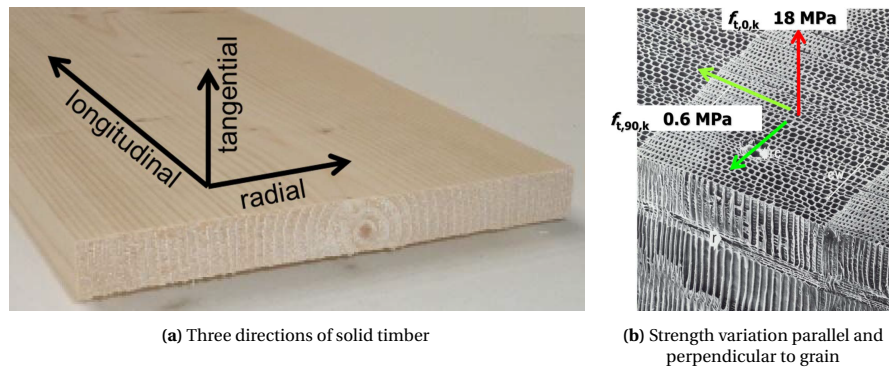


Figure 4.1: Wood directions [58]

Wood is a natural structural material that generally has a high strength-to-weight ratio, that represents a renewable resource, and that is considered by many to be aesthetically appealing. Due to its anisotropy properties, strength – and stiffness – can vary considerably with different load orientations. Wood is generally both strong and stiff when loaded parallel to the grain, but is relatively weak when loaded perpendicular to grain (i.e. in tangential and radial direction) equating to only 3 % of the capacity in longitudinal direction. This is shown in figure 4.1b, where one can observe the tubular-like microstructure of wood causing the anisotropy properties.

Therefore, more homogenised timber products became available on the market last decades, on which the junction typologies researched in this paper are based, using wood in a more efficient manner by reducing the variations. With the introduction of new products engineers start to experiment with building methods to figure out which one fits the products best. Besides, the acoustic performance either does vary and requires – for lightweight structures, like timber – special attention to prevent annoyance in multi-family buildings. At last, with all the essential knowledge given, various building methods using engineered timber products will be presented for the junction typologies.

4.1 ENGINEERED WOOD PRODUCTS

Wood is a natural product obtained from trees and therefore, its properties high vary for direction and location in cross-section. For example, as result of branches growing from the stem, knots appear in the wood affecting strength properties. At these locations the 'straw-structure' in a piece of solid timber bends around the knots and causes stress concentrations when loaded, therefore being the weak spot of wood.

Last decades the timber industry has innovated and new engineered wood products (EWP) entered the market with increased properties compared to solid timber. These products have more homogeneous physical and mechanical properties in the two plane directions by combining parallel and perpendicular layers in plane, as was shown in figure 4.1b, making them far more dimensionally stable. Furthermore, EWPs have a lower variance in properties since the weak knot spots are spread along the material or removed during the process. Last advantage of these products over solid wood is the variability of desired properties, like surface, shaping, dimensions and mechanical properties [58].

Depending on the desired end product, various processing techniques are available for transforming wood logs into a suitable material. By sawing the logs into boards, a CLT panel (see figure 4.2a) is produced and through peeling of a log veneers are obtained, which are glued together into panels or beams (see figure 4.2c and 4.2d). Smaller base materials, like strands and particles, are used for boards (e.g. OSB) that are produced by chipping a log into smaller portions which are assembled into desired dimensions. Even panels where its hard to distinguish the wood are available on the market where defibrated wood fibres are glued together into e.g. MDF panels. There even exist products which combine wood products of different processes into a new product, like the web of I-joist beams shown in figure 4.2b.

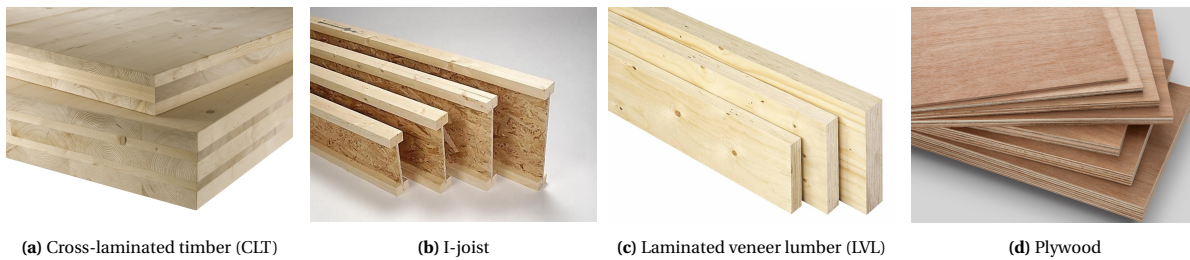


Figure 4.2: Engineered wood products

Cross-laminated timber

Cross-laminated timber (CLT) is a solid panel product that is classified as structural wood material only, unlike plywood, and therefore always used for load-bearing members, e.g. walls, roofs, floors and even lift shafts and stairs. It comprises of resin bonded board layers of softwood (see figure 4.2a), where the grain directions between adjacent layers run perpendicular to one another. All wood species used in practice nowadays are conifers, although first producers try to use beech. The major part of CLT panels is made of spruce, but also fir, pine, larch or Douglas fir are used for CLT panel production [3]. Thickness of the in-plane symmetrically aligned board layers generally vary between 15 and 40 millimetres, meaning a very wide range of panel thicknesses is possible (60 up to 400 mm). In general, producers glue together three up to eleven odd-numbered layers, such the panel is in-plane symmetric, to prevent twisting curvature when loaded.

I-joist

I-joists, or engineered wood joist, are beam elements with an high stiffness-to-weight ratio since material further from the neutral axis contributes more to the second moment of area. Therefore, the flanges are fabricated out of solid wood or a better EWP equivalent placing most material at the outer edges of the beam. For this thesis Finnjoist beams are used, which flanges are made of LVL with all veneers in longitudinal direction. In this manner, the material is used most efficiently resulting in high strength and stiffness.

The web is a Orientated Strand Board (OSB) connecting both flanges, which is a panel made from strands as mentioned earlier. Strands for top layers should preferably run parallel to the production direction, while those forming the middle layer should be random or perpendicular. The bending strength in the longitudinal direction of the board significantly exceeds that in the perpendicular direction.

Laminated veneer lumber

Laminated veneer lumber (LVL, see figure 4.2c) is produced by glueing multiple layers of veneers with phenol resin. These veneers, i.e. a thin sheets of wood, are normally produced by peeling process that cuts strips 0.5 to 6.0 mm thick from a peeled log. The veneers within a layer are generally connected by overlapping. The grain of veneers is either parallel only to the longitudinal direction of the panel or predominantly parallel and slightly (up to 25%) perpendicular [3].

Plywood

Plywood comprises at least three layers (plies) bonded to each other with perpendicular running grains to ensure a barrier effect in-plane (dimensional stability), like is shown in figure 4.2d. The in-plane properties of the x- and y-direction are closer to one another compared to LVL panels due to application of crosswise layers, whereby the veneers must be arranged symmetrically to the central plane. Accordingly, for plywood, a distinction is made as well between both axes running parallel and perpendicular to the grain of the top plies. Plywood is mainly used in construction as a sheathing material in horizontal (floors, roofs) and vertical (shear walls) diaphragms.

4.2 TIMBER BUILDING METHODS

With the development of new engineered wood products (EWP) the variety of timber building methods has increased. In the early days the majority of timber structures were built as a *timber frame system* with solid wood elements with panels mounted on these frames for walls and (solid) wooded beams with decking. Another manner of building is by a combining of beams and columns, called *column-beam systems*, to create multi-storey wood buildings with solid wood elements as well. Nowadays are still structures built using these method, though innovative EWP are used instead of solid wood elements because of better properties. Besides improvement of existing building methods also a new building method has developed, namely the so-called *Plate systems*. These structures consist out of plate components made from massive wood laminates, like for example CLT panels. In this section the components of the various building methods are described.

4.2.1 Floor types

For all timber building methods a distinction can be made between the floor and main load-bearing structure. The main function of a floor in static situation is transferring the vertically applied loads to the support through bending. Besides, the floor has to transfer lateral loads to shear elements by diaphragm action.

Beam floors with decking

The most commonly applied flooring construction consists out of beams spanning between the supports with a wooden decking on top. The beams are often engineered components, such as I-joist (see figure 4.3b), glulam or LVL beam and transverse bracing can be applied to transfer point loads partly to adjoining beams, which improves the vibration behaviour [70]. Engineered wood panels are commonly used as decking to cover the area between the beams and to enable the diaphragm action of the floor.

Massive timber floors

The first residential building made from cross laminated timber (CLT) was built in Austria in 1993 [23], and therefore, it is a relatively new material that will be implemented in the future revision of Eurocode 5 [4]. When applied as floor (see figure 4.3a), resilient material is often added to the home-separation junction to prevent sound transmission to adjoining units, as will be elaborated in section 4.3.1.



(a) CLT floor panel hoisted on top of CLT walls [25]



(b) I-joists as beams for flooring [33]

Figure 4.3: Floor types

4.2.2 Types of load-bearing structures

Vertical element transferring loads from the supported floors to the foundation are named load-bearing structures, and are mainly loaded with a normal force. Besides, in absence of a shear core, the (planar) element has to transfer the horizontal forces – due to e.g. wind load – to the foundation as well.

Timber frame wall

Timber structures with vertical studs between a top and bottom plate are called timber frame walls. The stud spacing is typically not exceeding 600 mm and often an insulation material is placed in between. Engineered

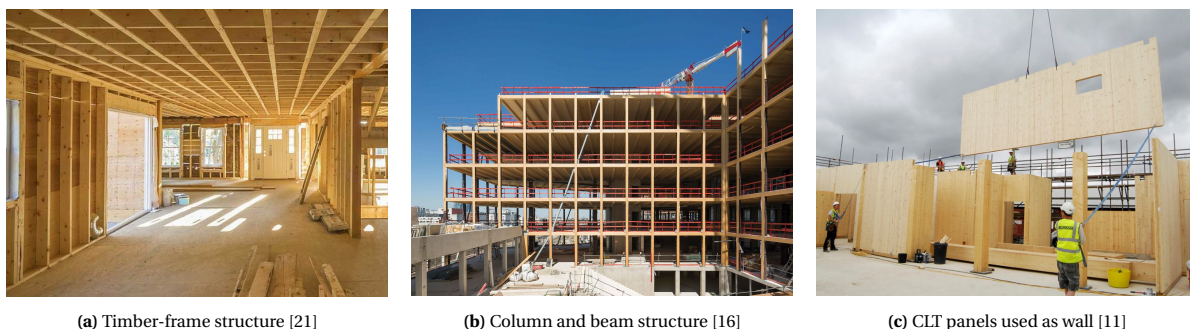
wood panels are fixed on the studs to close the frame and make it rigid. The studs are relatively small in cross-section (compared to columns) which limits the building height of this load-bearing system.

Column-and-beam structure

This system shows similarities with the timber framing but the bar elements are less densely placed and heavier in size. It consists out of vertical and horizontal elements which form a framework, as is shown in figure 4.4b. The horizontal element, i.e. a beam, supports the floor and transfers it through bending to the column, which thereafter carries the load to the foundation. This load-bearing structure is very suitable for multi-storey timber buildings, though it might bring some problems regarding vibrations. Cobelens [7] found that vibrations transmit easily to adjoining floor fields if the fundamental frequency of the beam and floor are close, so special attention to this phenomenon is necessary.

Massive timber walls

Cross laminated timber is not only suitable for floors, it is also used for walls and generally applied for both wall and floor, as is shown in figure 4.3a. These walls always have a load-bearing function, but are in some buildings also applied as shear wall for to its homogeneous character.



(a) Timber-frame structure [21]

(b) Column and beam structure [16]

(c) CLT panels used as wall [11]

Figure 4.4: Load-bearing structures

4.2.3 Damping in timber structures

The vibrations of an excited structure reduce over time (and eventually stop) through damping, due to dissipation of the energy. The damping of the system can be caused by internal friction of the material, external friction with other elements or an installed viscous damper. For a single beam the damping can easily be measured by the reduction of the amplitude in time. However, within structural designs it is hard to predict the absorbing elements of the structure and especially the amount of energy that is dissipated. Therefore are damping ratios susceptible to large uncertainties resulting in a wide range of values found in literature.

Level of damping is found to be depended on a large variety of conditions, like type of structure, support conditions, whether or not non-load bearing partitions are place, presence of people [1], placed furniture and type of floor- and ceiling finishing [8]. Adding (dead-)weight to the floor is generally assumed to increase the level of damping, though Weckendorf et al. have found by experiment that additional mass could reduce the damping ratio [69].

Many experiments are conducted to find consistent damping values for specific configurations, but since they are depended on many quantities they can often not be applied to other situations. In addition, Weckendorf attempted to create identical full-scale experiments (with same structure geometries) but found the ζ value to vary between 1.16 and 3.95. This spread causes uncertainties by having the damping a significant influence on the assessment of vibration performance.

Therefore is chosen for this work not to use damping values from experiments upon floors that are (quite) similar to those presented in section 4.4. Instead, the damping ratios presented by Abeysekera et al. for mass timber- and joist floors are used, studying sensitivity of the vibrations for damping being in a range between half and twice the values given in table 4.1. In this manner, the effect of an uncertain level of damping is investigated for varying values. In the table below are the values according to Abeysekera et al. their study given besides the damping ratios that are proposed for revised Eurocode 5. The latter disregards values for 4-sided supports for consistent interpretation by engineers, because in practice (almost) all floors are supported on

Table 4.1: Damping ratios after Abeyssekera [1] and values proposed for revised Eurocode 5 [5]

Floor type	Abeyssekera	Revised EC5
Joisted floors	$\zeta = 0,02$	$\zeta = 0,02$
Timber-concrete and mass timber floors	$\zeta = 0,025$	$\zeta = 0,025$
Joisted floors with floating layer	$\zeta = 0,03$	$\zeta = 0,03$
Timber-concrete and mass timber floors with floating layer	$\zeta = 0,035$	$\zeta = 0,04$
All floors with floating layer supported on 4-sides	$\zeta = 0,04$	-
All floors with floating layer supported on 4-sides on flexible bearings	$\zeta = 0,06$	-

four sides. Flexible bearings, described in next section, appear to have a positive effect on the damping level. However, this will not be considered in the damped assessment in chapter 6, which is on the conservative side.

4.3 ACOUSTIC PERFORMANCE OF DWELLINGS

Besides perception of dynamic vibrations as discussed in section 2.5, can hearing sounds sourcing in the adjacent apartment provoke annoyance as well. It is a key issue for medium-density and high-density timber housing, causing the need to properly design walls and floors between individual dwelling units to ensure acoustic privacy and prevent sound nuisance. Sound transmission between a “source room” and a “receiving room” can be related to two kinds of excitation: airborne or structure-borne. In the first case, a source generates a sound field inducing a vibrational state into the separating wall and radiating sound energy into the receiving room. Structure-borne sounds are generated by an impact (e.g. a heel-strike), causing a vibration that propagates through the structure and finally radiating in the receiving room.

Assessment of soundproofing in the Netherlands should be done, according Building Decree 2012, in line with NEN 1070 [36], where building elements are categorised into five classes (quality score k 1 to 5) based on acoustic performance. Class $k = 1$ relates to a quality level that is just achievable when one is applying state-of-the-art materials, $k = 3$ to currently applied building practices, and $k = 5$ to the lowest necessity when renovating buildings. In table 4.2 Limitations for these classes are given in $D_{nT;A}$ for airborne sound, expressing sound pressure difference between two rooms and corrected for reverberation time that depends of the size of the receiving room. Regarding impact sound insulation restrictions for $L_{nT;A}$ are provided, which measures the impact sound pressure in the receiving room and is corrected for reverb as well. Both these values are, however, not provided by Dataholz (which is an online catalog for timber construction elements that is used in this work) and comparison of the junction typologies presented in next section is therefore not possible using these A-weighted standardized level difference and standardized impact sound pressure level values.

Above mentioned descriptors express the insulation level of planar structural elements and only incorporating the direct sound transmission path. In EN 12354 [46, 47], a more comprehensive method is given including the flanking paths as well for airborne and impact sound transmission. In figure 4.5 the various paths are shown and one can observe that part of the sound power directly radiates into the receiving room (i.e. direct transmission). Other paths for sound to radiate to the receiving room is through the junction, where the vibrational state of a structural element is transferred to another. These so-called flanking paths depend on many input parameters like the sound reduction index of the element itself and improvements by additional layers for element, the element’s surface area, coupling length of the junction connecting receiving and flanking element and the vibration reduction index for structural coupling of elements. All flanking paths add up to the direct sound transmission and return to a lower value of sound insulation of the partition. Therefore would this method provide a more sufficient indication of the sound insulation of a structure, but many of it required parameters can only be obtained by experiments.

The website of Dataholz does only provide R_w and $L_{n,w}$ values (see Appendix) for the direct sound transmission path of the walls and floors to be presented in section 4.4, expressing the weighted sound reduction index and weighted normalized impact sound pressure level respectively. In line with the quantities provided in NEN 1070 are R_w and $L_{n,w}$ also corrected for reverb in the receiving room through the area of absorption, where $D_{nT;A}$ and $L_{nT;A}$ are corrected for reverberation time. The area and time are related to one another through Sabine’s formula given in ISO 140-4 [35]: $A = 0,16V/T$, where the equivalent absorption area A is expressed as the ratio of V , i.e. the volume of the receiving room, and reverberation time T . Therefore can

Table 4.2: Criteria for sound insulation with an external source [36]

Quality level	Airborne	Structure-borne
$k = 1$	$D_{nT;A} \geq 62$ dB	$L_{nT;A} \leq 43$ dB
$k = 2$	$D_{nT;A} \geq 57$ dB	$L_{nT;A} \leq 48$ dB
$k = 3$	$D_{nT;A} \geq 52$ dB	$L_{nT;A} \leq 53$ dB
$k = 4$	$D_{nT;A} \geq 47$ dB	$L_{nT;A} \leq 58$ dB
$k = 5$	$D_{nT;A} \geq 42$ dB	$L_{nT;A} \leq 63$ dB

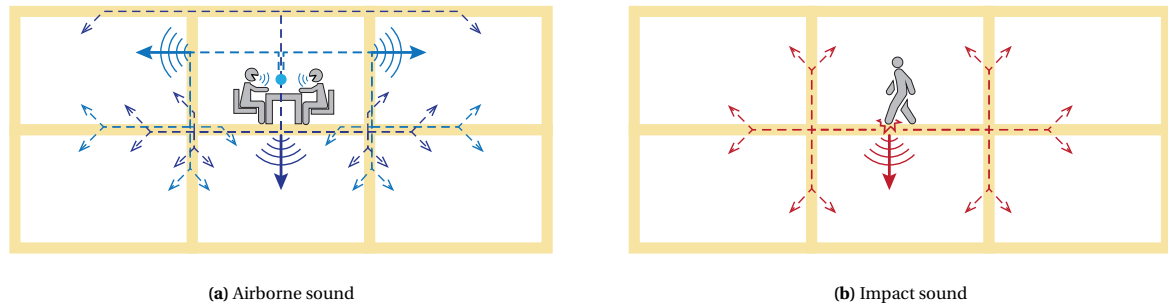


Figure 4.5: Visualization of direct (solid line) and flanking paths (dashed line)

be stated that R_w and $L_{n,w}$ have the same physical representation as the descriptors prescribed by the Dutch Building Decree 2012 (i.e. $D_{nT;A}$ and $L_{nT;A}$).

Sound classification in the Nordic countries

The single-number quantities R_w and $L_{n,w}$ are the most commonly used sound insulation descriptors in Europe [55], like in all Nordic countries where it is adopted in combination with spectrum adaptation terms (C , C_{tr} and C_I), taking different source spectra into account. For lightweight buildings [56] it is of importance to include the low-frequency spectrum adaptation term (down to 50 Hz). For simplicity, the behaviour of a partition is expressed as a single number using a special procedure relating the frequency behaviour to a reference curve, which is given in EN ISO 717 series [44, 45]. Finally, these values classify a wall or floor in a class, which are comparable to the classes developed in the Dutch NEN 1070 according to the graphs presented by Rasmussen [57]. This can be concluded as well by comparing classes given in table 4.2 and table 4.3. Quantities given in Nordic and Dutch codes are, up to some level, comparable and expressing both sound reductions.

For expression of a partition element's insulation level of airborne sound, Nordic countries use the descriptor Weighted sound reduction index R_w . This single number quantity, based on laboratory measurements, characterises the airborne sound insulation of a building element over a range of frequencies. The frequency-dependent value R is defined as $R = L_1 - L_2 + 10 \log(S/A)$ [35], where L_1 and L_2 are the sound pressure level (in dB) in the source and receiving room respectively, S the area of the separating element and A the equivalent absorption area of the receiving room. In other words, the insulation level depends on the difference in sound pressure level and the ability of the receiving room to absorb the sound, and therefore, partition elements with a higher R_w value insulate better.

For airborne sound insulation to include source spectra, two spectrum adaptation terms are defined in ISO 717 [44]: C , being the A-weighted pink noise spectrum, and C_{tr} incorporating the A-weighted urban traffic noise spectrum. The first spectrum is applied for separating walls and covers medium- and high-frequency noise of living activities, like talking, music, TV and playing children. The second spectrum applies to low- and medium-frequency noise like urban road traffic and aircrafts and corrects insulation levels of facades.

Since this thesis is about human-induced vibrations and heel-strikes during walking are a source for impact sound, one should include the weighted normalized impact sound pressure level $L_{n,w}$. This quantity is obtained by measuring the impact sound pressure level in the receiving room caused by a standardised tapping machine, and correcting it for the ratio of absorption area in the receiving room A and reference area A_0 . In contrast with airborne sounds means a lower insulation level $L_{n,w}$ a better performance, corresponding with lower sound levels in the receiving room.

The rating by $L_{n,w}$ appeared to be quite adequate for characterizing impact noise, like walking on wooden floors [45]. However, it insufficiently takes level peaks at single (low) frequencies into account of timber joist floors. Therefore a spectrum adaptation C_I is introduced and determined such that for massive floors (like concrete) with effective coverings its value is about zero. On the other hand, for timber joist floors with dominating low frequency peaks it is positive, i.e. worsening the impact sound insulation level.

Table 4.3: Main classes of sound insulation criteria in Danish standard (DS 490). Summarised by Rasmussen [56]

Sound class description	Evaluated as:		Sound insulation	
	Good	Poor	Airborne	Impact
A Excellent acoustic conditions. Occupants will be disturbed only occasionally by sound or noise.	> 90 %		$R'_w + C_{50-3150} \geq 63$ dB	$L'_{n,w} \leq 43$ dB and $L'_{n,w} + C_{1,50-2500} \leq 43$ dB
B Significant improvement compared to minimum in class C. Occupants may be disturbed sometimes.	70 to 85 %	< 10 %	$R'_w + C_{50-3150} \geq 58$ dB	$L'_{n,w} \leq 48$ dB and $L'_{n,w} + C_{1,50-2500} \leq 48$ dB
C Sound class intended as the minimum for new buildings.	50 to 65 %	< 20 %	$R'_w \geq 55$ dB	$L'_{n,w} \leq 53$ dB
D Sound class intended for older buildings with less satisfactory acoustic conditions, e.g. for renovated dwellings	30 to 45 %	25 to 40 %	$R'_w \geq 50$ dB	$L'_{n,w} \leq 58$ dB

4.3.1 Soundproofing measures

Various soundproofing measures are available on the market preventing acoustic convection of airborne or impact sound making use of different principles. Since acoustic waves and vibrations are both dynamic does improving the behaviour of one variable also influence the other. Improving rigidity of junctions is, for example, beneficial for reduction of vibration levels, but increases the convection of acoustic waves to adjacent walls and floors.

The measures mentioned in this section improve sound insulation all by making use of a different principle, and therefore, all affecting the vibrational behaviour in another way. Application of (wet) screed increases the mass – and therewith decreasing the eigenfrequencies and improving damping – such it requires more energy to excite the floor field and the energy dissipates faster through damping. If screed is applied as floating subflooring, the impact sound excitement is physically disconnected from the structure. Another soundproofing measure are resilient interlayers preventing transmittance of acoustic waves to other structural elements. They are often applied in (home-separating) junctions to prevent acoustic energy entering the neighbouring floor and walls and also dissipate energy through damping. Both measures are further elaborated below.

Screed

Floor screed is composed of cementitious material blended with water and sand to provide a levelled surface on the floor. For concrete structures it is applied to cancel the unevenness of structural concrete, but for timber structures it is used to add mass for better acoustic performance. Within the project 'Karel Doorman' by RHDHV the wooden floor system is topped with 55 mm anhydrite screed to meet the acoustic isolation demands [7, 14].

Since a floating screed acts like a dynamic mass-spring system, the SDOF system has eigenfrequencies and may cause resonance. The screed layer and quasi-permanent load on top of it are the mass of this dynamic system and the insulation layer being the spring. Therefore, the resonance frequency of the floating subflooring is given by equation 4.1 [62], where the dynamic stiffness per unit area of the resilient layer is given by s' (in N/m²) and m' is the mass per unit area of the slab (kg/m²).

$$f_{1,fsf} = \frac{1}{2\pi} \sqrt{\frac{s'}{m'}} \quad (4.1)$$

The study by Hamm, Richter and Winter [13] of floor vibrations comes with some vibration improvements by applying floating screeds to wooden floors based on performed tests. They investigated light floors as well as the heavier ones where anhydrite screed is applied, as shown in figure 4.6. From the research several demands are proposed regarding floors between different units as well as within one unit of use. Regarding vibrations were all heavy floating screeds observed to perform better than floating light screeds due to the

increased mass and stiffness of the floor. Moreover, they concluded that light floating screeds probably not applicable for timber beam floors between different units of use (see table 3.3), because of lack of sufficient mass.

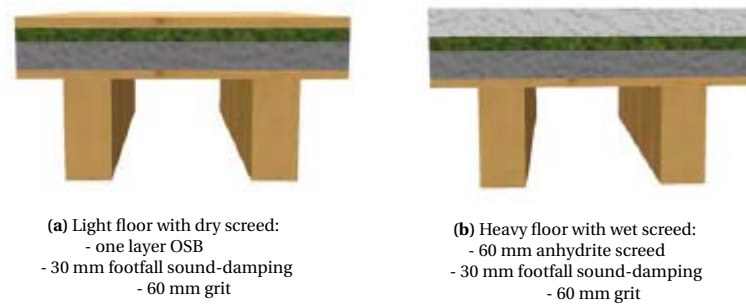


Figure 4.6: Two screed types types [13]

Resilient damping materials

Prevention of sound transmission from the floor to adjoining elements can be achieved by applying elastomers at the floors support (see figure 4.7). This measure is especially often applied in the junctions of massive timber structures. These resilient damping materials have a positive effect on the vibrations as well by its dissipating behaviour through damping. Weckendorf found the effects of elastomers to be dependent on the location where they were applied. Damping was considerably raised when applied at locations where high shear stress occurs [68], i.e. at the supports for single- and double span floor fields.

Jarnerö et al. [20] tested different support configurations, like resting on Sylomer (mixed cellular) elastomer interlayers, floating (i.e. no fastening to support) and screwed to the supporting beam. They measured, amongst others, the impulse velocity response of the structure, which appeared to reduce by adding elastic layers at the supports. There seems to be a clear correlation between improving the dynamic response and the use of elastomeric interlayers. Connection the floor to the supporting by screws gave the highest response, which makes sense since both elements are more fixed and the vibration energy cannot dissipate from the system. The application of flexible bearings increases the damping ratio according to Abeysekera et al. [1] by a factor 1,5. They propose $\zeta = 0,04$ for "all floors with a floating layer and supported on 4 sides", whereas for "all floors with a floating layer and supported on 4 sides by timber walls via flexible bearings" $\zeta = 0,06$ is proposed.



Figure 4.7: Application of resilient interlayer between walls and floor [60]

4.4 JUNCTION TYPOLOGIES

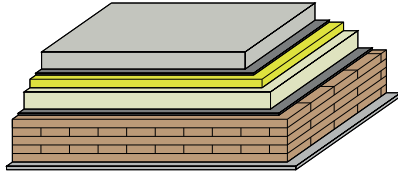
This section elaborates the different junction typologies, which are a combination of floor configurations and support types. First introducing the floors of CLT or I-joists with decking, and after that, the different support conditions that relate to building methods mentioned in section 4.2.

4.4.1 Introduction of floor configurations

Two structural floor types were introduced in section 4.2, namely cross-laminated timber and joists with decking. CLT floors are generally classified as low-frequency floor (LFF), whereas joists with decking have a higher fundamental frequency (HFF). Of both floors, two floors are configured to study the effect upon vibrations.

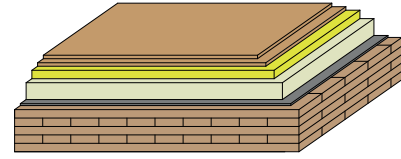
The structural elements of the first two typologies (F1 and F2) are CLT panels, where the difference lies in the applied screed type, i.e. wet and dry. The first is massive compared to a dry screed, and therefore no additional acoustic measures have to be applied. The CLT floor with dry screed has insufficient mass, and therefore, additional measures have to be taken. Secondly, two floors are configured (F3 and F4) using I-joists with LVL decking as a structural element. To study the effect of dead load regarding vibration levels, one of these configurations has ballasting added by a layer of sand (fill), and the other does Sufficient acoustic insulation is for the latter achieved by applying resilient channels to keep the plasterboard of the ceiling in place.

In table 4.4 provides the floor properties that are used next chapters. One can observe that CLT floors have both a low stiffness and high mass compared to joist floors. This explains why fundamental frequencies of CLT floors are generally low, and joist floors are classified as high-frequency floors.

F1: CLT floor with wet screed

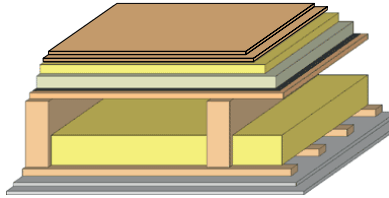
Dataholz code: gdmnxn01a-00
Damping ratio: $\zeta = 0,05$

Floor layer	t [mm]	Mass [kg/m ²]
Cement screed	50	100
Separation layer	0	0
Sound insulation	30	2
Fill (sand)	50	75
CLT	130	55
Plasterboard	12,5	10
	282,5	282

F2: CLT floor with dry screed

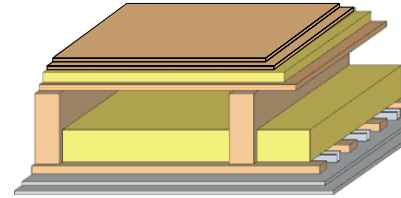
Dataholz code: gdmtnx01-00
Damping ratio: $\zeta = 0,04$

Floor layer	t [mm]	Mass [kg/m ²]
LVL (Kerto-Q)	27	14
Sound insulation	30	2
Fill (sand)	60	90
CLT	130	55
Plasterboard	12,5	10
	259,5	171

F3: Joist floor with fill

Dataholz code: gdrtnx01b-00
Damping ratio: $\zeta = 0,03$

Floor layer	t [mm]	Mass [kg/m ²]
LVL (Kerto-Q)	27	14
Sound insulation	30	2
Fill (sand)	50	75
LVL (Kerto-Q)	27	14
I-joist (FJI89x220)	220	27
Mineral wool	100	2
Spruce battens	25	11
Plasterboard (2x)	25	20
	404	165

F4: Joist floor without fill

Dataholz code: gdrtxa03b-00
Damping ratio: $\zeta = 0,025$

Floor layer	t [mm]	Mass [kg/m ²]
LVL (Kerto-Q)	27	14
Sound insulation	30	2
LVL (Kerto-Q)	27	14
I-joist (FJI89x220)	220	27
Mineral wool	100	2
Spruce battens	25	11
Resilient channels	27	3
Plasterboard (2x)	25	20
	356	93

Table 4.4: Properties of floors

Floor	Stiffness		Mass m [kg/m ²]	Sound insulation [15]	
	EI_L [Nm ² /m]	EI_T [Nm ² /m]		R_w (C) [dB]	$L_{n,w}$ (C _I) [dB]
F1 - CLT floor with wet screed	$1,73 \cdot 10^6$	$3,48 \cdot 10^5$	282	75 (-2)	45 (-1)
F2 - CLT floor with dry screed	$1,73 \cdot 10^6$	$3,48 \cdot 10^5$	171	62 (-5)	50 (-1)
F3 - Joist floor with fill	$3,53 \cdot 10^6$	$1,72 \cdot 10^4$	165	63 (-4)	58 (0)
F4 - Joist floor without fill	$3,53 \cdot 10^6$	$1,72 \cdot 10^4$	93	64 (-3)	52 (2)

Introduction of support types

Three load-bearing structures were introduced in section 4.2, namely *massive timber walls*, *column-and-beam structures* and *timber-frame walls*, whom relate to the manner floors are supported. The first two support types use a CLT wall as load-bearing structure, where one has a resilient elastomer applied between floor and wall to prevent excessive sound transmission, and the other does not. The other two supports both appear like a timber-frame, but use another load-bearing principle. To achieve high plan flexibility one of the supports is a Kerto-S beam (2x 50x260mm), whereas the other is a traditional timber-frame.

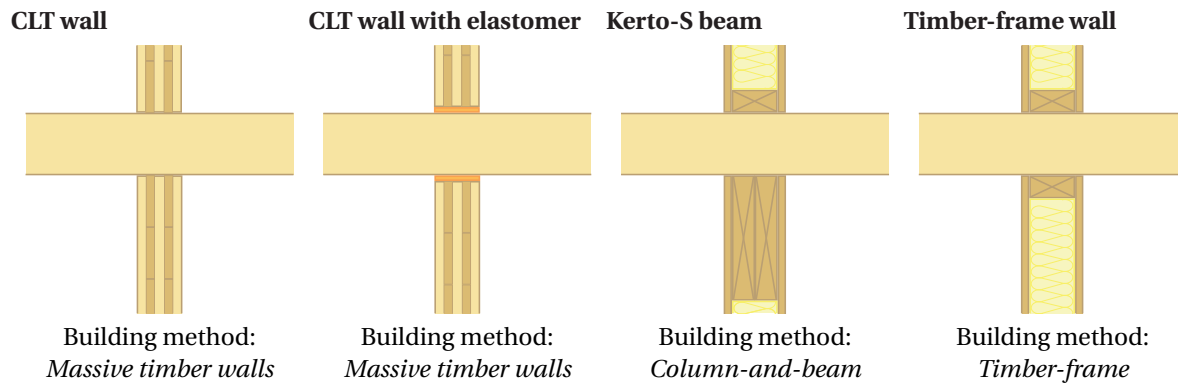


Table 4.5: Properties of walls after Dataholz [15]

Wall	Dataholz code	t_{const} [mm]	t_{tot} [mm]	m [kg/m ²]	R_w (C) [dB]
CLT - Double leaf	twmxxo03a-01	2x80	245	121,6	60 (0)
CLT - Single leaf	twmxxo04a-02	100	265	74,9	53 (-5)
CLT - Internal	iwmxxo01b-00	80	130	79,0	38 (-2)
Timber-frame - Double leaf	twrxxo03b-00	2x100	320	92,8	59 (-2)
Timber-frame - Single leaf	twrxxo01-00	120	250	82,4	60 (-1)
Timber-frame - Internal	iwrxxo01b-00	100	150	45,8	43 (-1)

Junction details

By combining the floor configurations and supports 8 junction typologies are formed. Floor 1 supported by beams is not studied since large beams are necessary to carry the heavy floor. Contrary is floor 2 investigated for 3 support types: CLT walls with elastomers (additional sound measure), Kerto-S beam and timber-frame wall. Both floor 3 and 4 are studied with beam as support besides a timber-frame.

Since the work focusses on multi-family timber buildings, additional measures have to be taken to prevent excessive transmittance of sound to neighbours. Therefore an insulating layer is added to the single leaf wall and for double leaf walls it is prevented through physical decoupling of both walls. Internal junction types are a single spanning variant, where the floor fields at both sides are discontinuous (single-span floor), and a continuous one (two-span floor). The continuity of a floor reduces the vibration levels in the same way it holds for static situations. However, it also excites the floor field at the other side of the junction from source perspective.

An overview of the configured junction details is given in figure 4.8. A more comprehensive version of all details are given in appendix A.

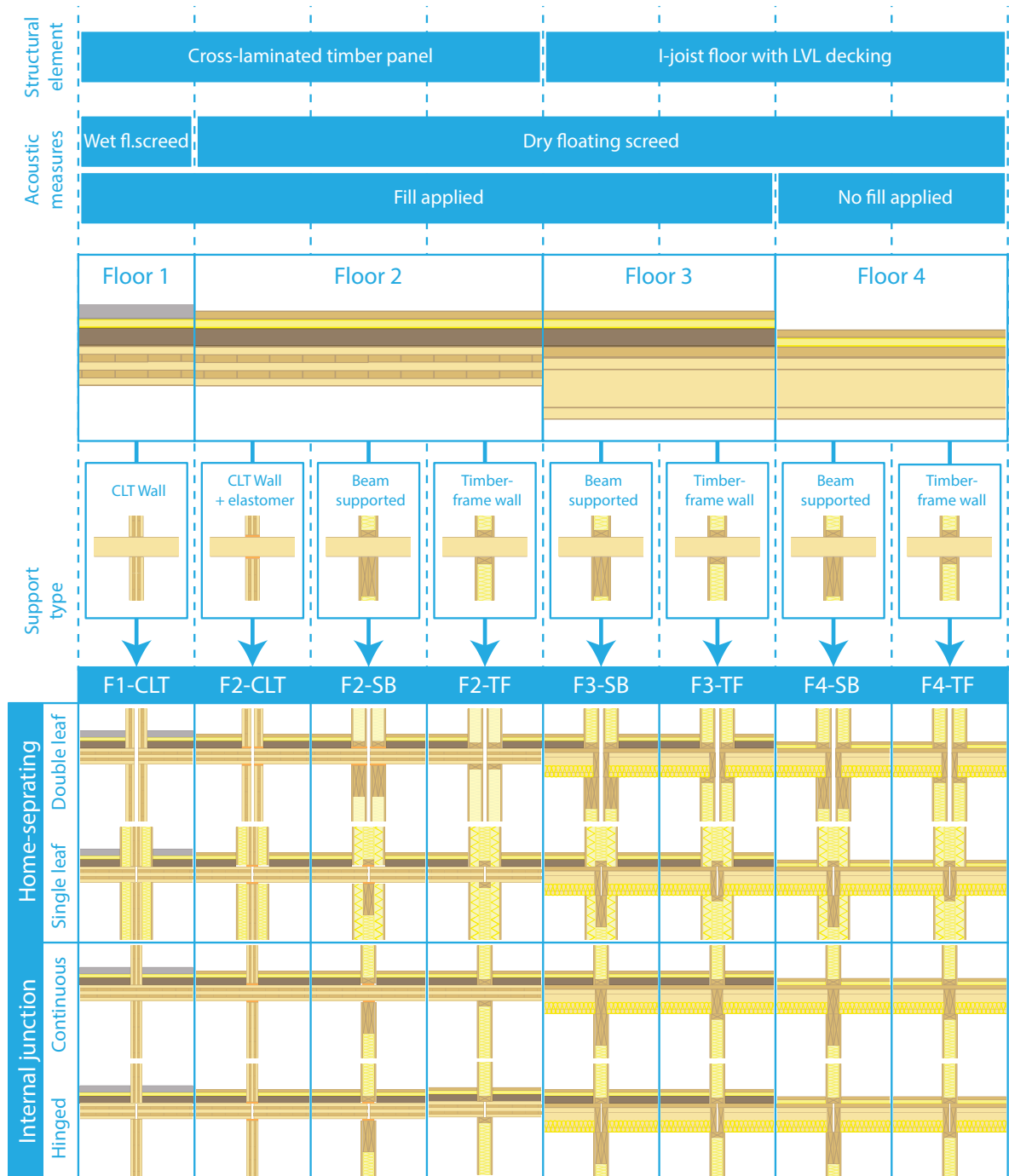


Figure 4.8: Overview of junction details for all floors and their supports (after Dataholz, edited by Oonk)

5

Parameter study

Combinations of support conditions and floor configurations are studied in this chapter by modelling the floor fields as a one-dimensional continuous system. A model with rotational springs describes floors that are supported by CLT panel walls to include clamping-like behaviour. A translational spring model represents floors supported by beams or timber-frame, where no rotational stiffness at the junction is assumed, but transmittance may occur from excited floor fields to adjoining structures.

As elaborated in section 2.5, especially when the vibrations are transmitted from one apartment to another, the levels of acceptance are low [14, 22] and should be prevented. Higher vibration levels are accepted by the receiver when the source is in the same apartment, in particular when the person causing the vibrations is in sight. Therefore, vibration transmittance to a floor in the same unit should be seen separate from vibrations transmitting to adjoining apartments.

A parameter study for floor configurations – and its four support conditions – investigates the effect of varying geometries and properties of the structure regarding human-induced vibrations. This is done for transmittance through the junction as well as excessive vibrations caused by resonance. Therefore the vibration shapes, natural frequencies and area contributing to modal mass are studied for varying parameters. Vibration shapes provide insight in the manner, and level of, vibrations transmit to adjoining fields, and natural frequencies determine the level of resonance, which should be prevented. Natural frequencies are the main variable for steady-state response, whereas the modal mass (and thus the area contributing to m^*) mainly affects the transient response.

First, the procedure from apartment to a Maple model using continuous systems is elaborated upon. After that, the vibration shapes and natural frequencies are studied for floor configurations that are supported by beams walls using a translational model, where several support parameters are varied. Thirdly, the effect of varying CLT wall thicknesses that support floors is studied. Finally, the stiffness and mass of floors are varying to provide insight into their effect upon comfort levels.

5.1 EXPLANATION OF SYSTEM

This chapter studies the effect of varying support- and floor parameter using continuous systems introduced in section 2.2. This section explains how to multi-family buildings study with these systems by boiling down from floor plans to the space-related part of the general solution.

5.1.1 Multi-family residential timber buildings

This work focusses on apartment buildings since people are living close to one another in this type of structures, and therefore transmittance of vibrations requiring special attention. Below shows how the floor fields can be possibly be arranged into useful floor plans, and the manner they are translated into computable systems.

Floor plans

Research by Cobelens [7] found alternating spans to be an effective way to reduce excessive vibration. Equal spans have matching eigenfrequencies (for similar properties) causing resonance and therefore transmitting vibrations more easily. In this research the standard span input for floor field 1 and 3 is chosen to be $L_1 = 3,6$ m and for field 2 and 4 the span is $L_2 = 4,5$ m. The standard input as supporting beam span is 3,6m, which lead to suitable grid sizes for rooms in family apartments.

A possible floor plan for an apartment meeting the grid dimensions is given in figure 5.1 where three floor fields are placed beside one another resulting in a 78 m^2 apartment. The smaller span (L_1) houses two sleeping rooms and a bathroom and the longer floor span for the kitchen and living room.



Figure 5.1: Apartment

Schematization as a beam

A one-dimensional continuous model represents the structure without damping consisting of 5 floor fields. Since the continuous system represents the vibration shape only in one dimension along the x-axis, the floor field has to be modelled as a beam. By picking a strip with 1,0 m width at midspan of the supporting wall or beam (see figure 5.2) a floor field transforms into one dimension. This simplification neglects the influence of the transverse direction and its mode shapes and eigenfrequencies, though it still gives a proper global estimation of vibrational behaviour. The width of 1,0 is chosen because of ease, since it does not influence the results for a 1D continuous system, affecting only EI and q in the equation for fundamental frequency, and thus, cancelling the width out of the system.

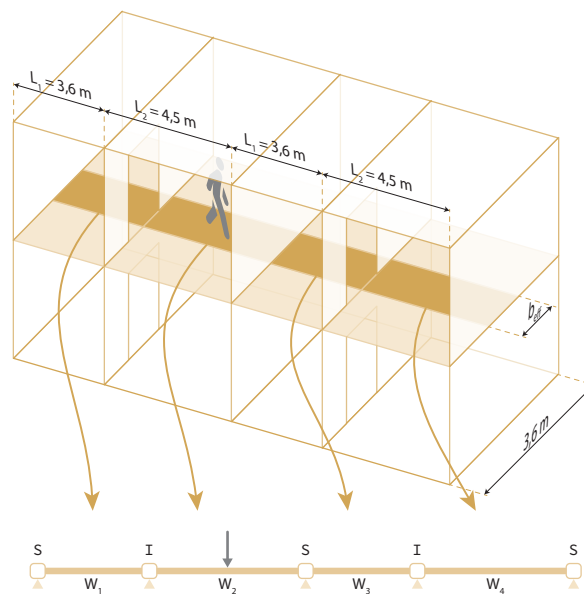


Figure 5.2: Physical representation of the model

5.1.2 Maple model

Solving continuous systems of more multiple floor fields can become complicated, and therefore, not be calculated by hand. For solving the systems of equation the algebraic software package Maple is used, such one finds expressions for the systems in terms of variables like EI , L_1 and L_2 and their values substituted later on in the process. The procedure of solving a system by hand is shown below, resulting in an elegant and simple equation describing the vibration shape in the space-related domain.

A disadvantage of separating space- and time is that damping can not be included, since a term $c \frac{\partial w(x,t)}{\partial t}$ has to be added to the equation of motion (given by equation 5.1). In that case, the solution to the differential equation can not be separated into a space-related and time-related part therewith increasing the computation time. However, for the purpose of this chapter results are not – or negligibly – affected by damping, and therefore left out of the study. Undamped vibrations shapes remain similar to damped ones, and damped fundamental frequencies f_D are only about 0,05% lower ($f_D = \sqrt{1 - \zeta^2} f$) if damping ratios are low, which is the case for timber structure ($\zeta \approx 0,03$).

$$\rho A \frac{\partial^2 w(x,t)}{\partial t^2} + EI \frac{\partial^4 w(x,t)}{\partial x^4} = f(t) \quad (5.1)$$

Elaboration of simply-supported floor

From theorem of continuum dynamics, the vibrations can be described in a continuous manner, where the supports are captured by boundary- and interface conditions as described in section 2.2. These conditions

characterize the relation at supports between floor fields in terms of displacement W , slope $\frac{\partial W}{\partial x}$, bending moment $EI \frac{\partial^2 W}{\partial x^2}$ and shear force $EI \frac{\partial^3 W}{\partial x^3}$. This results in a system of equations, which can be solved, such that the boundary- and interface conditions hold at any moment in time, and the value of $\beta_1 L$ is obtained. After that, modal mass and fundamental frequency of the floor is determined from this factor. Below, the procedure is shown for determination of $\beta_1 L$ for a simply-supported floor field:

In section 2.2 the general solution in the space domain is obtained, which is defined as:

$$W(x) = A \sin(\beta x) + B \cos(\beta x) + C \sinh(\beta x) + D \cosh(\beta x) \quad (5.2)$$

The vibration shape is found by substituting this solution into the boundary conditions, such that the solution holds at any given moment in time, and after that, the constants A , B , C and D can be solved. In the case of a simply-supported beam, both displacement and bending moment have to be equal to zero at the two boundaries:

$$\begin{aligned} x = 0: \quad & W(0) = 0 \quad \rightarrow B + D = 0 \\ & -\frac{\partial^2 W(0)}{\partial x^2} = 0 \quad \rightarrow -B + D = 0 \\ \\ x = L: \quad & W(L) = 0 \quad \rightarrow A \cdot \sin(\beta L) + C \cdot \sinh(\beta L) = 0 \\ & -\frac{\partial^2 W(L)}{\partial x^2} = 0 \quad \rightarrow A \cdot -\beta^2 \sin(\beta L) + C \cdot \beta^2 \sinh(\beta L) = 0 \end{aligned}$$

This set of equations read in matrix notation:

$$\mathbf{A}\bar{X} = 0 \quad = \quad \begin{bmatrix} 0 & 1 & 0 & 1 \\ 0 & -1 & 0 & 1 \\ \sin(\beta L) & 0 & \sinh(\beta L) & 0 \\ -\beta^2 \sin(\beta L) & 0 & \beta^2 \sinh(\beta L) & 0 \end{bmatrix} \cdot \begin{bmatrix} A \\ B \\ C \\ D \end{bmatrix} = \begin{bmatrix} 0 \\ 0 \\ 0 \\ 0 \end{bmatrix}$$

One finds the non-trivial solution of the set of equations by setting the determinant of matrix A equal to zero. For this case, one finds that the solution only holds if $B = C = D = 0$ and $A = 1$, such that one obtains:

$$\sin(\beta_n L) = 0 \quad (5.3)$$

The only unknown in this equation is β_n , which is a measure for the natural frequency. In most cases, it is impossible to find an analytical solution, and β_n has to be found transcendently using software packages. In this simple case, one can see that equation 5.3 is zero for:

$$\beta_n L = n\pi \quad \text{for } n = 1, 2, \dots, \infty \quad (5.4)$$

Therefore, the mode shapes ϕ_n (or eigenfunctions) are given by substituting this β_n and the values of A , B , C and D in the general solution of equation 5.2:

$$\phi_n(x) = A_n \sin(\beta_n x) = A_n \sin\left(\frac{n\pi}{L} x\right) \quad \text{for } n = 1, 2, \dots, \infty \quad (5.5)$$

The mass contributing to mode n is found by integrating the square of ϕ_n over the length times the distributed mass q :

$$m^* = \int_0^L q \phi_n^2(x) dx = \frac{1}{2} q L \quad (5.6)$$

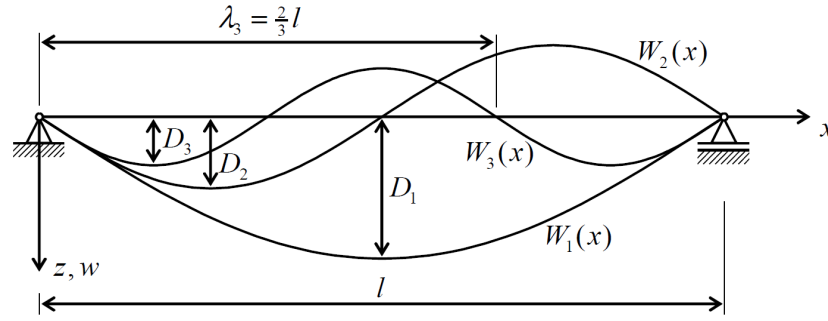


Figure 5.3: Mode shape ϕ_1 , ϕ_2 and ϕ_3 of a simply-supported beam [27]

Multiple floor field systems

Continuous systems describe the vibration shapes of a structure following from dynamic relations. It separates the variables of time and space, which is only possible for undamped systems, where the multiplication of both expressions results in the vibration in both space and time (see section 2.2). The parameter study focusses mainly on the space-related part since it holds the maximum amplitude at each location of the structure and is therefore suited for comparison of different configurations.

The following set of equations describes the space-related part of a structure with multiple floor fields as in figure 5.2:

$$\begin{aligned}
 W_1(x) &= A_1 \cosh(\beta x) + B_1 \sinh(\beta x) + C_1 \cos(\beta x) + D_1 \sin(\beta x) \\
 W_2(x) &= A_2 \cosh(\beta x) + B_2 \sinh(\beta x) + C_2 \cos(\beta x) + D_2 \sin(\beta x) \\
 W_3(x) &= A_3 \cosh(\beta x) + B_3 \sinh(\beta x) + C_3 \cos(\beta x) + D_3 \sin(\beta x) \\
 W_4(x) &= A_4 \cosh(\beta x) + B_4 \sinh(\beta x) + C_4 \cos(\beta x) + D_4 \sin(\beta x)
 \end{aligned} \tag{5.7}$$

The values of constants A_n , B_n , C_n and D_n can be obtained from the boundary conditions as shown in section 2.2 for a single floor field. In case multiple fields are connected, the relation between those are expressed using interface conditions at the connecting node. Floor field 2 holds the exciting force and therefore has to be split into 2 floor fields connected by the interface conditions describing continuity of displacement, slope and bending moment and shear force equilibrium with the exciting force.

By substituting the general solutions given in equation 5.7 one obtains a system of equations containing the constants. To find expressions for the constants for which does apply that the prerequisites of boundary- and interface conditions hold, the system of equations is solved linearly. Therefore, the vibration shape follows from the substitution of values for variables, independent of the magnitude. This algebraic property makes the method suitable for parametric study of floor fields since many slight variances can be studied using a consistent system.

Once the constants are solved for the interface- and boundary conditions one ends up with an expression for the vibration shape of field n with the following input quantities for the rotational ($W_{n,R}$) and translational model ($W_{n,T}$):

$$W_{n,R}(EI, \rho, A, q, L_1, L_2, P, x_f, r_s, r_i, f_s)$$

$$W_{n,T}(EI, \rho, A, q, L_1, L_2, P, x_f, k_s, k_i, f_s)$$

Where: EI Flexural stiffness of floor section in Nm^2/m
 ρ Mass density of structural floor element in kg/m^3
 A Cross-sectional area of structural floor element in m^2
 q Self-weight of floor and quasi-permanent load (e.g. furniture and partitions) in kg/m^2
 L_1 Floor span L_1 in m
 L_2 Floor span L_1 in m
 P Mass of one person in N
 x_f Location of person in field 2
 r_s Rotational stiffness of separating junction in Nm
 r_i Rotational stiffness of internal junction in Nm
 k_s Translational stiffness of separating junction in m/N

- k_i Translational stiffness of internal junction in m/N
 f_s Step frequency in Hz

Standard translational stiffness of the internal and home-separating junction is $k_s = k_i = 4.6 \cdot 10^3$ N/m. For junction 1 the standard width of the supporting wall is $b = m$, which is equivalent to a rotational stiffness of $r_s = r_i = 0.05$ Nm/rad. The standard width of the elastomeric supported floor of junction 2 is $b = m$ and corresponding with a rotational stiffness of $r_s = r_i = 0.01$ Nm/rad.

In section 2.2 the boundary conditions for a floor field are given, and by combining them, one can generate interface conditions for connecting multiple floor fields. Since the general solution follows from the fourth-order differential problem (see section 2.2), one needs four interface conditions at each connection node expressing the support conditions. Interface conditions can either be kinematic relation (i.e. displacement or slope related) or a dynamic force (i.e. related to moment or shear equilibrium).

At the boundaries, i.e. node A and E, only two conditions have to hold, and several situations are given in table 2.1. Below are the determined interface conditions summed up for the rotational model, which are used for junction typology 1 and 2, and for the translational model needed for junction typologies with supporting beams (i.e. 3, 4 and 5). Below are only general interface conditions regarding force- and moment equilibrium elaborated for a junction, where the node-specific ones are added in the Appendix table C.1.

Explanation of used graphs

The effect of changing parameters is explained in this chapter using three types of figures, namely the vibration shape, natural frequency and modal mass area. Below are each of these graphs briefly explained in terms of how they are obtained and what they represent.

Vibration transmission plots

The first graph is the vibration shape and visualises the effect of changing the parameter upon the first mode shape. Each time two different typologies are shown besides one another to easily compare them. It has to be noted that the displayed shape is the maximum amplitude in the space-domain and the floor oscillates in that specific shape around its resting position. The graphs aim to visualise the shape itself and not the magnitude, because there is in reality damping present affecting the magnitude, and therefore, no axes are shown in the graphs. One- and two-span fields are shown in the same plot for both double- and single leaf support conditions, where the typologies with a hinged internal junction (orange for double leaf, cyan for single leaf) are shown downwards and a continuous floor field upwards (red for double leaf, blue for single leaf).

Natural frequencies

Natural frequencies of typologies affected by the parameter are shown in the natural frequency graphs, where each of the four support conditions are shown separately. Natural frequencies are especially of interest for steady-state responses, since these only occurs if the fundamental frequency corresponds with one of the walking load harmonics. These natural frequencies are calculated from the βL values and floor properties using the following equation:

$$f_n = \frac{(\beta L)^2}{2\pi L_s^2} \sqrt{\frac{EI_L}{q}}$$

Floor area contributing to modal mass

The modal mass linearly decreases the initial velocity of transient responses, and therefore also included in the parameter study. As shown by equation 5.6 follows the modal mass from the area covered by the mode shape, which is the amount of mass that is set into motion. The floor area that contributes to the modal mass is displayed to make the graph more generic, where the modal mass is $m^* = q \cdot \lambda$. The equation used for approximating the modal mass area is derived from the modal mass approximation of a equivalent SDOF system in section 6.1. In this expression is accounted for the effective width of the floor by the equivalent spring stiffness K_{eq} .

$$\lambda = \frac{K_{eq,eff}}{EI_L} \left(\frac{L_s}{\beta_1 L} \right)^4$$

Maple sheets flowchart

Three graphs are generated in the software package Maple by connecting several worksheets, see figure 5.4 where an overview is shown. Two sheets illustrated at the sides function as input for the plot-generating sheets in the center. *Junction typology properties* holds the floor- and support properties to ensure consistency in all calculations. *System solver* provides solutions to the interface- and boundary conditions, like the general solution in the space-domain for study of transmittance, the characteristic frequency equation that has to be solved to find βL and the static solution for determining the modal mass area. Both the natural frequency and modal mass area are used in next chapter, when the floors are transformed into Single Degree of Freedom systems for assessment.

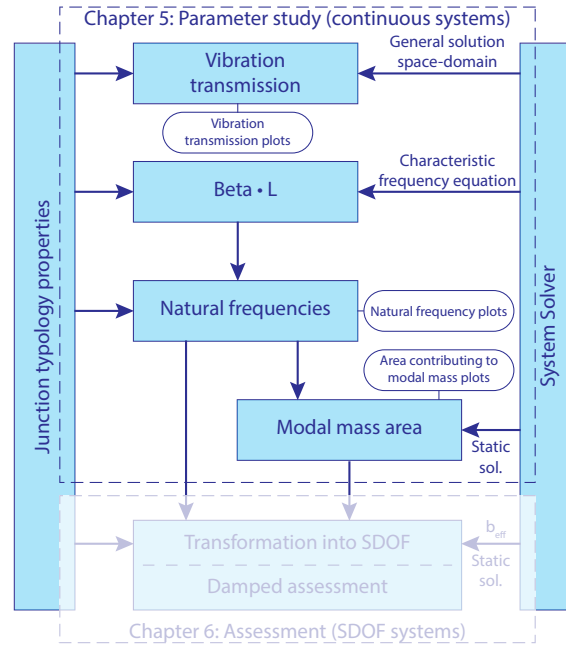


Figure 5.4: Flowchart of Maple sheets for chapter 5

5.2 TRANSLATIONAL STIFFNESS SUPPORT

This section introduces the translational model, where the nodes (i.e. junctions) are supported by springs. The type of load-bearing structure is represented by the spring stiffness. For timber-frame walls is the equivalent spring stiffness high, and, as a result, the junction almost acting like a rigid one. Since the influence of about 0,05 mm translation at the support is negligible for determination of natural frequencies and modal mass are timber-frame supports assumed to be rigid. Contrary, floors supported by beams are able to translate significantly, affecting the vibration shape and fundamental frequency. Besides, the location of the excitation source does affect the level of node translation.

With the translational model effects of support stiffness upon vibration shapes, natural frequencies and modal mass are studied. The first parameter is the height of the supporting beam at the home-separating junction, and second the height at the internal junction. Thirdly, the spanning length of the supporting beam is varied, and therewith the spring stiffness, where a relatively short span ($L \approx 0,6m$) represent a timber-frame wall.

5.2.1 Translational model

Floor 3 and 4 hold joists with decking as structural element thus is chosen their load-bearing components to be a timber-frame structure or a beam. One of the CLT floors, as introduced in section 4.4, either has a timber-frame (F2-TF) or beam (F2-SB) as support.

Because the grain directions are parallel to the contact surface of both timber-frame and Kerto-S beams, it is assumed that no clamping behaviour occurs at the nodes. Therefore, the bending moments of the floor are zero at the junction, except for a continuous floor field at the junction, where the bending moment left from the nodes equals the moment at the right. If the floor is supported by CLT walls, there are wood fibres parallel to the contact surface, and therefore clamping-like behaviour can occur as will be addressed in section 5.3.1

Boundary- and interface conditions of home-separating and internal junctions

In the translational model, nodes are able to translate vertically, but when it does so, a force from the supporting structure tries to restore it to the resting position. For timber-frame structures is this force equal to the E-modulus perpendicular to the grain times the structural wall width. Beams are relatively flexible compared to timber-frames, causing it to deflect under an applied point load. Therefore, contact stresses equal to timber-frames can not be reached and is the modelled spring stiffness k is equal to F/w . The resulting forces at the supports make equilibrium at the nodes with shear forces acting in the floor, as is shown in figure 5.5b-5.7b. These relations translate into interface conditions shown at (c) and schematize into springs given at (d).

Mechanical schemes

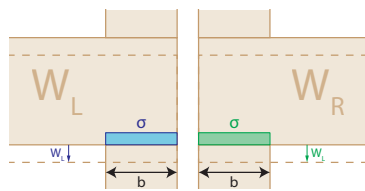
Each mechanical scheme translates in different interface conditions to ensure equilibrium of vertical forces at the node. Figure 5.8 shows the support conditions of interest being constructed using the junctions given previously. The home-separating junction consists of either one (single, figure 5.6) or two walls (double leaf, figure 5.5). The floor between two home-separating junctions is made out of one piece (figure 5.6) or split into two at the internal junction (figure 5.7).

Table C.2 in the appendix provides interface conditions of all nodes, including the conditions at the location of the force.

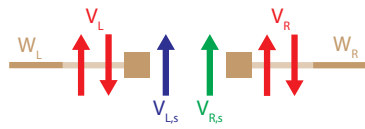
5.2.2 Location of force

In section 4.4 are four different floors introduced resting on three different types of supports. Two of them are relatively stiff wall supports, i.e. a Cross-laminated timber wall and timber-frame structure, since their dynamic translation is negligible in contrast to amplitudes in the floor. For floors supported on a beam does, however, the displacement at the junction contribute significantly to the total amplitude of the floor.

Floors supported by beams show significant higher amplitudes, see figure 5.9, compared to the previous situation because the floors its supports will displace as well due to lack of stiffness. Besides resulting in an



(a) Stresses due to translation



(b) Nodal force equilibrium

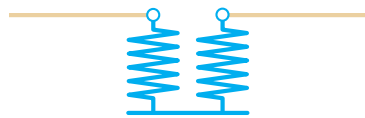
$$EI \frac{\partial^2 W_L}{\partial x^2} = 0$$

$$EI \frac{\partial^3 W_L}{\partial x^3} = kW_L$$

$$EI \frac{\partial^2 W_R}{\partial x^2} = 0$$

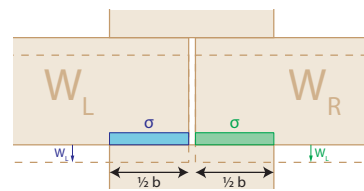
$$-EI \frac{\partial^3 W_R}{\partial x^3} = kW_R$$

(c) Interface conditions

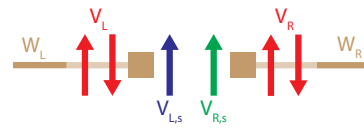


(d) Mechanical schematization

Figure 5.5: Double leaf junction



(a) Stresses due to translation



(b) Nodal force equilibrium

$$W_L = W_R$$

$$EI \frac{\partial^2 W_L}{\partial x^2} = 0$$

$$EI \frac{\partial^2 W_R}{\partial x^2} = 0$$

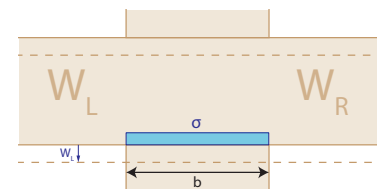
$$EI \left(\frac{\partial^3 W_L}{\partial x^3} - \frac{\partial^3 W_R}{\partial x^3} \right) = kW_L$$

(c) Interface conditions

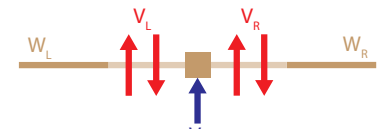


(d) Mechanical schematization

Figure 5.6: Single leaf junction with interrupted floor field



(a) Stresses due to translation



(b) Nodal force equilibrium

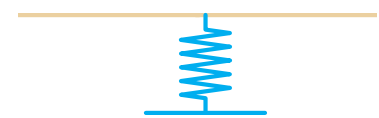
$$W_L = W_R$$

$$\frac{\partial W_L}{\partial x} = \frac{\partial W_R}{\partial x}$$

$$EI \left(\frac{\partial^2 W_L}{\partial x^2} \right) = EI \left(\frac{\partial^2 W_R}{\partial x^2} \right)$$

$$EI \left(\frac{\partial^3 W_L}{\partial x^3} - \frac{\partial^3 W_R}{\partial x^3} \right) = kW_L$$

(c) Interface conditions



(d) Mechanical schematization

Figure 5.7: Single leaf junction with continuous floor field

additional amplitude at the floor midspan, it either enables vibration transmittance to adjoining floor fields. Vibrations can be transmitted to neighbouring apartments, causing hindrance at low levels of vibrations, for the single leaf separating junctions. Especially when the exciting force is close to the home-separating junction (i.e. arrow in green), significant vibrations occur in the neighbouring floor field. Flexible hinged internal supports either cause rigid body rotation by a translating right edge, as shown in figure 5.9b and 5.9d. The same holds for the internal junction, where the highest amplitudes are found when the excited source is close to the internal wall (i.e. blue arrow).

Timber-frame structures are, likewise to cross-timber walls, acting really stiff, and therefore prevent transmittance of vibrations through the junction by rigid body movement. For these structure types, transmittance of vibrations only occurs for continuous floor fields where the dynamic hogging moment at the internal support results in bending at the other in-home floor field, such that it vibrates in anti-phase with the excited field. This phenomenon holds for the other two wall types as well, though the rigid-body rotation dominates for beam supported adjoining floor fields.

Now consequences for the vibration level of the force location in all four floor field are known, will the influence of several support- and floor parameters be studied regarding transmittance. Since the application of force at midspan generally results in the highest amplitudes will only this force location be studied. It

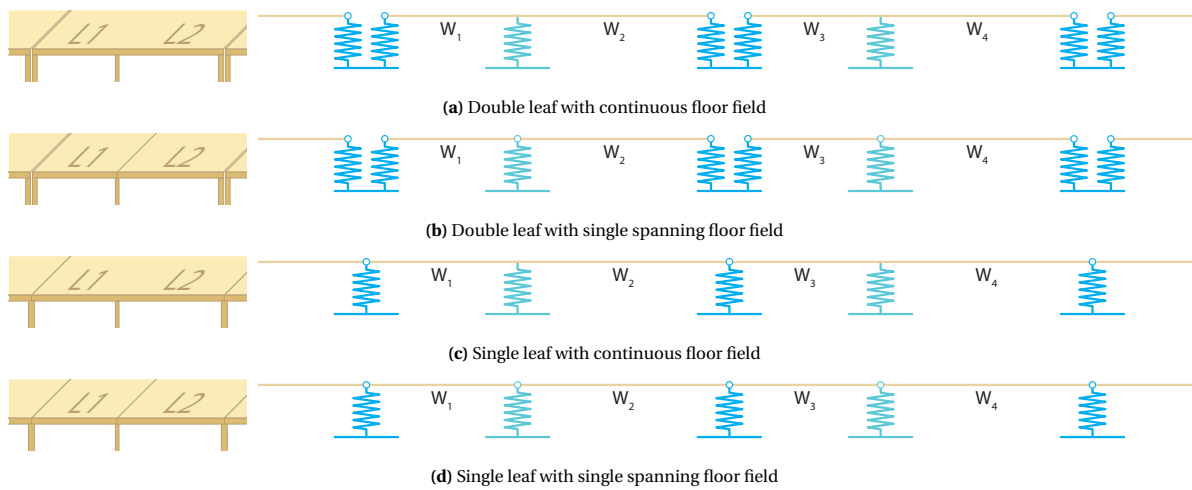


Figure 5.8: Mechanical schemes for translational model

should be noted that for the beam supported forced vibration shape higher values are obtained when one applies the force close to the edges of the excited floor field.

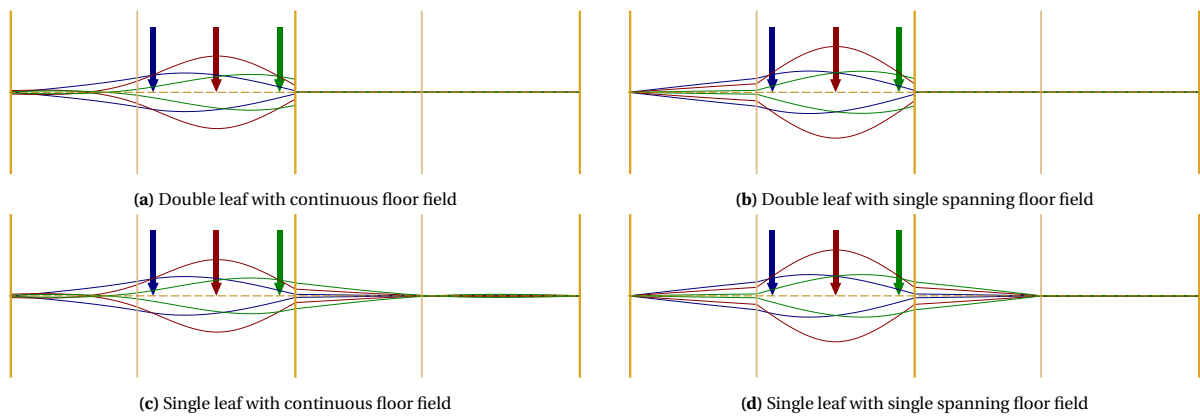


Figure 5.9: Vibration shapes of beam supported floor for various force locations

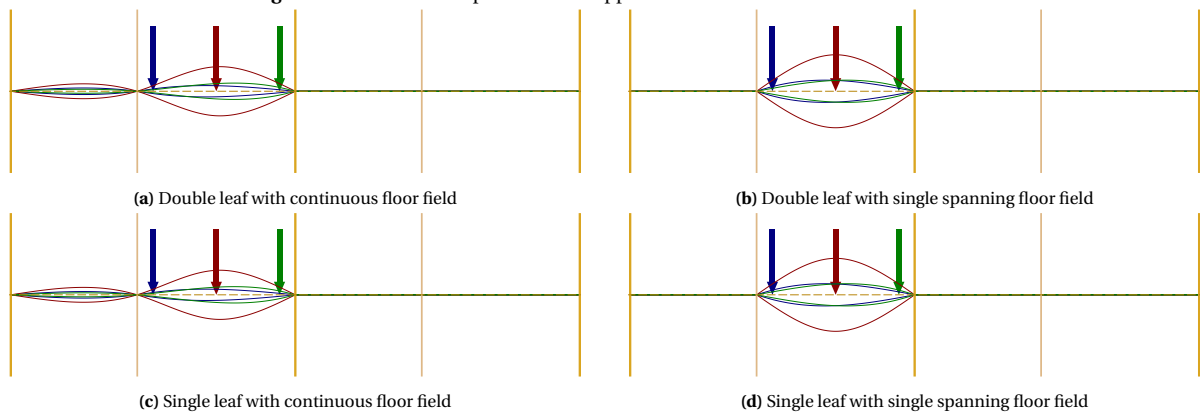


Figure 5.10: Vibration shapes of timber-frame supported floors for various force locations

5.2.3 Beam height at home-separating junction

As previously mentioned does the support stiffness significantly influence amplitudes of the floor, since these displacements add up to deflection of the floor itself. For beam heights of 180, 260 (original) and 400 mm the vibration shapes are shown in figure 5.11 for a CLT floor (F2-SB) and in figure 5.12 for an I-joist floor. It can be concluded that increasing the support stiffness results in significant amplitude reduction, where the I-joist floor is more sensitive due to its higher flexural floor stiffness. A beam height of 400mm (over a span of 3,6m) almost acts like a stiff wall, therewith decreasing transmittance of vibrations to neighbours for single leaf home-separating walls.

Lowering the beam height decreases the natural frequency with 2 to 3 Hz, which is the case for heights below about 250mm. Above that height, the natural frequency increases only slightly, because the beam at the internal junction is still 260mm which limits the positive effect of increasing home-separating beam height.

Besides, continuous floor fields (i.e. (a) and (c)) show two lines for natural frequencies, whereas hinged floors only show one. This is the consequence of floor field with span L_1 is connected to the excited field, and therefore either contributing to the system.

For the floor area that contributes to the modal mass (λ) the same can be concluded as for natural frequencies. For Double leaf typologies, the effect of supporting beam height is negligible, whereas for single leaf some beneficial effects are visible below 250mm (see figure 5.14) because some mass of adjoining apartments contributes to the vibration.

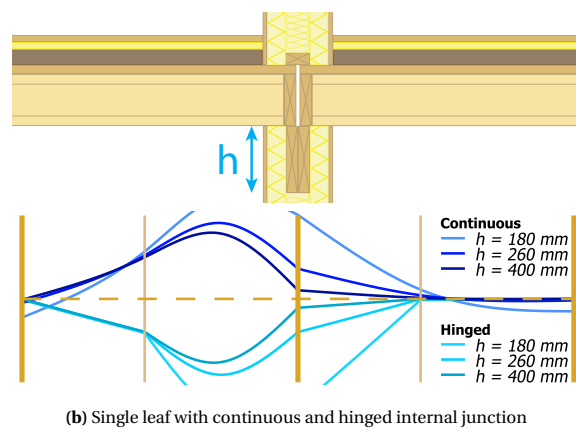
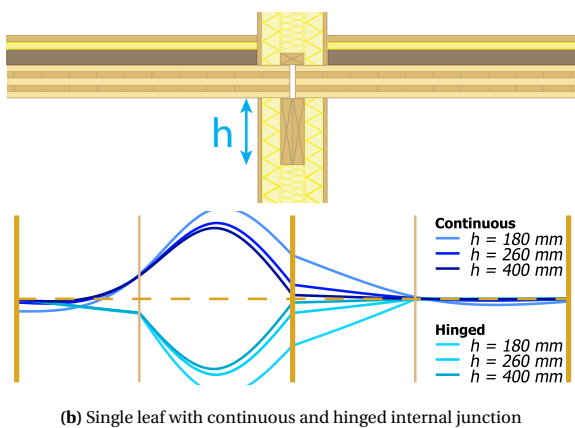
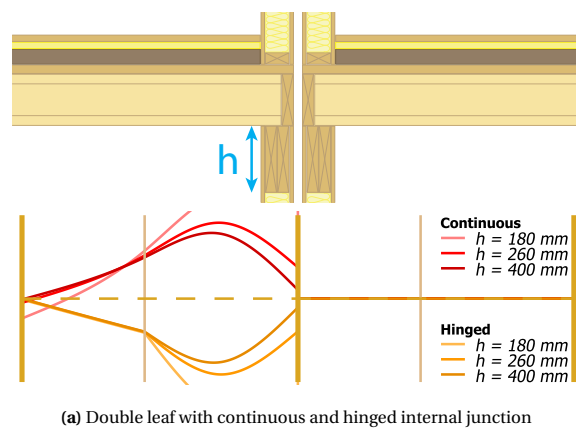
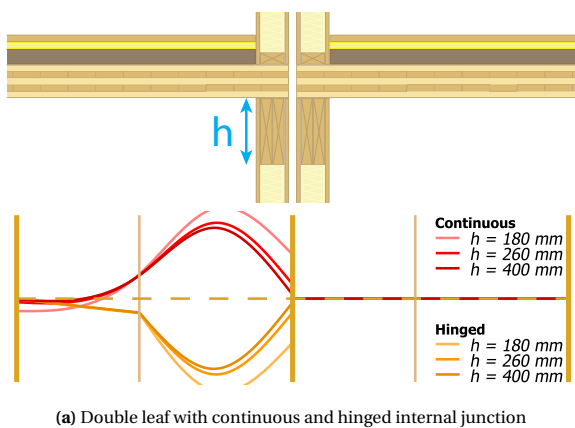


Figure 5.11: Vibration shapes of floor 2 supported by beams (F2-SB) for varying beam height at home-separating junctions

Figure 5.12: Vibration shapes of floor 3 supported by beams (F3-SB) for varying beam height at home-separating junctions

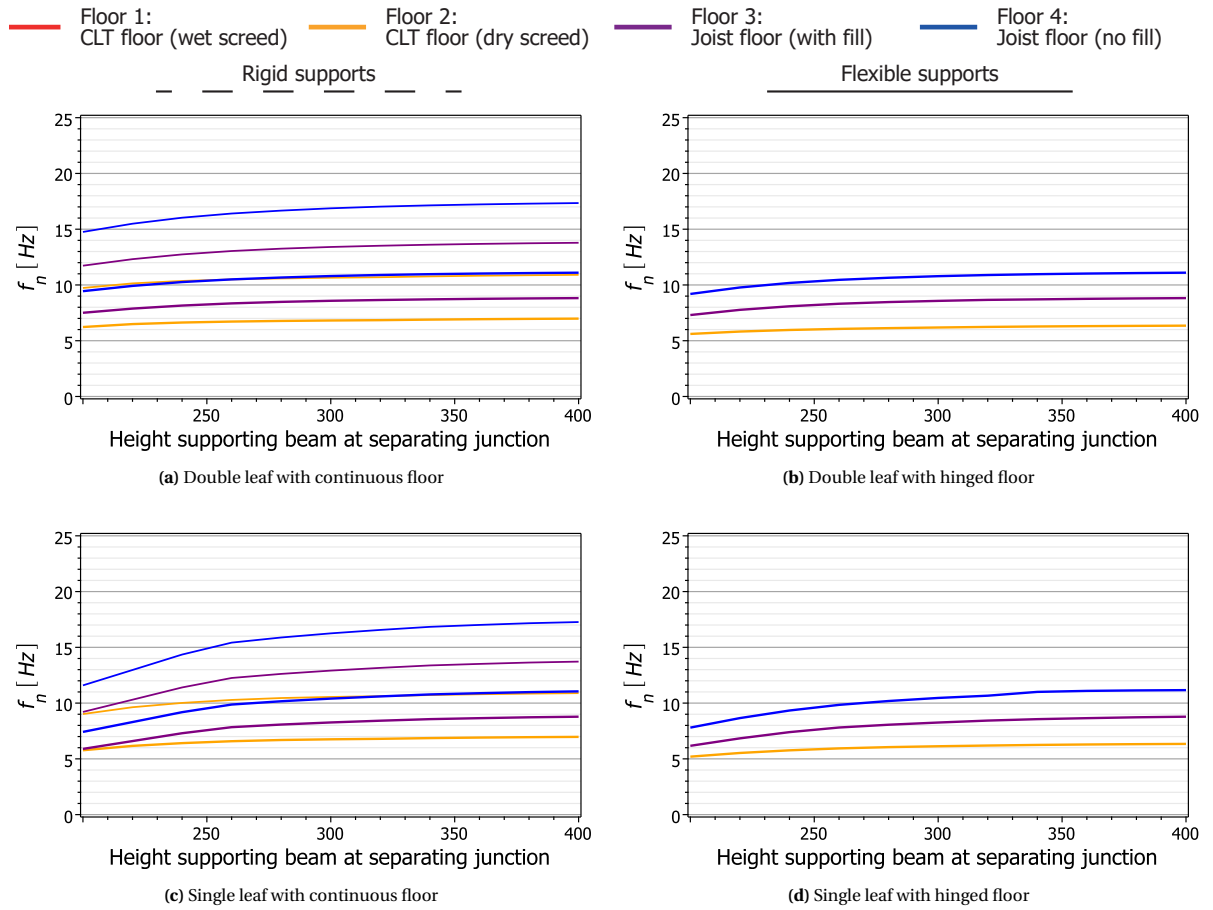


Figure 5.13: Natural frequencies for varying beam height at home-separating junctions

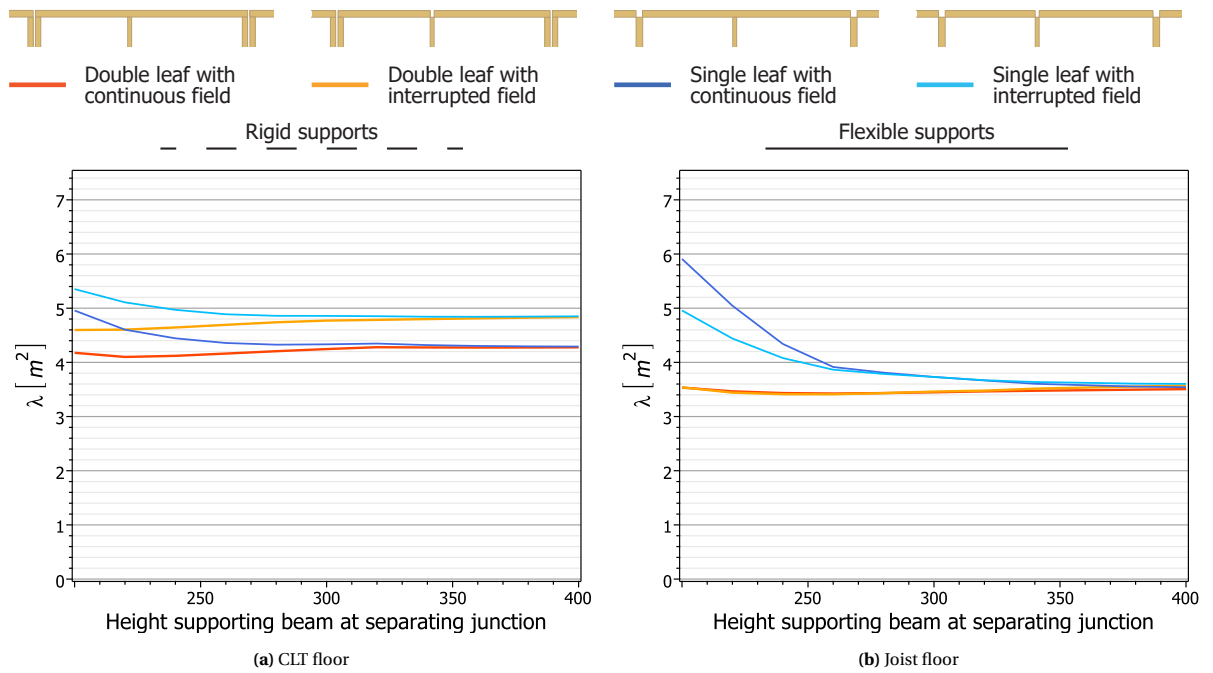


Figure 5.14: Modal mass area for varying beam height at home-separating junctions

5.2.4 Beam height at internal junction

Transmittance to the other home-field can be prevented through stiffness of the internal support. In figure 5.15 (CLT floor) and figure 5.16 (joist) are the shapes shown for the same beam heights as for the home-separating beam, i.e. 180, 260 and 400 mm. Likewise, increasing stiffness appears to be a useful parameter for preventing transmittance. In this case, the vibration levels in the other home-field L_1 are reduced, whereas for the neighbouring apartment, slight improvement is visible for increasing beam height. For single spanning floor, fields is the comfort level increased by reducing the rigid-body rotation of the other home-field. A stiff internal support prevents the shape to occur over the length of both floor fields for continuous floor fields, especially for the stiffer joist floor and reduces transmittance as well.

Improvements of about 4 to 5 Hz regarding natural frequencies are found for the continuous joist floors, see figure 5.17a and 5.17c, where a stiffer support enables the floor to activate its full flexural stiffness. CLT floors, having less longitudinal flexural stiffness, show improvements of about 2 Hz between a beam height of 200 and 400mm.

For CLT floors does the modal mass area not vary much, as can be observed in figure 5.18a, because the equivalent spring stiffness K_{eq} increases for higher beams (i.e. decreasing static deflection) as well as the βL values, partly counter interacting each others effects.

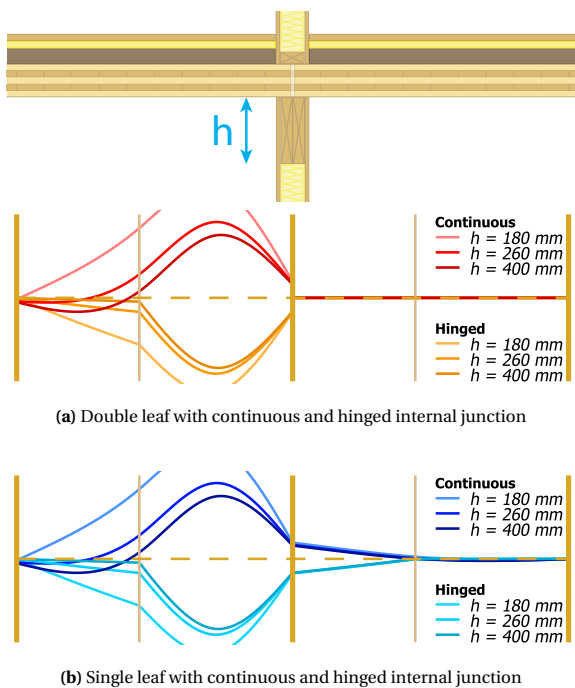


Figure 5.15: Vibration shapes of floor 2 supported by beams (F2-SB) for varying beam height at internal junctions

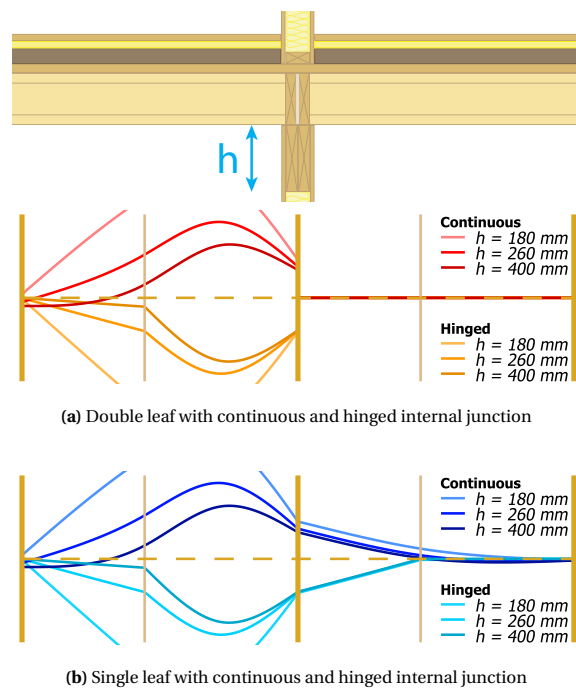


Figure 5.16: Vibration shapes of floor 3 supported by beams (F3-SB) for varying beam height at internal junctions

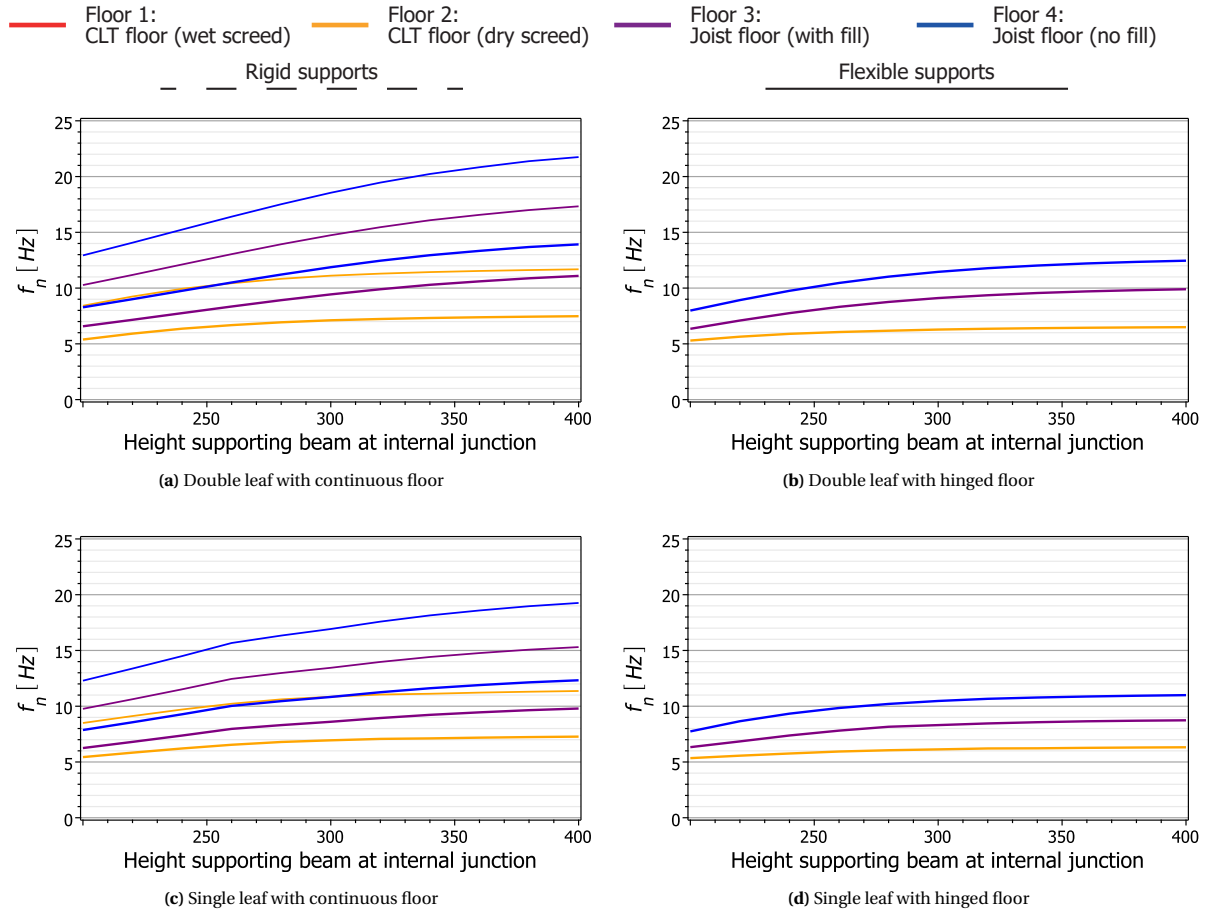


Figure 5.17: Natural frequencies for varying beam height at internal junctions

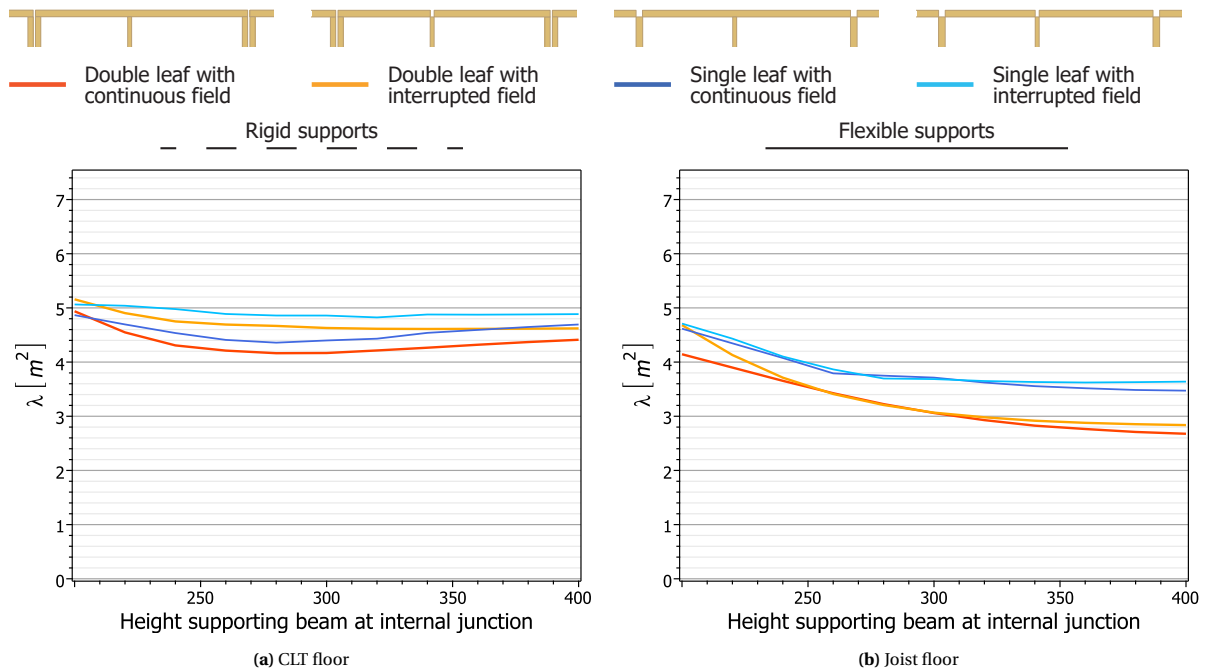


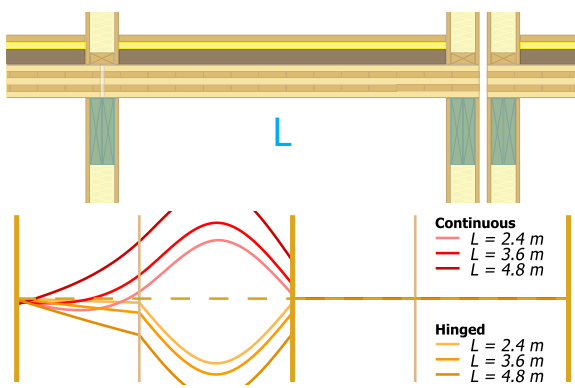
Figure 5.18: Modal mass area for varying beam height at internal junctions

5.2.5 Spanning length of supporting beam

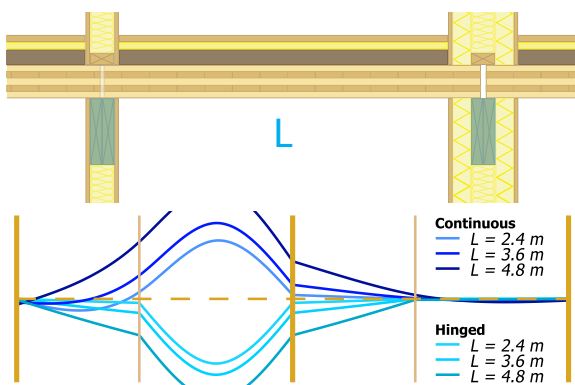
Contrary to the previous two cases, where the support stiffnesses were varied separately, both supports are modified similarly by spanning length of the supporting beams. This is shown in figure 5.19 for a CLT floor and in figure 5.20 for a joist floor, where spanning lengths of 2,4, 3,6 and 4,8 m are displayed. Equally to the case where support stiffnesses were varied separately, the amplitude does reduce for smaller spanning lengths due to less vertical translation of the support. Moreover, for joist floors (figure 5.20) stronger effects are visible than for CLT floors figure 5.19 because of higher flexural stiffness.

Figure 5.21 shows the natural frequencies for beam supported typologies F2-SB (green), F3-SB (purple) and F4-SB (blue). Frequencies read from the graph for a spanning length of 0,6m represent a timber-frame structure (i.e. almost rigid support). The effect of increasing spanning length (and thus reducing support stiffness) has a minor effect up to about 2 m, but for higher spans, the natural frequencies drop rapidly. Stiffness of the whole structure reduces due to the lack of stiffness at the supports, but for large spanning lengths, the graphs flatten again. This results in an S-shaped curve for the natural frequencies. It has to be noted that for a certain spanning length the natural frequencies of the excited floor field drops below the cut-off frequency of 8Hz, even for high-frequency joist floors. Besides, for single spanning floor situations, an additional resonance frequency is observed, since the other home-field contributes to the system as well.

Less stiffer supports result in larger amplitudes in either excited and adjoining floors (see figure 5.19 and 5.20). Since the modal mass depends on the area under these lines, increases the floor area also that contributes to the modal mass shown in figure 5.22. Although, higher comfort levels at adjoining floor fields should be prevented, especially to the more sensitive neighbours, may this increase in modal mass be beneficial for HFF floors, since mass is the dominant factor for transient responses.

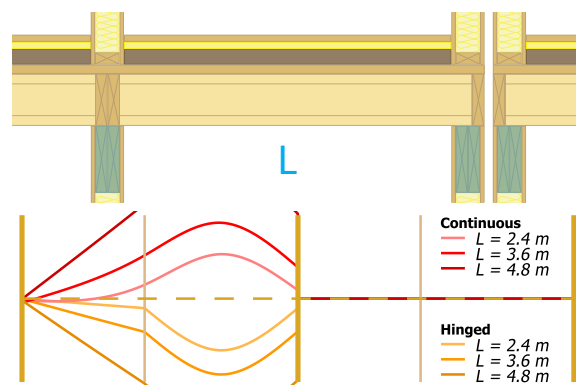


(a) Double leaf with continuous and hinged internal junction

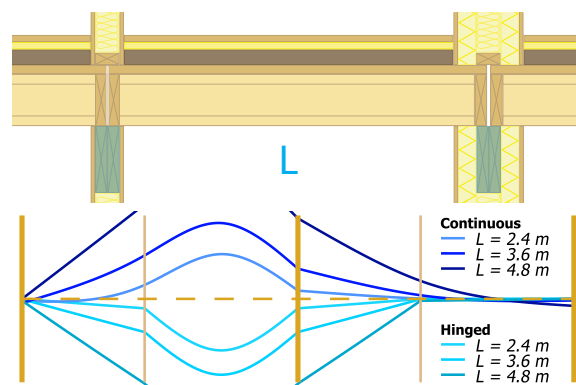


(b) Single leaf with continuous and hinged internal junction

Figure 5.19: Vibration shapes of floor 2 supported by beams (F2-SB) for varying spanning length of supporting beam



(a) Double leaf with continuous and hinged internal junction



(b) Single leaf with continuous and hinged internal junction

Figure 5.20: Vibration shapes of floor 3 supported by beams (F3-SB) for varying spanning length of supporting beam

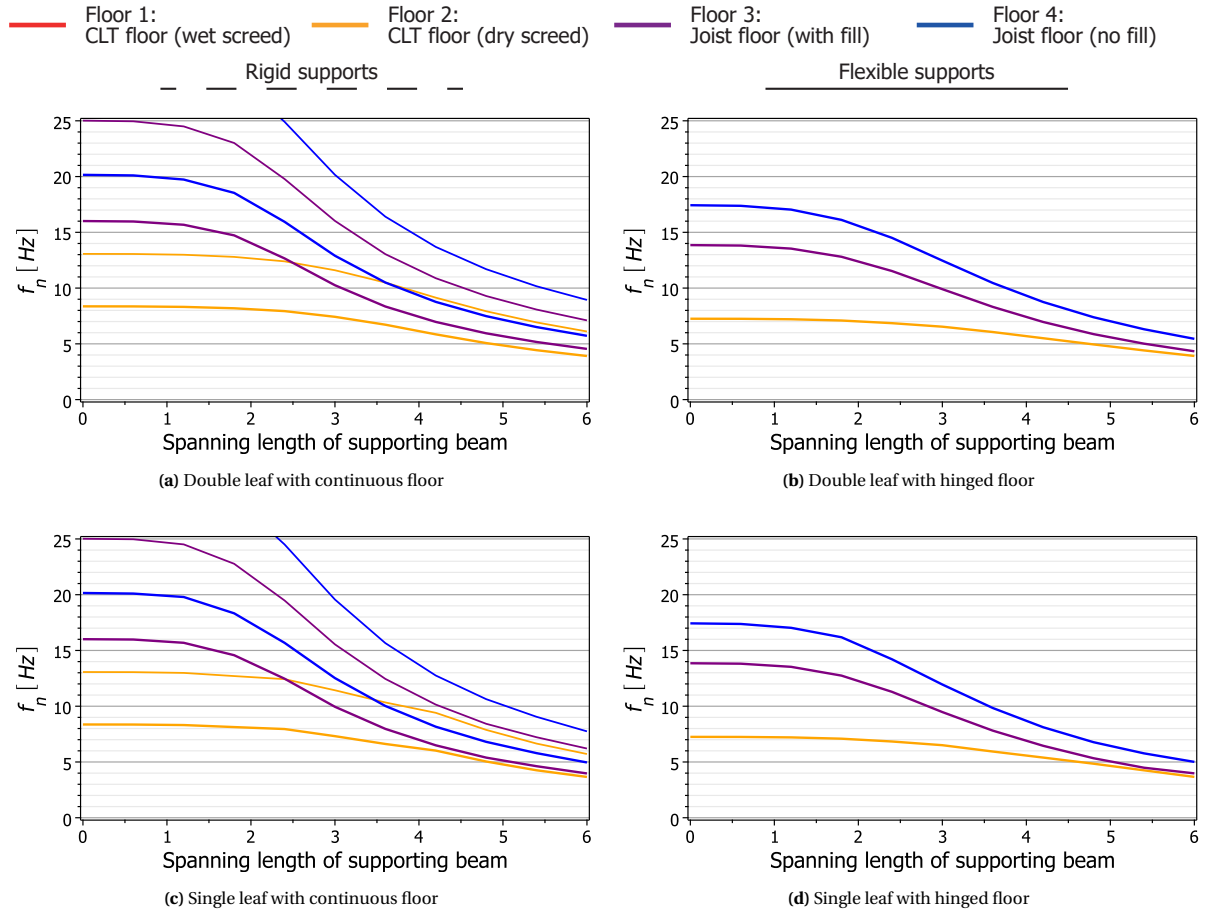


Figure 5.21: Natural frequencies for varying beam spanning length of supporting beam

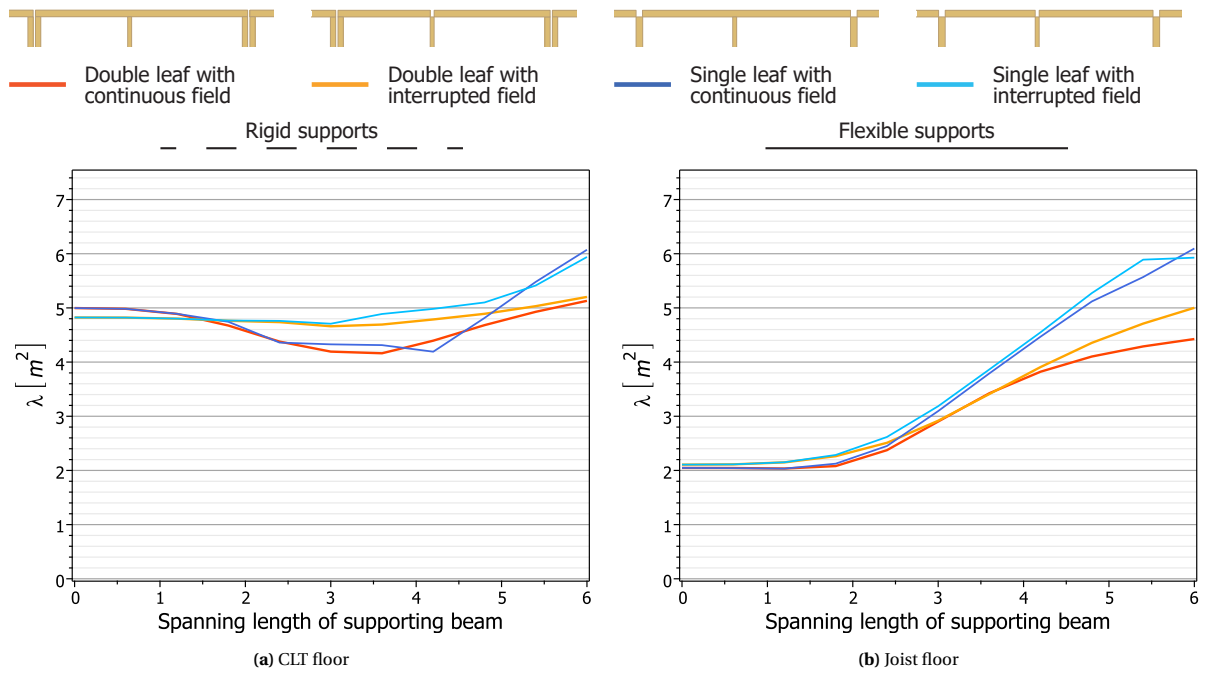


Figure 5.22: Modal mass area for varying beam spanning length of supporting beam

5.3 ROTATIONAL STIFFNESS SUPPORT

This thesis studies four different support conditions commonly applied in timber housing. Two types of home-separating junctions can be distinguished; namely, a double leaf junction physically disconnecting both apartments and a single leaf where both home's floor fields are supported by the same wall. Within the apartment the floor field can be single or double spanning, resulting in a continuous junction at the internal support or one with an interrupted floor.

5.3.1 Rotational model

The first two junction typologies consist of CLT floors supported by CLT panel walls. Massive timber walls do react stiff in the vertical direction, and therefore, displacement of the nodes can be neglected. Due to the stiff supports, influence of clamping-like behaviour under dynamic loading at the supports may develop. In static situations, the influence of clamping is negligible since high moments and rotations occur at the support needing much normal force for effect to appear.

Boundary- and interface conditions of home-separating and internal junctions

Rotations at the junctions are partly counteracted by clamping-like behaviour of the massive timber walls, as is schematized in figure 5.23a-5.25a. The use of algebraic equations for vibration shapes enables one to express both bending moments and rotation at the nodes in terms of the rotational stiffness r . If that variable is the only one left in the expression for equilibrium at the node, it can be solved and found.

Under dynamic loading the bending moments are relatively small compared to the rotations, and significantly less normal force is required for only compressive contact forces between the wall and floor to occur (see table 5.1). This effect increases a junction's rotational stiffness and, in addition to that, increasing eigenfrequencies of the floor structure since more modal mass transfers towards the supports. In general, higher natural frequencies result in lower vibration levels and thus can have a beneficial effect [78, 79].

For the clamping-like behaviour to be fully present, only compressive contact forces between the wall and floor structure may occur. Therefore, the normal forces introduced by the upper wall – or introduced by screws – require a certain magnitude to ensure the floor making contact with the wall over the full cross-section. Floor 2 has a resilient elastomer applied between floor and wall as acoustic measure, resulting in a very low rotational stiffness and almost acting like a pinned connection. For floor 1 no material is applied in between wall and floor, and more mass is added to increase airborne sound insulation.

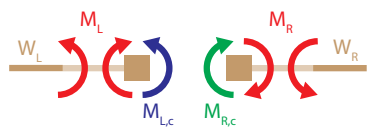
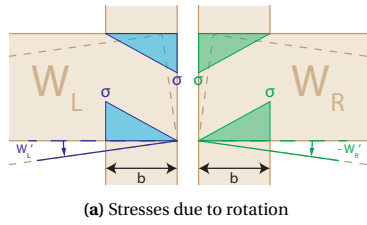
Bending moments due to vibrations are low and rotations at supports significant resulting in rotational fixity. For this phenomenon to occur sufficient normal force should be present resulting in only compressive contact forces between floor and wall. In this case the floor rotation results in compressive stresses resisting the floor to rotate by a moment. The rotational stiffness of the support is obtained by equilibrium of the moment from the compressive stresses and the bending moment in the beam. By substituting all variables except the rotational stiffness (r) into expressions of floor field one obtains the relations between the wall width and rotational stiffness (figure 5.23b-5.24b). With these relations, the rotational stiffness can be found for a certain wall width and substituted into the system.

Rotational stiffness of double leaf junction

Wall width of a double leaf junction is defined as the width of one wall, as shown in figure 5.23a, meaning the full width can be used for clamping-like behaviour. Since both walls are physically disconnected both floor fields have to make equilibrium at their node with the clamping moment (see figure 5.23b). This finally results in a relation between the separating wall width and rotational stiffness, which can be solved.

Rotational stiffness of single leaf junction with hinged floor

Single leaf junctions are equal to double leaf except only one wall being present. This means rotational fixity is only generated using half the wall width, and thus having a lower rotational stiffness. The equation in figure 5.24b has a factor $1/48$ instead of $1/6$ (i.e. double leaf) we see in figure 5.23b following from $b_{single} = (\frac{1}{2}b_{double})^3$.



$$b = \sqrt[3]{\frac{6EI \cdot \frac{\partial^2 W}{\partial x^2}(r)}{E_{supp} \cdot \frac{\partial W}{\partial x}(r)}}$$

(b) Nodal equilibrium and relation between r and b

$$\begin{aligned} W_L &= 0 \\ EI \frac{\partial^2 W_L}{\partial x^2} &= -r \frac{\partial W_L}{\partial x} \\ W_R &= 0 \\ -EI \frac{\partial^2 W_R}{\partial x^2} &= -r \frac{\partial W_R}{\partial x} \end{aligned}$$

(c) Interface conditions

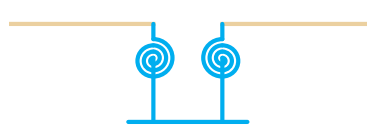
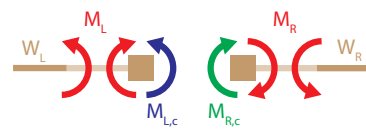
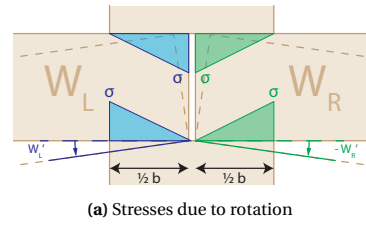


Figure 5.23: Double leaf junction



$$b = \sqrt[3]{\frac{48EI \cdot \frac{\partial^2 W}{\partial x^2}(r)}{E_{supp} \cdot \frac{\partial W}{\partial x}(r)}}$$

(b) Nodal equilibrium and relation between r and b

$$\begin{aligned} W_L &= 0 \\ EI \frac{\partial^2 W_L}{\partial x^2} &= -r \frac{\partial W_L}{\partial x} \\ W_R &= 0 \\ -EI \frac{\partial^2 W_R}{\partial x^2} &= -r \frac{\partial W_R}{\partial x} \end{aligned}$$

(c) Interface conditions

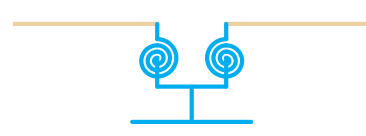
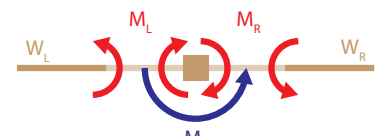
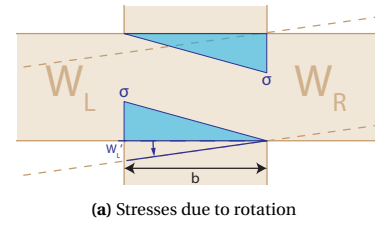


Figure 5.24: Single leaf junction with interrupted floor field



$$b = \sqrt[3]{\frac{6EI \cdot \left[\frac{\partial^2 W_L}{\partial x^2}(r) - \frac{\partial^2 W_R}{\partial x^2}(r) \right]}{E_{supp} \cdot \frac{\partial W_L}{\partial x}(r)}}$$

(b) Nodal equilibrium and relation between r and b

$$\begin{aligned} W_L &= 0 \\ W_R &= 0 \\ \frac{\partial W_L}{\partial x} &= \frac{\partial W_R}{\partial x} \\ EI \left(\frac{\partial^2 W_L}{\partial x^2} - \frac{\partial^2 W_R}{\partial x^2} \right) &= -r \frac{\partial W_L}{\partial x} \end{aligned}$$

(c) Interface conditions



Figure 5.25: Single leaf junction with continuous floor field

Rotational stiffness of single leaf junction with continuous floor

Continuous floor fields have, by definition, the same slope at both sides of the junction and use the full wall width for clamping like behaviour. Equally, they have only one node connecting to both floor fields, as shown in figure 5.25b. Therefore only one equation describes the equilibrium of moments in the junction.

Mechanical schemes

Using the nodes defined previously, the mechanical schemes for the four support conditions are generated in figure 5.26, where the physical representation is shown at the left. For the home-separating junctions (in blue) with double leaf wall, the interface conditions of figure 5.23c hold, whereas single leaf support conditions are represented by the interface conditions in figure 5.24c. The cases where the floor of an apartment consists of one piece (i.e. figure 5.26a and 5.26c) have a continuous internal junction, such interface conditions in figure 5.25c apply. Apartments with two one-span fields have an interrupted internal junction defined by the same conditions as a single leaf wall (figure 5.24c).

Table C.1 in the appendix provides interface conditions of all nodes, including the conditions at the location of the force.

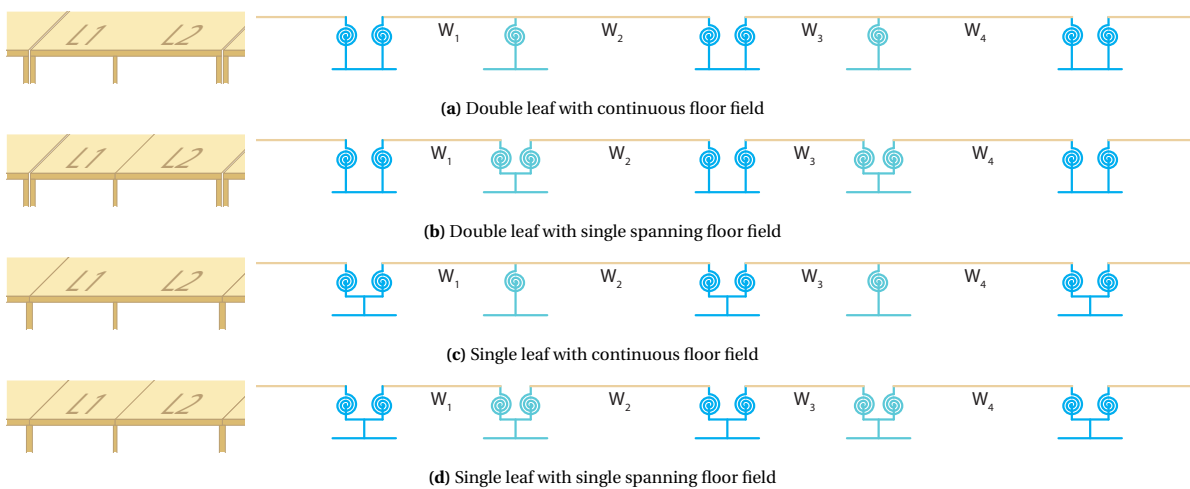


Figure 5.26: Mechanical schemes for rotational model

Rotational fixity supports

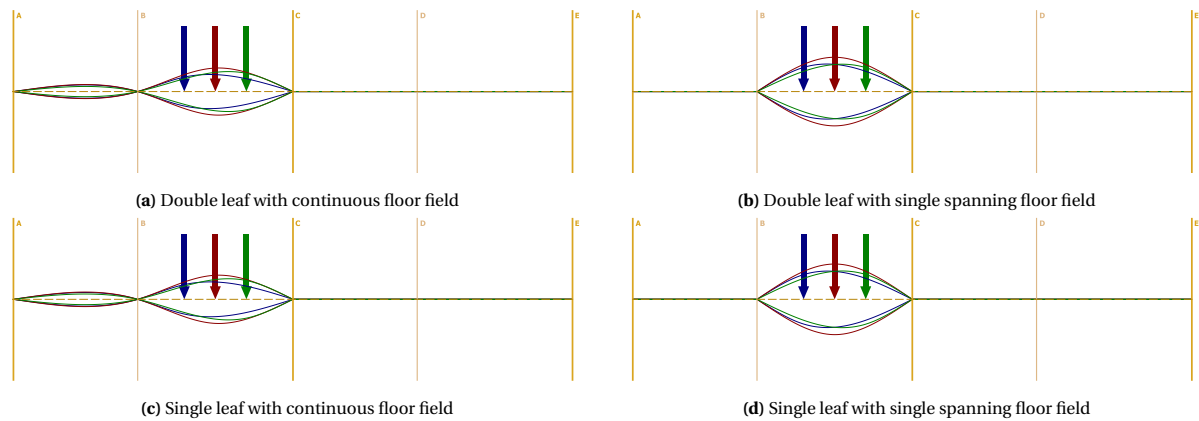
Due to the eccentricity of normal stresses at the upper- and lower side of the floor panel a moment occurs. The magnitude of the stresses highly depend on the stiffness at the contact areas, besides the wall width and slope, which differentiates junction typology 1 (no elastomer) and 2 (resilient elastomer). Therefore, the support stiffness of junction 1 depends on the Young's modulus perpendicular to the grain ($E_{\text{mean}} = 450 \text{ N/mm}^2$ [4]), which is low compared to in-plane stiffness of the walls. Since floor 2 has an elastomer interlayer applied (Rothoblaas Xylofon 70), the stiffness of those supports depend on the dynamic elastic modulus ($E' = 10,1 \text{ N/mm}^2$ [61]).

The magnitude of the moment resulting from rotational fixity at supports is small, especially for floor 2, as is shown in table 5.1. As expected, higher clamping moments at the separating junction (factor 4) are found for the double leaf walls compared to single leaf, even though the CLT panel of a single leaf is 120 mm and a double leaf consists of two panels of 100 mm. At the internal junction ($b = 80 \text{ mm}$) the highest moments are observed for the continuous floor field situations because full width of the wall is used for rigidity, and again are the moments negligible when resilient elastomers are applied.

In table 5.1 are the minimum required normal forces for full compressive contact stresses to occur given. In most cases is the self-weight of the upper wall sufficient (assuming a wall height of 3,2m), except for the double leaf wall support condition with continuous floors of junction 1 ($q_{\text{wall}} = 1,91 \text{ kN/m} < 2,50 \text{ kN/m}$). Therefore, the roof needs a minimum mass per square meter – or by introducing compressive forces by screws – to introduce the required forces. Since only half of roof span L_2 contributes to normal forces in the junction, a minimum mass of $26,8 \text{ kg/m}^2$ is required for support condition D-C.

Table 5.1: Dynamic clamping moment and required normal forces for standard quantities of the junctions

Supports:	$M_{dyn,cl}$ [Nm]				N_{req} [kN/m]			
	Separating		Internal		Separating		Internal	
	1	2	1	2	1	2	1	2
D-C	28,7	0,66	9,58	0,22	1,75	0,01	0,72	0,02
D-S	40,9	0,94	2,78	0,06	2,50	0,06	0,42	0,01
S-C	7,21	0,16	9,82	0,22	0,71	0,02	0,74	0,02
S-S	10,3	0,23	2,86	0,06	1,02	0,02	0,43	0,01

**Figure 5.27:** Vibration shapes of CLT wall supported floor for various force locations

5.3.2 Location of force

Mass timber walls are stiff and cause some clamping effects at the junctions. Therefore, are in the rotational model only the three locations at 0.25, 0.5 and 0.75 of the excited floor span length (see figure 5.27) integrated in the model. A person walking close to the wall would cause minor response of the floor since the applied force is almost fully directly transferred into the wall. Moreover, from figure 5.27 can be concluded that a walking person at midspan results in the highest amplitudes for all four support conditions.

5.3.3 Thickness home-separating CLT wall

Normal forces applied at junctions with CLT walls cause clamping-like behaviour reducing the amplitude. This especially holds for the first floor type with wet screed, since it is assumed that no flexible bearing is necessary for acoustic performance due to the increased screed mass. In figure 5.28 and 5.29 are the vibration shapes shown for all four support conditions, and home-separating wall thicknesses of 60, 100 and 210 mm. A marginal reduction of amplitude is found for double leaf structures. This type has the full wall width available for clamping contrary to single leaf walls, where the floors on both sides share the same wall.

Since clamping at junctions influence the natural frequencies, they are also studied. Floor 1 has a higher mass which results in a lower natural frequency. Figure 5.30 shows that the clamping-like behaviour of the junction does not compensate this lower f_1 —within the range of practical wall thicknesses—for all support conditions. One can observe two resonance frequencies for continuous, since the other home-field either resonates, though at a higher frequency due to its smaller span.

A significant effect upon the area contributing to the modal mass is found for increasing double leaf wall width. The area is reduced because more mass is transferred to the supports, analogous to static situations where the reaction force at the supports is higher for fixed support conditions compared to pinned.

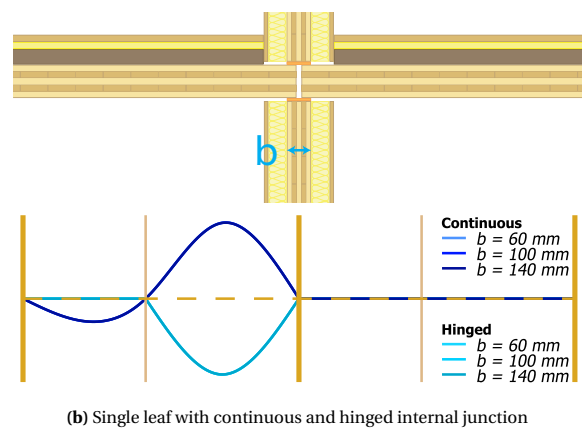
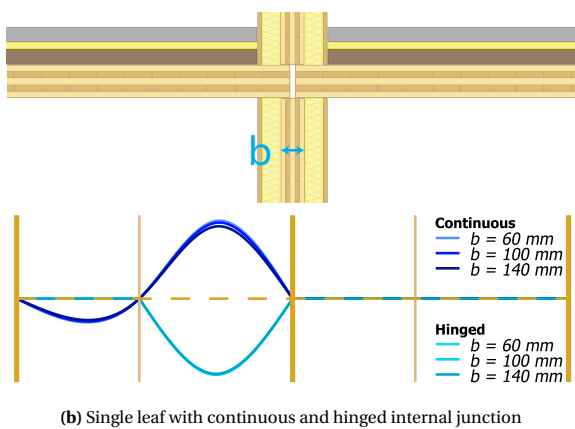
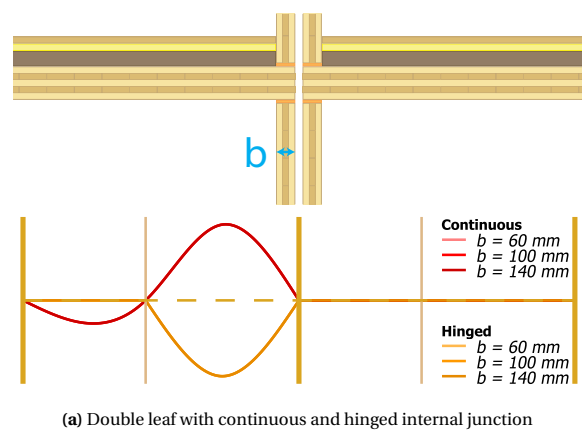
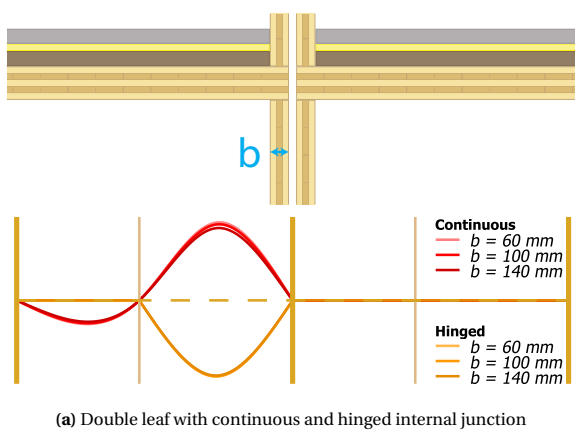


Figure 5.28: Vibration shapes of floor 1 supported by CLT walls (F1-CLT) for varying structural thickness of home-separating wall

Figure 5.29: Vibration shapes of floor 2 supported by CLT walls on elastomers (F2-CLT) for varying structural thickness of home-separating wall

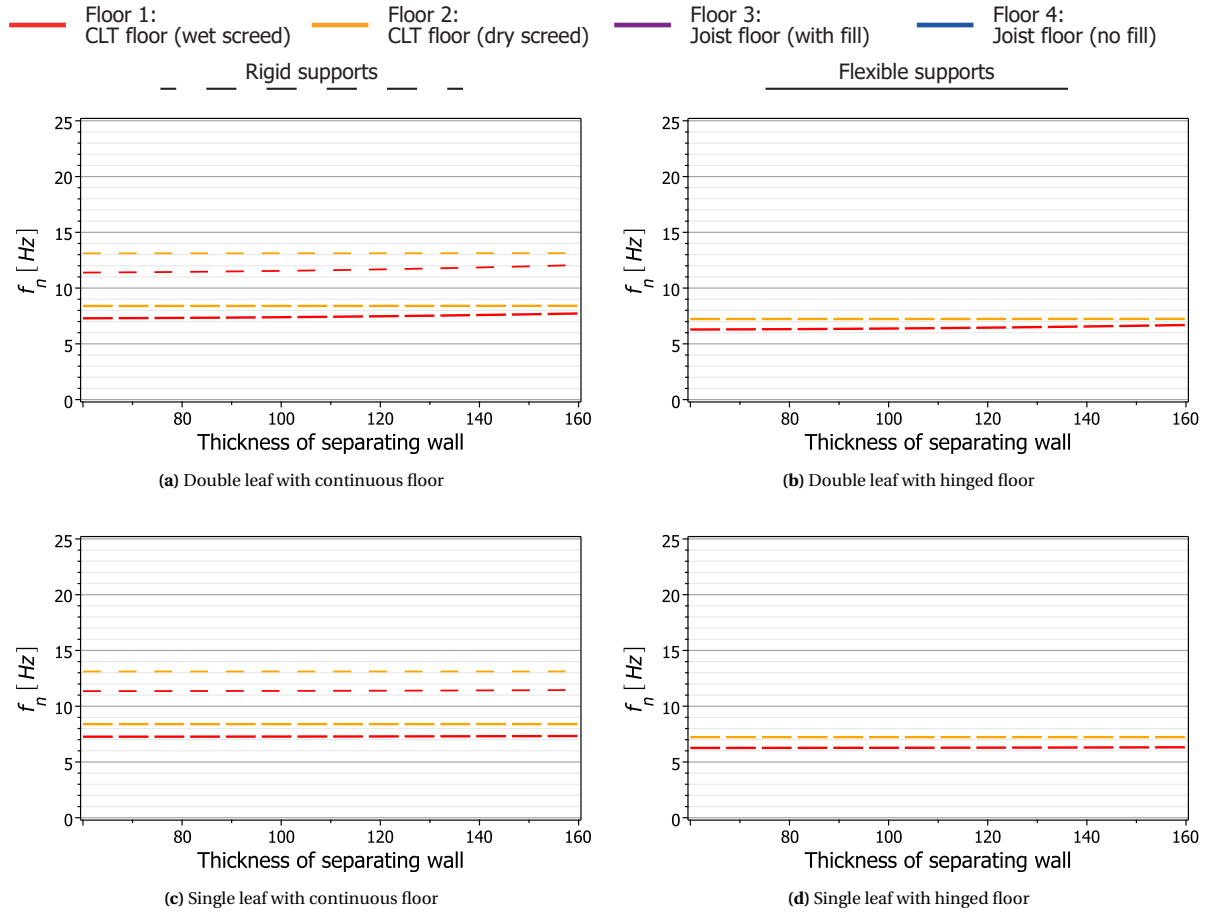


Figure 5.30: Natural frequencies for varying thickness of home-separating wall

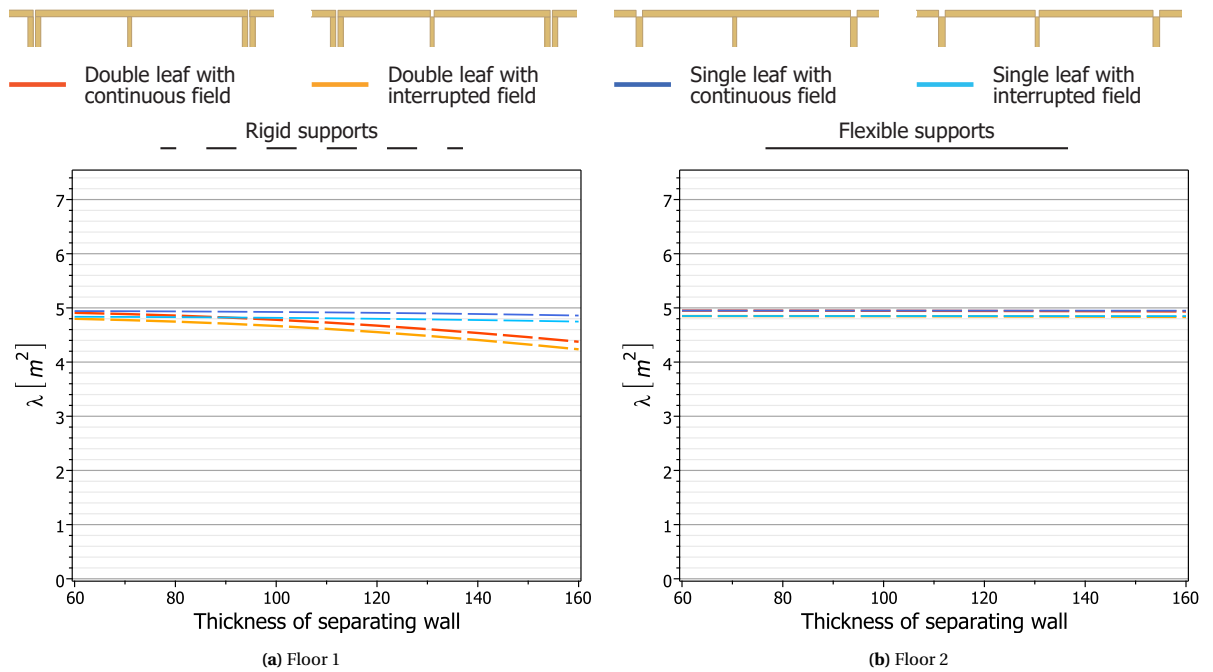


Figure 5.31: Modal mass area for varying thickness of home-separating wall

5.3.4 Thickness internal CLT wall

Fixity at the internal support results from the same principle as for the home-separating wall. However, no significant differences for internal wall thicknesses of 60, 80 and 210mm are found for floor 1 and 2, as can be observed from figure 5.32 and 5.33 respectively. The single spanning floor field cases have insufficient wall width available for development of significant clamping forces, likewise to single leaf home-separating junctions. The results for continuous floor fields can be explained from the ratio between the clamping moment and hogging moment due to the continuous floor. Apparently, the fixity is insignificant to the resistance applied by the other field. Therefore, increasing wall thicknesses are a doubtful manner of obtaining better comfort levels.

Neither do the natural frequencies change significantly for increasing internal wall width, as is shown in figure 5.34, which corresponds with observations regarding vibration shapes.

Figure 5.35a shows minor variation of the floor area contributing to the modal mass for floor 1. High internal wall thicknesses (i.e. ≈ 140 mm) result in the clamping moment at the junction becoming dominant compared to the effect of having a two-span floor, meaning the moment resistance of the second span is marginal compared to clamping.

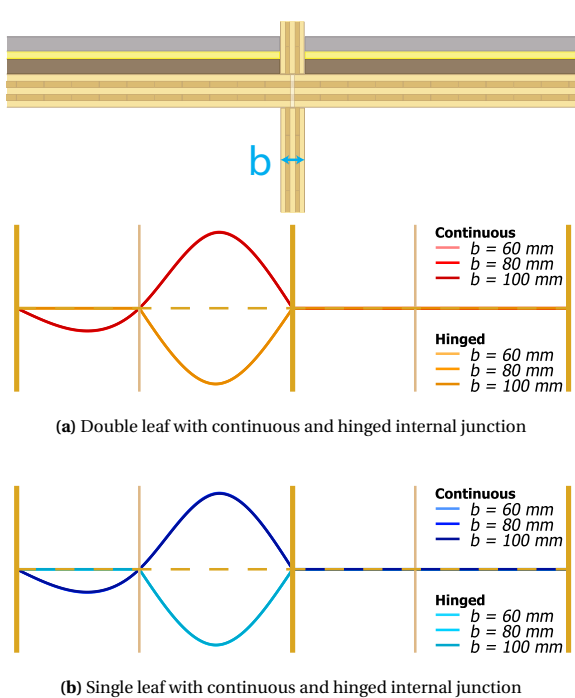


Figure 5.32: Vibration shapes of floor 1 supported by CLT walls (F1-CLT) for varying structural thickness of internal wall

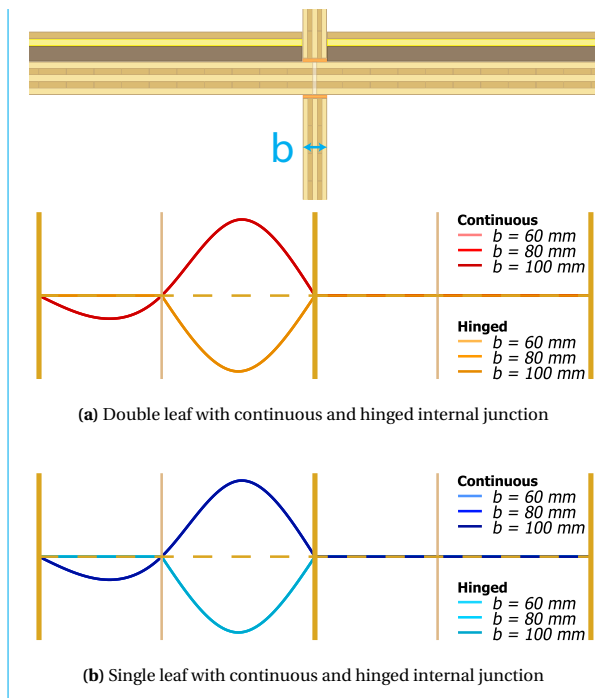


Figure 5.33: Vibration shapes of floor 2 supported by CLT walls on elastomers (F2-CLT) for varying structural thickness of internal wall

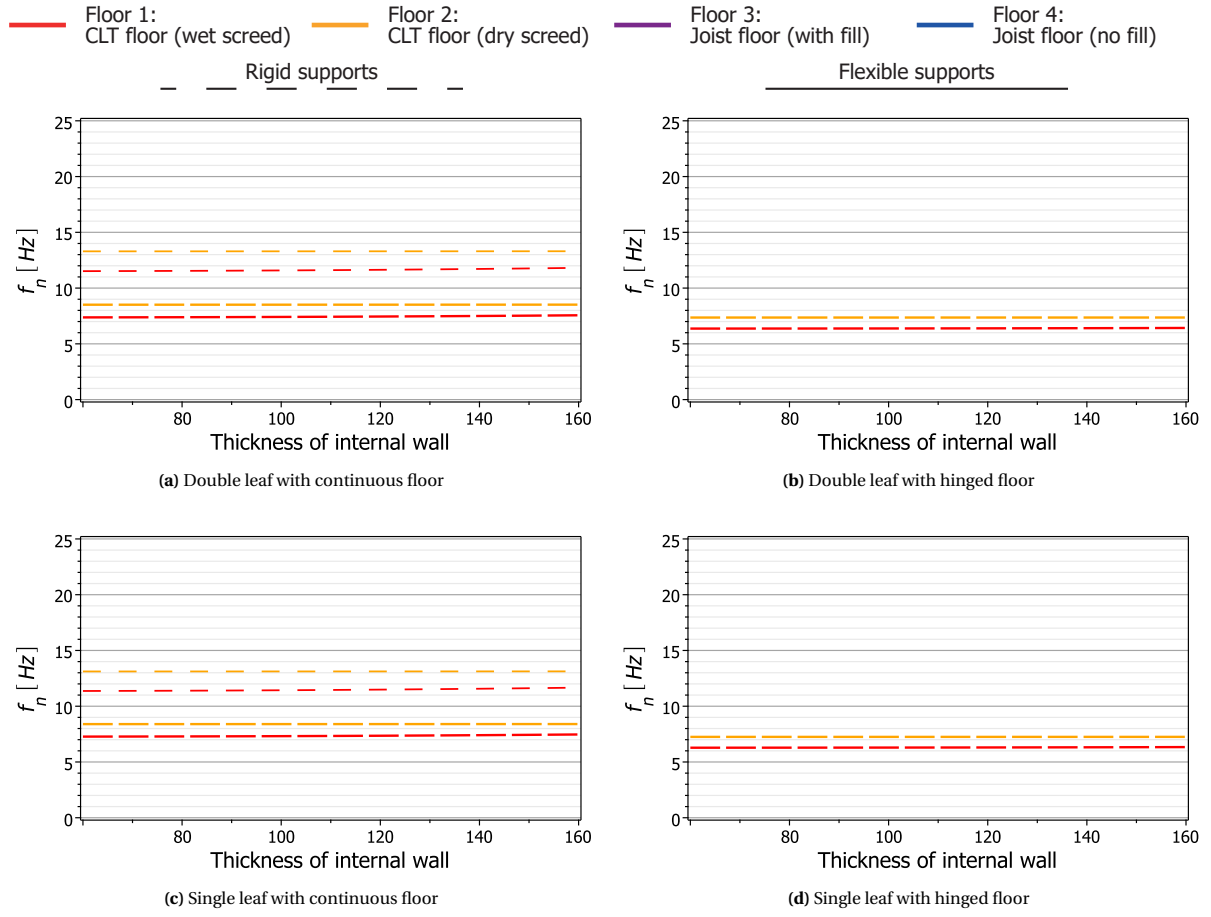


Figure 5.34: Natural frequencies for varying thickness of internal wall

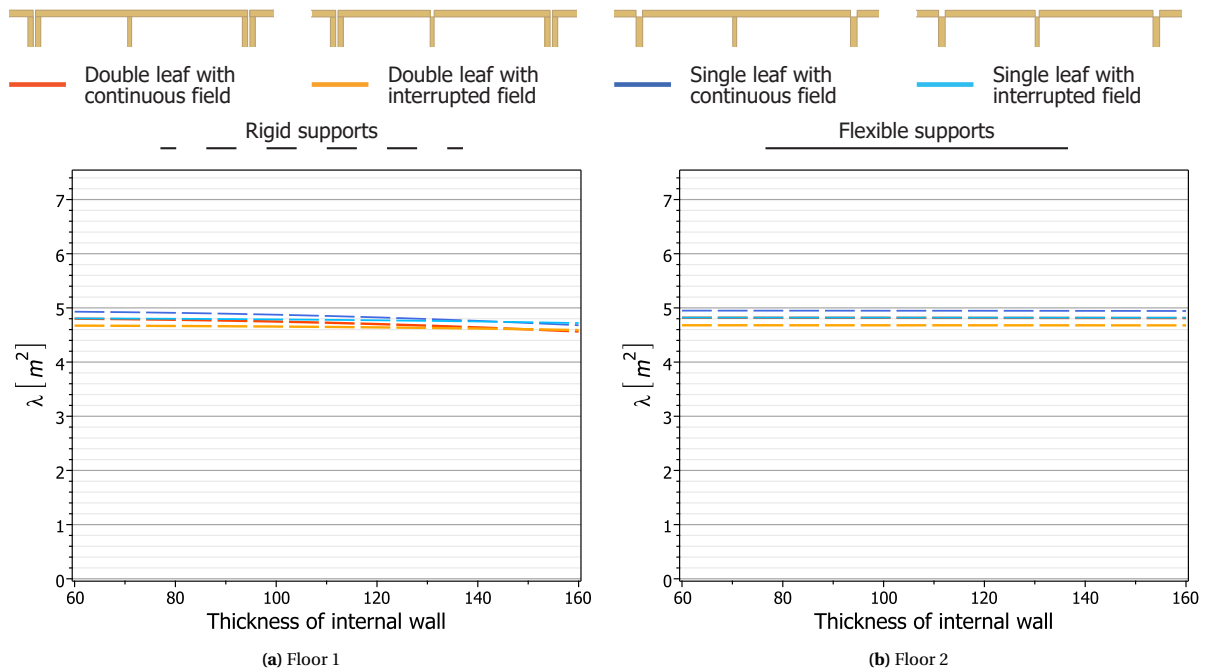


Figure 5.35: Modal mass area for varying thickness of internal wall

5.4 FLOOR CONFIGURATION

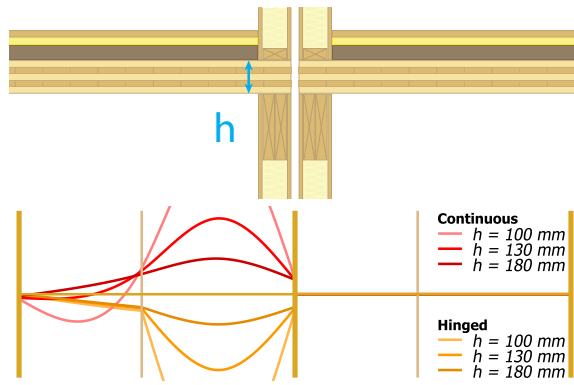
Like previously discussed support parameters, changing the floor also affect the vibration shape and natural frequencies. This section elaborates upon the influence of floor parameters related to longitudinal stiffness and mass, which are both main parameters for natural frequencies as square root of the stiffness over mass.

5.4.1 Floor stiffness

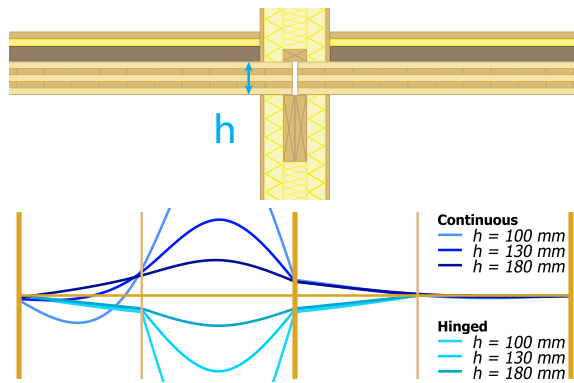
The stiffness of a floor affects the vibration shape in the same manner as it does for static deflection, i.e. higher stiffnesses result in the floor to bend less strongly. In figure 5.36 are the vibration shapes for CLT panels with a thickness of 100, 130 and 180 mm of floor 2 supported by beams shown and in figure 5.38 for rigid supports. Increasing the thickness significantly reduces the vibration amplitude. Similar results are found for the vibration shapes of joist floors (see figure 5.37 for supports and figure 5.39 for rigid) supports. Amplitudes at neighbouring floor fields are minorly affected by a changing floor stiffness.

Natural frequencies of rigidly supported floors increase almost linearly with both the thickness of the CLT panel (figure 5.40) and height of the I-joist (figure 5.41). Joist floors show more linear lines because a higher beam means a higher web and the flanges of the I-joist remain the same. Therefore the floor mass increases only marginally, where for thicker CLT panels the self-weight either increases linearly.

Flexible supported floors tend to reach a plateau from a certain stiffness, because the supporting beams prevent linear improvement of the system's eigenfrequency. It can be concluded that increasing the floor its stiffness is only effective up to some level depending on the support stiffnesses. Therefore, it can be concluded that beam supports outweigh the beneficial effect of increased stiffness, and has to be kept in mind when the flexural stiffness is increased to impede resonance with walking load harmonics.

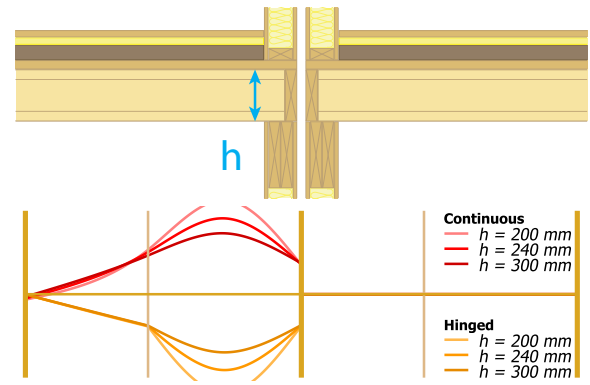


(a) Double leaf with continuous and hinged internal junction

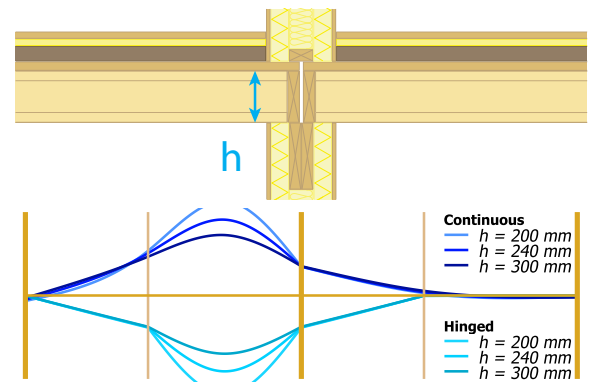


(b) Single leaf with continuous and hinged internal junction

Figure 5.36: Vibration shapes of floor 2 supported by beams (F2-SB) for varying floor stiffness

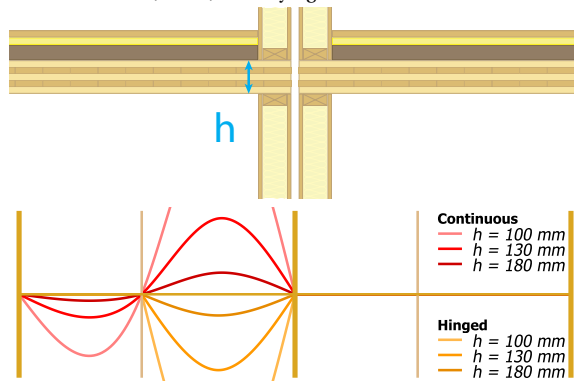


(a) Double leaf with continuous and hinged internal junction

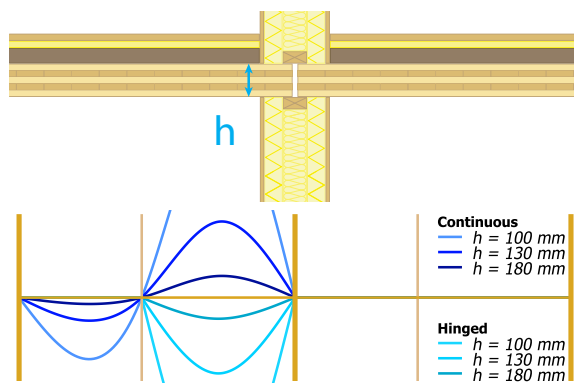


(b) Single leaf with continuous and hinged internal junction

Figure 5.37: Vibration shapes of floor 3 supported by beams (F3-SB) for varying floor stiffness

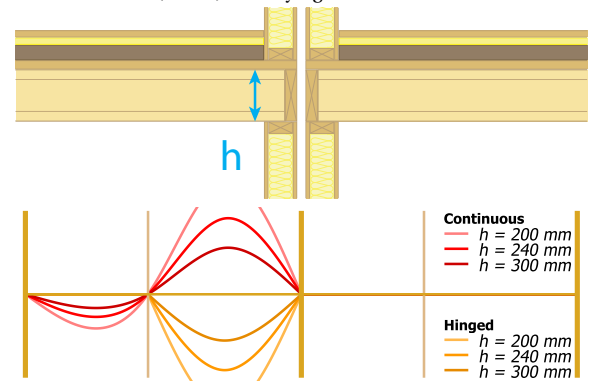


(a) Double leaf with continuous and hinged internal junction

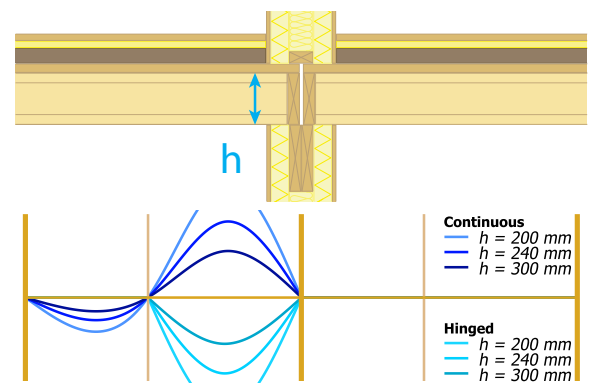


(b) Single leaf with continuous and hinged internal junction

Figure 5.38: Vibration shapes of floor 2 supported by timber-frame (F2-TF) for varying floor stiffness



(a) Double leaf with continuous and hinged internal junction



(b) Single leaf with continuous and hinged internal junction

Figure 5.39: Vibration shapes of floor 3 supported by timber-frame (F3-TF) for varying floor stiffness

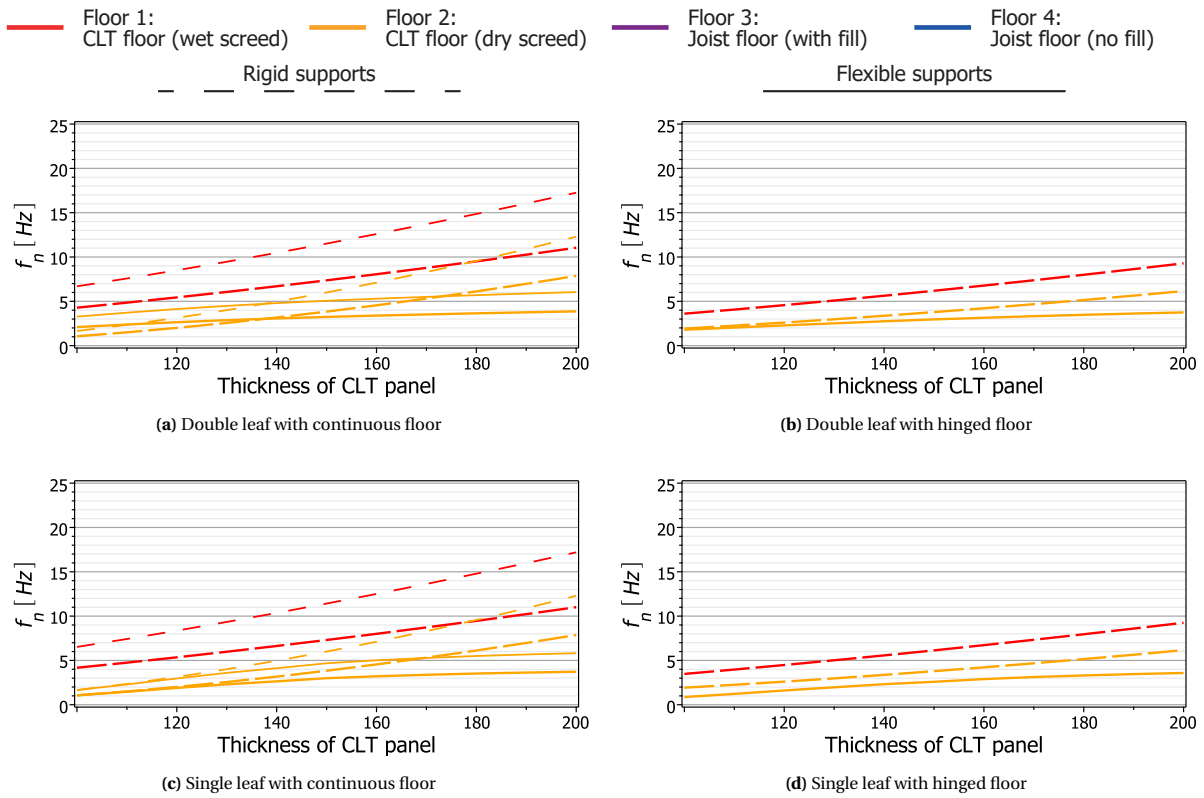


Figure 5.40: Natural frequencies for varying thickness of structural CLT floor

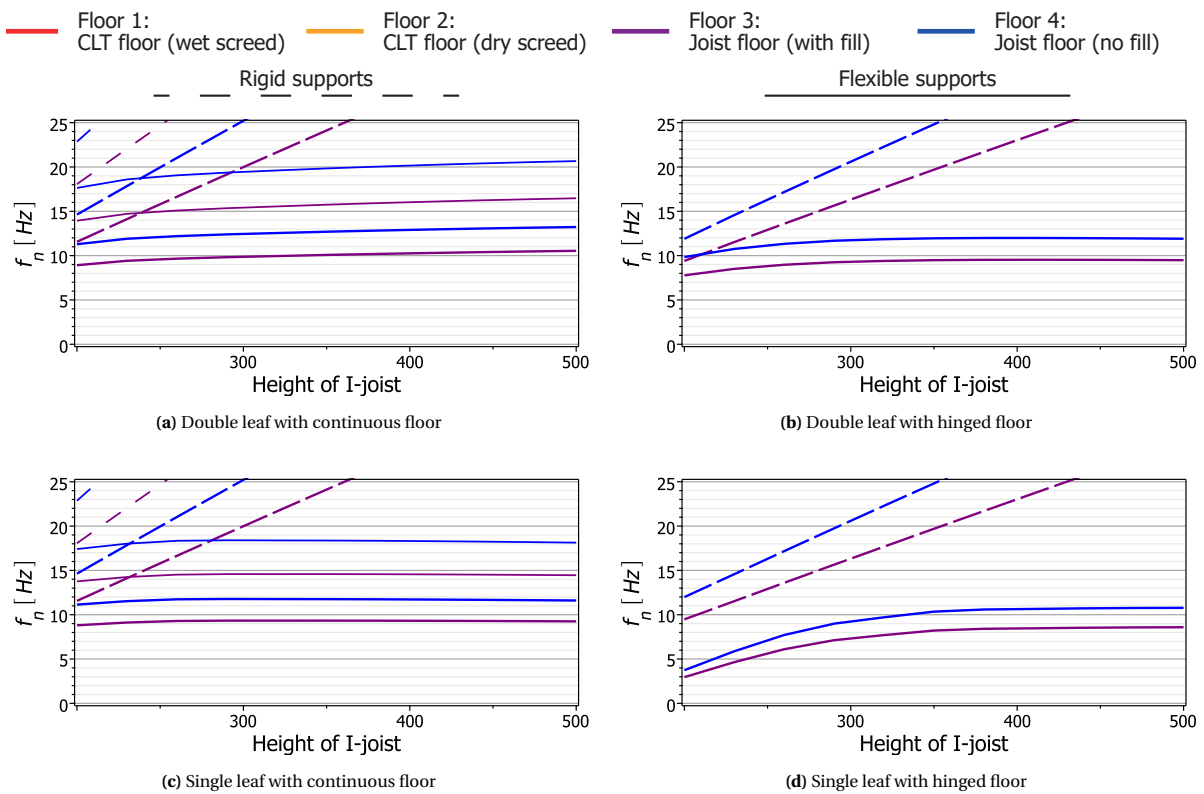


Figure 5.41: Natural frequencies for varying height of I-joists

5.4.2 Additional mass by non-structural floor layers

Another major parameter for natural frequencies is the floors mass, which reduces the natural frequency but improves the level of damping. In figure 5.42 the natural frequencies are shown, from which the same can be concluded regarding f_n . In the figure floor 1 and 3 are not visible, because they overlap with floor 2 and 4, since their distinguishing property is the mass of non-structural layers.

The figure shows that joist floors always have a higher natural frequency compared to CLT floors because of their higher stiffness-to-mass ratio. Moreover, it shows that, independent of the additional mass, flexible supported CLT floors always will resonance with one of harmonics.

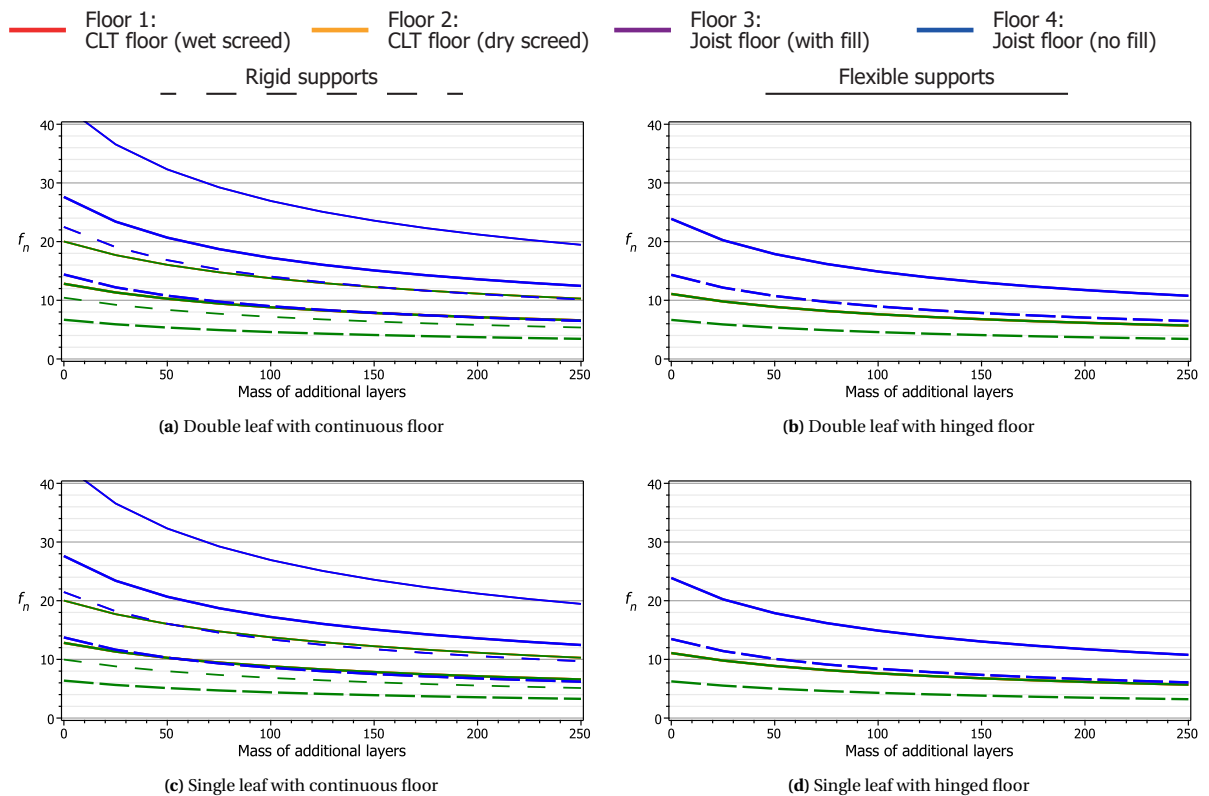


Figure 5.42: Natural frequencies for varying mass of non-structural floor layers

5.5 COMPARISON WITH FUTURE EC5 REVISION

This section compares the fundamental frequencies obtained in this chapter with the equations proposed in the future revision of Eurocode 5 for the standard typology properties given in section 4.4. First, the formulas in the revision of EC5 are described briefly, and after that the resulting fundamental frequencies are compared to the ones found with the Maple model

Fundamental frequency according to code

The working draft of EC5 [5] provides three formulas for determination of the fundamental frequency, where one relates to rigid supports and the other two approximate the eigenfrequency of systems containing flexible supports (see section 3.3).

1. Rigid supports

The future revision proposes an exact solution for f_1 of a system supported rigidly (i.e. walls). This equation is derived from classical vibration theory and is similar to the theorem where the model is based on. For the comparison is the following equation used for rigid supports.

$$f_1 = k_{e,1} k_{e,2} \frac{\pi}{2l^2} \sqrt{\frac{(EI)_L}{m}}$$

2. Flexible supports: deflection of system

From the maximum deflection can the fundamental frequency be approximated, where the floor weight is applied in a single bay only. The following formula is proposed:

$$f_1 = \frac{18}{\sqrt{\delta_{sys}}}$$

3. Flexible supports: Dunkerley's approximation

Dunkerley derived a equation to approximate the fundamental frequency by summing the fundamental frequencies of all structural elements in the system. In this equation is $f_{1, floor}$ the eigenfrequency of the floor on rigid supports, and $f_{1, sb}$ and $f_{1, sbi}$ the fundamental frequencies of the supporting beams at the home-separating and internal junction respectively, where the mass of the supporting beam is the tributary floor area supported by the beam plus its self weight.

$$f_1 = \sqrt{\frac{1}{\frac{1}{f_{1, floor}^2} + \frac{1}{3 \cdot f_{1, sb}^2} + \frac{1}{3 \cdot f_{1, sbi}^2}}}$$

Comparison of fundamental frequencies

In table 5.2 the frequencies are given from the model, and f_1 calculated according to the future revision of Eurocode 5 for either the rigid formula or the equation for flexible supports. The first column holds the floor typology in line with the ones given in figure 4.8. J_s is the home-separating junction type, namely a double leaf (D) or a single leaf (S), where J_i names the internal junction being continuous (C) or hinged (H). The column besides gives the support type: either rigid (R) or flexible (F).

The model performs very accurately for rigid supports, which makes sense, since the model is based on the same theory as the formula for rigid supports in revised EC5. Almost all the fundamental frequencies that are found with the Maple model deviate marginally.

For flexible supports is the model less accurate, as expected, because it simplifies the floor into a one-dimensional element. Fundamental frequencies acquired by the model are far off the frequencies approximated by the formula that uses the deflection of the system, with f_1 from the model being 23% to 39% lower.

Compared to the third equation based on Dunkerley's approximation, are the frequencies from the model slightly higher, ranging from 1 to 13 percent. Based on these observations is the model also accurate when the supports are flexible.

Floor	Supports			Model	Future revision Eurocode 5								
	J_s	J_i		f_1	Eq. 1	%	δ_{sys}	Eq. 2	%	$f_{1,bs}$	$f_{1,bi}$	Eq. 3	%
F1-CLT	D	C	R	7,05	7,06	0%	-	-	-	-	-	-	-
	D	H	R	6,08	6,09	0%	-	-	-	-	-	-	-
	S	C	R	6,95	7,06	-2%	-	-	-	-	-	-	-
	S	H	R	5,99	6,09	-2%	-	-	-	-	-	-	-
F2-CLT	D	C	R	8,18	8,16	0%	-	-	-	-	-	-	-
	D	H	R	7,04	7,04	0%	-	-	-	-	-	-	-
	S	C	R	8,18	8,16	0%	-	-	-	-	-	-	-
	S	H	R	7,04	7,04	0%	-	-	-	-	-	-	-
F2-SB	D	C	F	6,54	-	-	3,84mm	9,19	-29%	8,69	6,48	6,05	8%
	D	H	F	5,90	-	-	5,23mm	7,87	-25%	8,69	6,48	5,54	6%
	S	C	F	6,44	-	-	3,84mm	9,19	-30%	6,48	6,48	5,69	13%
	S	H	F	5,78	-	-	5,23mm	7,87	-27%	6,48	6,48	5,26	10%
F2-TF	D	C	R	8,14	8,16	0%	-	-	-	-	-	-	-
	D	H	R	7,06	7,04	0%	-	-	-	-	-	-	-
	S	C	R	8,14	8,16	0%	-	-	-	-	-	-	-
	S	H	R	7,06	7,04	0%	-	-	-	-	-	-	-
F3-SB	D	C	F	8,35	-	-	1,89mm	13,09	-36%	8,85	6,59	7,95	5%
	D	H	F	8,32	-	-	2,74mm	10,87	-23%	8,85	6,59	7,64	9%
	S	C	F	7,97	-	-	1,89mm	13,09	-39%	6,59	6,59	7,21	10%
	S	H	F	7,81	-	-	2,74mm	10,87	-28%	6,59	6,59	6,98	12%
F3-TF	D	C	R	16,01	16,06	0%	-	-	-	-	-	-	-
	D	H	R	13,85	13,85	0%	-	-	-	-	-	-	-
	S	C	R	16,01	16,06	0%	-	-	-	-	-	-	-
	S	H	R	13,85	13,85	0%	-	-	-	-	-	-	-
F4-SB	D	C	F	10,50	-	-	1,21mm	16,36	-36%	11,78	8,78	10,44	1%
	D	H	F	10,46	-	-	1,75mm	13,61	-23%	11,78	8,78	9,99	5%
	S	C	F	10,02	-	-	1,21mm	16,36	-39%	8,78	8,78	9,50	6%
	S	H	F	9,84	-	-	1,75mm	13,61	-28%	8,78	8,78	9,15	8%
F4-TF	D	C	R	20,16	20,20	0%	-	-	-	-	-	-	-
	D	H	R	17,43	17,40	0%	-	-	-	-	-	-	-
	S	C	R	20,16	20,20	0%	-	-	-	-	-	-	-
	S	H	R	17,43	17,40	0%	-	-	-	-	-	-	-

Table 5.2: Comparison of fundamental frequencies from model with future revision EC5

6

Assessment of junction typologies

Second part of the study of timber junction typologies focusses on the assessment of low- and high-frequency floors for a person walking in a apartment. It aims for quantification of the 32 combinations of floor- and wall configurations (8) and support conditions (4) such they are comparable regarding vibrational behaviour (in home and at neighbour), acoustic performance and their mass.

This chapter addresses the last Maple sheet *Damped Assessment* using SDOF properties determined previously, like natural frequencies and modal mass. For the last SDOF property, equivalent spring stiffness K_{eq} , the static solution and effective width are imported from *System Solver*, and floor and support properties (EI , q , k_s and k_i) from *Junction typology properties*. Each floor is transformed into a SDOF system according to the methodology noted in previous section 6.1, and the vibration levels are determined in *Damped assessment of junction typologies* following below noted procedure.

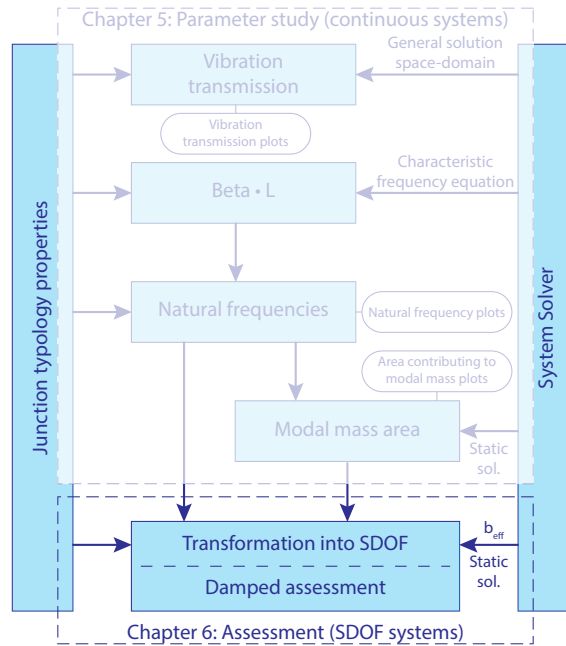


Figure 6.1: Flowchart of Maple sheets for chapter 6

6.1 TRANSFORMATION OF FLOORS INTO SDOF SYSTEMS

Though amplitudes can be obtained from the continuous model in previous chapter, do they not correspond with practice because of damping left out of the system. Therefore the floors are transformed into a system that does not require a lot of computing power to include damping, which are Single Degree of Freedom systems.

In this section, the procedure is demonstrated to obtain the properties of a mass-spring-dashpot system that is equivalent to the floor in a certain point. By choosing most unfavourable the location, i.e. midspan for the excited field and at the connecting junction for adjoining fields, the maximum vibration levels are found for the floor field.

The fundamental frequencies determined in previous chapter, and found to be close to the ones obtained using formulas in the future revision of EC5, are visualized in figure 6.2. The cut-off frequency of 8 Hz is also shown, which is believed to distinct between the steady-state response of LFF and transient response of HFE.

Figure 6.2b shows the second natural frequency of floor span L_1 , which is caused by that floor set into motion by an excitement in floor field L_2 . This is the case for two-span floor fields (in red and dark blue) and typologies where the floor is supported by beams. The second mode has either to be accounted for in transient responses, because all natural frequencies up to twice the fundamental one have to be considered according to Sedlacek et al. [63].

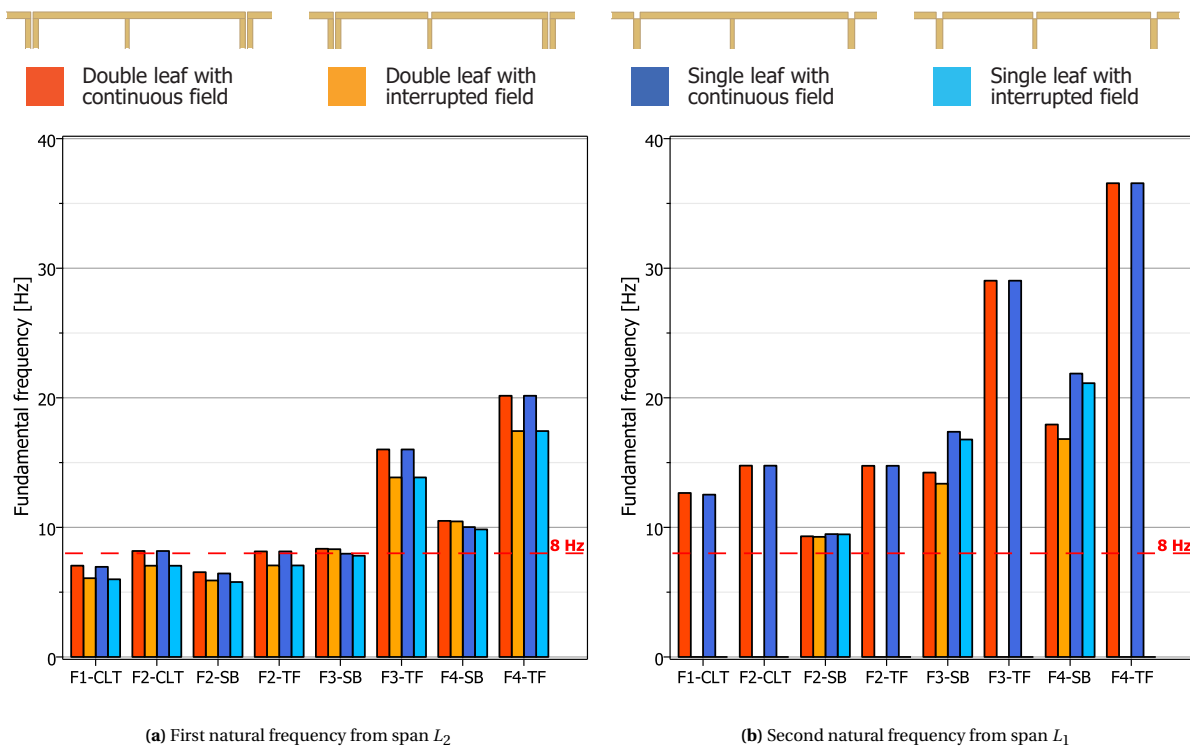


Figure 6.2: Natural frequencies of floor typologies

6.1.1 Methodology

A downside of using a continuous system is that incorporating damping requires lots of computing power for complex multi-field systems. However, it is very suitable for obtaining βL values and thus finding fundamental frequencies and modal masses. Therefore, two approaches presented in this work are combined, namely the continuous system and representing a beam as a Single Degree of Freedom (SDOF) system, as introduced in section 2.3. The example below demonstrates the relationship between these two methods and the relation of mass to fundamental frequency and damping ratio.

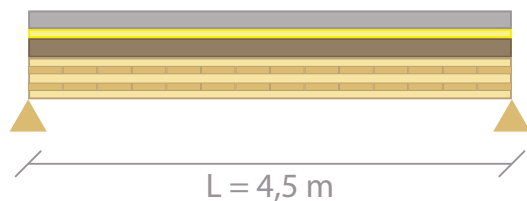
Continuous systems mathematically represent the beam structure as a whole and is, therefore, an exact method for determination of fundamental frequencies. The second approach, SDOF systems, is a simplification of the beam by describing the dynamic amplitude at midspan, where a spring represents the floor stiffness and the floor its contributing weight concentrates in a lumped mass. For the case of a simply-supported beam, the mass of the equivalent mass-spring-system is equal to the modal mass of the floor, which is about 0,49 times mass of the floor. In other cases, modal mass are determined by substituting $\beta_1 L$ into the general solution, such one obtains the mode shape, and after that, integrating the mode shape over the beam length.

Single spanning low-frequency floor (LFF)

Cross-laminated timber floors generally classify as low-frequency floor due to their low stiffness-to-mass ratio. Therefore, the fundamental frequency is determined below for a 130 mm thick panel with 5 layers (30-20-30-20-30). Below the floor its properties are given for floor 2 supported by a timber-frame wall (F2-TF), where EI is the longitudinal stiffness, q the mass and L the floor span.

$$\begin{aligned} EI_L &= 1,734 \cdot 10^6 \text{ Nm}^2/\text{m} & q &= 280 \text{ kg}/\text{m}^2 & L &= L_2 = 4,5 \text{ m} \\ EI_T &= 3,476 \cdot 10^5 \text{ Nm}^2/\text{m} & b_{eff} &= 2,08 \text{ m} \end{aligned}$$

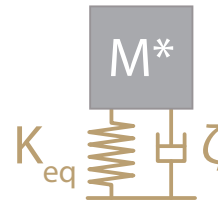
Continuous system



$$\beta_1 L = \pi$$

$$f_{1,cont} = \frac{(\beta_1 L)^2}{2\pi \cdot (L)^2} \sqrt{\frac{EI_L}{q}} = 6,10 \text{ Hz}$$

Single Degree of Freedom (SDOF) system



$$K_{eq} = \frac{F}{w} = \frac{48 \cdot EI_L \cdot b_{eff}}{L^3} = 1,890 \cdot 10^6 \text{ N}/\text{m}$$

$$M^* = \frac{1}{2} \cdot q \cdot b_{eff} \cdot L = 1310 \text{ kg}$$

$$f_{1,SDOF} = \frac{1}{2\pi} \sqrt{\frac{K_{eq}}{M^*}} = 6,04 \text{ Hz}$$

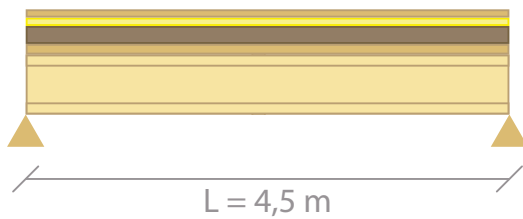
Fundamental frequency of the floor is below 8 Hz and thus, is classified as low-frequency floor. The frequency found using the SDOF approach differs less than 1 % from the exact continuous method. Therefore it can be concluded that the method is appropriate for simply-supported floor fields.

Single spanning high-frequency floor (HFF)

Floors with a high stiffness-to-mass ratio classify as a high-frequency floor, which are in practice joist floors with panel decking. For this example, I-joists (FJI89/220@300mm) are chosen with a 27 mm thick LVL panel on top. This set-up results in the following floor properties for typology F3-TF:

$$\begin{array}{lll} EI_L = 6,047 \cdot 10^6 \text{ Nm}^2/\text{m} & q = 190 \text{ kg/m}^2 & L = L_2 = 4.5 \text{ m} \\ EI_T = 1,722 \cdot 10^4 \text{ Nm}^2/\text{m} & b_{eff} = 0,95 \text{ m} & B = 3,6 \text{ m} \end{array}$$

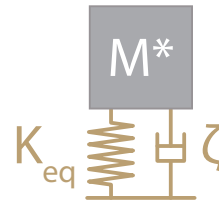
Continuous system



$$\beta_1 L = \pi$$

$$f_{1,cont} = \frac{(\beta_1 L)^2}{2\pi \cdot (L)^2} \sqrt{\frac{EI_L}{q}} = 13,84 \text{ Hz}$$

Single Degree of Freedom (SDOF) system



$$K_{eq} = \frac{F}{w} = \frac{48 \cdot EI_L \cdot b_{eff}}{L^3} = 3,026 \cdot 10^6 \text{ N/m}$$

$$M^* = \frac{1}{2} \cdot q \cdot b_{eff} \cdot L = 406 \text{ kg}$$

$$f_{1,SDOF} = \frac{1}{2\pi} \sqrt{\frac{K_{eq}}{M^*}} = 13,74 \text{ Hz}$$

Like the low-frequency floor, a fundamental frequency is found from the mass-spring system slightly lower (1 %), and therefore being on the conservative side. The chosen joist-floor in this example classifies as high-frequency floor.

Effective width

A floor field bends in both the longitudinal and transverse direction when a force is applied. Since the method simplifies the floor into a beam has there to be accounted for the force redistribution in transverse direction. The effective width expresses the floor width that contributes to resistance of the load such that similar deflections are found for the equivalent beam. In table 6.1 are the static deflections given, as such they are acquired from software package SCIA Engineer, and the corresponding effective width.

The effective flexural stiffness EI_{eff} is found by multiplying the effective width with the flexural rigidity per unit length (see table 4.4), which is thereafter used to determine the equivalent spring stiffness. Therefore, the effective width is accounted for by K_{eq} in the SDOF system.

Table 6.1: Static deflection and corresponding effective width

		Span L_2		Span L_1	
		$w_{st,1kN}$ [mm]	b_{eff} [mm]	$w_{st,1kN}$ [mm]	b_{eff} [mm]
CLT	Double span	0.254	1968	0.064	2272
	Single span	0.350	2077	0.088	2950
Joist	Double span	0.178	849	0.037	1188
	Single span	0.231	952	0.048	2504

Determining modal mass SDOF system from continuous fundamental frequency

Previous two examples for a LFF and HFF shows that fundamental frequencies found for the equivalent SDOF system are about equal to the exact formulation of eigenfrequencies for continuous beams. This outcome is used to transform the floor vibration at a specific location into an equivalent mass-spring-dashpot system for all combinations of floors and support conditions.

First, for the SDOF system to be equivalent, the fundamental frequency has to be equal to the one found for the continuous system: $f_{1,cont} = f_{1,SDOF}$. Secondly, the equivalent spring stiffness K_{eq} is found from the point load divided by the static deflection of the floor such that the lowest stiffness is found. Now the only unknown is M^* , and can, therefore, be determined:

$$\frac{(\beta_1 L)^2}{2\pi \cdot (L_s)^2} \sqrt{\frac{EI_L}{q}} = \frac{1}{2\pi} \sqrt{\frac{K_{eq,eff}}{M^*}} \quad \Rightarrow \quad M^* = \frac{K_{eq,eff}}{(2\pi f_1)^2} = K_{eq,eff} \cdot \frac{q}{EI_L} \left(\frac{L_s}{\beta_1 L} \right)^4 \quad (6.1)$$

Thus, equation 6.1 expresses the modal mass either in terms of equivalent spring stiffness and fundamental frequency or, more comprehensively, in terms of equivalent stiffness, ratio of mass over longitudinal flexural stiffness and ratio to the power 4 of span length over $\beta_1 L$. The parameters q , EI_L and $\beta_1 L$ (which includes the support conditions) are system dependent, and therefore constant along the whole floor, where $K_{eq,eff}$ and L_s depend on the location that the SDOF system has to represent. Equivalent stiffness is the static counterpart of mode shapes describing continuous systems, meaning it accounts for the position of the exciting person and where the receiving person locates. L_s is the system length of the span one wants to determine the modal mass, that is in this case, L_2 (first mode) and L_1 (second mode for two-span fields only).

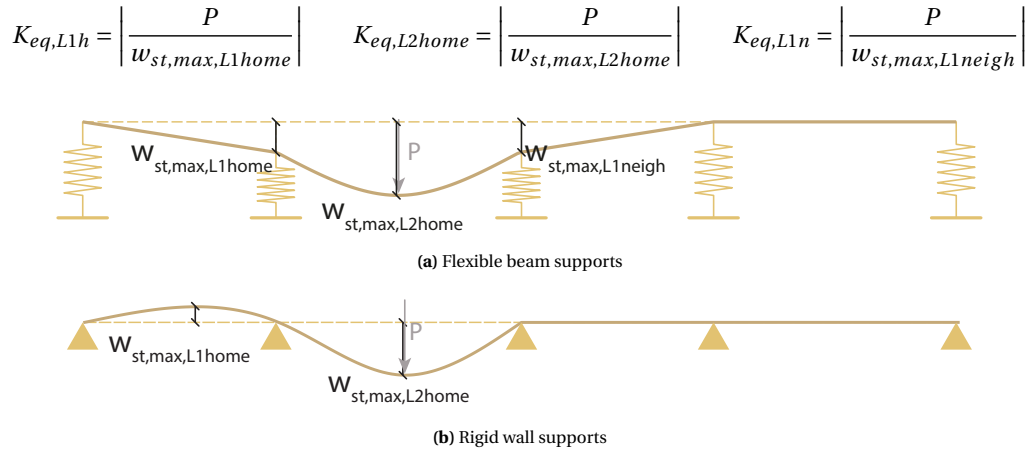


Figure 6.3: Static deflection definition of different floor fields

6.1.2 SDOF properties of all floors

This section determines the mass- and stiffness properties of mass-spring-dashpot systems that correlate to the floor- and support combinations. To study the effects of transmittance not only the excited home floor field L_2 is transformed, but its adjacent floor fields L_1 at the other home room and span L_1 at the neighbouring apartment as well. It is not necessary to validate floor field L_2 in the neighbouring apartment since in section 5.2 is found that amplitude levels in L_1 are always higher compared to L_2 for the neighbouring unit.

Expression 6.1 can be used to generate an equivalent SDOF system that could represent vibrations at any floor location. However, the lowest –and governing– modal mass is found for lowest equivalent spring stiffness. The latter relates to the most unfavourable case where both load location and receiver's point are positioned such that the deflection in the floor field maximizes.

In this work, the static deflection is determined using the theorem of continuum mechanics since it is the static counterpart of a continuous system. In this manner, the effective floor width is found by modelling the floors in the software package SCIA Engineer. However, in practice, it is more suitable to determine the equivalent spring stiffness directly with such software packages, which are often already used to verify the strength and deflection of a floor.

The proposed procedure is used to determine modal masses of all floor combinations for all previously mentioned three floor fields. In table 6.2 and 6.3 properties of the equivalent SDOF system are summed up and the modal mass is compared to values found according to the equation provided in revised EC5.

6.1.3 Comparison with revised Eurocode 5

Input values for both steady-state and transient response of the transformed SDOF systems are compared to the values calculated from the formulas proposed in the future revision of EC5.

In table 6.2 are the properties given used to determine the steady-state response. The fundamental frequency was already found to be quite comparable in previous chapter. The input variable that represents the structure in the model differs from the one used in EC5 revision, since the model uses equivalent spring stiffness $K_{eq,eff}$ where EC5 prescribes the modal mass M^* for defining the structure, and therefore, these are not comparable to one another. However, steady-state responses below the fundamental frequency are stiffness dominated, whereas above that, the mass dominates the response [64]. Since the model either validates the steady-state response of higher fundamental frequencies of joist floors, the use of $K_{eq,eff}$ is more correct. For the case of assuming resonance, like in the revision of EC5, is the response damping dominated, and therefore the use of mass is either correct. Since the mass is either needed for the transient response, did they probably choose to use the modal mass to keep the future code compact.

The Dynamic Modification Factor (DMF) describes the level of resonance compared to the static deflection, and is acquired from the model using *Square Root Sum of the Squares (SRSS)* method to combine the DMFs of all harmonics. In the formula for a_{rms} proposed in EC5 revision assumes resonance with the natural frequency and given by $1/2\zeta$, and are only applied to floors with $f_1 < 8$ Hz. Since no resonance occurs for higher fundamental frequencies, the DMF of the model diverges from the revision of EC5 for these floor types.

The Dynamic Load Factor (DLF) accounts for the contribution of each harmonic to the total walking load curve, and is given for the dominating harmonic for $f_{s,dom}$. Revision of EC5 proposes the factor α to determine the dynamic force of the walking load by $e^{-0,4f_1}$.

Transient responses both use the method where the heel-strike impulse divided by the modal mass gives the initial velocity. The Maple model used in this work also allows to determine the modal masses of adjoining floor fields through the transformation into mass-spring-dashpot systems, where the revision of Eurocode 5 only provides a formula for the modal mass of the excited field for single spanning situations. Therefore, can only M_{L2h}^* be compared to M^* , which values are quite similar for rigidly supported floors. However, the future revision of EC5 does not account for the additional mass of adjoining floor fields, which explains the higher modal masses for especially floor F3-SB and F4-SB.

For determination of the initial velocity is the same procedure followed in both methods, as previously mentioned. However, future revision of EC5 states that a walking frequency of 1,5 Hz has to be applied, but a higher f_s results in a more strong impact by the heel-strike (we tend to walk more brisk). Since the average walking frequency of humans is about 2 Hz, the initial velocity is underestimated by $v_{1,peak}$ as adopted in EC5. If one corrects for this and substitutes the dominant walking frequency $f_{s,dom}$ for the impulse value, the initial velocity is similar for rigid supported floors, where flexible supports show higher values due to the lower modal mass.

Floor	ζ [-]	Model					Revision EC5			
		f_1 [Hz]	$f_{s,dom}$ [Hz]	$K_{eq,eff}$ [N/m]	DMF [-]	DLF [-]	f_1 [Hz]	M^* [kg]	DMF [-]	DLF [-]
F1-CLT	DC 0,05	7,05	2,35	$2,74 \cdot 10^6$	5,12	0,061	7,06	1316,0	10,0	0,059
	DS 0,05	6,08	2,05	$2,00 \cdot 10^6$	9,93	0,057	6,09	1316,0	10,0	0,088
	SC 0,05	6,95	2,35	$2,74 \cdot 10^6$	5,26	0,061	7,06	1316,0	10,0	0,059
	SS 0,05	5,99	2,00	$2,00 \cdot 10^6$	9,01	0,056	6,09	1316,0	10,0	0,088
F2-CLT	DC 0,04	8,18	2,05	$2,74 \cdot 10^6$	5,15	0,057	8,16	984,2	12,5	0,038
	DS 0,04	7,04	2,35	$2,00 \cdot 10^6$	12,72	0,061	7,04	984,2	12,5	0,060
	SC 0,04	8,18	2,05	$2,74 \cdot 10^6$	5,15	0,057	8,16	984,2	12,5	0,038
	SS 0,04	7,04	2,35	$2,00 \cdot 10^6$	12,72	0,061	7,04	984,2	12,5	0,060
F2-SB	DC 0,04	6,54	2,50	$1,48 \cdot 10^6$	5,57	0,064	5,44	984,2	12,5	0,113
	DS 0,04	5,90	1,95	$1,36 \cdot 10^6$	12,56	0,055	5,72	984,2	12,5	0,102
	SC 0,04	6,44	2,50	$1,49 \cdot 10^6$	5,98	0,064	5,44	984,2	12,5	0,113
	SS 0,04	5,78	1,95	$1,36 \cdot 10^6$	12,13	0,055	5,72	984,2	12,5	0,102
F2-TF	DC 0,04	8,14	2,50	$2,74 \cdot 10^6$	5,16	0,064	8,16	984,2	12,5	0,038
	DS 0,04	7,06	2,35	$2,00 \cdot 10^6$	12,75	0,061	7,04	984,2	12,5	0,060
	SC 0,04	8,14	2,50	$2,74 \cdot 10^6$	5,16	0,064	8,16	984,2	12,5	0,038
	SS 0,04	7,06	2,35	$2,00 \cdot 10^6$	12,75	0,061	7,04	984,2	12,5	0,060
F3-SB	DC 0,03	8,35	2,10	$1,79 \cdot 10^6$	16,49	0,058	6,93	406,4	16,7	0,062
	DS 0,03	8,32	2,10	$1,77 \cdot 10^6$	15,92	0,058	8,27	406,4	16,7	0,037
	SC 0,03	7,97	2,00	$1,80 \cdot 10^6$	8,44	0,051	6,93	406,4	16,7	0,062
	SS 0,03	7,81	1,95	$1,77 \cdot 10^6$	6,80	0,050	8,27	406,4	16,7	0,037
F3-TF	DC 0,03	16,01	2,50	$3,91 \cdot 10^6$	2,57	0,064	16,06	406,4	16,7	0,002
	DS 0,03	13,85	2,50	$3,03 \cdot 10^6$	2,95	0,064	13,85	406,4	16,7	0,004
	SC 0,03	16,01	2,50	$3,91 \cdot 10^6$	2,57	0,064	16,06	406,4	16,7	0,002
	SS 0,03	13,85	2,50	$3,03 \cdot 10^6$	2,95	0,064	13,85	406,4	16,7	0,004
F4-SB	DC 0,025	10,50	2,50	$1,79 \cdot 10^6$	9,91	0,064	8,73	256,5	20,0	0,030
	DS 0,025	10,46	2,50	$1,77 \cdot 10^6$	10,49	0,064	10,41	256,5	20,0	0,016
	SC 0,025	10,02	2,50	$1,80 \cdot 10^6$	20,16	0,061	8,73	256,5	20,0	0,030
	SS 0,025	9,84	2,45	$1,77 \cdot 10^6$	16,89	0,060	10,41	256,5	20,0	0,016
F4-TF	DC 0,025	20,16	2,50	$3,91 \cdot 10^6$	2,30	0,064	20,22	256,5	20,0	0,000
	DS 0,025	17,43	2,50	$3,03 \cdot 10^6$	2,44	0,064	17,43	256,5	20,0	0,001
	SC 0,025	20,16	2,50	$3,91 \cdot 10^6$	2,30	0,064	20,22	256,5	20,0	0,000
	SS 0,025	17,43	2,50	$3,03 \cdot 10^6$	2,44	0,064	17,43	256,5	20,0	0,001

Table 6.2: Steady-state response input variables for model and revision EC5

Floor	ζ [-]	Model						Revision EC5			
		f_1 [Hz]	$f_{s,dom}$ [Hz]	M_{L1h}^* [kg]	M_{L2h}^* [kg]	M_{L1n}^* [kg]	$v_{0,L2h}$ [mm/s]	f_1 [Hz]	M^* [kg]	$v_{1,peak}$ [mm/s]	$v_{1,fsdom}$ [mm/s]
F1-CLT	DC 0,05	7,05	2,05	4726,2	1398,9	-	8,05	7,06	1316,0	2,98	10,97
	DS 0,05	6,08	2,05	-	1370,0	-	8,19	6,09	1316,0	3,62	10,95
	SC 0,05	6,95	2,05	4852,9	1436,4	-	7,97	7,06	1316,0	2,98	10,97
	SS 0,05	5,99	2,05	-	1409,0	-	7,83	6,09	1316,0	3,62	10,57
F2-CLT	DC 0,04	8,18	2,35	3507,7	1038,3	-	7,35	8,16	984,2	3,25	9,99
	DS 0,04	7,04	2,35	-	1020,5	-	11,04	7,04	984,2	3,94	14,73
	SC 0,04	8,18	2,35	3509,9	1038,9	-	7,35	8,16	984,2	3,25	9,99
	SS 0,04	7,04	2,35	-	1021,2	-	11,04	7,04	984,2	3,94	14,73
F2-SB	DC 0,04	6,54	1,95	1437,9	876,5	-	15,46	9,19	984,2	5,51	22,49
	DS 0,04	5,90	1,95	1542,2	988,2	-	10,98	7,87	984,2	5,17	14,79
	SC 0,04	6,44	1,95	1482,6	908,1	1380,2	15,22	9,19	984,2	5,51	22,49
	SS 0,04	5,78	1,95	1606,3	1029,4	1606,3	10,83	7,87	984,2	5,17	14,79
F2-TF	DC 0,04	8,14	2,35	3537,6	1047,1	-	9,73	8,16	984,2	3,25	13,27
	DS 0,04	7,06	2,35	-	1014,7	-	11,06	7,04	984,2	3,94	14,73
	SC 0,04	8,14	2,35	3537,5	1047,1	-	9,73	8,16	984,2	3,25	13,27
	SS 0,04	7,06	2,35	-	1014,9	-	11,06	7,04	984,2	3,94	14,73
F3-SB	DC 0,03	8,35	2,1	925,9	649,8	-	11,83	13,09	406,4	8,89	30,97
	DS 0,03	8,32	2,1	776,8	647,4	-	11,94	10,87	406,4	7,07	24,62
	SC 0,03	7,97	2,1	1016,6	719,2	921,1	10,59	13,09	406,4	8,89	28,88
	SS 0,03	7,81	2,1	880,3	733,6	880,3	10,28	10,87	406,4	7,07	22,15
F3-TF	DC 0,03	16,01	2,5	1307,9	386,2	-	10,96	16,06	406,4	2,98	13,33
	DS 0,03	13,85	2,5	-	399,4	-	12,79	13,85	406,4	3,62	16,17
	SC 0,03	16,01	2,5	1307,9	386,2	-	10,96	16,06	406,4	2,98	13,33
	SS 0,03	13,85	2,5	-	399,4	-	12,79	13,85	406,4	3,62	16,17
F4-SB	DC 0,025	10,50	2,5	585,3	410,7	-	17,83	16,36	256,5	9,62	46,68
	DS 0,025	10,46	2,5	491,0	409,2	-	17,99	13,61	256,5	7,65	37,12
	SC 0,025	10,02	2,5	642,7	454,7	582,3	17,11	16,36	256,5	9,62	46,68
	SS 0,025	9,84	2,5	554,5	462,1	554,5	16,75	13,61	256,5	7,65	36,06
F4-TF	DC 0,025	20,16	2,5	825,4	243,8	-	12,87	20,20	256,5	3,23	15,66
	DS 0,025	17,43	2,5	-	252,2	-	15,02	17,40	256,5	3,91	19,00
	SC 0,025	20,16	2,5	825,4	243,8	-	12,87	20,20	256,5	3,23	15,66
	SS 0,025	17,43	2,5	-	252,2	-	15,02	17,40	256,5	3,91	19,00

Table 6.3: Transient response input variables for model and revision EC5

6.2 COMFORT LEVELS OF COMBINED RESPONSE

By transforming the different combinations into a single degree of freedom system can their vibration performance be assessed. First the response factors based on r.m.s. acceleration are presented for the excited floor field as well as adjoining floor fields in home and at neighbouring apartment. Thereafter, showing graphs for r.m.s. velocities of the same floor fields. Finally, sensitivity of SDOF systems for the damping ratio is studied since these susceptible to wide variations in literature.

6.2.1 Methodology

Since damping is included in the system, we can now assess the floor fields for appropriate comfort. This calculation focusses on span L2 in the home (i.e. the excited floor field), but the same procedure holds for the other fields:

1. Determine steady-state response to walking load harmonics
2. Define transient response as a result of footfall heel-strike
3. Calculate 90 % quantile acceleration r.m.s. and velocity of combined steady-state and transient responses
4. Transform a_{rms} and v_{rms} into response factor R and classify the floor field

The following mass-spring-dashpot properties are used in this calculation:

$$\begin{aligned} f_{1,L2} &= 8,14 \text{ Hz} & M_{L2h,m1}^* &= 1047,1 \text{ kg} & K_{eq,L2h} &= 2,742 \cdot 10^6 \text{ N/mm} \\ f_{2,L1} &= 14,75 \text{ Hz} & M_{L2h,m2}^* &= 428,9 \text{ kg} & & \end{aligned}$$

Steady-state response

The steady-state response is a periodically constant vibration that is forced by one of the walking load harmonics, meaning the structure only reacts to that dynamic force. It is in mathematical terms defined by the particular solution for an SDOF system W_{ss} , which follows from equation 2.22 introduced in section 2.3.2.

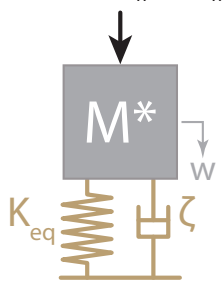
$$P \sin(2\pi f_h t - \varphi_h) \quad W_{ss} = \frac{P}{K_{eq}} \cdot DMF(n \cdot f_s, f_1) \cdot DLF(n \cdot f_s) \cdot \sin(2\pi n f_s t - \varphi_n) \quad (6.2)$$


Figure 6.4: Equivalent SDOF system for steady-state vibration

In expression 6.2 a harmonic function with an amplitude is given by factors that include the level of resonance and the strength of forcing load. The first part of the amplitude is given by the static displacement multiplied with a factor that considers the amplification level such that the maximum dynamic amplitude is found. Static displacement is the magnitude of force P (weight of one person, taken as $P = 700$ N) divided by the equivalent stiffness. Level of resonance depends on the Dynamic Magnification Factor (DMF) that depends on the ratio of harmonic load frequency and the fundamental frequency. Secondly, the amplitude depends on the strength of the force, which is taken into account by the Dynamic Load Factor (DLF). It incorporates how strongly each harmonic contributes to the total walking load by the Fourier coefficient.

Walking load decomposes into four harmonics contributing separately to the vibration and together form the steady-state response. First, determining the response of the equivalent mass-spring-dashpot system to each harmonic, and secondly, summing these responses to find the total response.

One finds the most extreme responses when resonance occurs with one – or more – harmonics. Therefore, the structure has to be checked within the whole range of step frequencies, which is between 1,5 and 2,5 Hz according to several studies regarding walking harmonics [63, 72]:

- $f_{h1} = 1f_s$ Frequency range: 1,5-2,5 Hz
- $f_{h2} = 2f_s$ Frequency range: 3,0-5,0 Hz
- $f_{h3} = 3f_s$ Frequency range: 4,5-7,5 Hz
- $f_{h4} = 4f_s$ Frequency range: 6,0-10,0 Hz

Let us assume for now that $f_s = 2,72$ Hz results in the strongest response, thus $f_{h1} = 2,72$ Hz, $f_{h2} = 5,44$ Hz, $f_{h3} = 8,16$ Hz and $f_{h4} = 10,88$ Hz. Later on will be shown that this step frequency resonates most strongly with the structure.

The closer the forcing frequency gets to the fundamental frequency, the stronger the effect of resonance will be. The Dynamic Magnification Factor (DMF) accounts for this by factoring the static SDOF displacement; thus $DMF = 2$ means the dynamic amplitude is twice the static displacement.

$$\begin{aligned} DMF_{h1} &= \frac{1}{\sqrt{\left(1 - \frac{f_{h1}^2}{f_1^2}\right)^2 + \left(2\zeta \frac{f_{h1}}{f_1}\right)^2}} = 1,091 \\ DMF_{h3} &= \frac{1}{\sqrt{\left(1 - \frac{f_{h3}^2}{f_1^2}\right)^2 + \left(2\zeta \frac{f_{h3}}{f_1}\right)^2}} = 3,937 \end{aligned} \quad \left| \quad \begin{aligned} DMF_{h2} &= \frac{1}{\sqrt{\left(1 - \frac{f_{h2}^2}{f_1^2}\right)^2 + \left(2\zeta \frac{f_{h2}}{f_1}\right)^2}} = 1,502 \\ DMF_{h4} &= \frac{1}{\sqrt{\left(1 - \frac{f_{h4}^2}{f_1^2}\right)^2 + \left(2\zeta \frac{f_{h4}}{f_1}\right)^2}} = 2,811 \end{aligned}$$

Dynamic Load Factor (DLF) expresses the contribution of each harmonic to the total walking load and obtained by Fourier transformation of displacement-time curves of walking experiments. Wilford et al. [72] combined multiple studies and found the following expressions for mean values:

$$DLF_{h1} = 0,37(f_{h1} - 0,95) < 0,5 \quad \Rightarrow \quad DLF_{h1} = 0,5 \quad (6.3)$$

$$DLF_{h2} = 0,054 + 0,0044f_{h2} \quad \Rightarrow \quad DLF_{h2} = 0,080 \quad (6.4)$$

$$DLF_{h3} = 0,026 + 0,0050f_{h3} \quad \Rightarrow \quad DLF_{h3} = 0,071 \quad (6.5)$$

$$DLF_{h4} = 0,010 + 0,0051f_{h4} \quad \Rightarrow \quad DLF_{h4} = 0,071 \quad (6.6)$$

Due to the presence of damping a slight phase shift occurs under a forced vibration, since the damper slightly resists the SDOF system of moving. This effect is taken into account by the phase lag, which is defined – in line with equation 2.23 – as:

$$\begin{aligned} \varphi_{h1} &= \arctan\left(\frac{2\zeta f_{h1}}{\pi(f_{h1}^2 - f_1^2)}\right) = -0,00043 \\ \varphi_{h3} &= \arctan\left(\frac{2\zeta f_{h3}}{\pi(f_{h3}^2 - f_1^2)}\right) = 0,10043 \end{aligned} \quad \left| \quad \begin{aligned} \varphi_{h2} &= \arctan\left(\frac{2\zeta f_{h2}}{\pi(f_{h2}^2 - f_1^2)}\right) = -0,00070 \\ \varphi_{h4} &= \arctan\left(\frac{2\zeta f_{h4}}{\pi(f_{h4}^2 - f_1^2)}\right) = 0,00049 \end{aligned}$$

Now all components of the steady-state response are known, displacement over time of each harmonic can be determined:

$$W_{L2h,h1}(t) = \frac{P}{K_{eq,L2h}} \cdot DMF_{h1} \cdot DLF_{h1} \sin(2\pi n f_s t - \varphi_{h1}) = 0,1409 \sin(18,85t + 0,00044) \quad (6.7)$$

$$W_{L2h,h2}(t) = \frac{P}{K_{eq,L2h}} \cdot DMF_{h2} \cdot DLF_{h2} \sin(2\pi n f_s t - \varphi_{h2}) = 0,0445 \sin(37,70t + 0,00084) \quad (6.8)$$

$$W_{L2h,h3}(t) = \frac{P}{K_{eq,L2h}} \cdot DMF_{h3} \cdot DLF_{h3} \sin(2\pi n f_s t - \varphi_{h3}) = 0,0762 \sin(56,56t + 0,00174) \quad (6.9)$$

$$W_{L2h,h4}(t) = \frac{P}{K_{eq,L2h}} \cdot DMF_{h4} \cdot DLF_{h4} \sin(2\pi n f_s t - \varphi_{h4}) = 0,0154 \sin(75,41t - 0,00033) \quad (6.10)$$

Above expressions define the response to each harmonic and according to the superposition-principle the total response is a summation of equations 6.7-6.10. In figure 6.5 are the responses to each harmonic (equations 6.7-6.10) plotted besides the combined total response.

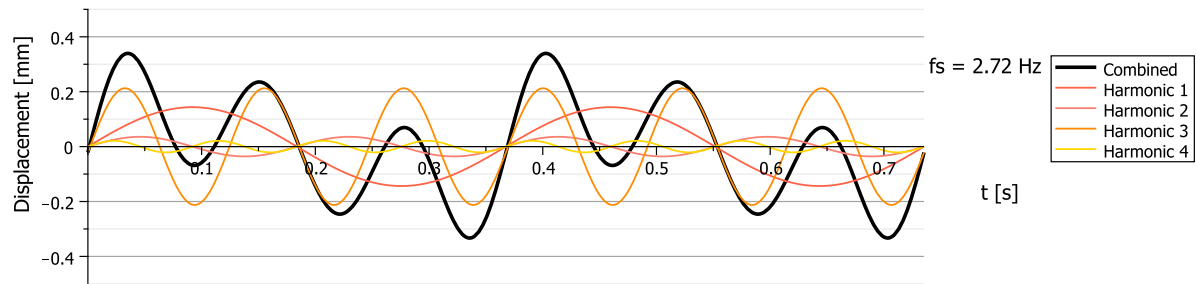


Figure 6.5: Maximum steady-state response of floor 2 with timber-frame walls (F2-TF) and double leaf continuous floor field (DC)

Equations 6.7-6.10 are displayed in figure 6.5 together with the summation of all four. One can observe that the total steady-state response predominantly consists of the combination of harmonic 1 and 4. This makes sense since harmonic 4 ($f_{h4} = 8,20$ Hz) strongly resonates with the structure ($f_1 = 8,14$ Hz) and harmonic 1 has a high DLF compared to the other harmonics.

Transient response

Transient response relates to the homogeneous solution W_{tr} , which is introduced in section 2.3.1 with equation 2.20, and defined by the absence of a force.

$$W_{tr} = \frac{v_0}{2\pi f_1} \cdot e^{-2\pi\zeta f_1 t} \cdot \sin(2\pi f_1 t) \quad (6.11)$$

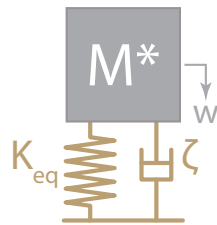


Figure 6.6: Equivalent SDOF system for transient vibration

The vibration occurs due to an initial displacement W_0 and velocity v_0 whereafter the structure oscillates freely back to its origin due to energy dissipating from the system. For the case of walking vibrations, the initial displacement is equal to zero and initial velocity defined as energy added by a heel striking the floor making a mass move:

$$W_0 = 0 \quad v_0 = \frac{\partial W_{t=0}}{\partial t} = \frac{I}{M^*}$$

Initial velocity is thus given by dividing the impulse of that heel-strike over modal mass of the structure. The second term in equation 6.11 incorporates the energy dissipating from the system through damping. Finally, the oscillation is included by the sinusoidal term.

Transient responses are also known as free vibrations since the floor vibrates freely without an external force being present. These vibrations are a combination of all vibration modes according to the superposition principle, where the first mode is most dominant.

$$v_{0,L2h,m1} = \frac{I_{m1}}{M_{L2h,m1}^*} = 12,63 \text{ mm/s} \quad \text{where:} \quad I_{m1} = 42 \frac{f_s^{1.43}}{f_{1,L2}^{1.3}} = 11,50 \text{ Ns} \quad (6.12)$$

$$W_{L2h,m1}(t) = \frac{v_{0,L2h,m1}}{2\pi f_{1,L2}} \cdot e^{-2\pi\zeta f_{1,L2} t} \cdot \sin(2\pi f_{1,L2} t) = 0,469 \cdot e^{-2,047t} \sin(51,17t) \quad (6.13)$$

All natural vibration modes with eigenfrequencies up to twice the fundamental frequency have to be considered according to multiple studies [63, 72, 75]. Therefore, the second mode of structures where a dynamic force at span L2 excites floor span L1, i.e. double span and beam supported floors, has also to be taken into account. Eigenfrequency of the second mode is $f_{1,L1}$ resulting in modal mass $M_{L2h,m2}^*$. Furthermore, displacement over time of the second SDOF system is found in the same manner as for the first mode.

$$v_{0,L2h,m2} = \frac{I_{m2}}{M_{L2h,m2}^*} = 14,25 \text{ mm/s} \quad \text{where:} \quad I_{m2} = 42 \frac{f_s^{1.43}}{f_{1,L1}^{1.3}} = 5,31 \text{ Ns} \quad (6.14)$$

$$W_{L2h,m2}(t) = \frac{v_{0,L2h,m2}}{2\pi f_{1,L2}} \cdot e^{-2\pi\zeta f_{1,L1}t} \cdot \sin(2\pi f_{1,L1}t) = 0,154 \cdot e^{-3,708t} \sin(92,69t) \quad (6.15)$$

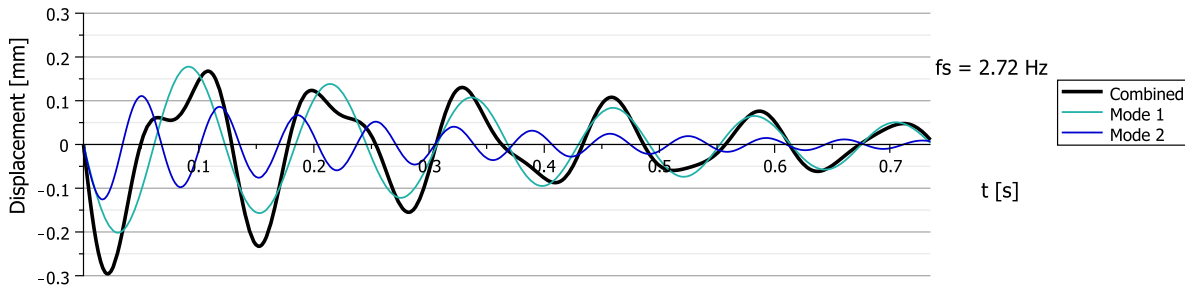


Figure 6.7: Maximum transient response

In figure 6.7 are equations 6.13 (mint) and 6.15 (blue) displayed for $t = 0 \dots 2T_s$. In reality is the transient response given by the summation of both equations (black) according to the superposition principle. The second mode has a higher natural frequency which causes more cycles than the first mode in the same period, and thus more energy is dissipated from the system. Therefore decays the second mode faster than the first mode.

Root-mean-square acceleration and velocity

Now the profile of both responses is known, their root-mean-square values for acceleration and velocity can be determined. Since humans perceive acceleration more strongly for lower frequencies and velocity for the higher ones, the r.m.s. values are weighted for human perception with $H_{W,a}$ for acceleration and $H_{W,v}$ for velocity:

$$H_{W,a} = \frac{1}{\sqrt{1 + \left(\frac{f}{5,6}\right)^2}} \quad H_{W,v} = \frac{1}{\sqrt{1 + \left(\frac{5,6}{f}\right)^2}} \quad (6.16)$$

Since the floor is relatively short, all harmonics have to be corrected for the inability to fully build up resonance with factor ρ (see section 2.4.2). The formula is repeated below, where L_2 is the floor span and v_s the walking speed, which is 1,62 m/s for $f_s = 2,05$ Hz [63].

$$\rho = 1 - \exp^{-2\pi\zeta f_1 T_w} = 0,916 \quad \text{where:} \quad T_w = \frac{L_2}{v_s} = \frac{L_2}{1,67 f_s^2 - 4,83 f_s + 4,5} = 1,21 \quad (6.17)$$

As mentioned in section 2.5.2, the root-mean-square is defined as the square root of the mean square, where the mean square is obtained by integrating the square of a function over one period and dividing it by that same period. The period of one step T_s , i.e. the time between two footsteps, is given by:

$$T_s = \frac{1}{f_s} = 0,368 \text{ s}$$

$$a_{rms,h1} = H_{W,a}(f = f_{h1}) \cdot \rho \cdot \sqrt{\frac{1}{T_s} \int_0^{T_s} \left(\frac{\partial^2 W_{L2h,h1}(t)}{\partial t^2} \right)^2 dt} = 0,90 \cdot 0,916 \cdot 29,7 = 24,44 \text{ mm/s}^2 \quad (6.18)$$

$$a_{rms,h2} = H_{W,a}(f = f_{h2}) \cdot \rho \cdot \sqrt{\frac{1}{T_s} \int_0^{T_s} \left(\frac{\partial^2 W_{L2h,h2}(t)}{\partial t^2} \right)^2 dt} = 0,72 \cdot 0,916 \cdot 29,5 = 19,41 \text{ mm/s}^2 \quad (6.19)$$

$$a_{rms,h3} = H_{W,a}(f = f_{h3}) \cdot \rho \cdot \sqrt{\frac{1}{T_s} \int_0^{T_s} \left(\frac{\partial^2 W_{L2h,h3}(t)}{\partial t^2} \right)^2 dt} = 0,57 \cdot 0,916 \cdot 395,0 = 204,75 \text{ mm/s}^2 \quad (6.20)$$

$$a_{rms,h4} = H_{W,a}(f = f_{h4}) \cdot \rho \cdot \sqrt{\frac{1}{T_s} \int_0^{T_s} \left(\frac{\partial^2 W_{L2h,h4}(t)}{\partial t^2} \right)^2 dt} = 0,46 \cdot 0,196 \cdot 69,77 = 29,25 \text{ mm/s}^2 \quad (6.21)$$

$$a_{rms,tr} = \sqrt{\frac{1}{T_s} \int_0^{T_s} \left(\frac{\partial^2 H_{W,a}(f = f_{1,L2}) \cdot W_{L2h,m1}(t) + H_{W,a}(f = f_{1,L1}) \cdot W_{L2h,m2}(t)}{\partial t^2} \right)^2 dt} = 238,9 \text{ mm/s}^2 \quad (6.22)$$

Acceleration over time is by definition the second derivative of $W(t)$ over time and used to determine the root-mean-square values of acceleration. These values are multiplied with the weighting function $H_{W,a}$ and resonance build up factor ρ . From equations 6.18–6.21 one can observe that the first harmonic is perceived most strongly and the fourth harmonic the least.

The same procedure is followed for obtaining root-mean-square velocity values, where velocity over time is the first derivative of $W(t)$ over time:

$$v_{rms,h1} = H_{W,v}(f = f_{h1}) \cdot \rho \cdot \sqrt{\frac{1}{T_s} \int_0^{T_s} \left(\frac{\partial W_{L2h,h1}(t)}{\partial t} \right)^2 dt} = 0,44 \cdot 0,916 \cdot 1,74 = 0,69 \text{ mm/s} \quad (6.23)$$

$$v_{rms,h2} = H_{W,v}(f = f_{h2}) \cdot \rho \cdot \sqrt{\frac{1}{T_s} \int_0^{T_s} \left(\frac{\partial W_{L2h,h2}(t)}{\partial t} \right)^2 dt} = 0,70 \cdot 0,916 \cdot 0,86 = 0,55 \text{ mm/s} \quad (6.24)$$

$$v_{rms,h3} = H_{W,v}(f = f_{h3}) \cdot \rho \cdot \sqrt{\frac{1}{T_s} \int_0^{T_s} \left(\frac{\partial W_{L2h,h3}(t)}{\partial t} \right)^2 dt} = 0,82 \cdot 0,916 \cdot 7,70 = 5,82 \text{ mm/s} \quad (6.25)$$

$$v_{rms,h4} = H_{W,v}(f = f_{h4}) \cdot \rho \cdot \sqrt{\frac{1}{T_s} \int_0^{T_s} \left(\frac{\partial W_{L2h,h4}(t)}{\partial t} \right)^2 dt} = 0,89 \cdot 0,916 \cdot 1,02 = 0,83 \text{ mm/s} \quad (6.26)$$

$$v_{rms,tr} = \sqrt{\frac{1}{T_s} \int_0^{T_s} \left(\frac{\partial H_{W,v}(f = f_{1,L2}) \cdot W_{L2h,m1}(t) + H_{W,v}(f = f_{1,L1}) \cdot W_{L2h,m2}(t)}{\partial t} \right)^2 dt} = 6,74 \text{ mm/s} \quad (6.27)$$

Since humans perceive velocity more strongly for higher frequencies and resonance build up is similar to a_{rms} contribute higher harmonics more to weighted root-mean-square velocity than the lower ones.

Response factor of combined total response

Different root-mean-square values can be combined by a procedure known as 'Square root sum of the squares' according to Wilford [72]. As a consequence, have low r.m.s. values a low contribution to the total value, where high values dominate the r.m.s. total value.

$$a_{rms,SS} = \sqrt{a_{rms,h1}^2 + a_{rms,h2}^2 + a_{rms,h3}^2 + a_{rms,h4}^2} = 209,2 \text{ mm/s}^2 \quad (6.28)$$

$$a_{rms,Tr} = a_{rms,tr} = 238,9 \text{ mm/s}^2 \quad (6.29)$$

$$a_{rms} = \sqrt{a_{rms,SS}^2 + a_{rms,Tr}^2} = 317,5 \text{ mm/s}^2 \quad (6.30)$$

$$v_{rms,SS} = \sqrt{v_{rms,h1}^2 + v_{rms,h2}^2 + v_{rms,h3}^2 + v_{rms,h4}^2} = 5,94 \text{ mm/s} \quad (6.31)$$

$$v_{rms,Tr} = v_{rms,tr} = 6,74 \text{ mm/s} \quad (6.32)$$

$$v_{rms} = \sqrt{v_{rms,SS}^2 + v_{rms,Tr}^2} = 8,99 \text{ mm/s} \quad (6.33)$$

Both steady-state and transient response contribute to total a_{rms} and v_{rms} value. When above explained procedure is followed for each walking frequency the following graphs are obtained:

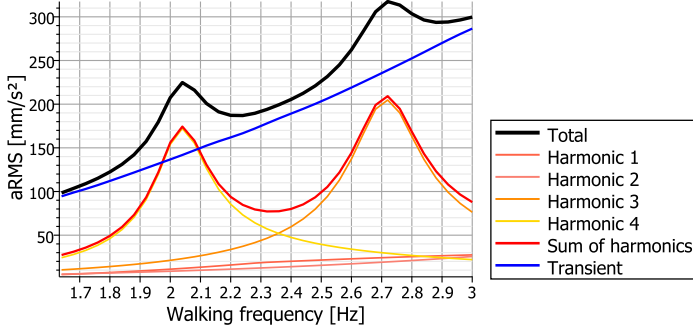


Figure 6.8: aRMS-values within the walking frequency range

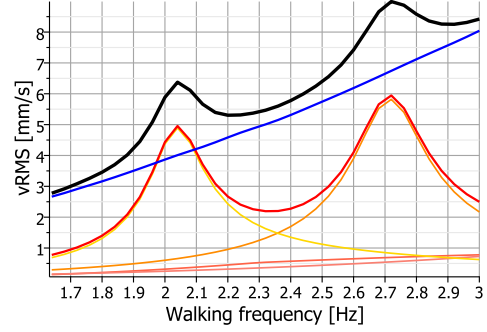


Figure 6.9: vRMS-values within the walking frequency range

Above shown figures explain why $f_s = 2,72$ Hz was assumed to be the dominant walking frequency since this results in the strongest resonance in the steady-state regime. Transient response increases almost linearly with the walking frequency since the impact force of a heel-strike rises with f_s .

Simply using the highest a_{rms} and v_{rms} would be insufficient, since high walking frequencies have a low probability of occurring. Therefore, the stochastic demographic distribution of Waarts [67] is applied to find the root-mean-square values with only 10 % chance on exceeding. Figure 6.10 and 6.11 show the cumulative probability of a_{rms} and v_{rms} respectively, where 90% quantile values can be read of the graphs: $a_{rms90} = 215,63 \text{ mm/s}^2$ and $v_{rms90} = 6,10 \text{ mm/s}$.

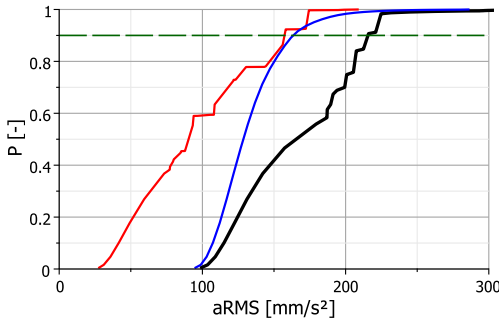


Figure 6.10: Probability of aRMS-values

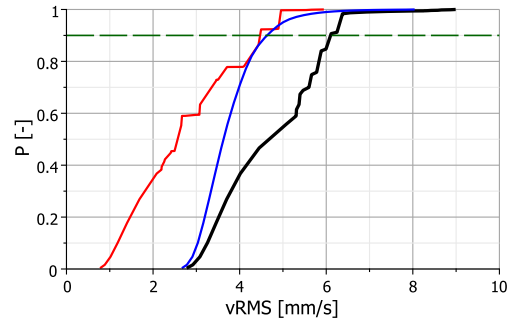


Figure 6.11: Probability of vRMS-values

Concluding, the response factor is determined for both a_{rms90} and v_{rms90} , and the maximum of these two classifies the floor:

$$R_{L2h,a} = \frac{a_{rms90,L2h}}{5} = 43,1 \quad R_{L2h,v} = \frac{v_{rms90,L2h}}{0.1} = 61,0$$

$$R_{L2h} = \max(R_{L2h,a}, R_{L2h,v}) = 61,0$$

6.2.2 Quantification using root-mean-square values

For each of the floor typologies, and their four support condition variations, the vibrations due to humans walking are quantified in terms of root-mean-square values, and the found results for these combinations are elaborated below.

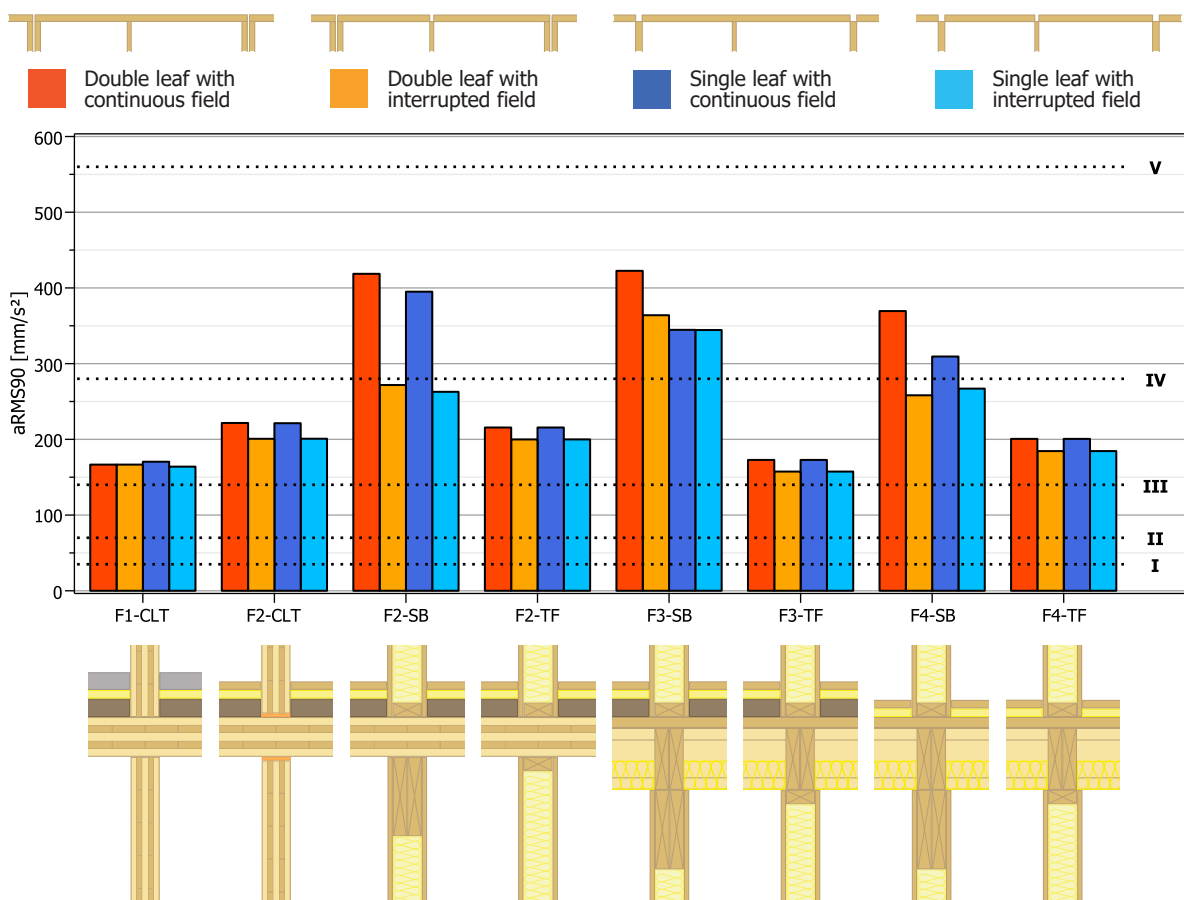
Acceleration

Figure 6.12a summarises the r.m.s. acceleration values calculated for all floor typologies shown below the column graph. All beam supported floors show higher $a_{r.m.s.}$ compared to their equivalents on rigid supports, which has two causes. 1) The static deflection due to a single person is higher for flexible supports, because the displacement of the supporting beam adds up to the floor deflection, resulting in a stronger steady-state response. 2) Impact values by a heel-strike for transient responses increase for lower fundamental frequencies, which can not be fully compensated by the increased modal mass, and therefore, have flexible supported a higher initial velocity.

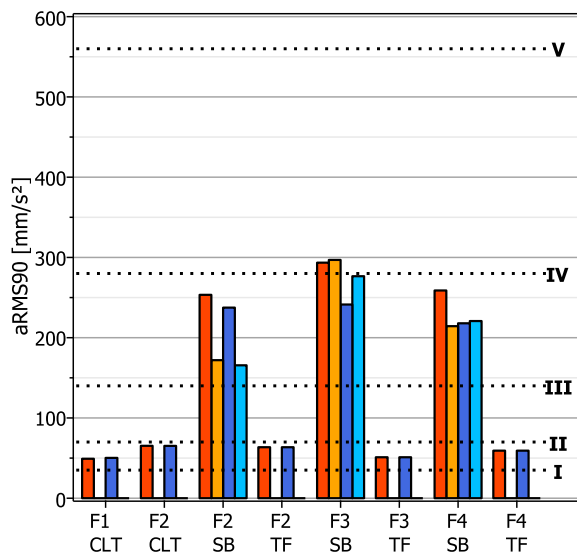
The CLT-floor with a wet screed (F1-CLT) performs better than the one with a dry screed (F2-CLT and F2-TF) for all support conditions, where the wet screed shows higher values for the continuous field, and the dry screed for the hinged internal junction. This is due to the dominant walking frequency $f_{s,dom}$, as can be read from table ??.

Floor 3 (with additional mass, F3-TF) performs slightly better than the other rigidly supported joist floor (F4-TF). This attributes to the increased mass resulting in a lower initial velocity, and thus a weaker transient response.

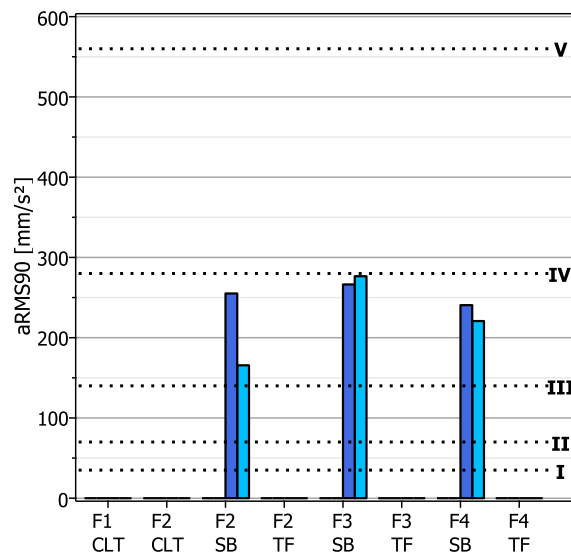
Vibration levels found in the floor fields in home (figure 6.12b) and neighbouring apartment (figure 6.12c) are lower than in the excited field. Especially continuous floor fields result in higher vibration levels in these adjoining fields.



(a) Excited home field (L2)



(b) Other home field (L1)

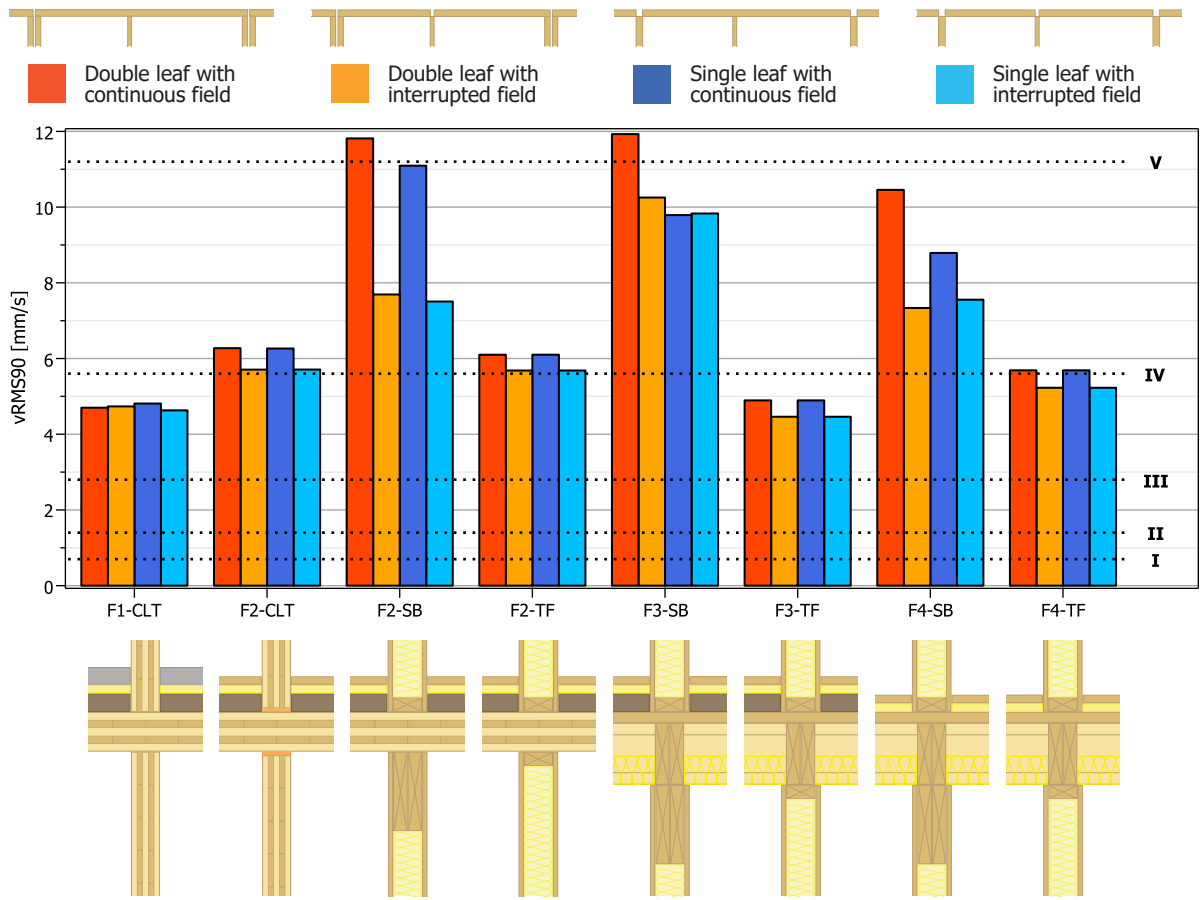


(c) Neighbour field (L1)

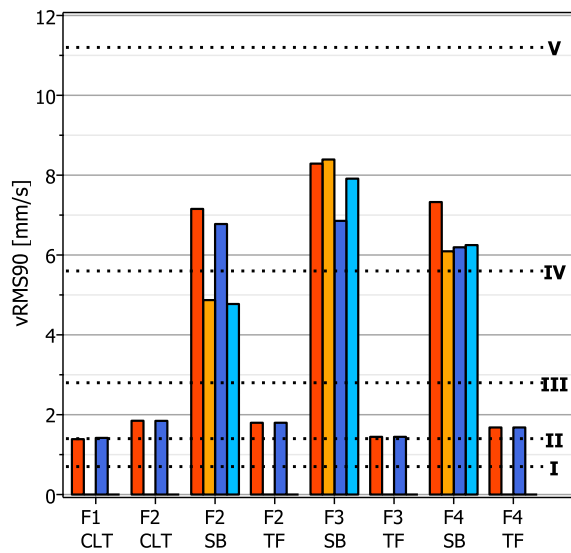
Figure 6.12: a_{rms} values of floor typologies

Velocity

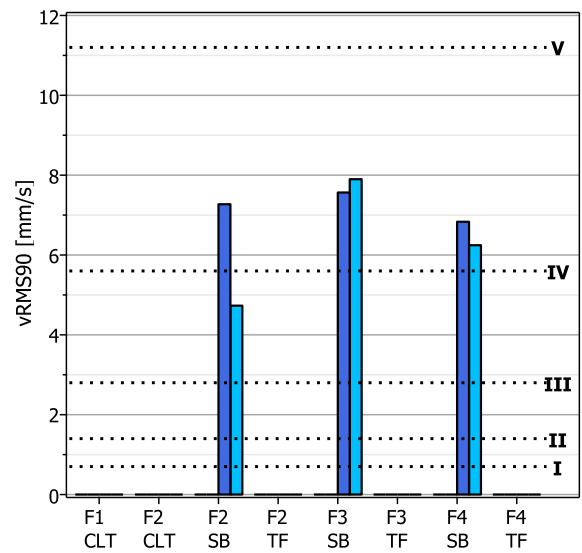
Vibration levels in terms of root-mean-square velocity are shown in figure 6.13, from which can be observed that flexibly supported floors also perform about twice as worse than their rigid equivalent. Of all rigid floors,



(a) Excited home field (L2)



(b) Other home field (L1)



(c) Neighbour field (L1)

Figure 6.13: v_{rms} values of floor typologies

floor 2 shows, on average, the highest v_{rms} values.

6.2.3 Contribution transient response

Generally it is assumed that the transient response can be neglected for low-frequency floors, and steady-state response contributes marginally for high-frequency floors. One of the aims of this work is to check that hypothesis, especially for floors with a fundamental frequency around 8 Hz. The contribution of the transient to the total response is calculated with the following equation for acceleration and velocity respectively:

$$\left(\frac{a_{rms,Tr}}{a_{rms,tot}} \right)^2 \cdot 100\% \quad \left(\frac{v_{rms,Tr}}{v_{rms,tot}} \right)^2 \cdot 100\%$$

In figure 6.14a are the contributions of the transient to the total response shown for acceleration, which is the quantity often used to assess low frequency floors, for example the future revision of EC5. Based on this study can be concluded that transient response do contribute significantly to low-frequency floors (between 30 and 60 % for rigid supports), and therefore, neglecting the transient response results in underestimated vibration levels. On the other hand, vibrations of high frequency floors (F3 and F4) consist almost fully out transient responses when expressed in a_{rms} .

When the root-mean-square velocity is applied as vibration level quantity, as is commonly done for high-frequency floors, the total response consists, for the major part, of transient response contribution (see figure 6.14b).

Therefore can be concluded based on this work that transient responses contribute always to the vibration levels, independent of whether the floor is classified as LFF or HFF. Regarding the steady-state response it is correct to assume that it can be neglected for high-frequency floors.

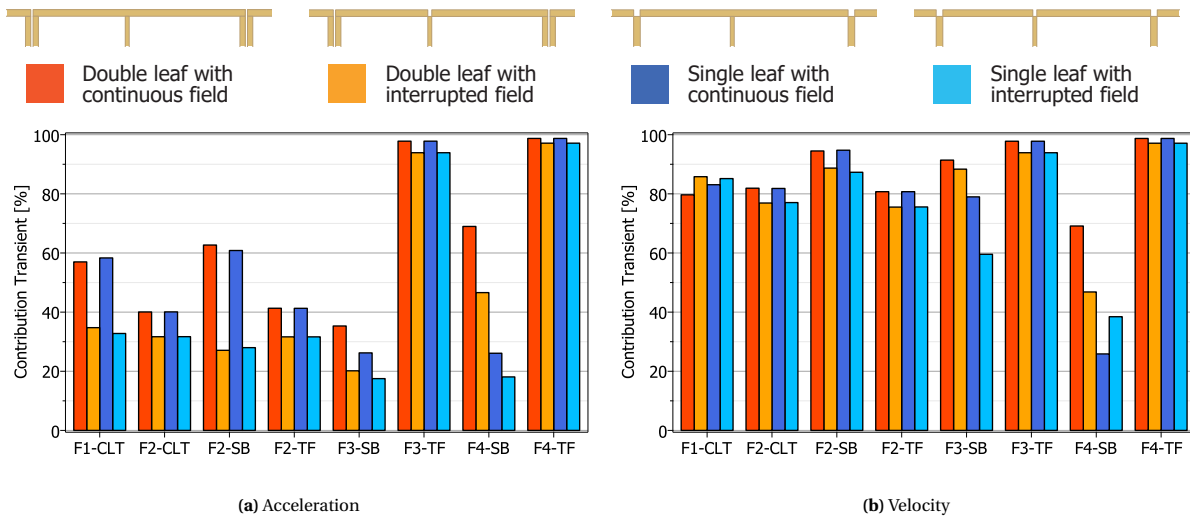


Figure 6.14: Contribution of transient to total response

6.2.4 Classification using response factors

We now have two values that define the floor vibrations, namely the root-mean-square acceleration and velocity. Since the annoyance depends on the frequency range do we have to introduce the response factor to find the lowest comfort level of the two. This response factor is defined by R and relates to the base curve of ISO 10137 [17] where $R = 1$ relates to hardly perceptible vibrations given in the frequency range. Below are the definitions given of R , where a_{rms} is in mm/s^2 and v_{rms} in mm/s .

$$R = \frac{a_{w,rms}}{5} = \frac{v_{w,rms}}{0.1} \quad (6.34)$$

Table 6.4: Response factors as given in revision of EC5 [5] and newly determined for combined response

	Performance level	R_{EC5}	$R_{comb.}$	a_{rms90}	v_{rms90}
I	Quality	4	7	35 mm/s ²	0,7 mm/s
II	Quality	8	14	70 mm/s ²	1,4 mm/s
III	Quality	16	28	140 mm/s ²	2,8 mm/s
IV	Base	32	56	280 mm/s ²	5,6 mm/s
V	Economy	64	112	560 mm/s ²	11,2 mm/s

The determined reponse factor classifies the floor for comfort and depends on the type of use. Since this study focusses on multi-family buildings will only deliberated on these response factors given in the future revision of Eurocode 5. For these factors is, however, the assumption made that LFFs are only subjected to the steady-state response and HFF to transient response only, where this work studies the combination of both responses, and therefore, the classes have to be adopted for appropriate classification. The response factors of the most elementary floors, e.g. single-span floor on rigid supports, are calculated for steady-state or transient response only and compared to the response factors from the combined responses. Thereafter, the new response factors classes are found such that similar classifications are found, given in table 6.4. It should be noted that these proposed factors are only an estimation that reflects the comfort levels for combined responses and further research is required for actual classification of floors.

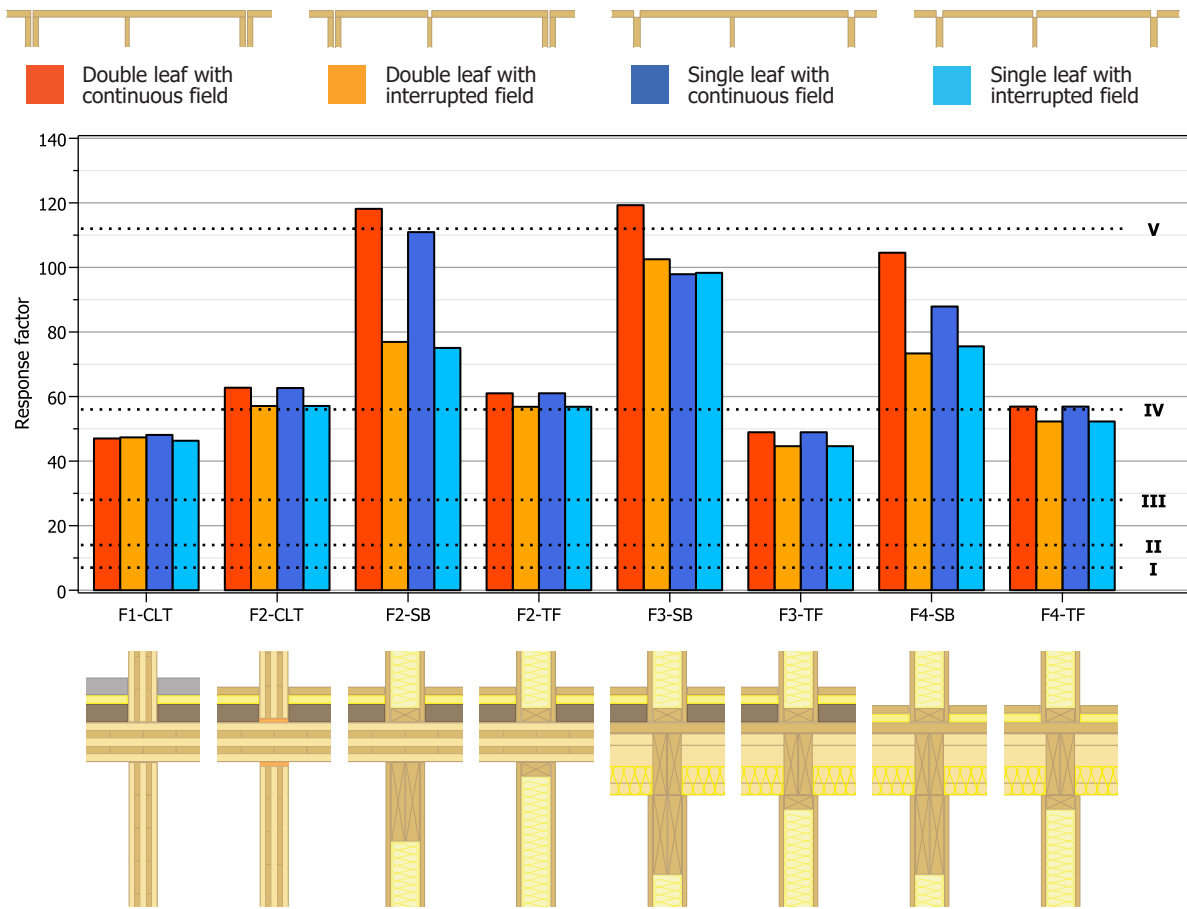
Generally can be stated that rigid supports are the best measure that could be taken to prevent transmittance of vibrations. Since neighbours get annoyed at lower vibration levels due to a source that is hard to address should especially the separating wall be designed such that it behaves rigid. The internal junction can still be executed with supporting beams for flexibility reasons as long as the beam has sufficient stiffness (i.e. a height above 300 mm).

When observing the four floor configurations on rigid supports do floor 1 and 3 perform quite similarly, where floor 3 shows slightly bigger differences between the single- (red and dark blue) and two-span (orange and light blue). Thereafter follows floor 4, and floor 2 the worst of all. From figure 6.15 can be concluded that increasing the stiffness (floor 3 with joists) either reduces vibrations, besides the commonly applied measure by increasing the mass (floor 1). Moreover, when building in CLT sufficient mass should be added to prevent excessive vibrations, preferably by applying wet screeds since it increases the impact sound insulation. Joists with decking floors are generally lighter resulting in a higher fundamental frequency, and therefore not susceptible to steady-state vibrations. Leaving out the additional mass of the floor configuration (floor 4) results higher in initial velocities compared to floors with higher modal masses (floor 3).

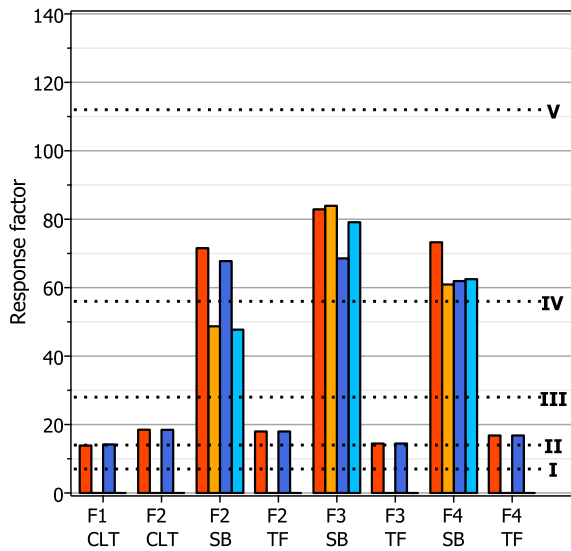
Concluding, for multi-family buildings where the permanent load on the foundation does not play a role in the design process the most efficient design choice is to increase the floor its mass, since it improves both the vibration comfort and impact sound insulation. When the structure is a vertical extension or build on soil with low load-bearing capacity, and thus the mass plays a role, an joist floor should be applied because vibrations are controlled by sufficient stiffness. Mass could be added to the floor for acoustic reasons as long as the fundamental frequency is kept above 12 Hz to prevent resonance with walking load harmonics, i.e. negligible steady-state response. In case that limit is reached and more mass is still required, the stiffness should either be increased.

No significant differences are found between single- and two-span floors, but single-span floors perform in general slightly better especially for HFF where the second mode introduced by the shorter floor span increases the vibration levels.

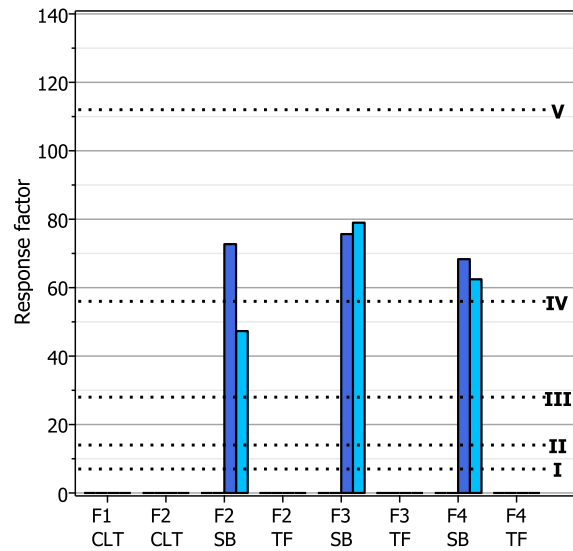
Flexible supported home-separating junctions where both floors are supported should be prevented or sufficient stiff beams (above 400mm height) have to be applied. Generally it is a safer measure to apply two beams (double leaf typology) in that home-separating junction such that vibration transmittance is prevented. For rigid support types, no differences are found between single- and double leaf regarding transmittance, thus applying a single leaf wall preferable for reducing mass, since both wall types have similar sound insulation.



(a) Excited home field (L2)



(b) Other home field (L1)



(c) Neighbour field (L1)

Figure 6.15: Response factor

6.3 SENSITIVITY RESPONSE FACTORS FOR DAMPING RATIO

The response factors are, besides the fundamental frequency, highly dependent on the damping ratio. Since the values in literature widely vary and structure specific values can only be obtained by full-scale experiments, the sensitivity of the R factors for ζ is studied in this section. The values are varied by a factor ranging from 0,5 to 2,0 (see figure 6.5), where the results are shown in a boxplot (figure 6.16), such that the response range can be studied. A wider ranging boxplot means a higher sensitivity for the damping ratio.

The damping ratios are based on values provided by Abeysekera [1], which are adopted in the future revision of EC5. According to Abeysekera, resilient elastomers in the junction do have a positive effect on the damping ratio, but since more experiments have to be done for realistic ζ values, the resilient interlayers are neglected for damping ratios. Besides, the absence of a fill for floor 4 is encountered by reducing the damping ratio with 0,5%.

	Floor 1	Floor 2	Floor 3	Floor 4
0,50 ζ =	0,025	0,02	0,015	0,0125
0,60 ζ =	0,03	0,024	0,018	0,015
0,70 ζ =	0,035	0,028	0,021	0,0175
0,80 ζ =	0,04	0,032	0,024	0,02
0,90 ζ =	0,045	0,036	0,027	0,0225
ζ =	0,05	0,04	0,03	0,025
1,11 ζ =	0,056	0,044	0,033	0,0278
1,25 ζ =	0,063	0,05	0,038	0,031
1,43 ζ =	0,071	0,057	0,043	0,038
1,67 ζ =	0,083	0,067	0,05	0,0417
2,00 ζ =	0,1	0,08	0,06	0,05

Table 6.5: Damping ratios used for sensitivity study

Beam supported floors tend to be more sensitive for varying damping ratios, meaning their vibration levels are more controlled by damping, which is a consequence of their lower system stiffness. Most boxplots are quite symmetric in their mean value, but some show a longer tail upwards, like the double leaf walls and continuous floor field in figure 6.16b. The symmetry of the plot declares the dependency on damping, the more symmetric the more linear the response increases with increasing damping ratio.

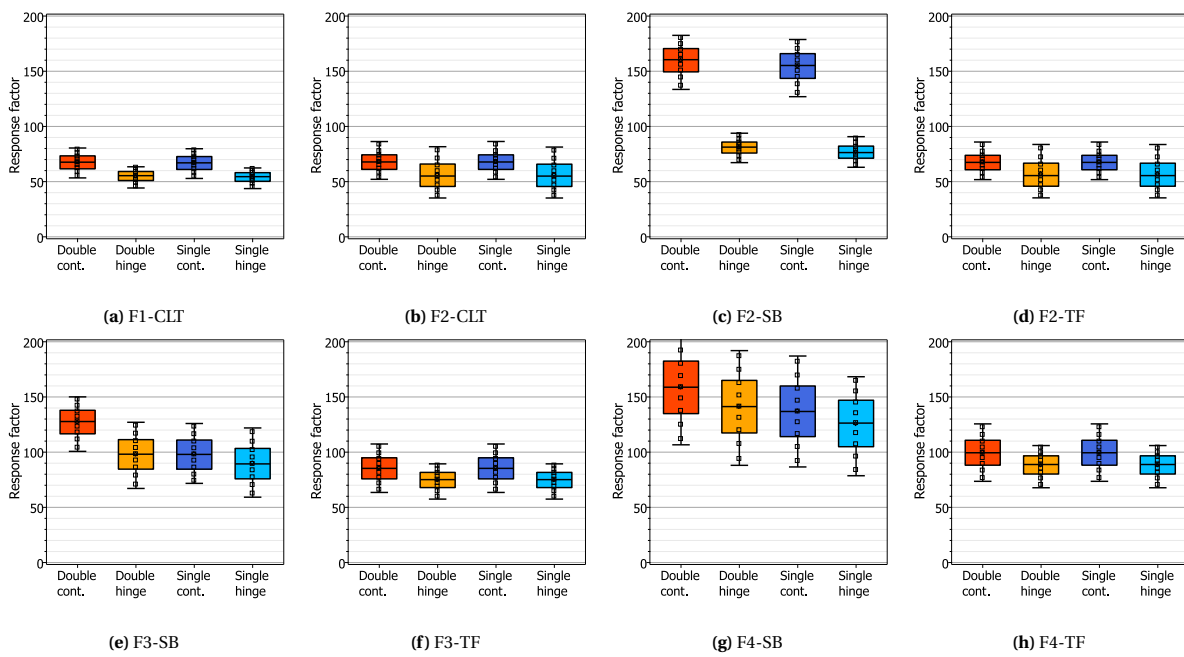


Figure 6.16: Response factors of combined responses for $0,5\zeta$ to 2ζ

6.4 COMPARISON RESULTS WITH OTHER METHODS

The Maple model is validated by comparing the vibration levels with values calculated in line with the future revision of EC5 and experiments conducted by TNO for the project 'De Karel Doorman' by RHDHV.

Revision Eurocode 5

Eurocode 5 allows one to only assess the excited field and not vibration levels at adjoining floor fields. Therefore, only floor span L_2 is compared in this section. Moreover, the code assumes resonance with one of the harmonics and neglects the others. Therefore, to correctly compare the model to EC5, only the a_{rms} value of the strongest contribution harmonic at the dominant walking frequency is shown in table 6.6 for steady-state response from the model.

As elaborated in section 6.1 (table 6.2 and 6.3) does not only the procedure of assessment differ, but also input values like modal mass and initial velocity. To account for this, the mass-spring-dashpot properties are obtained by transformation into a SDOF system also applied for validation according to the EC5 procedure. Below the equations for a_{rms} and v_{rms} are given according to future revision of EC5. Explanation of these equations can be found in section 3.3.

$$a_{rms} = \frac{0,4\alpha F_0}{\sqrt{2}M^*2\zeta}$$

$$v_{rms} = \beta \cdot K_{imp} \cdot K_{red} \frac{42 \frac{f_s^{1.43}}{f_1^{1.3}}}{M^* + 70}$$

Steady-state response

Steady-state responses of low-frequency floors are validated with the quantity a_{rms} in EC5, where the geometry floor properties are enclosed by M^* and α (which depends on f_1).

Values found for the dominating harmonic by the Maple model are of the same order of magnitude as the ones obtained in line with EC5, but the variances are significant. Especially for flexible supported typologies are large differences visible in table 6.6, which may be caused by the fact that not all the formulas that are proposed are suited for floors supported on beams, as already mentioned in section 6.1. When SDOF properties obtained in this work are used as input for EC5, the values for a_{rms} of the model neither do approach the ones from the code. This may be due the different procedure that is used, since the future revision of EC5 determines the vibration level based on the modal mass, applies this work the use of equivalent stiffness K_{eq} for assessment of steady-state responses.

Transient response

High-frequency floors, with a fundamental frequency above 8 Hz, are assumed to be transient according to future revision of EC5 so are only the v_{rms} values for transient response from the model used for comparison.

As was already stated in section 3.3, the assumption in EC5 that the walking frequency is 1,5 Hz leads to an underestimation of the impact by a heel-strike. This mainly explains the difference in v_{rms} values between the model and EC5, as table 6.6 shows.

When floor properties obtained by the model are substituted in the formulas of EC5, more similar vibration levels are found. For the magnitude of the impact the dominant walking frequency is used. However, for support conditions with a continuous floor field (DC and SC) the model generally gives higher values because it also includes the second mode in the displacement-time expression for the floor.

Floor		Steady-state: a_{rms} [mm/ ²]			Transient: v_{rms} [mm/s]		
		Model		EC5	Model		EC5
		Input: Model	Input: EC5	Input: Model	Input: Model	Input: EC5	Input: Model
F1-CLT	DC	132,67	89,29	84,48	6,76	1,19	4,56
	DS	154,95	131,82	127,06	5,54	1,47	5,74
	SC	129,66	89,29	85,38	6,70	1,19	4,52
	SS	156,97	131,82	127,80	5,45	1,47	5,68
F2-CLT	DC	205,70	95,96	90,44	6,78	1,27	4,32
	DS	221,79	150,57	144,98	4,42	1,58	4,44
	SC	205,71	95,96	90,48	6,78	1,27	4,32
	SS	221,44	150,57	145,02	4,42	1,58	4,44
F2-SB	DC	259,44	245,93	206,22	16,05	2,06	8,19
	DS	257,86	255,65	236,23	8,13	2,11	8,16
	SC	253,92	285,25	207,06	15,52	2,26	8,12
	SS	253,89	294,49	237,86	7,63	2,31	7,78
F2-TF	DC	204,75	95,96	90,93	6,74	1,27	4,31
	DS	224,02	150,57	144,64	4,43	1,58	4,45
	SC	204,77	95,96	90,93	6,74	1,27	4,31
	SS	223,97	150,57	144,65	4,43	1,58	4,45
F3-SB	DC	389,33	379,01	180,04	12,77	5,14	11,74
	DS	396,71	296,95	183,08	8,01	4,60	11,48
	SC	365,39	506,93	189,36	9,07	5,92	10,49
	SS	370,35	424,70	197,64	6,90	5,42	10,25
F3-TF	DC	45,84	13,17	14,12	8,53	1,67	7,98
	DS	99,06	31,94	32,38	7,51	2,12	9,74
	SC	45,84	13,17	14,12	8,53	1,67	7,98
	SS	99,06	31,94	32,38	7,51	2,12	9,74
F4-SB	DC	628,53	326,13	144,50	13,52	5,36	12,24
	DS	629,29	239,89	147,43	8,95	4,79	11,91
	SC	579,87	470,29	158,07	10,10	6,21	11,17
	SS	563,08	376,37	167,11	7,90	5,67	10,89
F4-TF	DC	31,54	4,75	5,12	9,94	1,66	8,58
	DS	48,49	14,49	14,70	8,88	2,14	10,64
	SC	31,54	4,75	5,12	9,94	1,66	8,58
	SS	48,49	14,49	14,70	8,88	2,14	10,64

Table 6.6: Comparison of steady-state and transient responses from model with revision EC5

Experiments TNO 'De Karel Doorman'

When during construction of 'De Karel Doorman' excessive vibrations were felt it was set on hold. TNO conducted experiments to come up with effective measures to reduce vibrations, especially regarding transmittance to adjoining fields. Beneficial about this research is that both a situation with flexible supports only (as designed) and with rigid supports at the home-separating junction (as built) were measured.

The results are documented in *Trilling- en geluidsonderzoek aan vloeren van het Linea Nova gebouw* [22], where the vibration levels are obtained with the OS-RMS₉₀ method, which accounts for the probability of occurring of walking frequencies and the persons weight. The vibration levels obtained with the Maple model are partly processed in line with this method to be able to compare the model with the experiments. Only the stochastic distribution of walking frequency is considered, where the persons weight is set equal to the mean value (i.e. 760 N). This does not influence the results by much because vibration levels increase linearly over the force.

Moreover, more adjustments are made to the model to create conditions similar to the experiments, where the vibrations were the result of the heeldrop test. A person stands on his toes and lets his heel hit the floor, which causes an impact lower than from a heel-strike. Therefore, the formula for the impact in the model is replaced by one that represents a heeldrop, which can be approximated with the following equation according to Ohlsson [50]:

$$I = \sqrt{\frac{30000}{(f_1)^4}}$$

The properties of the equivalent SDOF system is given in table 6.7, where the fundamental frequency was given in the document and K_{eq} determined from the static deflection in a software package. The modal mass follows from these two values by equation 6.1.

		f_1 [Hz]	K_{eq} [N/m]	M^* [kg]
Designed	Home	6,1	$2,028 \cdot 10^6$	1380,8
	Neighbour	6,7	$2,169 \cdot 10^6$	1224,0
Built	Home	6,7	$6,135 \cdot 10^6$	865,5
	Neighbour	6,5	$9,091 \cdot 10^7$	4360,2

Table 6.7: Input values of equivalent SDOF for 'De Karel Doorman'

The calculated v_{rms} values are given in table 6.8 for both home and neighbouring apartment besides the values as measured by TNO. The table provides the mean and 90 % probability value of the cumulative probability, which are also graphically displayed in figure 6.17 for the situation 'as designed' and in figure 6.17 'as built'.

The model approaches the measured values quite well, especially for the designed situation where the floors were supported by HE220A steel beams. For the built situation, the model is less accurate, which may be due to the manner the supports are constructed. TNO advised to add steel columns between the steel beams to make the supports act more rigidly, as is shown in figure 6.19. The two-dimensional effects of vibrations transmitted by this support type are hard to catch in a one-dimensional model.

	Quantile	Home		Neighbour	
		Model	TNO	Model	TNO
Designed	50%	1,50 mm/s	1,5 mm/s	1,35 mm/s	0,9 mm/s
	90%	1,57 mm/s	2,4 mm/s	1,42 mm/s	1,4 mm/s
Built	50%	1,86 mm/s	1,7 mm/s	0,40 mm/s	0,9 mm/s
	90%	1,97 mm/s	2,3 mm/s	0,42 mm/s	1,4 mm/s

Table 6.8: v_{rms} quantile values from model for 'De Karel Doorman'

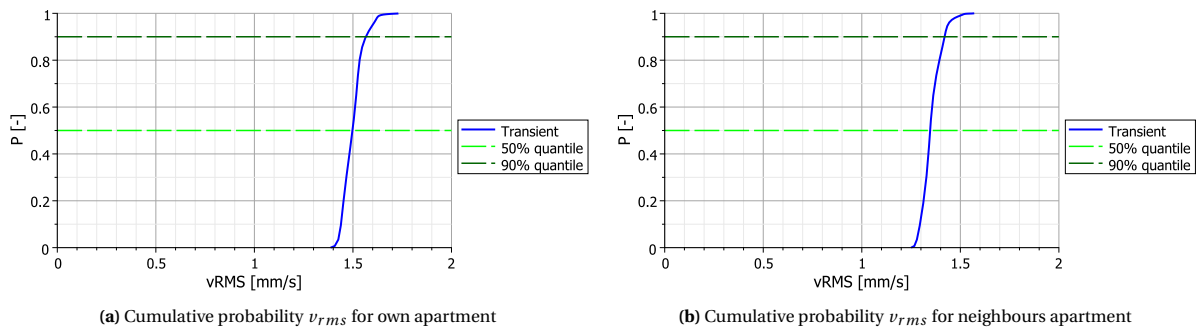


Figure 6.17: Results from model for 'De Karel Doorman' as designed

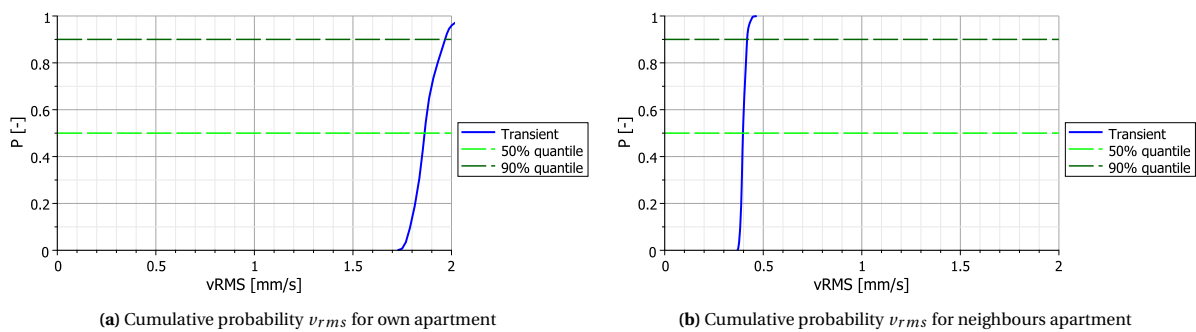


Figure 6.18: Results from model for 'De Karel Doorman' as built

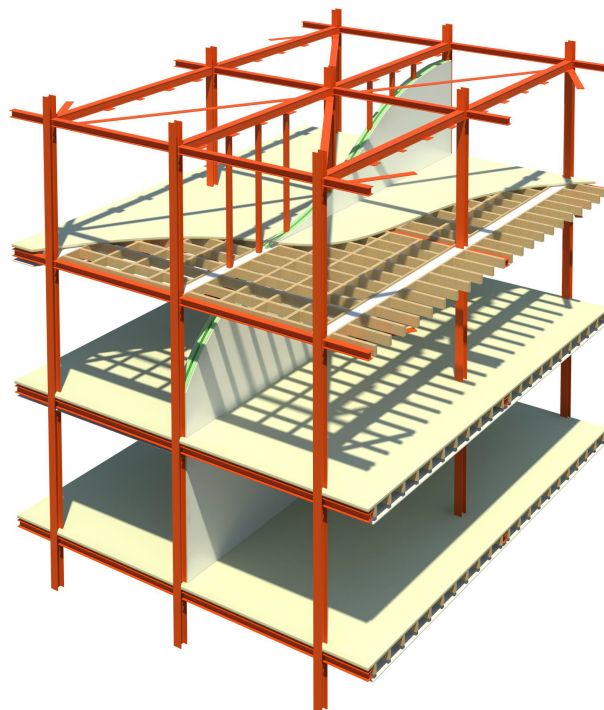


Figure 6.19: Home-separating junction of 'De Karel Doorman' [14]

7

Conclusion

7.1 CONCLUSION

Vibration problems can be solved by adding sufficient mass to increase the damping of the structure and to improve the acoustic performance of dwellings. However, adding mass decreases the eigenfrequencies, cancelling the benefit regarding damping partially out. When aiming for an ultra-lightweight structure, simply adding mass is not desirable and therefore, the problems regarding vibrations and acoustics have to be solved in another manner. Instead, adding stiffness to the structure is a more efficient way of achieving vibration comfort since it reduces the vibration amplitude. It does this firstly by increasing the eigenfrequency, and thereby, decreasing the resonance of the structure. Secondly, the stiffness dominated steady-state responses as result external walking loads are handled in a mathematical more logic manner.

In the parameter study, the effects of varying the geometry at the supports were visualised with mode shapes, showing the ease with which vibrations can transmit from one floor to another when the beam that supports both beam is insufficiently stiff (i.e. a beam height below about 400 mm). Moreover, the natural frequencies decrease to such a level for flexible supports that joist floors that were not susceptible to resonance with the walking load harmonic show increasing vibration levels for the steady-state response. Floors with rigid supports, like timber-frame or CLT walls, show no transmittance of vibrations to adjoining floor fields except when the floor in home spans both rooms. Weight reduction is possible by using single leaf separating walls, which have comparable acoustic performance compared to their double leaf equivalent. Clamping-like behaviour of CLT floors by CLT walls is found to have a negligible effect on natural frequencies and mode shapes. Increasing the floor stiffness shows a linear increase of natural frequencies if supports are rigid, otherwise, f_1 reaches a plateau caused by flexible supports. Natural frequencies calculated with continuous undamped systems are found to be similar to the ones from the rigid fundamental frequency proposed in the future revision of Eurocode 5, and for flexible supports the values are comparable to the Dunkerley's approximation.

Two CLT floors (one with wet and one with dry screed) and two I-joist floors with LVL decking are assessed with respect to human-induced vibrations by transforming the floors into Single Degree of Freedom systems. Steady-state and transient responses are combined for determination of vibration levels, where the transient response is found to contribute significantly to the total response. This contradicts the assumption in the future revision of EC5 that transient responses can be neglected for low-frequency floors. Moreover, the heel-strike impact magnitude is underestimated by assuming a walking frequency of 1,5 Hz, and the proposed formula for determination of the modal mass neglects increasing mass for flexible supports or two-span beams. Therefore, the following equation for modal mass is proposed to approximate the modal mass, where w_{1kN} is the maximum deflection of the floor field in *mm* and determined similar to EC5's stiffness criterion:

$$M^* = \frac{10^6}{w_{1kN} (2\pi f_1)^2}$$

Joist floors are found most suitable for lightweight timber buildings, where mass can be increased to reduce transient responses as long as the fundamental frequency stays above 12 Hz to prevent resonance with the walking load harmonics. Transmittance to adjoining apartments is avoided with rigid supports, or by applying two beams in the home-separating junction if more plan flexibility is asked. When no requirements are set regarding mass for the multi-family building, CLT panels with sufficient mass are the best choice since the weight improves both vibrations and impact sound insulation. No significant differences were found between single- and two-span floors on rigid supports.

7.2 DISCUSSION

The results in this work can be applied to timber buildings with rectangular floor fields constructed from material with a transverse stiffness up to 20 % of the longitudinal flexural stiffness. For floors that are supported on four sides, this research can either be used, but gives conservative results. It is suitable for simple floor fields and structure studies in preliminary design, otherwise more comprehensive methods have to be used for vibration assessment, like Finite Element modelling.

Floors are approached from one-dimensional perspective by modelling them as a beam. Therefore, beneficial planar effects regarding vibrations are not taken into account. The only two-dimensional part that is incorporated is for the damped assessment, where the equivalent stiffness includes the floor's effective width. As a consequence, natural frequencies may not exactly meet realistic values, especially for CLT panels which have a significant transverse flexural stiffness compared to EI_L .

Models simplify by definition reality, which also holds for the Maple models used in this work. Transforming floors into Single Degree of Freedom system hinders modelling of a person walking along a path, but it is partially covered by accounting for resonance built-up. Besides, the dynamic load of only a single person is considered, whereas in reality more people may walk along a floor, which may result in higher vibration levels.

Damping is considered as a factor that is hard to predict because it is a result of dry friction of structural elements and differs from floor to floor. Moreover, inhabitants of buildings either influence the level of damping by the furniture that is placed on the floor and type of flooring that is chosen. The sensitivity study showed that response factors vary quite strongly with changing damping ratios.

7.3 RECOMMENDATIONS

The preliminary stage in development of a timber building concept for residential multi-family buildings is covered by this work. Within the subject of human-induced vibration, extensive research with timber as structural material regaining attention. Below are several areas described that require more research.

Where often it is assumed that modal masses of low-frequency floors are sufficiently high that transient responses are negligible compared to the steady-state, this work shows that the contribution to the total response is significant. Extensive research needs to be done on this topic to examine whether this is the result of simplification by the model, or that the assumption in the future revision of EC5 is incorrect and engineers have to account for both responses when designing a light-weight floor structure.

Timber floors are simplified in this work by almost fully neglecting two-dimensional effects. For the development of a lightweight timber building concept for multi-family houses, this effect has to be studied further using, for example, Finite Element software. Since vibrations are a Serviceability Limit State, stochastic variables like source and receiver location, walking frequency and person's weight should be included in this study.

Bibliography

- [1] I.K. Abeysekera, P. Hamm, T. Toratti, and A. Lawrence. Development of a floor vibration design method for Eurocode 5. In R. Görlacher, editor, *INTER*, pages 445–459, Tallinn (ES), 2018.
- [2] D.E. Allen and T.M. Murray. Design criterion for vibrations due to walking. *Engineering Journal*, 30(4): 117–129, 1993.
- [3] H.J. Blaß and C. Sandhaas. *Timber engineering: Principles for design*. KIT Scientific publishing, Karlsruhe, 2017.
- [4] CEN TC250 SC5.T1. *Working draft of design of cross laminated timber in a revised Eurocode 1995-1-1*. European Committee for Standardization, 2018.
- [5] CEN TC250 SC5.T3. *Working draft of design of timber structures - Revised section 9.3 Vibrations*. European Committee for Standardization, 2018.
- [6] A.K. Chopra. *Dynamics of structures*. Prentice Hall, New Jersey (USA), 2007.
- [7] R.V.M. Cobelens. *Building light and comfortable*. Msc thesis, Delft University of Technology, 2018.
- [8] M. Feldmann, C. Heinemeyer, C. Butz, E. Caetano, A. Cunha, F.M.B. Galanti, A. Goldack, O. Hechler, S.J. Hicks, A. Keil, M. Lukic, R. Obiala, M. Schlaich, G. Sedlacek, A.L. Smith, and P.H. Waarts. *Design of floor structures for human induced vibrations*. Office for Official Publications of the European Communities, Luxembourg, 2009.
- [9] G. Fink, D. Honfi, J. Kohler, and P. Dietsch. *Basis of Design Principles for Timber Structures: A state-of-the-art report by COST Action FP1402 / WG 1*. Shaker Verlag, Aachen (DE), 2018.
- [10] O. Flodén. *Vibration transmission in lightweight buildings: Numerical prediction models*. Doctoral thesis, Lund University, 2016.
- [11] GreenBuildingAdvisor. Can Wood Replace Concrete and Steel in Skyscrapers?, 2015. URL <https://www.finehomebuilding.com/2015/09/16/can-wood-replace-concrete-and-steel-in-skyscrapers>.
- [12] P. Hamm and A. Richter. Bemessungs- und Konstruktionsregeln zum Schwingungsnachweis von Holzdecken. In *Fachtagungen Holzbau 2009*, pages 15–29, Leinfelden-Echterdingen, 2009.

- [13] P. Hamm, A. Richter, and S. Winter. Floor vibrations - new results. In *11th World Conference on Timber Engineering (WCTE 2010)*, pages 2765–2775, Riva da Garda (IT), 2010.
- [14] M. Hermens, M. Visscher, and J. Kraus. Ultra Light Weight Solutions for Sustainable Urban Densification. In *CTBUH 2014 Shanghai*, pages 542–549, 2014.
- [15] Holzforschung Austria. Dataholz: an online catalog for timber construction. URL <https://www.dataholz.eu/>.
- [16] I. Ijeh. Timber frames: will we see wooden skyscrapers in the future?, 2019. URL <https://www.building.co.uk/buildings/timber-frames-will-we-see-wooden-skyscrapers-in-the-future/5097471.article>.
- [17] ISO. *ISO 10137 - Bases for design of structures - Serviceability of buildings and walkways against vibrations*. International Organization for Standardisation, Geneva, Switzerland, 2007. URL <https://archive.org/details/et.iso.10137.2007>.
- [18] N.A. Jacobs, J. Skorecki, and J. Charnley. Analysis of the vertical component of force in normal and pathological gait. *Journal of Biomechanics*, 5:11–34, 1972.
- [19] K. Jarnerö. *Vibrations in timber floors – Dynamic properties and human perception*. PhD thesis, Linnaeus University, 2014.
- [20] K. Jarnerö, Å. Bolmsvik, A. Brandt, and A. Olsson. Effect of flexible supports on vibration performance of timber floors. In *Noise Control (Euronoise)*, pages 214–219, Prague, 2012.
- [21] M. Kohler and C. Lecomte. Lumber choices for wood frame construction - choosing timber for framing and building homes, 2013. URL <https://www.ecohome.net/guides/2283/best-material-choices-for-wood-frame-construction/>.
- [22] A. Koopman, S.S.K. Lentzen, and F.M.B. Galanti. *Trilling- en geluidsonderzoek aan vloeren van het Linea Nova gebouw*. TNO Bouw en Ondergrond, Delft, 2009.
- [23] N. Labonnote. *Damping in Timber Structures*. PhD thesis, Norwegian University of Science and Technology, 2012.
- [24] N. Labonnote, A. Rønnquist, and A.M. Kjell. Experimental evaluations of material damping in timber beams of structural dimensions. *Wood Science Technology*, 47:1033–1050, 2013.
- [25] D. Malone. Military giants: Cross-laminated timber construction gets a salute from the Army, 2016. URL <https://www.bdcnetwork.com/military-giants-cross-laminated-timber-construction-gets-salute-army>.
- [26] N.J. Mansfield. *Human response to vibration*. CRC Press, Boca Raton, Florida (USA), 2005.
- [27] A V Metrikine. *Dynamics, Slender structures and an Introduction to continuum mechanics*. Delft University of Technology, Delft (NL), 2014.
- [28] MetsäWood. Adding new storeys of wood: New housing potential for big cities in Germany. URL <https://www.metsawood.com/global/news-media/articles/Pages/Adding-new-storeys-of-wood-New-housing-potential-for-big-cities-of-Germany.aspx>.
- [29] A.S. Mohammed, A. Pavic, and V. Racic. Improved model for human induced vibrations of high-frequency floors. *Engineering Structures*, 2018.
- [30] Z. Muhammad, P. Reynolds, O. Avci, and M. Hussein. Review of Pedestrian Load Models for Vibration Serviceability Assessment of Floor Structures. *Vibration*, 2(1):1–24, 2018. doi: 10.3390/vibration2010001.
- [31] T.M. Murray, D.E. Allen, E.E. Ungar, and D.B. Davis. *Vibrations of steel-framed structural systems due to human activity*. American Institute of Steel Construction, Chicago (USA), 2016.

- [32] K. Nabielek, D. Hamers, and D. Evers. *Cities in Europe - Facts and figures on cities and urban areas*. PBL Netherlands Environmental Assessment Agency, The Hague (NL), 2016.
- [33] Naopt. Engineered floor joist. URL <http://naopt.info/engineered-floor-joist/>.
- [34] J. Negreira. *Vibrations in lightweight buildings: Perception and prediction*. Licentiate dissertation, Lund University, 2013.
- [35] NEN. *ISO 140-4 Acoustics — Measurement of sound insulation in buildings and of building elements — Part 4: Field measurements of airborne sound insulation between rooms*. Netherlands Standards Institute, Delft (NL), 1998.
- [36] NEN. *NEN 1070 - Noise control in buildings – Specification and rating of quality*. Netherlands Standards Institute, Delft (NL), 1999.
- [37] NEN. *EN 1990 - Eurocode: Basis of structural design*. Netherlands Standards Institute, Delft (NL), 2002.
- [38] NEN. *EN 1991-2 - Eurocode 1: Actions on structures - Part 2: Traffic loads on bridges*. Netherlands Standards Institute, Delft (NL), 2003.
- [39] NEN. *EN 1995-1-1 - Eurocode 5: Design of timber structures - Part 1-1: General - Common rules and rules for buildings*. Netherlands Standards Institute, Delft (NL), 2005.
- [40] NEN. *EN 1993-1-1 - Eurocode 3: Design of steel structures - Part 1-1: General rules and rules for buildings*. Netherlands Standards Institute, Delft (NL), 2006.
- [41] NEN. *EN 1990 - National Annex to NEN-EN 1990+A1+A1/C2: Eurocode: Basis of structural design*. Netherlands Standards Institute, Delft (NL), 2011.
- [42] NEN. *EN 1991-2 - National Annex to NEN-EN 1991-2+C1: Eurocode 1: Actions on structures - Part 2: Traffic loads on bridges*. Netherlands Standards Institute, Delft (NL), 2011.
- [43] NEN. *EN 1993-2 - Eurocode 3: Design of steel structures - Part 2: Steel bridges*. Netherlands Standards Institute, Delft (NL), 2011.
- [44] NEN. *NEN-EN-ISO 717-1 - Acoustics - Rating of sound insulation in buildings and of building elements - Part 1: Airborne sound insulation*. Netherlands Standards Institute, Delft (NL), 2013.
- [45] NEN. *NEN-EN-ISO 717-2 - Acoustics - Rating of sound insulation in buildings and of building elements - Part 2: Impact sound insulation*. Netherlands Standards Institute, Delft (NL), 2013.
- [46] NEN. *ISO 12354-2 - Building acoustics - Estimation of acoustic performance of buildings from the performance of elements - Part 2: Impact sound insulation between rooms*. Netherlands Standards Institute, Delft (NL), 2017. URL <https://connect.nen.nl/standard/openpdf/?artfile=590868&RNR=3532142&token=3b567325-88ac-479e-a32d-5d562ddc39ac&type=pdf#page=mode=bookmarks>.
- [47] NEN. *ISO 12354-1 - Building acoustics - Estimation of acoustic performance of buildings from the performance of elements - Part 1: Airborne sound insulation between rooms*. Netherlands Standards Institute, Delft (NL), 2017.
- [48] I. Newton, I. Cohen, and A. Whitman. *The Principia: mathematical principles of natural philosophy*. University of California Press, Berkeley, 1999.
- [49] S. Ohlsson. *Springiness and human-induced floor vibrations: A design guide*. Swedish Council for Building Research, Stockholm, Sweden, 1988.
- [50] S. Ohlsson. Ten years of floor vibration research - a review of aspects and some results. *Proceedings of the symposium/workshop on serviceability of buildings (movements, deformations, vibrations)*, 1: 419–434, 1988.
- [51] K.C. Parsons and M.J. Griffin. Whole-body vibration perception thresholds. *Journal of Sound and Vibration*, 121(2):237–258, 1988.

- [52] A. Pavic, P. Reynolds, P. Waldron, and K.J. Bennett. Critical review of guidelines for checking vibration serviceability of post-tensioned concrete floors. *Cement and Concrete Composites*, 23:21–31, 2001.
- [53] PlusWonen. Appartementen: Gevarieerd wonen, flexibele architectuur. Technical report, VolkerWessels, Amersfoort, 2012.
- [54] J.H. Rainer, G. Pernica, and D.E. Allen. Dynamic Loading and Response of Footbridges. *Canadian Journal of Civil Engineering*, 15:66–71, 1988.
- [55] B. Rasmussen. *Sound insulation between dwellings - Overview of the variety of descriptors and requirements in Europe*. European Acoustics Association - EAA, Aalborg (DK), 2011. ISBN 9788469415207.
- [56] B. Rasmussen. Sound classification of dwellings in the Nordic countries – Differences and similarities between the five national schemes Sound classification of dwellings in the Nordic countries – Differences and similarities between the five national schemes Introdunct. In *Baltic-Nordic Acoustics Meeting (BNAM) 2012*, Odense (DK), 2012.
- [57] B. Rasmussen. Sound classification of dwellings - Quality class ranges and intervals in national schemes in Europe. In *European Conference on Noise Control*, pages 1178–1183, Prague, 2012. ISBN 9788001050132.
- [58] G. Ravenshorst. *Course Timber Structures 1: Engineered Timber*, 2017.
- [59] RFCS. *Human Induced Vibration of Steel Structures (HiVoSS) - Vibration Design of Floors: Guideline*. European Commission - Research Fund for Coal and Steel, Brussels, 2007.
- [60] Rothoblaas. *Soundproofing solutions*. Technical report, Rothoblaas SRL, 2017.
- [61] Rothoblaas. *Xylofon: High-performance resilient soundproofing profile*. Technical report, Rothoblaas, Cortaccia (IT), 2018.
- [62] A. Schiavi, A. P. Belli, and F. Russo. Estimation of acoustical performance of floating floors from dynamic stiffness of resilient layers. *Building Acoustics*, 12(2):99–113, 2005. ISSN 1351010X. doi: 10.1260/1351010054037938.
- [63] G. Sedlacek, C. Heinemeyer, C. Butz, B. Völling, P.H. Waarts, F. Van Duin, S.J. Hicks, P.J. Devine, and T. Demarco. *Generalisation of criteria for floor vibrations for industrial, office, residential and public building and gymnastic halls*. Office for Official Publications of the European Communities, Luxembourg, 2006.
- [64] Siemens PLM. The FRF: Dynamic Stiffness, Compliance, Mobility, and more..., 2019. URL <https://community.plm.automation.siemens.com/t5/Testing-Knowledge-Base/The-FRF-Dynamic-Stiffness-Compliance-Mobility-and-more/ta-p/573101>.
- [65] A.L. Smith, S.J. Hicks, and P.J. Devine. *Design of floors for vibration - A new approach*. The Steel Construction Institute, Ascot (UK), 2009.
- [66] T. Toratti and A. Talja. Classification of human induced floor vibrations. *Building acoustics*, 13:211–221, 2006.
- [67] P.H. Waarts. *Trillingen van vloeren door lopen. Richtlijn voor het voorspellen, meten en beoordelen*. SBR, Rotterdam (NL), 2005.
- [68] J. Weckendorf. *Dynamic response of structural timber flooring systems*. PhD thesis, Edinburgh Napier University, Edinburgh (UK), 2009.
- [69] J. Weckendorf, B. Zhang, A. Kermani, D. Reid, and P. Andersen. Damping Characteristics of Timber Flooring Systems with Respect to Low-Frequency Vibration Modes Lecturer in Structural Engineering Senior Lecturer in Structural Engineering. In *Proceedings of the 10th World Conference on Timber Engineering*, Miyazaki, Japan, 2008.

- [70] J. Weckendorf, T. Toratti, I. Smith, and T. Tannert. Vibration serviceability performance of timber floors. *European Journal of Wood and Wood Products*, 74:353–367, 2016.
- [71] J. Wheeler. Prediction and control of pedestrian induced vibration in footbridges. *Journal of the Structural division ASCE*, 108:2045–2065, 1982.
- [72] M.R. Wilford and P. Young. *A design guide for footfall induced vibration of structures*. The Concrete Centre, Camberley (UK), 2006. ISBN 1-904482-29-5.
- [73] T.A. Wyatt. *Design guide on the vibration of floors*. The Steel Construction Institute, Ascot (UK), 1989.
- [74] T.A. Wyatt and A.F. Dier. Building in steel, the way ahead. *International symposium: building in steel, the way ahead*, 1989.
- [75] P. Young. Improved floor vibration prediction methodologies. In *Engineering for Structural Vibration – Current developments in research and practice, Arup Vibration seminar*. Institution of Mechanical Engineers, 2001.
- [76] S. Zegers. *Lightweight floor system for vibration comfort*. PhD thesis, Eindhoven University of Technology, 2011.
- [77] B. Zhang, B. Rasmussen, A. Jorissen, and A. Harte. Comparison of vibrational comfort assessment criteria for design of timber floors among the European countries. *Engineering Structures*, 52:592–607, 2013.
- [78] S. Zhang, J. Zhou, J. Niederwestberg, and Y.H. Chui. Effect of end support restraints on vibration performance of cross laminated timber floors: An analytical approach. *Engineering Structures*, 189: 186–194, 2019. ISSN 18737323. doi: 10.1016/j.engstruct.2019.03.042.
- [79] S.E. Zimmer and M. Augustin. Vibrational behaviour of cross-laminated timber floors in residential buildings. In *World conference on timber engineering 2016*, pages 4835–4844, Vienna, Austria, 2016. URL <http://repositum.tuwien.ac.at/obvutwoa/content/pageview/1559788>.
- [80] S. Živanović, A. Pavic, and P. Reynolds. Vibration serviceability of footbridges under human-induced excitation: A literature review. *Journal of Sound and Vibration*, 279:1–74, 2005.

A

Junction details and properties

F1-CLT: JOIST FLOORS WITH A WET SCREED ON CLT WALLS (NO INTERLAYER)

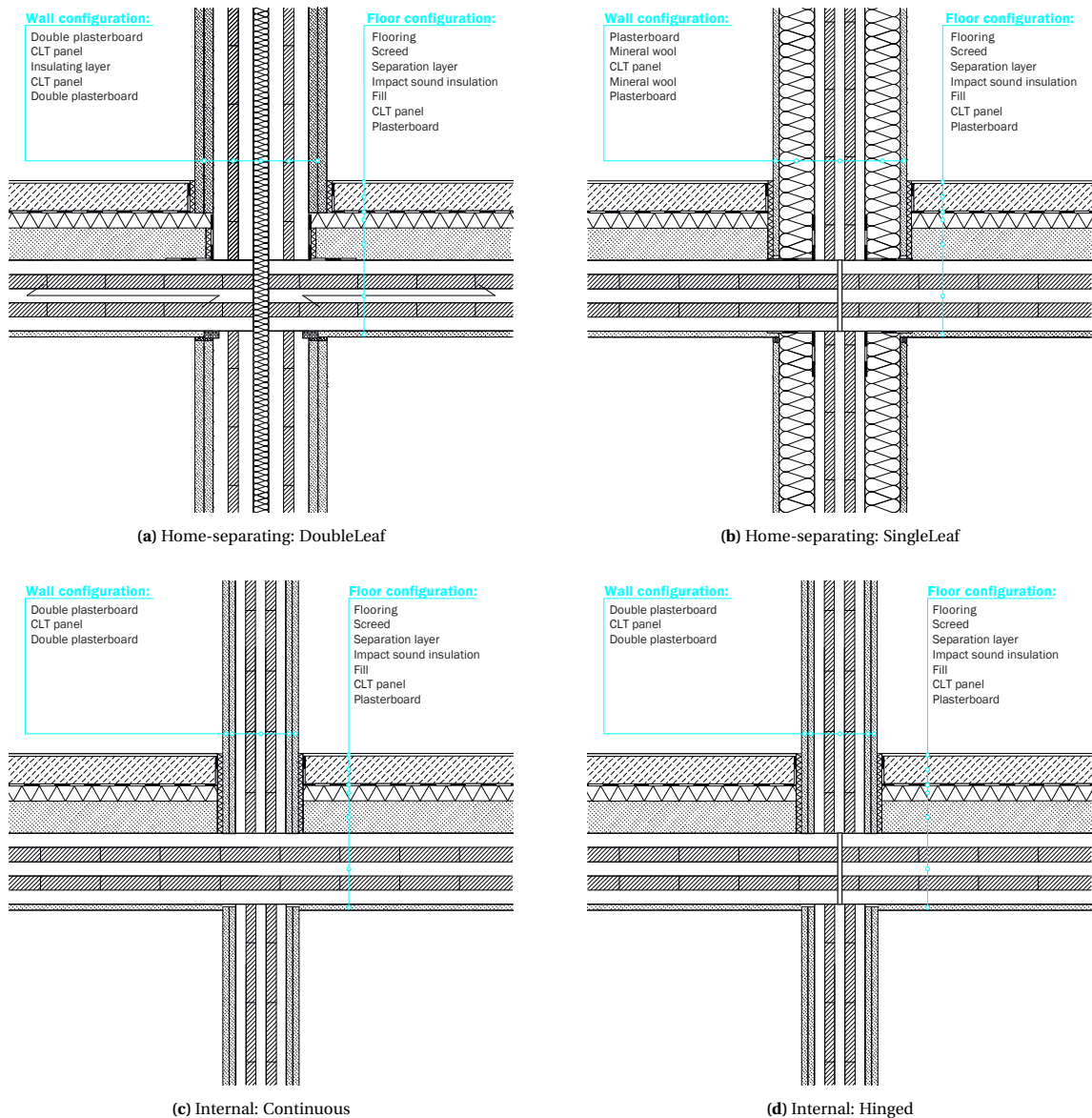


Figure A.1: Junctions of CLT floors with a wet screed on CLT walls without elastomeric interlayer

F2-CLT: CLT FLOORS WITH DRY SCREED ON CLT WALLS

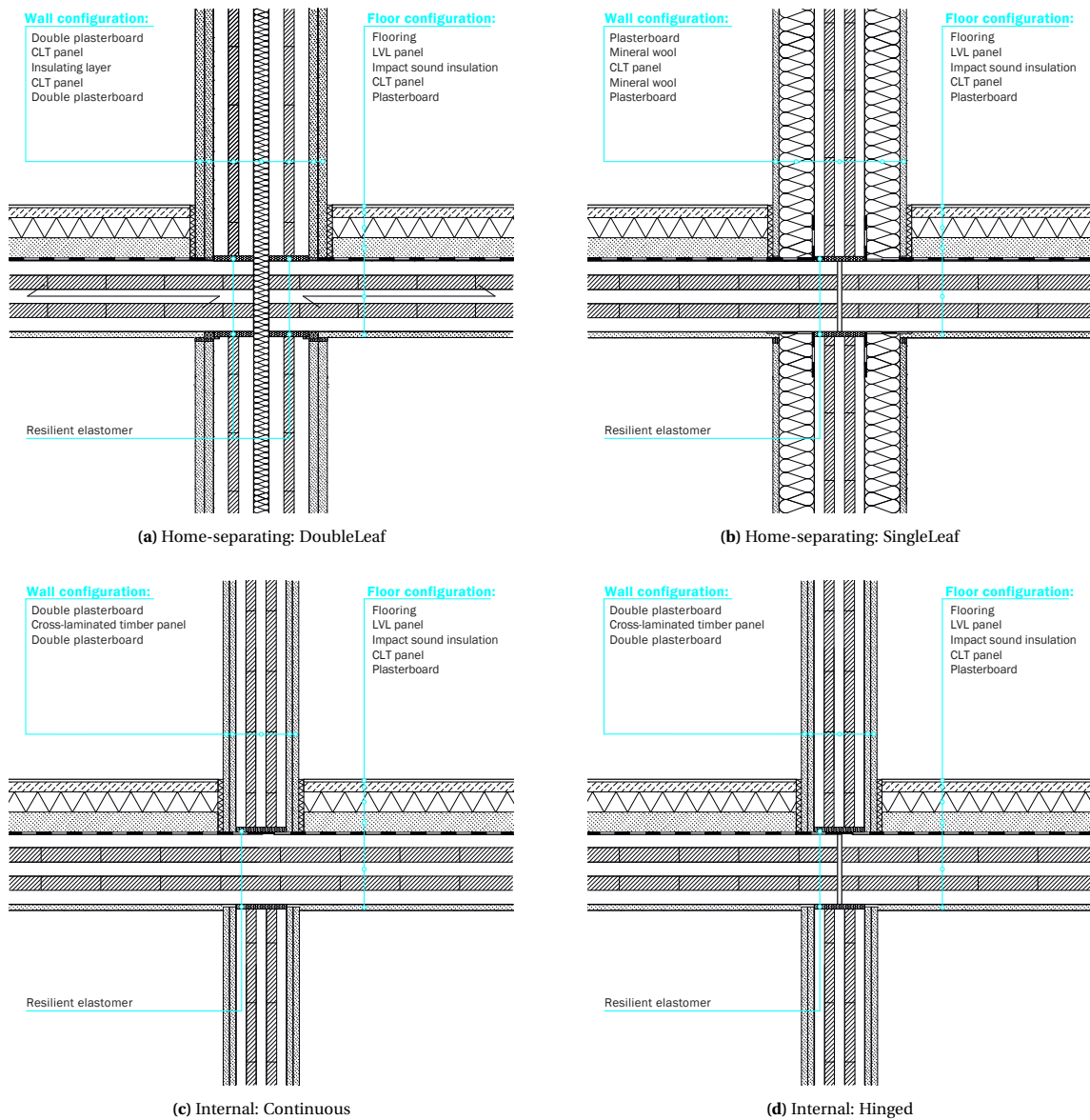


Figure A.2: Junctions of CLT floors with a dry screed on CLT walls with elastomeric interlayer

F2-SB: CLT FLOORS WITH DRY SCREED ON SUPPORTING BEAM

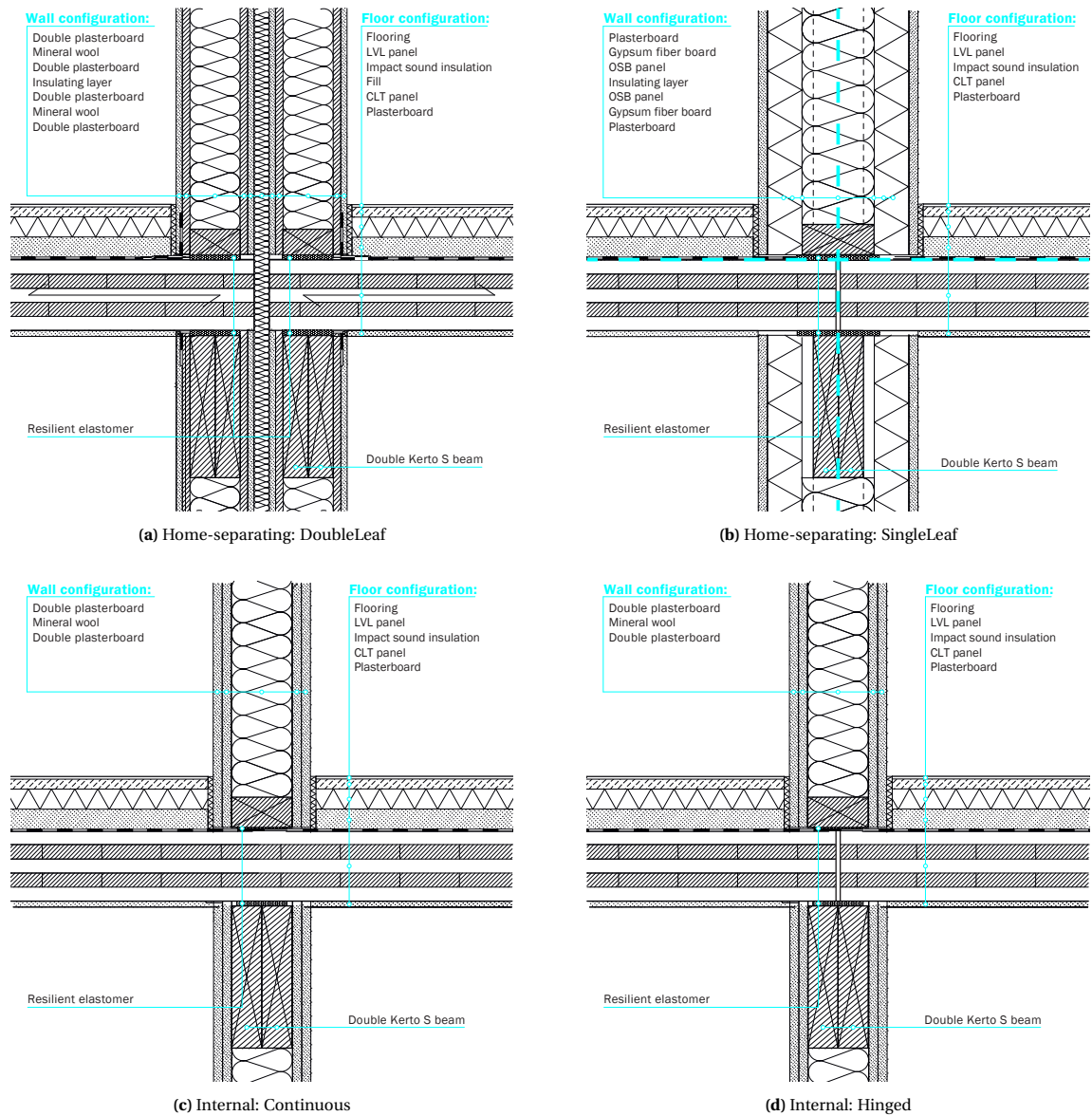


Figure A.3: Junctions of CLT floors with a dry screed on supporting LVL beam with elastomeric interlayer

F2-TF: CLT FLOORS WITH DRY SCREED ON TIMBER-FRAME

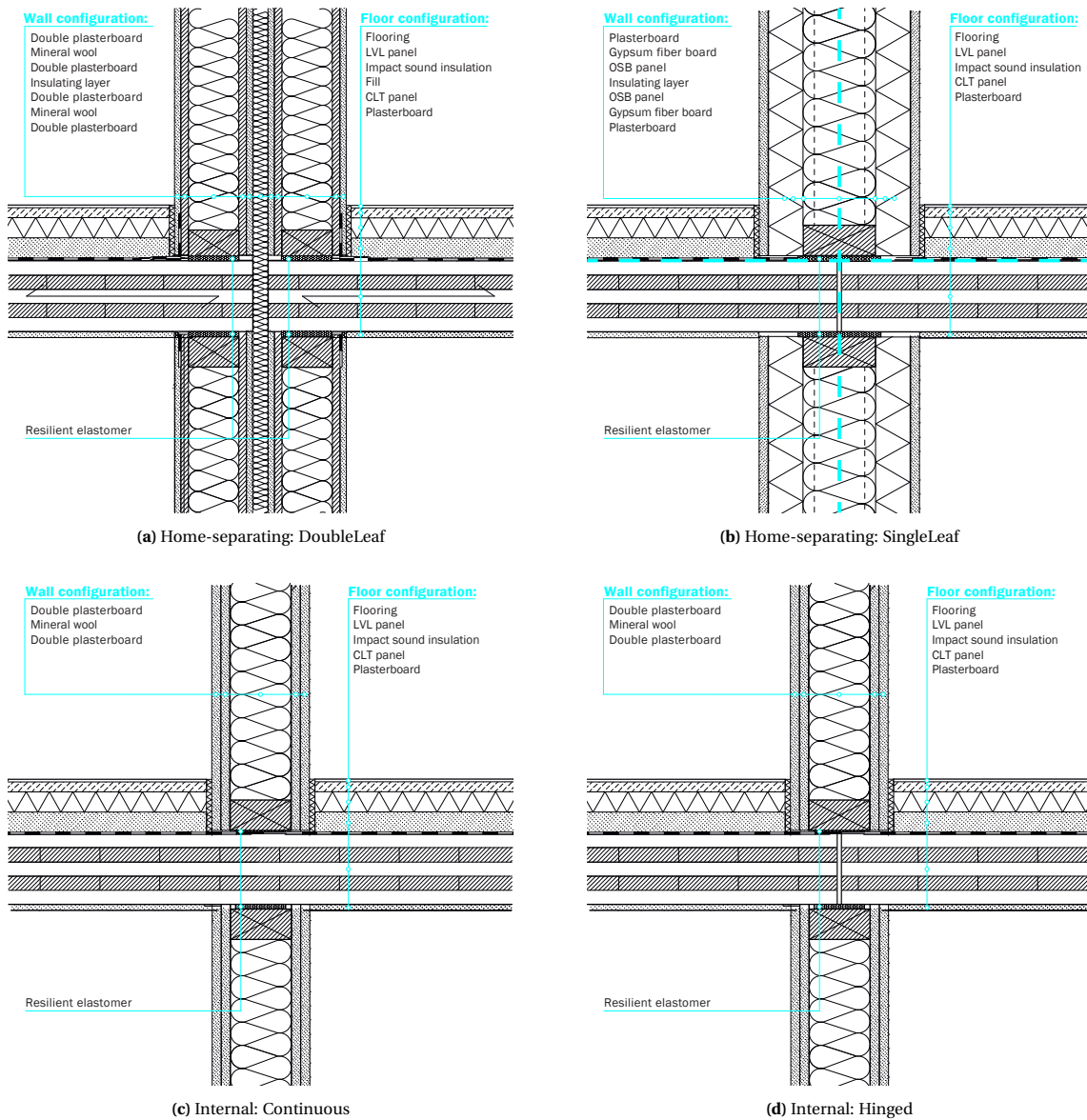


Figure A.4: Junctions of CLT floors with a dry screed on timber-frame wall with elastomeric interlayer

F3-SB: JOIST FLOORS WITH FILL ON SUPPORTING BEAM

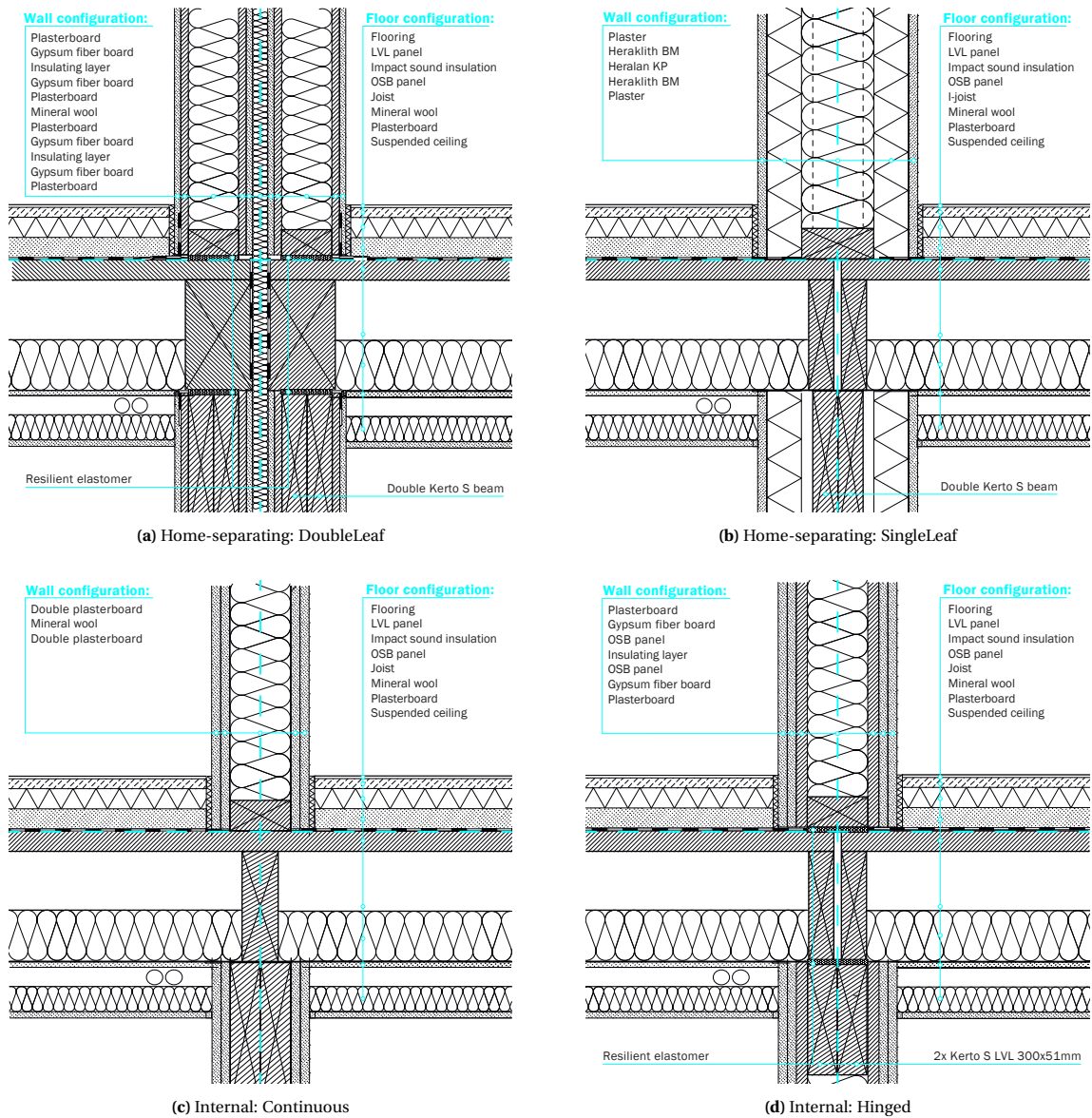


Figure A.5: Junctions of joist floor with fill on supporting LVL beam with elastomeric interlayer

F3-TF: JOIST FLOORS WITH FILL ON TIMBER-FRAME

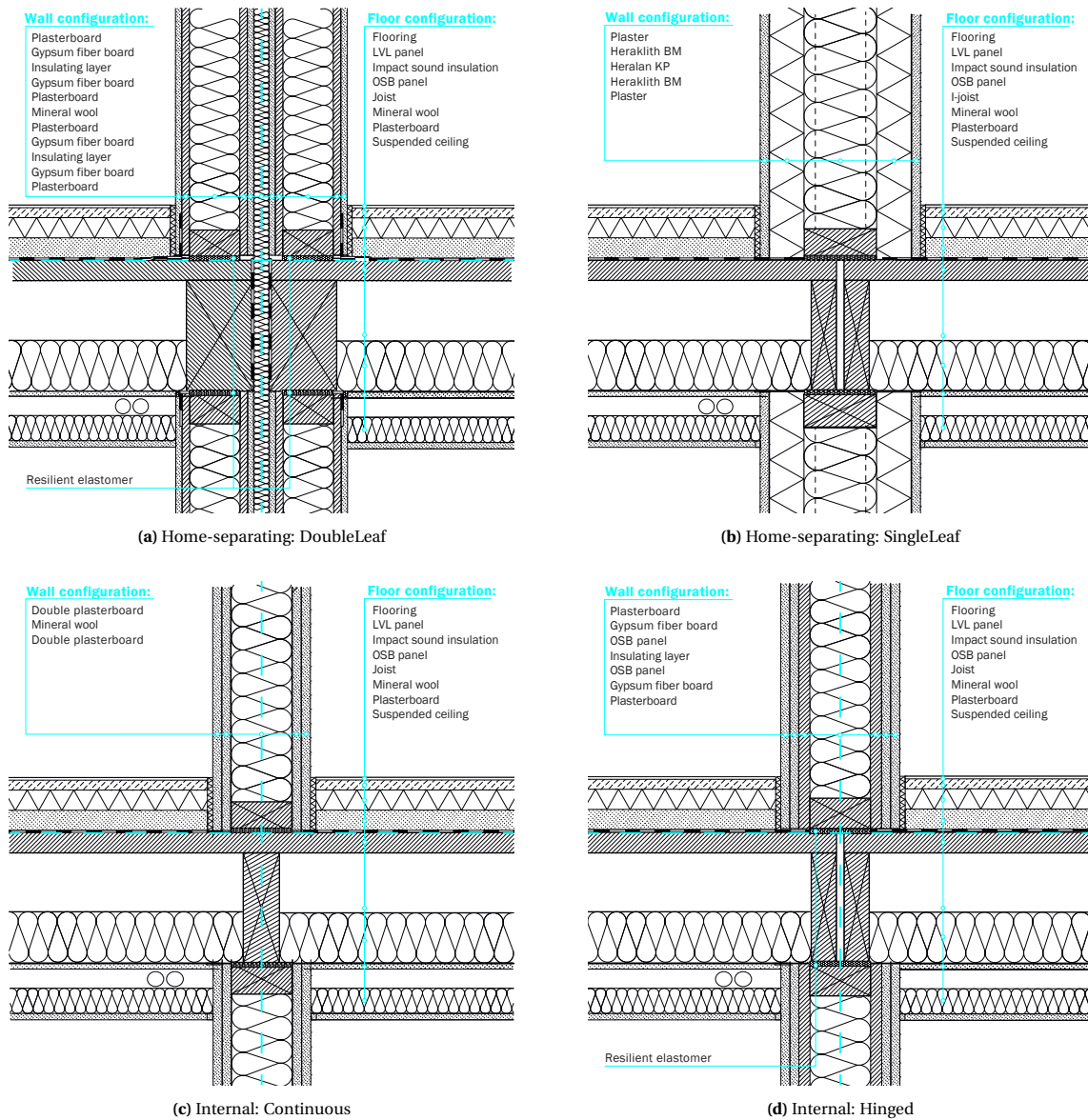


Figure A.6: Junctions of joist floor with fill on timber-frame wall with elastomeric interlayer

F4-SB: CLT FLOORS WITHOUT FILL ON SUPPORTING BEAM

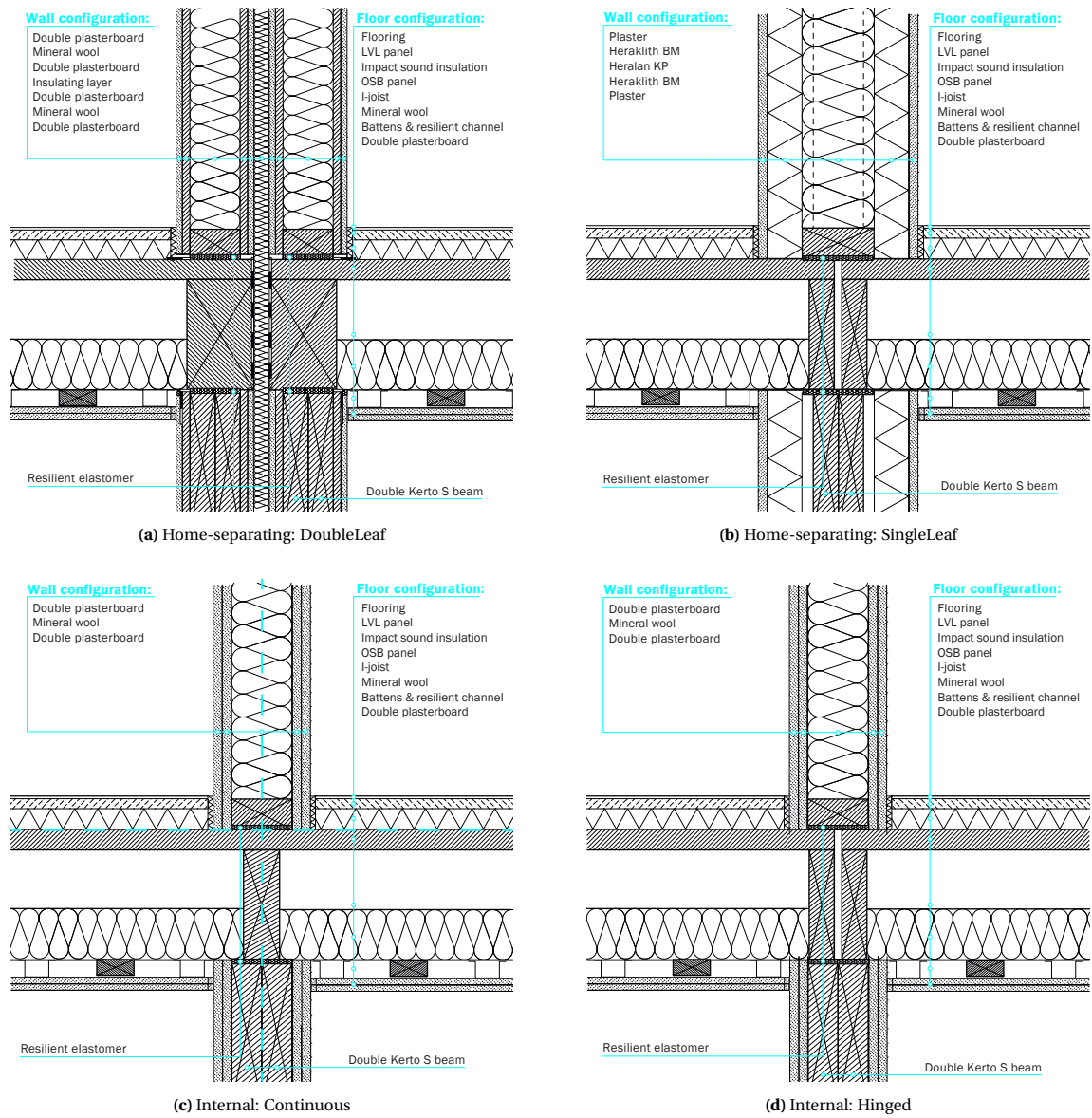


Figure A.7: Junctions of joist floor without fill on supporting LVL beam with elastomeric interlayer

F4-TF: CLT FLOORS WITHOUT FILL ON TIMBER-FRAME

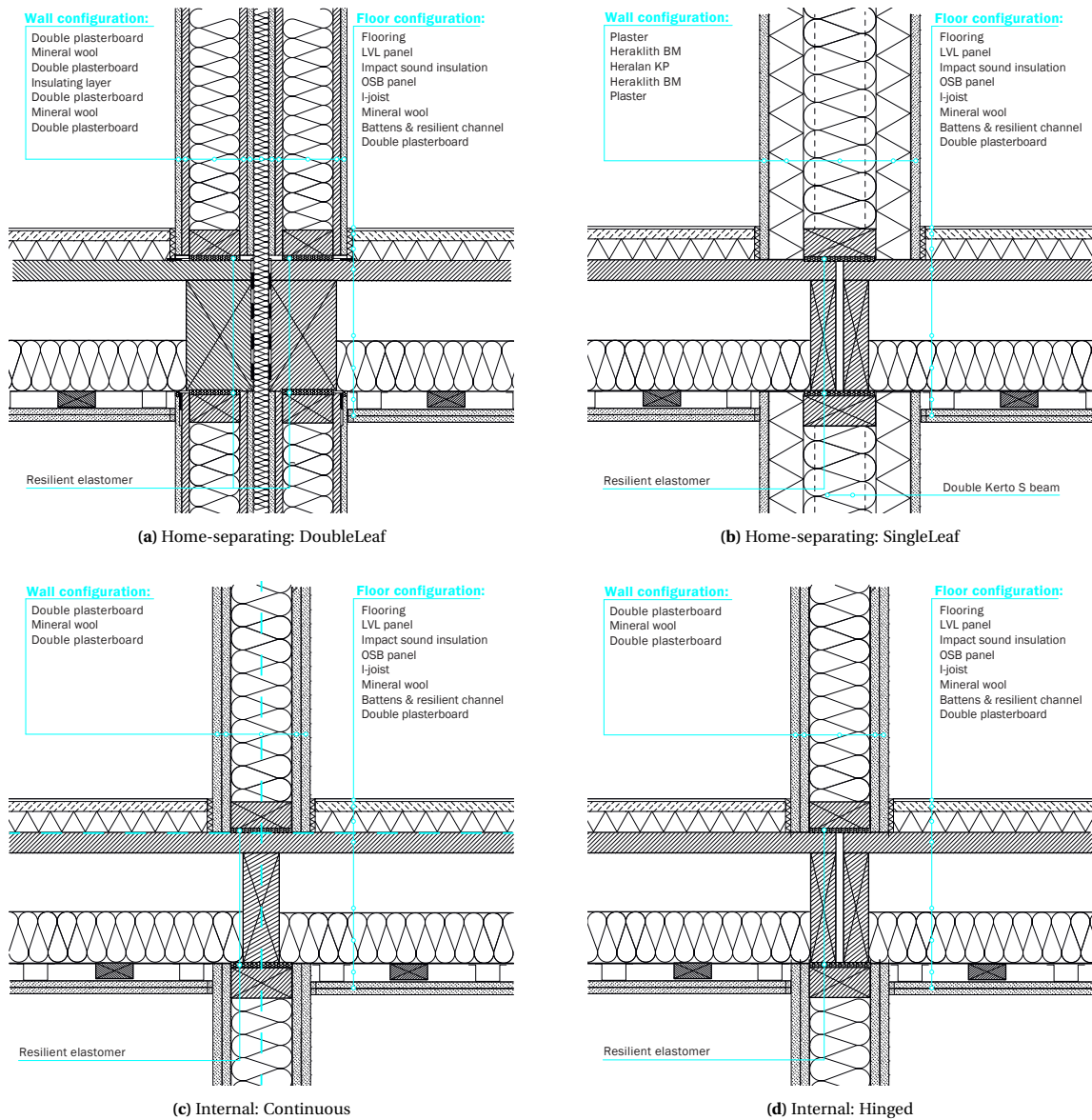


Figure A.8: Junctions of joist floor without fill on timber-frame wall with elastomeric interlayer

B

Dataholz datasheets

Intermediate floor - gdmnxn01a-00

intermediate floor, solid wood construction, directly, wet, with filling, other surface

Performance rating

Fire protection performance REI 60

maximum span = 5 m; maximum load $E_{d,fi} = 3,66 \text{ kN/m}^2$ (without floor construction)
 Classified by HFA

Germany

F60

Load $E_{d,fi}$ according to the German certification document

Corresponding proof: manufacturer-specific

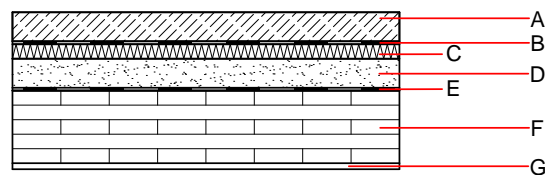
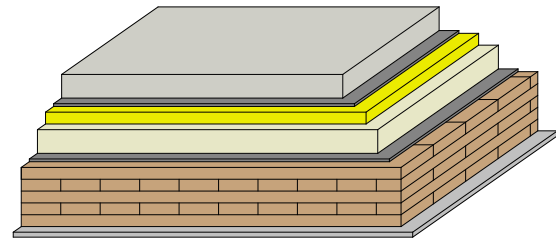
Thermal performance U Diffusion suitable

Acoustic performance $R_w (C; C_{tr})$ 75(-2;-8) dB
 $L_{n,w} (C_i)$ 45(-1)

Assessed by Müller-BBM

Mass per unit area m 315.30 kg/m²

Calculation based on gypsum plaster board type DF



Register of building materials used for this application, cross-section (from outside to inside, dimensions in mm)

	Thickness	Building material	Thermal performance				Reaction to fire EN
			λ	μ min - max	ρ	c	
A	60.0	cement screed	1.330	50 - 100	2000	1.080	A1
B	0.2	plastic separation layer	0.200	100000	1400	1.400	E
C	30.0	impact sound absorbing subflooring MW-T [$s' = 10 \text{ MN/m}^3$]	0.035	1	68	1.030	A1
D	60.0	elastic bonded fill (m' approx. 90 kg/m ²) elastic bonded, $m' = 90 \text{ kg/m}^2$	0.700	1	1500	1.000	A1
E	0.2	trickling protection					E
F	150.0	cross laminated timber	0.130	50	500	1.600	D
G	12.5	gypsum plaster board type DF	0.250	10	800	1.050	A2
G	12.5	gypsum fibre board	0.320	21	1000	1.100	A2

Sustainability rating (per m²)

Database ecoinvent

O13_{kon} 2.5

Calculated by TUM

Database GaBi (ÖKOBAUDAT)

Built-in renewable materials kg 73.410
 Biogenic carbon in kg CO₂-e. kg CO₂ 105.680
 Energy use of Primary Energy MJ 1,032.850
 Share of renewable PE % 31.250

Calculated by TUM

Intermediate floor - gdmtn01-00

intermediate floor, solid wood construction, without lining, dry, with filling, wooden surface

Performance rating

Fire protection performance REI 60

maximum span = 5 m; maximum load $E_{d,fi}$ = 5 kN/m²
 Classified by HFA

Germany

REI60

Load $E_{d,fi}$ according to the German certification document

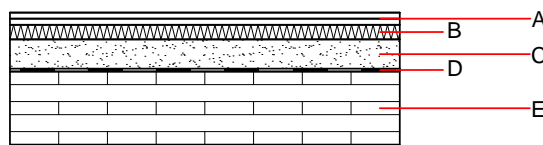
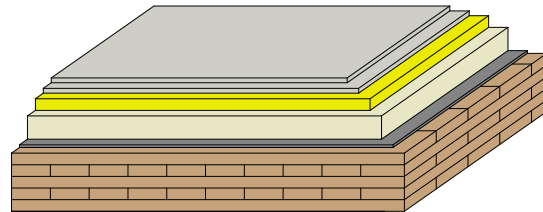
Corresponding proof: manufacturer-specific

Thermal performance U Diffusion suitable

Acoustic performance R_w (C;C_{tr}) 62(-5;-13) dB
 $L_{n,w}$ (C_i) 50(-1)

Assessed by Müller-BBM

Mass per unit area m 202.50 kg/m²



Register of building materials used for this application, cross-section (from outside to inside, dimensions in mm)

	Thickness	Building material	Thermal performance				Reaction to fire EN
			λ	μ min – max	ρ	c	
A	25.0	dry screed	0.210	8	900	1.050	A1
B	30.0	impact sound absorbing subflooring MW-T [$s' = 40MN/m^2$]	0.040	1	160	0.840	A2
C	60.0	elastic bonded fill (m' approx. 90 kg/m ²) elastic bonded, $m' = 90$ kg/m ²	0.700	1	1500	1.000	A1
D	0.2	trickling protection					E
E	140.0	cross laminated timber	0.130	50	500	1.600	D

Sustainability rating (per m²)

Database GaBi (ÖKOBAUDAT)

Built-in renewable materials	kg	68.520
Biogenic carbon in kg CO ₂ e.	kg CO ₂	98.630
Energy use of Primary Energy	MJ	967.990
Share of renewable PE	%	31.210

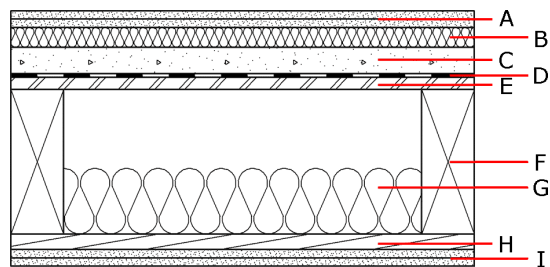
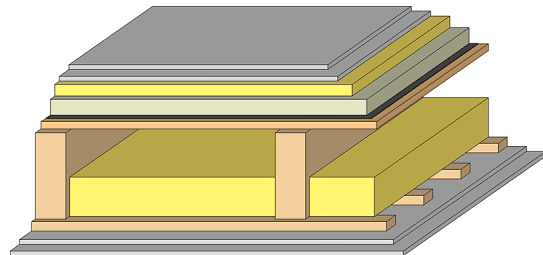
Calculated by TUM

Geschossdecke - gdrtn01b-00

Geschossdecke, Holzrahmen/Holztafel, auf Lattung, trocken, mit Schüttung, andere Oberfläche

Bauphysikalische Bewertung

Brandschutz	REI	60
max. Spannweite = 5 m; max. Last $E_{d,fl}$ = 3,66 kN/m ² Klassifizierung durch IBS		
Wärmeschutz	U Diffusionsverhalten	0,26 W/(m ² K) geeignet
Berechnung durch HFA		
Schallschutz	R_w (C;C _{tr}) $L_{n,w}$ (C _i)	63(-4;-11) dB 58(0)
Beurteilung durch TGM		
Flächenbezogene Masse	m	144,30 kg/m ²
Berechnet mit GF		



Bemerkung: e=625;

Baustoffangaben zur Konstruktion, Schichtaufbau (von außen nach innen, Maße in mm)

	Dicke	Baustoff	Wärmeschutz				Brandverhaltensklasse EN
			λ	μ min – max	ρ	c	
A	25,0	Trockenestrich	0,210	8	900	1,050	A1
B	30,0	Trittschalldämmung MW-T	0,035	1	68	1,030	A1
C	40,0	Schüttung	0,700	1	1800	1,000	A1
D		Rieselschutz					E
E	18,0	OSB	0,130	200	600	1,700	D
F	220,0	Konstruktionsholz (80/..; e=*)	0,120	50	450	1,600	D
G	100,0	Mineralwolle [040; ≥16; <1000°C]	0,040	1	16	1,030	A1
H	24,0	Holz Fichte Sparschalung (24/100; a=400)	0,120	50	450	1,600	D
I	25,0	Gipsplatte Typ DF (GKF) (2x12,5 mm) oder	0,250	10	800	1,050	A2
I	25,0	Gipsfaserplatte (2x12,5 mm)	0,320	21	1000	1,100	A2

Ökologische Bewertung (pro m² Konstruktionsfläche)

Datenbasis ecoinvent

O13_{kon} 7,4

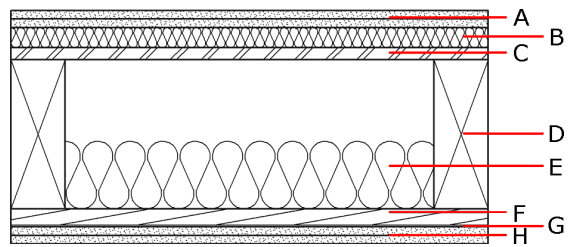
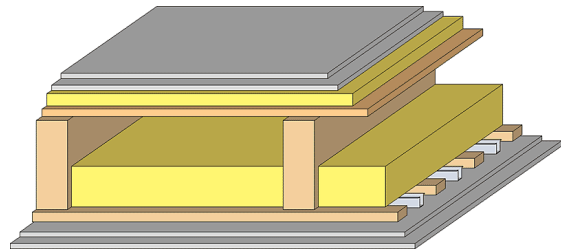
Berechnung durch IBO

Intermediate floor - gdrta03b-00

intermediate floor, timber frame construction, suspended, dry, without filling, other surface

Performance rating

Fire protection performance	REI	60
maximum span = 5 m; maximum load $E_{d,fi} = 3,66 \text{ kN/m}^2$		
Thermal performance	U Diffusion	0.26 $\text{W}/(\text{m}^2\text{K})$ suitable
Acoustic performance	$R_w (C;C_{tr})$ $L_{n,w} (C)$	64(-3;-10) dB 52(2)
Mass per unit area	m	72.30 kg/m^2
Calculation based on GF		



Note: e=625;

Register of building materials used for this application, cross-section (from outside to inside, dimensions in mm)

	Thickness	Building material	Thermal performance				Reaction to fire EN
			λ	μ min – max	ρ	c	
A	25.0	dry screed	0.210	8	900	1.050	A1
B	30.0		0.040	1	180	1.030	A1
C	18.0	OSB	0.130	200	600	1.700	D
D	220.0	construction timber (80/..; e=625) (80/..; e=*)	0.120	50	450	1.600	D
E	100.0	mineral wool [040; ≥ 16 ; <1000°C]	0.040	1	16	1.030	A1
F	24.0	spruce wood cladding with spacing of cladding boards(24/100); a=400	0.120	50	450	1.600	D
G	27.0	resilient channel (placed between open formwork)	0.156				
H	25.0	gypsum plaster board type DF (2x12,5 mm) or	0.250	10	800	1.050	A2
H	25.0	gypsum fibre board (2x12,5 mm)	0.320	21	1000	1.100	A2

Sustainability rating (per m^2)

Database ecoinvent

$OI3_{Kon}$ 7.0

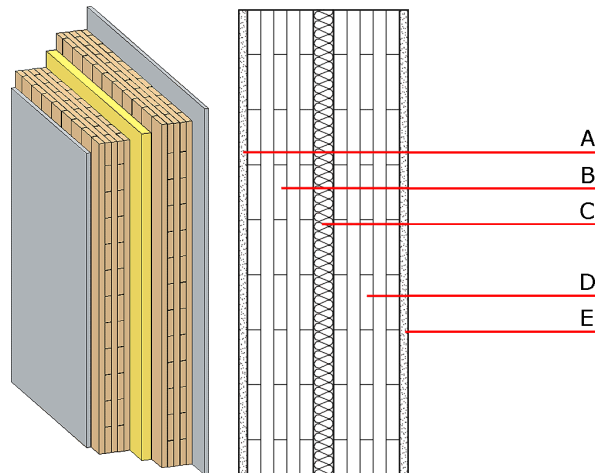
Calculated by IBO

Trennwand - twmxxo03a-01

Trennwand, Holzmassivbau, ohne Installationsebene, zweischalig, Holz sichtbar

Bauphysikalische Bewertung

Brandschutz	REI	60
max. Wandhöhe = 3 m; max. einwirkende Last $E_{d,fi} = 35 \text{ kN/lm}$ Klassifizierung durch MA39		
Wärmeschutz	U Diffusionsverhalten	0,29 $\text{W}/(\text{m}^2\text{K})$ geeignet
Berechnung durch HFA		
Schallschutz	R_w ($C; C_{tr}$) $L_{n,w}$ (C_i)	60 dB
Beurteilung durch TU-GRAZ		
Flächenbezogene Masse	m	121,60 kg/m^2
Berechnet mit GKF		



Bemerkung: Bei Verwendung von Brettsperholz:
 Varianten 00-01: $d \geq 78,0$; mind. 3-lagig, Decklage mind. 25mm
 Variante 02: $d \geq 94,0$; mind. 3-lagig, Decklage mind. 30mm
 $C=2 \times 30 \text{ mm}$,

Baustoffangaben zur Konstruktion, Schichtaufbau (von außen nach innen, Maße in mm)

	Dicke	Baustoff	Wärmeschutz				Brandverhaltensklasse EN
			λ	μ min – max	ρ	c	
A	12,5	GKF/Gipsfaserplatte	0,250	10	800	1,050	A2
B	78,0	Massivholz verleimt (z. B. Brettsperholz, Brettstapel)	0,130	50	500	1,600	D
C	60,0	Trittschalldämmung MW-T	0,035	1	68	1,030	A1
D	78,0	Massivholz verleimt (z.B. Brettsperholz, Brettstapel)	0,130	50	500	1,600	D
E	12,5	GKF/Gipsfaserplatte	0,250	10	800	1,050	A2

Ökologische Bewertung (pro m^2 Konstruktionsfläche)

Datenbasisecoinvent

$O13_{kon}$	-0,1
Berechnung durch IBO	

Ökologische Bewertung im Detail

Datenbasis Datenbankecoinvent

GWP [kg CO_2 Äqv.]	AP [kg SO_2 Äqv.]	PEI ne [MJ]	PEI e [MJ]	EP [kg PO_4 Äqv.]	POCP [kg C_2H_4 Äqv.]
-115,9	0,220	786,7	2.040,5	0,033	0,014

Trennwand - twmxxo04a-02

Trennwand, Holzmassivbau, ohne Installationsebene, einschalig, andere Oberfläche

Bauphysikalische Bewertung

Brandschutz REI 90
 max. Wandhöhe = 3 m; max. einwirkende Last $E_{d,fi} = 35 \text{ kN/lfm}$
 Klassifizierung durch HFA

Deutschland
 REI60; ACHTUNG: REI 90 möglich mit 2x12,5mm GKF/GF
 Last $E_{d,fi}$ gemäß des deutschen Verwendbarkeitsnachweises
 Nachweis: herstellerepezifisch

Wärmeschutz U Diffusionsverhalten 0,27 W/(m²K) geeignet

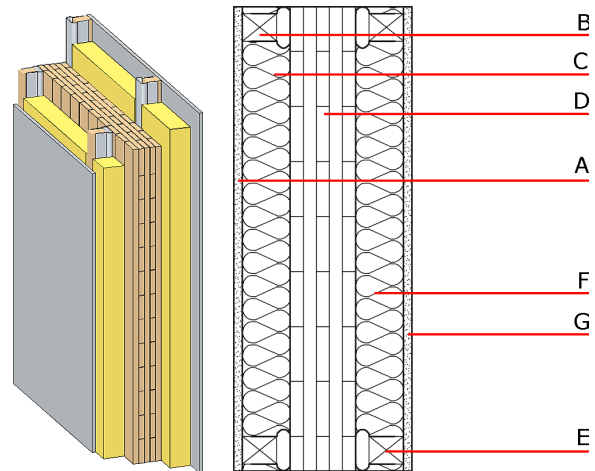
Berechnung durch TUM

Schallschutz $R_w (C;C_{tr})$ 53(-5;-13) dB
 $L_{n,w} (C_i)$

Beurteilung durch Müller-BBM

Flächenbezogene Masse m 74,90 kg/m²

Berechnet mit GKF



Bemerkung: Der Feuerwiderstand gilt beim Einsatz als Trennwand mit einseitiger Beflammung. ACHTUNG: REI 90 in Deutschland nur mit 2x12,5mm GKF/GF Bei Verwendung von Brettsperrholz: mind. 5-lagig, Decklage mind. 19mm

Baustoffangaben zur Konstruktion, Schichtaufbau (von außen nach innen, Maße in mm)

	Dicke	Baustoff	Wärmeschutz				Brandverhaltensklasse EN
			λ	$\mu \text{ min} - \text{max}$	ρ	c	
A	12,5	Gipsplatte Typ DF (GKF) oder	0,250	10	800	1,050	A2
A	12,5	Gipsfaserplatte	0,320	21	1000	1,100	A2
B	60,0	Mineralwolle [040; 11; <1000°C]	0,040	1	11	1,030	A1
C	70,0	Holz Fichte Lattung auf Schwingbügel (60/60)	0,120	50	450	1,600	D
D	97,0	Massivholz verleimt (z.B. Brettsperrholz, Brettstapel)	0,130	50	500	1,600	D
E	70,0	Holz Fichte Lattung auf Schwingbügel (60/60)	0,120	50	450	1,600	D
F	60,0	Mineralwolle [040; 11; <1000°C]	0,040	1	11	1,030	A1
G	12,5	Gipsplatte Typ DF (GKF) oder	0,250	10	800	1,050	A2
G	12,5	Gipsfaserplatte	0,320	21	1000	1,100	A2

Ökologische Bewertung (pro m² Konstruktionsfläche)

Datenbasis ecoinvent

$OI3_{kon}$ -11,1
 Berechnung durch IBO

Datenbasis GaBi (ÖKOBAUDAT)

Verbaute Menge an Nawaros	kg	53,050
Biogener Kohlenstoff in kg CO ₂ Äqv.	kg CO ₂	76,500
Einsatz Primärenergie	MJ	645,710
Davon Anteil erneuerbar	%	35,350

Berechnung durch TUM

Internal wall - iwmxo01b-00

internal wall, solid wood construction, without dry lining, other surface

Performance rating

Fire protection performance REI 90

maximum ceiling height = 3 m; maximum load $E_{d,fi} = 32,0 \text{ kN/m}$
 Classified by MA39

Germany

REI60

Load $E_{d,fi}$ according to the German certification document

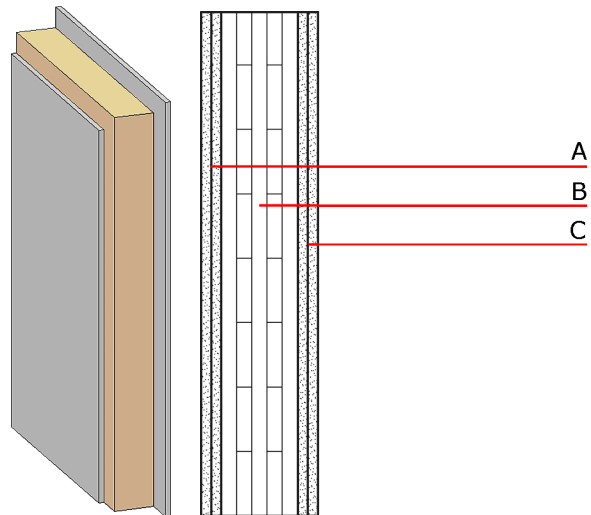
Corresponding proof: manufacturer-specific

Acoustic performance $R_w (C; C_{tr})$ 38(-2;-5) dB
 $L_{n,w} (C_i)$

Assessed by TU-GRAZ
 Assessed by Müller-BBM

Mass per unit area m 79.00 kg/m²

Calculation based on gypsum plaster board type DF



Note: The fire resistance is only valid when wall is used as partition with only one side exposed to fire.

Register of building materials used for this application, cross-section (from outside to inside, dimensions in mm)

	Thickness	Building material	Thermal performance				Reaction to fire EN
			λ	μ min – max	ρ	c	
A	25.0	gypsum plaster board type DF (2x... mm) or	0.250	10	800	1.050	A2
A	25.0	gypsum fibre board (2x...mm)	0.320	21	1000	1.100	A2
B	78.0	solid wood (e.g. cross laminated timber: thickness $\geq 78\text{mm}$; 3-ply at least, surface layer at least 25mm)	0.130	50	500	1.600	D
C	25.0	gypsum plaster board type DF (2x...mm) or	0.250	10	800	1.050	A2
C	25.0	gypsum fibre board (2x...mm)	0.320	21	1000	1.100	A2

Sustainability rating (per m²)

Database ecoinvent

O13_{Kon} -17.1
 Calculated by HFA

Database GaBi (ÖKOBAUDAT)

Built-in renewable materials kg 38.170
Biogenic carbon in kg CO₂-e. kg CO₂ 54.950
Energy use of Primary Energy MJ 541.040
Share of renewable PE % 31.590

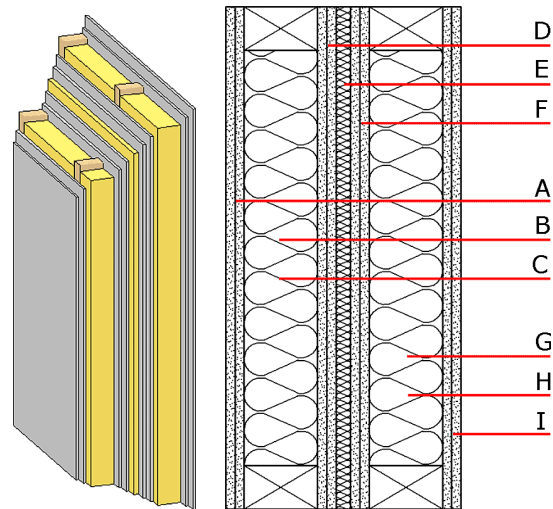
Calculated by TUM

Compartment wall - twrxo03b-00

compartment wall, timber frame construction, without dry lining, double-layer, other surface

Performance rating

Fire protection performance	REI	60
apply to each individual load-bearing wall; the whole wall: EI90; maximum ceiling height = 3 m; maximum load $E_{d,fi} = 50,0 \text{ kN/m}$ Classified by MA39		
Thermal performance	U Diffusion	0.19 $\text{W}/(\text{m}^2\text{K})$ suitable
Calculated by HFA		
Acoustic performance	R_w (C;C _{tr}) $L_{n,w}$ (C _i)	59(-2;-10) dB
Assessed by MA39		
Mass per unit area	m	92.80 kg/m^2
Calculation based on gypsum plaster board type DF		



Note: layer A, D, F, I: planking: 2x12,5mm; e=625

Register of building materials used for this application, cross-section (from outside to inside, dimensions in mm)

	Thickness	Building material	Thermal performance				Reaction to fire EN
			λ	μ min – max	ρ	c	
A	25.0	gypsum plaster board type DF or	0.250	10	800	1.050	A2
A	25.0	gypsum fibre board	0.320	21	1000	1.100	A2
B	100.0	construction timber (60/100; e=*)	0.120	50	450	1.600	D
C	100.0	mineral wool [040; ≥ 16 ; $< 1000^\circ\text{C}$]	0.040	1	16	1.030	A1
D	25.0	gypsum plaster board type DF or	0.250	10	800	1.050	A2
D	25.0	gypsum fibre board	0.320	21	1000	1.100	A2
E	20.0	mineral wool [040; ≥ 16 ; $< 1000^\circ\text{C}$]	0.040	1	16	1.030	A1
F	25.0	gypsum plaster board type DF or	0.250	10	800	1.050	A2
F	25.0	gypsum fibre board	0.320	21	1000	1.100	A2
G	100.0	construction timber (60/100; e=*)	0.120	50	450	1.600	D
H	100.0	mineral wool [040; ≥ 16 ; $< 1000^\circ\text{C}$]	0.040	1	16	1.030	A1
I	25.0	gypsum plaster board type DF or	0.250	10	800	1.050	A2
I	25.0	gypsum fibre board	0.320	21	1000	1.100	A2

Sustainability rating (per m^2)

Database ecoinvent

O13_{Kon} 2.1

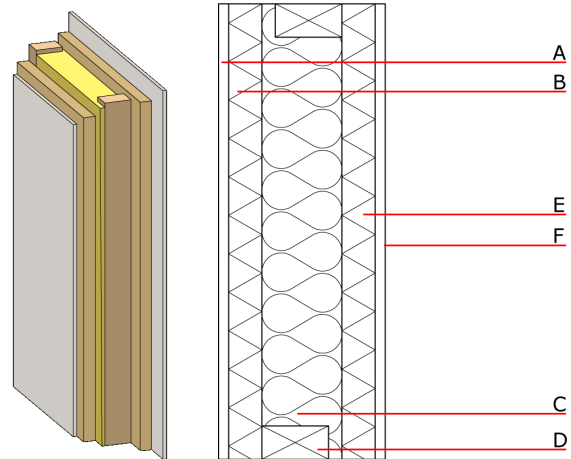
Calculated by IBO

Compartment wall - twrxo01-00

compartment wall, timber frame construction, without dry lining, single-layer, other surface

Performance rating

Fire protection performance	REI	60
maximum ceiling height = 3 m; maximum load $E_{d,fi}$ = 19,2 kN/m Classified by MA39		
Thermal performance	U Diffusion	0.25 W/(m ² K) suitable
Calculated by HFA		
Acoustic performance	R _w (C;C _{tr}) L _{n,w} (C _i)	60(-1;-6) dB
Assessed by TGM		
Mass per unit area	m	82.40 kg/m ²



Register of building materials used for this application, cross-section (from outside to inside, dimensions in mm)

	Thickness	Building material	Thermal performance				Reaction to fire EN
			λ	μ min - max	ρ	c	
A	15.0	plaster	0.700	10	1300	1.000	A1
B	50.0	Heraklith BM	0.090	2 - 5	370	2.000	B
C		construction timber (60/100; e=625)	0.120	50	450	1.600	D
D	120.0	Heralan KP	0.040	1	28	1.030	A1
E	50.0	Heraklith BM	0.090	2 - 5	370	2.000	B
F	15.0	plaster	0.700	10	1300	1.000	A1

Sustainability rating (per m²)

Database ecoinvent

OI_{3kon} -10.5

Calculated by IBO

Details of sustainability rating

Database ecoinvent

GWP [kg CO ₂ -e.]	AP [kg SO ₂ -e.]	PEI ne [MJ]	PEI e [MJ]	EP [kg PO ₄ -e.]	POCP [kg C ₂ H ₄ -e.]
1.7	0.103	354.9	348.4	0.013	0.020

Internal wall - iwrxo01b-00

internal wall, timber frame construction, without dry lining, other surface

Performance rating

Fire protection performance REI 60

maximum ceiling height = 3 m; maximum load $E_{d,fi} = 50,0$ kN/m
 Classified by MA39

Germany

F30/F60 (depending on the corresponding proof)

Load $E_{d,fi}$ according to the German certification document

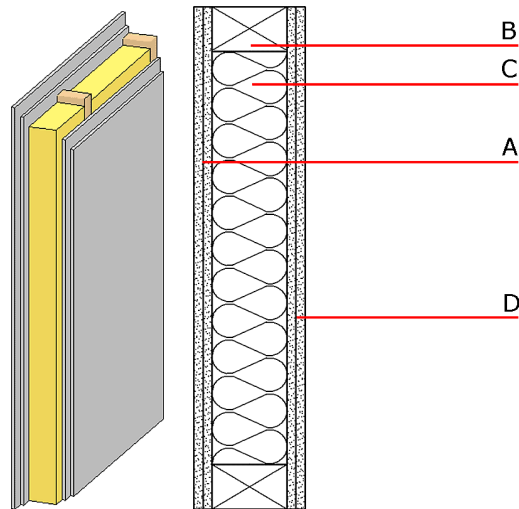
Corresponding proof: F30: DIN 4102-4:2016-05, Tabelle 10.5, Zeile 5; F60: DIN 4102-4:2016-05, Tabelle 10.5, Zeile 10 (if gypsum plaster board type DF or gypsum fibre board 15 mm inside) or manufacturer-specific

Acoustic performance $R_w (C; C_{tr})$ 43(-1;-5) dB
 $L_{n,w} (C_i)$

Assessed by Müller-BBM

Mass per unit area m 45.80 kg/m²

Calculation based on gypsum plaster board type DF



Note: The fire resistance is only valid when wall is used as partition with only one side exposed to fire.
 (B=60/100); e=625

Register of building materials used for this application, cross-section (from outside to inside, dimensions in mm)

	Thickness	Building material	Thermal performance				Reaction to fire EN
			λ	μ min – max	ρ	c	
A	25.0	gypsum plaster board type DF (2x12,5 mm) or	0.250	10	800	1.050	A2
A	25.0	gypsum fibre board (2x12,5 mm)	0.320	21	1000	1.100	A2
B	100.0	construction timber (60/100 or 60/160; e=*)	0.120	50	450	1.600	D
C	100.0	mineral wool [040; ≥ 16 ; $< 1000^\circ\text{C}$]	0.040	1	16	1.030	A1
D	25.0	gypsum plaster board type DF (2x12,5 mm) or	0.250	10	800	1.050	A2
D	25.0	gypsum fibre board (2x12,5 mm)	0.320	21	1000	1.100	A2

Sustainability rating (per m²)

Database ecoinvent

OI3_{Kon} -17.7

Calculated by IBO

Database GaBi (ÖKOBAUDAT)

Built-in renewable materials	kg	4.730
Biogenic carbon in kg CO ₂ -e.	kg CO ₂	6.910
Energy use of Primary Energy	MJ	261.110
Share of renewable PE	%	17.750

Calculated by TUM

C

Boundary- and interface conditions

Table C.1: Boundary- and interface conditions for rotational model

Node	Double leaf with continuous floor	Double leaf with single spanning floor	Single leaf with continuous floor	Single leaf with single spanning floor
A	$W_1 = 0$	$W_1 = 0$	$W_1 = 0$	$W_1 = 0$
	$-EI \frac{\partial^2 W_1}{\partial x^2} + r_{s,d} \frac{\partial W_1}{\partial x} = 0$	$-EI \frac{\partial^2 W_1}{\partial x^2} + r_{s,d} \frac{\partial W_1}{\partial x} = 0$	$-EI \frac{\partial^2 W_1}{\partial x^2} + r_{s,s} \frac{\partial W_1}{\partial x} = 0$	$-EI \frac{\partial^2 W_1}{\partial x^2} + r_{s,s} \frac{\partial W_1}{\partial x} = 0$
B	$W_1 = 0$	$W_1 = 0$	$W_1 = 0$	$W_1 = 0$
	$W_{2a} = 0$	$W_{2a} = 0$	$W_{2a} = 0$	$W_{2a} = 0$
	$\frac{\partial W_1}{\partial x} - \frac{\partial W_{2a}}{\partial x} = 0$	$EI \frac{\partial^2 W_1}{\partial x^2} + r_i \frac{\partial W_1}{\partial x} = 0$	$\frac{\partial W_1}{\partial x} - \frac{\partial W_{2a}}{\partial x} = 0$	$EI \frac{\partial^2 W_1}{\partial x^2} + r_i \frac{\partial W_1}{\partial x} = 0$
	$EI \left(\frac{\partial^2 W_1}{\partial x^2} - \frac{\partial^2 W_{2a}}{\partial x^2} \right) + r_i \frac{\partial W_1}{\partial x} = 0$	$-EI \frac{\partial^2 W_{2a}}{\partial x^2} + r_i \frac{\partial W_{2a}}{\partial x} = 0$	$EI \left(\frac{\partial^2 W_1}{\partial x^2} - \frac{\partial^2 W_{2a}}{\partial x^2} \right) + r_i \frac{\partial W_1}{\partial x} = 0$	$-EI \frac{\partial^2 W_{2a}}{\partial x^2} + r_i \frac{\partial W_{2a}}{\partial x} = 0$
P	$W_{2a} - W_{2b} = 0$	$W_{2a} - W_{2b} = 0$	$W_{2a} - W_{2b} = 0$	$W_{2a} - W_{2b} = 0$
	$\frac{\partial W_{2a}}{\partial x} - \frac{\partial W_{2b}}{\partial x} = 0$	$\frac{\partial W_{2a}}{\partial x} - \frac{\partial W_{2b}}{\partial x} = 0$	$\frac{\partial W_{2a}}{\partial x} - \frac{\partial W_{2b}}{\partial x} = 0$	$\frac{\partial W_{2a}}{\partial x} - \frac{\partial W_{2b}}{\partial x} = 0$
	$EI \left(\frac{\partial^2 W_{2a}}{\partial x^2} - \frac{\partial^2 W_{2b}}{\partial x^2} \right) = 0$	$EI \left(\frac{\partial^2 W_{2a}}{\partial x^2} - \frac{\partial^2 W_{2b}}{\partial x^2} \right) = 0$	$EI \left(\frac{\partial^2 W_{2a}}{\partial x^2} - \frac{\partial^2 W_{2b}}{\partial x^2} \right) = 0$	$EI \left(\frac{\partial^2 W_{2a}}{\partial x^2} - \frac{\partial^2 W_{2b}}{\partial x^2} \right) = 0$
	$EI \left(\frac{\partial^3 W_{2a}}{\partial x^3} - \frac{\partial^3 W_{2b}}{\partial x^3} \right) + P = 0$	$EI \left(\frac{\partial^3 W_{2a}}{\partial x^3} - \frac{\partial^3 W_{2b}}{\partial x^3} \right) + P = 0$	$EI \left(\frac{\partial^3 W_{2a}}{\partial x^3} - \frac{\partial^3 W_{2b}}{\partial x^3} \right) + P = 0$	$EI \left(\frac{\partial^3 W_{2a}}{\partial x^3} - \frac{\partial^3 W_{2b}}{\partial x^3} \right) + P = 0$
C	$W_{2b} = 0$	$W_{2b} = 0$	$W_{2b} = 0$	$W_{2b} = 0$
	$EI \frac{\partial^2 W_{2a}}{\partial x^2} + r_{s,d} \frac{\partial W_{2b}}{\partial x} = 0$	$EI \frac{\partial^2 W_{2a}}{\partial x^2} + r_{s,d} \frac{\partial W_{2b}}{\partial x} = 0$	$EI \frac{\partial^2 W_{2a}}{\partial x^2} + r_{s,s} \frac{\partial W_{2b}}{\partial x} = 0$	$EI \frac{\partial^2 W_{2a}}{\partial x^2} + r_{s,s} \frac{\partial W_{2b}}{\partial x} = 0$
	$W_3 = 0$	$W_3 = 0$	$W_3 = 0$	$W_3 = 0$
	$-EI \frac{\partial^2 W_3}{\partial x^2} + r_{s,d} \frac{\partial W_3}{\partial x} = 0$	$-EI \frac{\partial^2 W_3}{\partial x^2} + r_{s,d} \frac{\partial W_3}{\partial x} = 0$	$-EI \frac{\partial^2 W_3}{\partial x^2} + r_{s,s} \frac{\partial W_3}{\partial x} = 0$	$-EI \frac{\partial^2 W_3}{\partial x^2} + r_{s,s} \frac{\partial W_3}{\partial x} = 0$
D	$W_3 = 0$	$W_3 = 0$	$W_3 = 0$	$W_3 = 0$
	$W_4 = 0$	$W_4 = 0$	$W_4 = 0$	$W_4 = 0$
	$\frac{\partial W_3}{\partial x} - \frac{\partial W_4}{\partial x} = 0$	$EI \frac{\partial^2 W_3}{\partial x^2} + r_i \frac{\partial W_3}{\partial x} = 0$	$\frac{\partial W_3}{\partial x} - \frac{\partial W_4}{\partial x} = 0$	$EI \frac{\partial^2 W_3}{\partial x^2} + r_i \frac{\partial W_3}{\partial x} = 0$
	$EI \left(\frac{\partial^2 W_3}{\partial x^2} - \frac{\partial^2 W_4}{\partial x^2} \right) + r_i \frac{\partial W_3}{\partial x} = 0$	$-EI \frac{\partial^2 W_4}{\partial x^2} + r_i \frac{\partial W_4}{\partial x} = 0$	$EI \left(\frac{\partial^2 W_3}{\partial x^2} - \frac{\partial^2 W_4}{\partial x^2} \right) + r_i \frac{\partial W_3}{\partial x} = 0$	$-EI \frac{\partial^2 W_4}{\partial x^2} + r_i \frac{\partial W_4}{\partial x} = 0$
E	$W_4 = 0$	$W_4 = 0$	$W_4 = 0$	$W_4 = 0$
	$EI \frac{\partial^2 W_4}{\partial x^2} + r_{s,d} \frac{\partial W_4}{\partial x} = 0$	$EI \frac{\partial^2 W_4}{\partial x^2} + r_{s,d} \frac{\partial W_4}{\partial x} = 0$	$EI \frac{\partial^2 W_4}{\partial x^2} + r_{s,s} \frac{\partial W_4}{\partial x} = 0$	$EI \frac{\partial^2 W_4}{\partial x^2} + r_{s,s} \frac{\partial W_4}{\partial x} = 0$

